



UNIVERSITY OF  
BIRMINGHAM

**Synthesis of Asymmetric DMAP Derivatives and Their  
Applications in Asymmetric Catalysis and Sensing**

by

**Daniel Tony Payne**

A thesis submitted to the

**University of Birmingham**

for the degree of

**DOCTOR OF PHILOSOPHY**

*School of Chemistry*

*College of Engineering and Physical Sciences*

*University of Birmingham*

*October 2016*

UNIVERSITY OF  
BIRMINGHAM

**University of Birmingham Research Archive**

**e-theses repository**

This unpublished thesis/dissertation is copyright of the author and/or third parties. The intellectual property rights of the author or third parties in respect of this work are as defined by The Copyright Designs and Patents Act 1988 or as modified by any successor legislation.

Any use made of information contained in this thesis/dissertation must be in accordance with that legislation and must be properly acknowledged. Further distribution or reproduction in any format is prohibited without the permission of the copyright holder.

## Abstract

A library of novel chiral DMAP derivatives were synthesised from 4-chloropyridine and 3,5-dibromo-4-chloropyridine to give a diverse range of DMAP derivatives focusing on modifications at the 3-position and 3,5-positions of pyridine in DMAP. Characteristics were included in the catalyst design to allow for the formation of intramolecular cation- $\pi$  interactions, which were studied with fluorescence spectroscopy. In order to achieve the desired catalyst structure, methodology was developed to allow for the facile syntheses of a diverse range of hydrocinnamaldehydes, which were subsequently used in optimised synthetic routes towards the DMAP derivatives.

The synthesised catalysts were studied in the kinetic resolution of secondary alcohols, leading to enantioenrichment of the ester and the remaining alcohol. Attempts were made to probe the pyridinium intermediate using fluorescence spectroscopy, with characteristic cation- $\pi$  fluorescence responses observed when the catalysts were both alkylated and acylated.

*In memory of*

***Gladys Payne and Phineas Samuel Payne***

*You never got the chance to see this or see who I have become but  
you've been with me always.*

# Abbreviations

<b>Ac</b>	Acyl
<b>Aq.</b>	Aqueous
<b>Ar</b>	Aryl
<b>CAL</b>	<i>Candida antartica lipase</i>
<b>CD</b>	Circular dichroism
<b>Conc.</b>	Concentration
<b>C</b>	Conversion
<b>Conv.</b>	Conversion
<b>CuAAC</b>	Copper catalysed azide-alkyne Cycloaddition
<b>CBS</b>	Corey-Bakshi-Shibata
<b>°C</b>	Degrees Celcius
<b><i>dr</i></b>	Diastereomer ratio
<b>DCM</b>	Dichloromethane
<b>DME</b>	Dimethoxyethane
<b>DMAP</b>	Dimethylaminopyridine
<b>DMSO</b>	Dimethylsulfoxide
<b><i>ee</i></b>	Enantiomeric excess
<b>EP</b>	Enantiopure
<b>H<sub>0</sub></b>	Enthalpy
<b>equiv.</b>	Equivalent
<b>Et</b>	Ethyl
<b>e.g.</b>	<i>Exempli gratia</i>
<b>F</b>	Fluorescence
<b>GC</b>	Gas chromatography
<b>G<sub>0</sub></b>	Gibb's free energy
<b>GSK</b>	Glaxo-Smith-Klein
<b>Hex</b>	Hexane
<b>HPLC</b>	High performance liquid chromatography
<b>h/hrs</b>	Hour(s)
<b>i.e.</b>	<i>Id est</i>
<b><sup>i</sup>Pr</b>	Iso-propyl

<b>LG</b>	Leaving group
<b>LDA</b>	Lithium Diisopropylamine
<b>MHz</b>	Mega hertz
<b>Me</b>	Methyl
<b>MW</b>	Microwave
<b>mins</b>	Minutes
<b>M</b>	Molar
<b>mol</b>	Mole
<b>MBH</b>	Morita-Baylis-Hilman
<b>DMF</b>	<i>N,N</i> -dimethylformamide
<b>nm</b>	Nano meters
<b>NBS</b>	<i>N</i> -Bromosuccinamide
<b>NMO</b>	<i>N</i> -Methylmorpholine- <i>N</i> -oxide
<b>NMR</b>	Nuclear magnetic resonance
<b>nOe</b>	Nuclear Overhauser effect
<b>S<sub>N</sub>Ar</b>	Nucleophilic aromatic substitution
<b>ppm</b>	Parts per million
<b>Ph</b>	Phenyl
<b>PCL</b>	<i>Pseudomonas cepacia</i> lipase
<b>PCC</b>	Pyridinium chlorochromate
<b>PDC</b>	Pyridinium dichromate
<b>PPY</b>	4-Pyrrolidinopyridine
<b>rt</b>	Room temperature
<b>Sat.</b>	Saturated
<b>s</b>	Selectivity factor
<b>NaAsc</b>	Sodium ascorbate
<b><sup>t</sup>Bu</b>	Tertiary butyl
<b>TBAF</b>	Tetrabutylammonium fluoride
<b>THF</b>	Tetrahydrofuran
<b>TLC</b>	Thin layer chromatography
<b>TEA</b>	Triethylamine
<b>TMS</b>	Trimethylsilyl or Tetramethylsilane
<b>XRD</b>	X-ray diffraction

# Acknowledgements

I would like to thank my supervisor, Dr John Fossey, for all the fantastic opportunities he has given me over the past four years, his guidance throughout my PhD and his enthusiastic attitude even when times are hard.

The Fossey group members past and present. Especially, Mark Dutton, Rama Byravan, William Brittain, Wenlei Zhai, Xingjian Li, Akina Yoshizawa, Antonio Feula, Yiming Zhao, Glenn Lees, all our Undergraduate students and summer students. My time in the Fossey group wouldn't have been the same without you all.

A massive thanks need to go to my (little) army of proof readers, they are definitely the superstars when it comes to getting a thesis finished. Massive thanks to William Brittain (again!) and Brette Chapin for their speedy reading skills.

Next up is the team of analytical chemists at the University of Birmingham, especially Louise Male, Chi Tsang, Neil Spencer, Peter Ashton, Cécile Stephanie Le Duff and Allen Bowden.

The big ones are my amazing friends and family, I couldn't have done it without you all. Especially my Mom and Dad (Lesley and Andrew) for their support throughout my time at University and for pushing me into higher education from an early age. My Nan and Robert, who have always been there whenever I have needed them, whatever that may be.

I am grateful for funding awarded from organisations including, The University of Birmingham, Engineering and Physical Sciences Research Council, Royal Society of Chemistry and the Society of Chemical Industry.

# Table of Contents

<b>Abstract</b> .....	<b>iii</b>
<b>Abbreviations</b> .....	<b>v</b>
<b>Acknowledgements</b> .....	<b>vii</b>
Table of Contents .....	viii
<b>Introduction</b> .....	<b>1</b>
Nucleophilic (Lewis Base) Catalysis .....	1
4-Dimethylaminopyridine (DMAP) and Related Compounds .....	2
Chiral DMAP Derived Catalysts .....	5
Kinetic Resolution of Secondary Alcohols .....	6
Chiral DMAP Derived Catalysts .....	8
Cation- $\pi$ interactions .....	20
Pre-organised Intramolecular Cation- $\pi$ Stacking .....	22
Intramolecular Cation- $\pi$ Interactions in Non-Restricted Systems .....	23
Cation- $\pi$ Stacking in Catalysis with Chiral DMAP Derivatives .....	24
Summary and Perspective .....	27
<b>Concept &amp; Aims</b> .....	<b>28</b>
<b>Synthesis of Catalyst Core Structure</b> .....	<b>33</b>
Investigated Route 1 .....	33
Investigated Route 2 .....	35
Investigated Route 3 .....	37
Increasing Structural Diversity .....	41
Chiral HPLC Separation of Enantiomers of 60a .....	42
Enantioenriched Catalyst using Asymmetric Synthesis .....	46
Enzymatic Resolution .....	46
Oxidation and Asymmetric Reduction .....	47
Section Summary .....	53
<b>Synthesis of Analogues</b> .....	<b>54</b>
Linker Aromatic Unit Modification .....	55
Hydrocinnamaldehyde Derivatives Synthesis .....	56
Synthesis of DMAP Derivatives with Phenyl Modifications .....	70
Silylated Derivative .....	71
Substitution of Methylene Linker .....	72
Increasing Linker Rigidity .....	74
Section Summary .....	78



<b>Synthesis of 3,5-Disubstituted DMAP Derivatives.....</b>	<b>80</b>
Application of previously developed route.....	81
Lutidine Modifications .....	82
Vilsmeier-Haack Reaction .....	84
Sonogashira Reaction.....	85
Grignard Reaction .....	88
Section Summary .....	90
<b>Catalysis .....</b>	<b>92</b>
Kinetic Resolution of Secondary Alcohols.....	93
Optimisation of Catalysis Conditions .....	94
Catalyst Comparison and Summary .....	111
<b>Fluorescence .....</b>	<b>113</b>
<b>Conclusion .....</b>	<b>118</b>
<b>Experimental .....</b>	<b>123</b>
General Information .....	123
Synthesis of Catalyst Core Structure.....	124
Synthesis of Analogues .....	137
Witting By-Product.....	137
Heck Cross-Coupling to Synthesise Cinnamaldehydes 72d,e,h,p,q .....	137
Synthesis of hydrocinnamaldehyde derivatives <sup>94</sup> .....	140
Knoevenagel Condensation to Synthesise 75b-o .....	140
Olefin Reduction to Synthesise 76b-h,j-l,n,o.....	147
Hydrolysis & Decarboxylation to Synthesise 76b-h,j,l,n,o .....	154
Carboxylic Acid Reduction to Synthesise 78b-e,g,h,j,l .....	159
Swern Oxidation to Synthesise 74b,d,e,g,h,j .....	162
Synthesis of 60b,d,e,g,h, 82, 87 and 90 .....	165
Synthesis of 51b,d,e,g,h, 84, 86 and 89. ....	171
Synthesis of 50b,d,e,g,h, 81, 85 and 92 .....	176
Synthesis of 3,5-Disubstituted DMAP Derivatives .....	181
Kinetic Resolution of Secondary Alcohols .....	194
GC Parameters .....	198
Gas Chromatography Correction factors and Retention Times .....	199
<b>Appendix .....</b>	<b>200</b>
HPLC Data.....	200
HPLC separation of R and S 60a·HCl.....	200
HPLC separation of R and S 60b .....	200

HPLC separation of R and S 60d .....	201
HPLC separation of R and S 60e .....	201
HPLC separation of R and S 60g .....	202
HPLC separation of R and S 82 .....	202
HPLC separation of R and S 90 .....	203
X-Ray Structures.....	204
Compound rac-60a.....	204
Compound (S)-60a .....	209
Compound (S)-51a .....	213
Compound 67 .....	217
Compound 82.....	224
Compound 87 .....	228
Compound 126.....	235
<b>References.....</b>	<b>241</b>

# Introduction

## Nucleophilic (Lewis Base) Catalysis

Catalysts are fundamental to chemistry, used in a variety of applications for a large number of chemical transformations to provide materials that were previously inaccessible. Catalysts are used to accelerate the rate of reaction and in effect can make a previously impossible reaction (due to the rate being painfully slow) possible through a large rate acceleration.

Nucleophilic catalysis, or more accurately catalysis utilising a Lewis base leading to the formation of a Lewis adduct as a reaction intermediate, is currently one of the less thoroughly investigated forms of catalysis.<sup>1-3</sup> It has been suggested that this is because of the lack of potential Lewis acidic sites in organic molecules and the limited opportunity for valence expansion at carbon centres.<sup>2</sup>

Catalysts can come in many shapes, sizes and compositions, however there are some key properties that a catalyst should adhere to. In terms of Lewis base catalysis these guidelines were concisely summarised by Denmark as: <sup>2</sup>

*“Lewis base catalysis is the process by which an electron pair donor increases the rate of a given chemical reaction by interacting with an acceptor atom in one of the reagents or substrates. The binding event may enhance either the electrophilic or nucleophilic character of the bound species. Furthermore, the Lewis base should not be consumed or altered during the course of the reaction—a hallmark of any catalytic process”*

Pyridine was an early example of a nitrogen-containing reaction promoter for acylation reactions which has led to a considerable amount of research into related compounds and their catalytic activity.<sup>4</sup>

## 4-Dimethylaminopyridine (DMAP) and Related Compounds

Pyridine (**1**) was an early example of a nitrogen-containing reaction promoter, reported in 1898 by Einhorn and Hollandt, used as a catalyst for the acetylation of phenols and alcohols.<sup>4</sup> In hindsight it only exhibits a relatively small rate increase compared with the uncatalysed reaction and the substrate scope was limited. These limitations were eventually overcome in 1967, six decades later, by Litvinenko and Kirichenko, who reported the use of 4-dimethylaminopyridine (DMAP, **2**) for the benzoylation of anilines.<sup>5</sup> Use of DMAP as a catalyst led to a 15000 fold increase in rate compared to use of catalytic triethylamine and a 6000 fold increase over pyridine (**1**).<sup>5</sup>

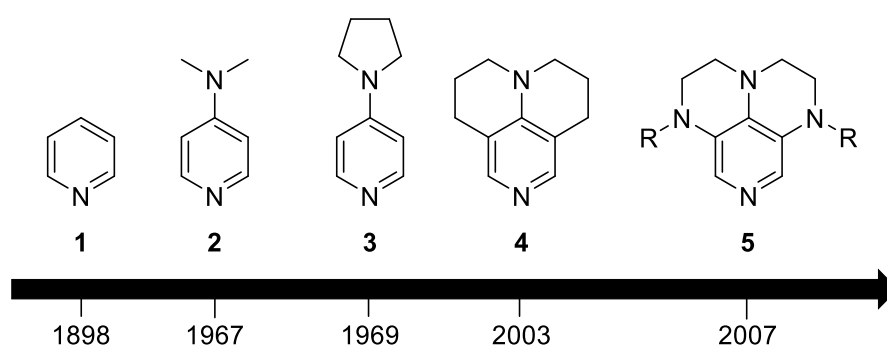


*Figure 1 – Development timeline of key pyridine containing nucleophilic catalysts*

The use of DMAP did not become widespread until a simple large scale synthesis of the catalyst was developed (Figure 2).<sup>6-7</sup> This meant that, as well as being easy to handle and highly active in a range of reactions (Figure 4), DMAP was now readily accessible.<sup>8</sup>

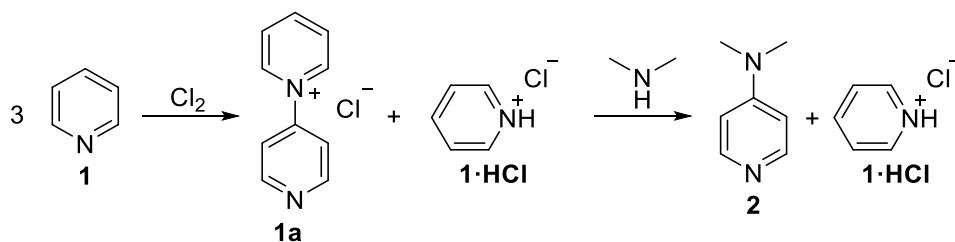


*Figure 2 - Large scale synthesis of DMAP*

Since 1967 a range of DMAP related catalysts have been reported (Figure 1).<sup>4</sup> In 1969 Steglich and Höfle reported 4-pyrrolidinopyridine (PPY, **3**) to be a superior catalyst to DMAP, giving a further increase in the rate of the acetylation of oxazolinones.<sup>9</sup> This led to the syntheses of numerous 4-alkylaminopyridines, but none could surpass the high catalytic activity of PPY in both acylation reactions and the Steglich rearrangement.<sup>10</sup> In 1978 this led to Steglich, Höfle and Vorbrüggen stating that they felt that it was unlikely that a better acyl transfer reagent than PPY would be found because a further increase in the basicity of pyridine was hardly possible.<sup>10</sup> However, in 2003 Steglich had to retract the previous statement due to his development of a tricyclic DMAP analogue (**4**) which surpassed PPY as a nucleophilic catalyst.<sup>11</sup> This was due to the restricted rotation of the dialkyl nitrogen giving a superior p- $\pi$  overlap and therefore greater facile formation of the acyl-pyridinium reactive intermediate (additionally, the electron donating properties of the alkyl groups at the 3-position of the pyridine giving further stabilisation).<sup>11</sup>

In 2007 another small increase in catalytic activity was achieved by the introduction of two additional alkylamines at the 3-position of the pyridine (**5**).<sup>12</sup> This could be explained by the electron donating properties of the additional amines, which further stabilise the acyl-pyridinium intermediate. An additional benefit of these derivatives is that diversity can be introduced by altering the alkyl substituents on these amines.<sup>12</sup>

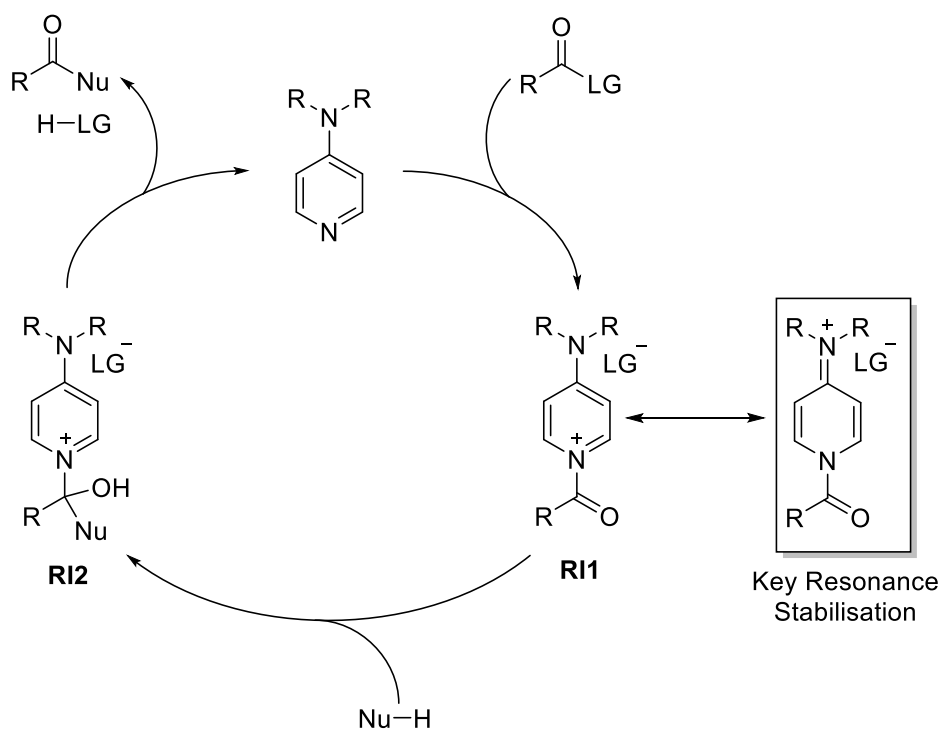


*Figure 3 - Catalytic cycle for DMAP and related compounds*

The catalytic cycle for acylation reactions using DMAP and its related compounds as a catalyst are analogous to one another (Figure 3) and, as mentioned previously, stabilisation of the acyl-pyridinium reactive intermediate (**R11**) contributes towards the improvements in reactivity of 4-aminopyridines.

The catalytic cycle shows that nucleophilic attack of the carbonyl and expulsion of the leaving group (LG), which can include but is not limited to halides, triflates and carboxylates, leads to the formation of the acyl-pyridinium species (**R11**), which is stabilised by the key resonance form shown. This is followed by nucleophilic attack on the activated carbonyl to afford the tetrahedral intermediate (**R12**), which will then eliminate the pyridinium leading to the reformation of the carbonyl and regeneration of the catalyst.

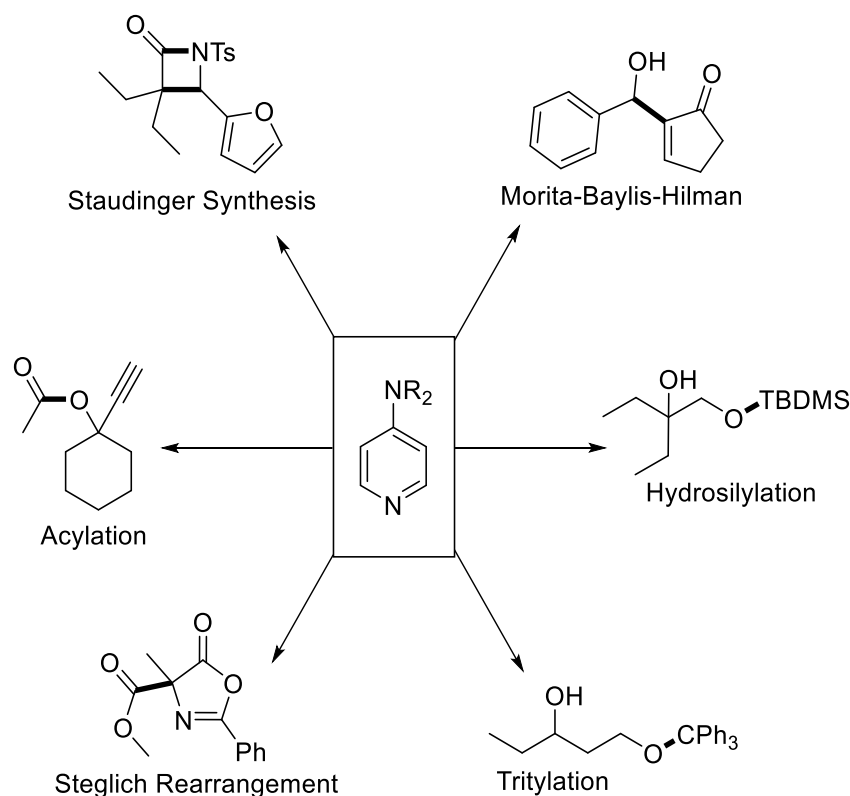


*Figure 4 - Selection of reactions catalysed by DMAP and PPY with bonds formed in bold*

The most widely reported pyridine based catalysts in literature to date are DMAP and PPY and over the last half century these have been used in a number of reactions some of which are shown in Figure 4.<sup>1-2,10, 13-16</sup> Points of interest from these are that DMAP can be used for regioselective silylations and tritylations, as well as the acylation of tertiary alcohols, which is difficult without a catalyst present.<sup>10, 13, 15</sup>

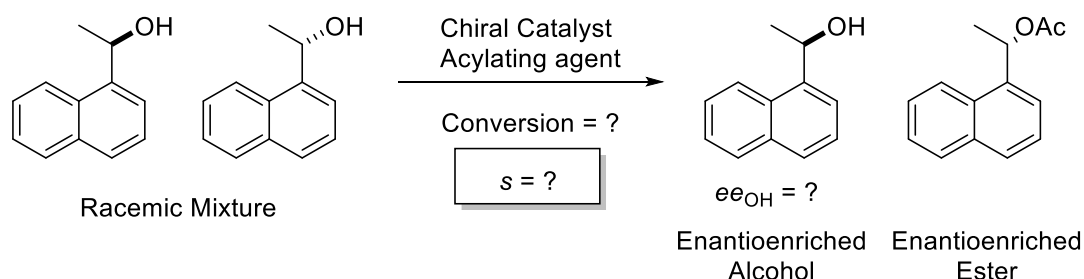
## Chiral DMAP Derived Catalysts

When considering the products of the reactions in Figure 4, there are numerous applications for asymmetric catalysis. These can include the kinetic resolution of secondary and tertiary alcohols and amines via stereoselective acylation, silylation or tritylation.<sup>10, 13-15</sup> Additionally, there are opportunities for stereoselective Morita-Baylis-

Hilman (MBH) reactions, Steglich rearrangements and Staudinger syntheses via the introduction of a defined stereocentre into the products formed.<sup>17-18</sup>

## Kinetic Resolution of Secondary Alcohols

The kinetic resolution of secondary alcohols can be viewed as the benchmark reaction for the effectiveness of asymmetric DMAP derivatives. The reaction takes a racemic mixture of a secondary alcohol and aims to use a catalyst to acylate one enantiomer of a racemic mixture faster than the other. The chromatographic separation of enantioenriched alcohol and enantioenriched ester can then be achieved. This difference in rate is possible because of the formation of a diastereomeric transition state between the single enantiomer acyl-pyridinium catalyst and the secondary alcohol enantiomers leading to a matched and mis-matched pair of diastereoisomers. An effective catalyst will show an energetically more favoured transition state leading to a difference in the rate of reaction. A theoretical example of this reaction is shown in Scheme 1.<sup>19</sup>



*Scheme 1 - General scheme for the kinetic resolution of a secondary alcohol*

The effectiveness of a catalyst at carrying out this reaction is measured by a selectivity factor ( $s$ ). The selectivity factor is the ratio of the rates of reaction of each individual enantiomer (Equation 1) giving a number that must be greater than or equal to 1. If  $s$  is 1 then both enantiomers are reacting at the same rate and a number greater than one shows that catalyst is reacting preferentially with one enantiomer.<sup>20</sup>



$$S = \frac{\text{Larger rate constant}}{\text{Smaller rate constant}} = \frac{\ln[(1 - ee_{OH})(1 - C)]}{\ln[(1 + ee_{OH})(1 - C)]}$$

*Equation 1 - Selectivity factor calculation*

As the rate of reaction for each enantiomer can be troublesome to determine experimentally an equation has been derived by Kagan which relates the *ee* of the recovered alcohol and the conversion to the ester with selectivity factor (Equation 1) making the determination of *s* more rapid.<sup>20</sup>

The above derived equation can be plotted graphically demonstrating the *ee* change with respect to conversion (Figure 5). Furthermore, the conversion and *ee* can be determined for a range of selectivity factors. For example, a selectivity factor of 20 would require the reaction to reach 65% conversion to isolate >99% *ee* alcohol giving a 35% yield. If the ideal case is considered where an alcohol of >99% *ee* is recovered at 50% conversion then theoretically the selectivity factor would need to be in excess of 1057.<sup>21-22</sup>

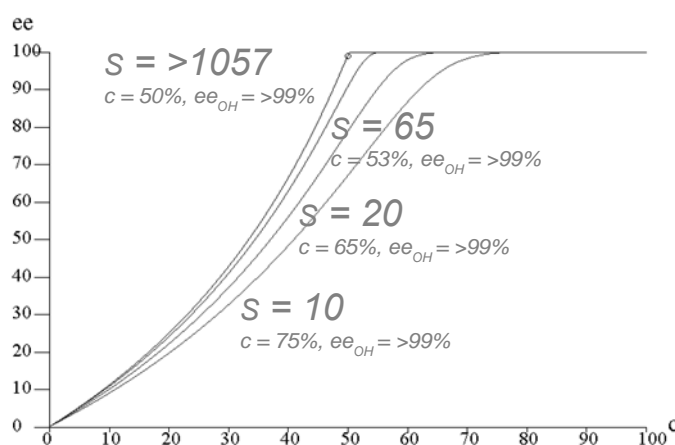
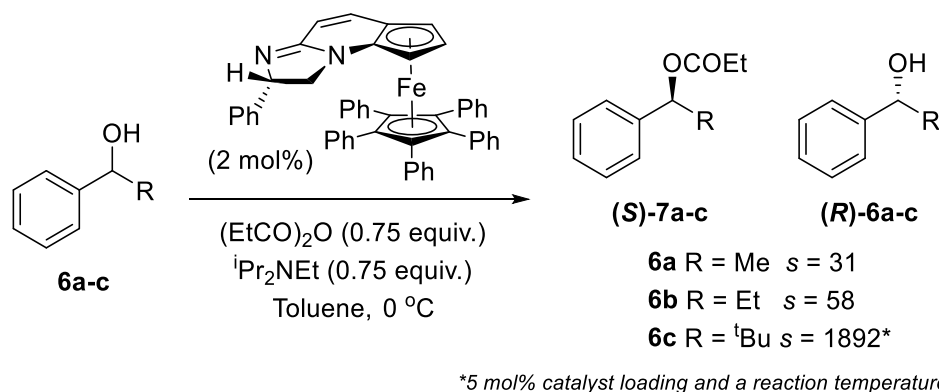


*Figure 5 - Graphical representation of selectivity factor (s) created in online selectivity factor calculator by Goodman et al.<sup>21-22</sup>*

Numerous catalysts have been reported which can carry out the kinetic resolution of secondary alcohols, however selectivity factors reaching values greater than 1000 are rare. When considering enzymes, which are generally seen to be superior to synthetic

catalysts at reactions such as this, selectivity factors can be as high as 1160 or 98 for *Pseudomonas cepacia* lipase (PCL) or *Candida antarctica* lipase (CAL) respectively, when studies in the resolution of 1-phenylethanol using 1-phenylvinyl acetate as the acylating agent.<sup>23</sup>



*Scheme 2 - Secondary alcohol kinetic resolution using a ferrocene-based planar chiral acyl transfer catalyst (Fc-PIP).*

An example of a non-enzymatic catalyst capable of carrying out the kinetic resolution of secondary alcohols is shown in Scheme 2. This system has reported large *s* factors compared to other synthetic catalysts in this type of resolution with values as high as 1892, albeit at lower temperatures, for the resolution of 2,2-dimethyl-1-phenylpropan-1-ol (**6c**).<sup>24</sup> It has also been used for sterically hindered and bulky secondary alcohols obtaining selectivity factors as high as 46.<sup>25</sup> Furthermore, recent advances with this system have led to the removal of the ferrocene moiety and replacement with extend  $\pi$ -systems, introducing axial chirality, which has achieved impressive selectivity factors of greater than 400.<sup>26</sup>

## Chiral DMAP Derived Catalysts

Chiral DMAP derivatives utilising a range of methods to introduce chirality into the system have been reported, a selection of which are shown in Figure 6.

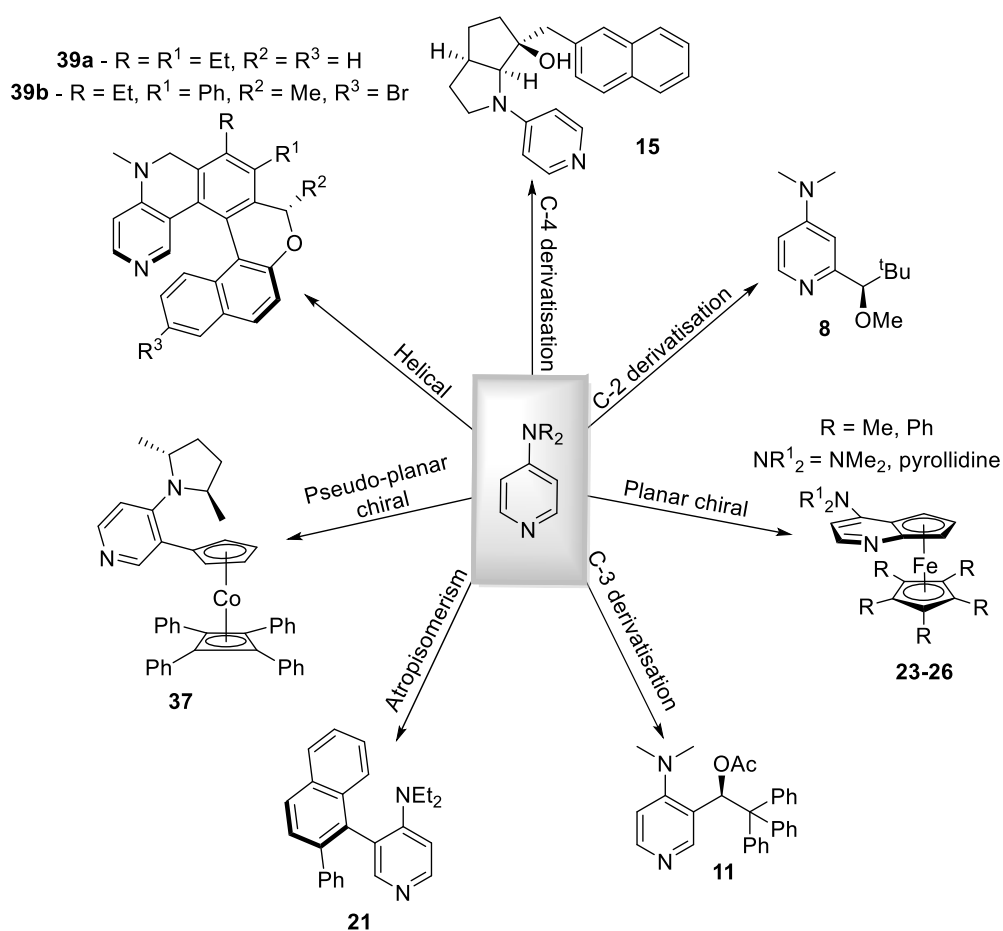
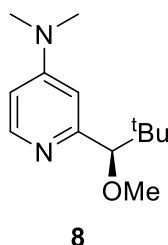


*Figure 6 - Selection of asymmetric DMAP related catalysts*

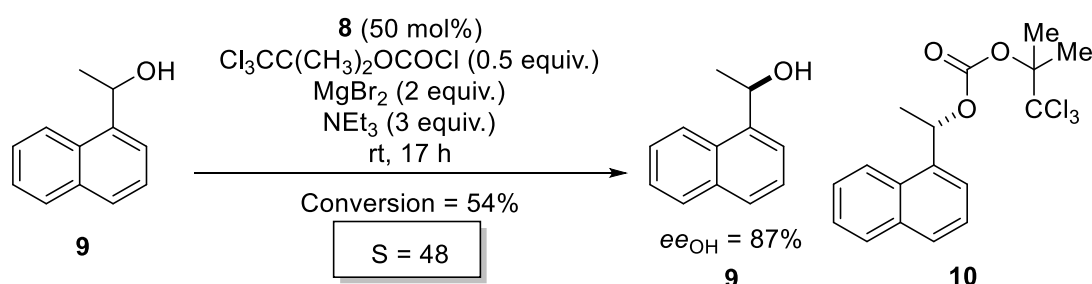
In order to utilise DMAP derivatives in asymmetric catalysis a form of chirality needs to be introduced into the catalyst and the catalyst need to be obtained in a non-racemic form. The most common way to do this has been by introducing a stereocentre into the catalyst, which normally would cause either a steric clash or have a directing effect with the substrate.<sup>27-28</sup> Alternative methods have utilised atropisomerism, planar chirality and helical chirality.<sup>18, 27, 29</sup> Below are some examples of the more successful asymmetric DMAP and related catalysts. Although the following is not an exhaustive review of the applications of asymmetric DMAP derivatives, it does give an indication of scope. Some of the most popular substrates will be focused on, for example 1-(1-naphthyl)ethanol,

however it is again important to note that a larger range of substrates may have been studied.

### Pyridine 2-Position Derivatisation



Vedejs reported one of the earliest asymmetric DMAP derived catalysts in 1996, which was derivatised at the 2-position of the pyridine and contained a defined stereocentre.<sup>30</sup> This was easily synthesised utilising a pyridine nitrogen directed lithiation followed by trapping with the corresponding acid chloride.<sup>30</sup> The ketone was then reduced asymmetrically and methylated to afford **8** with an *ee* of greater than 99%.<sup>30</sup> This catalyst could be used for the kinetic resolution of secondary alcohols, obtaining conversions in the region of 20-44% and *ee*'s of up to 90%, however reaction times were long (usually around 48 hours) and in some cases pseudo-stoichiometric amounts of catalyst were needed (Scheme 3).<sup>30</sup>

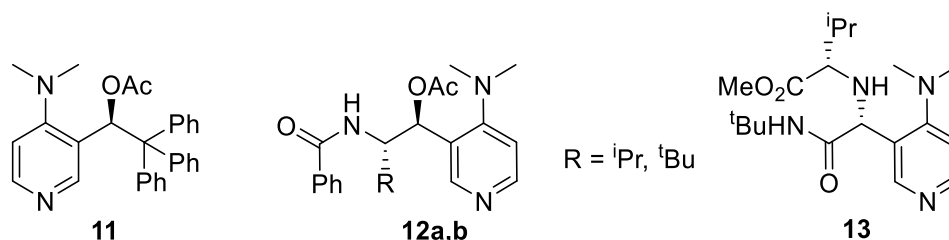


*Scheme 3 - Kinetic resolution of 1-(1-naphthyl)ethanol using 8*

The main limitation of this catalyst is that it is less effective as substituents become larger, causing reductions in yield and lowering of *ee*'s, and therefore exceptionally long reaction

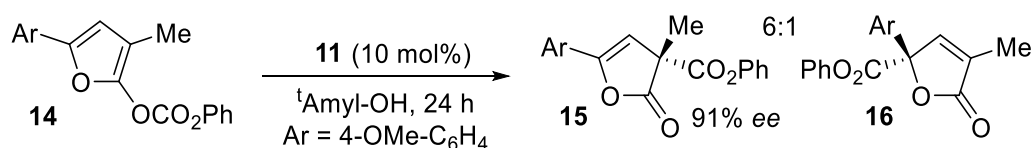
times are need.<sup>30</sup> This is due to the steric clash between the tert-butyl and methoxy groups and the substrates which are being resolved.

### Pyridine 3-Position Derivatisation



As mentioned above the original C-2 derivatised DMAP catalyst encountered problems due to steric clashes with the substrates. Therefore, in order to minimise this, derivatisation at the 3-position of the pyridine seemed the most attractive alternative, however the key problem can be that the chiral information needs to be relayed over a larger distance.<sup>8, 31</sup> This drawback can however be resolved by using bulkier groups (such as CPh<sub>3</sub>, **11**) which can more effectively influence the environment around the pyridine nitrogen.<sup>8, 31-32</sup>

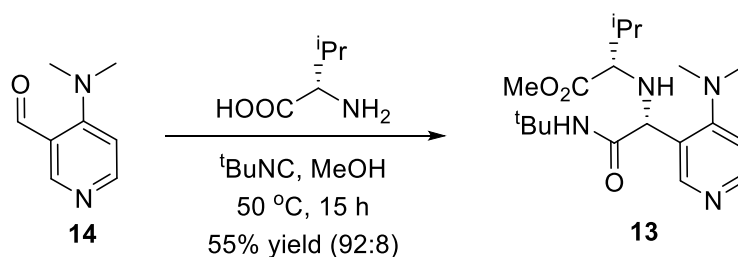
Catalyst **11** has been shown to be active in the Steglich rearrangement, the carboxyl migration of 3-methyl-5-arylfurans (Scheme 4) and 3-substituted 2-alkoxycarbonyloxyindoles.<sup>8, 31</sup> For the Steglich rearrangement *ee*'s between 73 and 95% were obtained as well as yields as high as 99%. However, the catalyst was not suitable for the rearrangement of indolyl acetates and carbonates which led to a redesign of the catalyst.<sup>33</sup>



*Scheme 4 - 3-Methyl-5-arylfuran enol carbonate rearrangement*

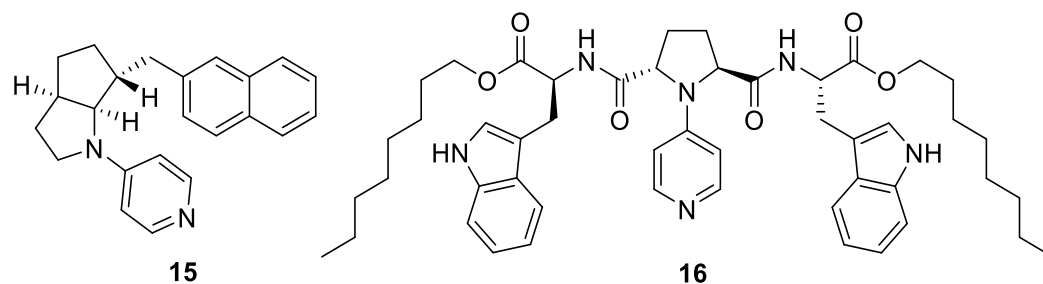
The structure of **11** was difficult to derivatise, as there are not many sites where modifications can be made. Therefore, Vedejs redesigned the catalyst to give **12** which allowed for a greater range of modification in order to tune the catalyst for the reaction being conducted.<sup>33</sup> Additionally, the core chirality is amino acid derived which minimises complexity and minimised the purification of diastereoisomers. The tert-butyl derivative was the most effective for the enantioselective rearrangement of indolyl acetates and carbonates and in most cases gave yields and *ee*'s greater than 90%.<sup>33</sup>

Derivative **13**, reported in 2015 by Suga and co-workers, has been applied to the kinetic resolution of secondary alcohols, obtaining a selectivity factor of 8.1 for the resolution of 1-phenylethanol, and also in the enantioselective Steglich rearrangement. Although enantioselectivities for both of these reactions were low when compared to other chiral DMAP derivatives, the synthesis of the catalyst is interesting. It has been synthesised in one step from commercially available starting materials in good enantiopurity (Scheme 5). Furthermore, because the chirality is derived from amino acids a library of catalysts can be readily synthesised and catalyst chiral resolution is not required.<sup>34</sup>

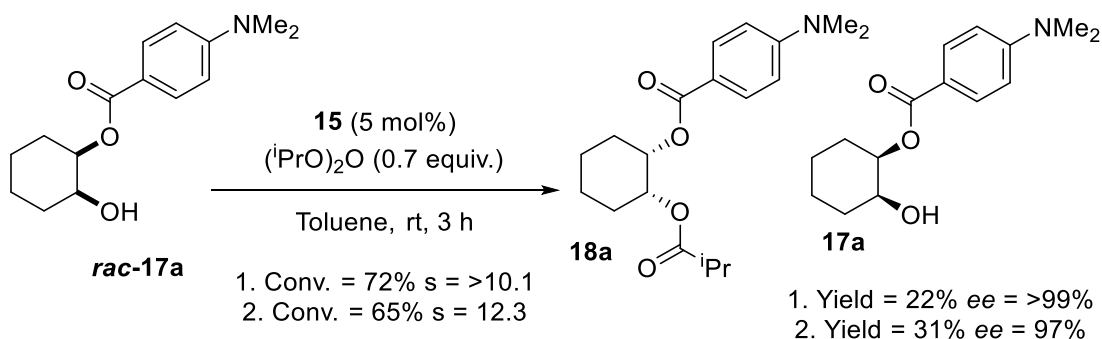


*Scheme 5 - Synthesis of catalyst 13*

### Pyridine 4-Position Derivatisation



The first chiral DMAP catalyst with derivatisation at the pyridine 4-position (**15**) was reported by Fuji, it was proposed that this design would place the aromatic substituent over the pyridine ring due to the stereochemistry of the carbon it is attached to.<sup>35</sup> Additionally, the directing effect may have been further enhanced due to a suspected cation- $\pi$  interaction between the acyl-pyridinium intermediate and the electron rich aromatic group.<sup>35</sup> A representative example of a secondary alcohol kinetic resolution for this catalyst can be seen in Scheme 6.

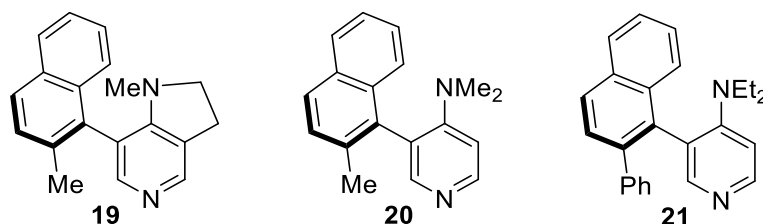


*Scheme 6 - Kinetic resolution of a cyclohexanediol derivative with 15*

In 2007 Kawabata reported a  $C_2$  symmetric C-4 substituted PPY derivative (**16**) with a niche application.<sup>28</sup> It was able to carry out the acylation of monosaccharides regioselectively and chemoselectively due to the indole side arms being able to conduct substrate recognition, thereby directing the monosaccharide to the active site.<sup>28</sup> The alkyl chains were used to aid solubility and the PPY catalyst core was used due to its increased activity compared to DMAP and that the single diastereoisomer can be readily synthesised from

proline.<sup>28</sup> Both  $C_2$  symmetric diastereoisomers were synthesised for the indole carbon, however **16** gave the best results when screened for monosaccharide acylation.<sup>28</sup> This catalyst could obtain the 4-position monoacylation of some sugars with yields of 99% and regioselectivity of greater than 99%.<sup>28</sup>

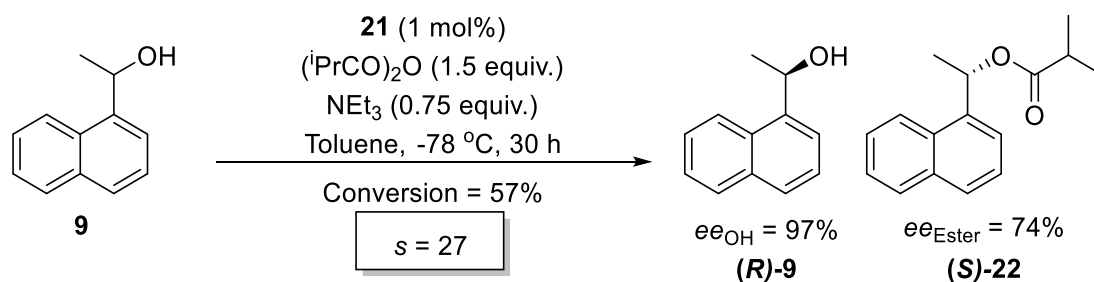
### *Atropisomerism*



The initial design of atropisomeric DMAP derivatives by Spivey and co-workers was based on **19**, which used a conformationally locked 4-position amine.<sup>29</sup> This meant that the aromatic substituents at the 3-position of the pyridine exhibits restricted rotation around the Ar-Ar bond leading to two possible conformers.<sup>29</sup> This restriction was induced by a steric clash between the methyl and the aromatic 3-position derivative. However when this aromatic substituent is a phenyl no atropisomeric effects are observed.<sup>36</sup> Additionally, when using the 4-dimethylaminopyridine equivalent (**20**), atropisomeric effects are observed, which is a much simpler catalyst to synthesise, however for **19** and **20** some racemisation was observed during chiral HPLC separation.<sup>36</sup>

A large selection of derivatives have been synthesised based on this core structure, such as regioisomers and a range of R groups and these have been studied in the kinetic resolution of secondary alcohols.<sup>29, 36-37</sup> It was however hypothesised that a greater left to right differentiation was needed in order to increase selectivity, which was introduced using the 4- diethylaminopyridine (**21**).<sup>37</sup>

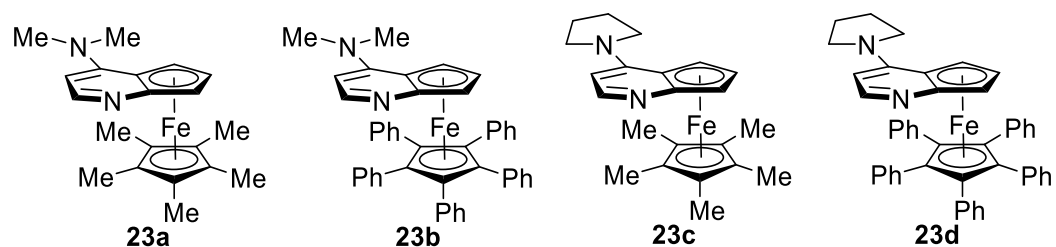




*Scheme 7 - Kinetic resolution of 1-(1-naphthyl)ethanol using 21*

When using the optimised catalyst (**21**) the kinetic resolution of 1-(1-naphthyl)ethanol could be carried out at 1 mol% catalyst loading which gave a conversion of 56% when using isobutyric anhydride and an *ee* for the acetate of 73.7% and 97.0% for the remaining (*R*)-1-(1-naphthyl)ethanol was obtained (Scheme 7).<sup>37</sup> This means that this resolution had a selectivity factor of 27 and additionally, 96% of the catalyst could be recovered with an *ee* of greater than 99%.<sup>37</sup> In contrast, when this resolution was carried out with **19** the selectivity factor was 1.1.

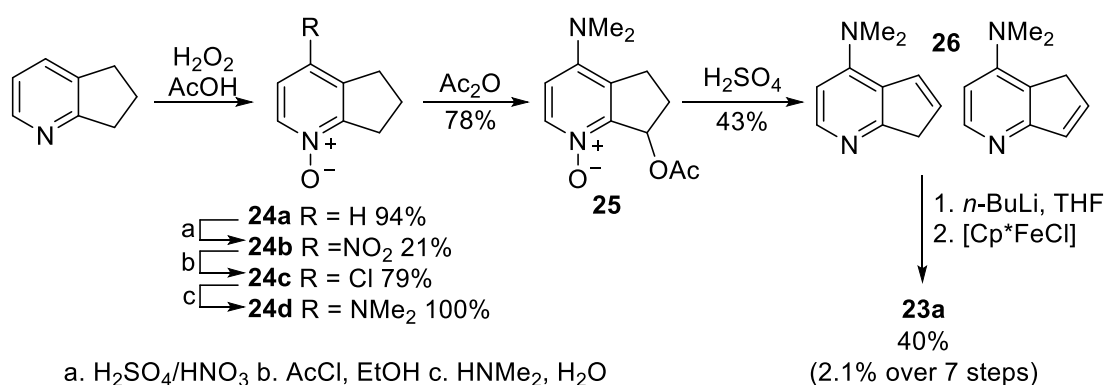
#### *Planar Chiral*



Arguably, the most well known of all asymmetric DMAP based catalysts were first reported by Fu in 1996.<sup>38</sup> The key features of the catalyst are they attempted to remove the symmetry of DMAP by using a 2,3-cyclopentadiene substituent in order to remove the left to right symmetry and the formation of a substituted ferrocene using this cyclopentadiene to remove facial symmetry.<sup>38</sup> They have been synthesised in both the dimethylamino and pyrrolidino forms and methyl and phenyl groups have also been used as cyclopentadiene substituents.<sup>38-39</sup> Rather than using central chirality (such as the incorporation of a

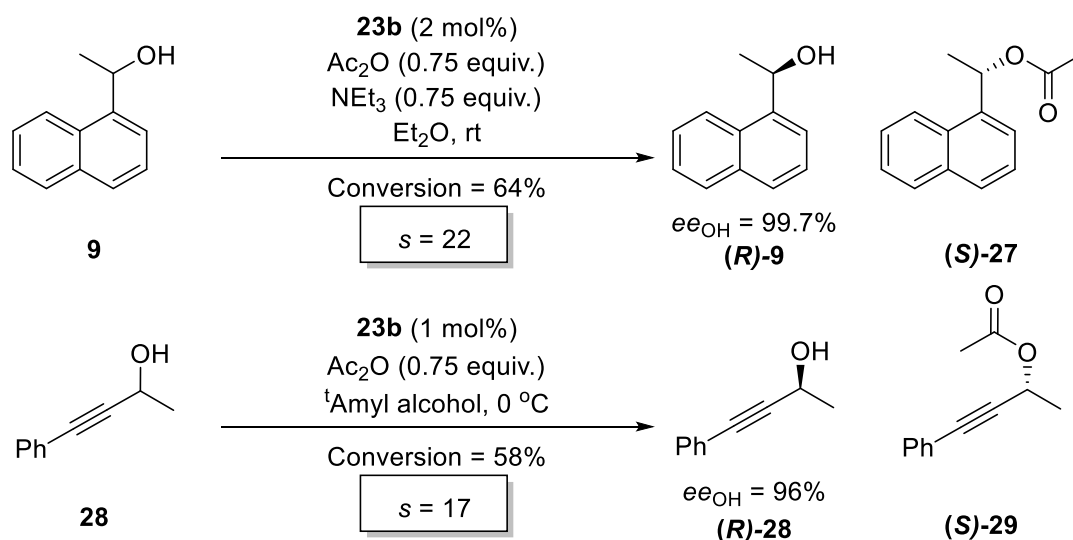
stereocentre), Fu's catalyst incorporates planar chirality which was a game changing moment in asymmetric DMAP catalysis as previously only installation of a stereogenic centre near the catalytically active site had been investigated with limited success.

The synthesis of Fu's planar chiral DMAP derivative is shown in Scheme 8, a total of seven synthetic steps are required in order to obtain racemic catalyst which was then resolved using chiral HPLC. Pyridine-*N*-oxide **24a** was synthesised from 6,7-dihydro-1,5-pyridine in 94% yield using a literature procedure.<sup>40</sup> *N*-Oxide **24a** was then taken through a series of aromatic substitution reactions to obtain the 4-dimethylamino derivative **24d** which was subsequently deprotected and the acetate group installed in one pot to afford **25**. An acid catalysed elimination process was used to give olefin **26** as a mixture of regioisomers, which was taken through to the synthesis of catalyst **23b** via a deprotonation of the cyclopentadiene moiety with <sup>n</sup>BuLi and complexation with a preformed Cp\*FeCl.<sup>38</sup> This could be viewed as a lengthy synthesis for an asymmetric catalyst (7 steps) and the final product is obtained in a low overall yield (2.1%). To obtain a single enantiomer the compound was resolved using preparative HPLC with a chiral stationary phase, further lowering the final yield for an enantiopure catalyst.



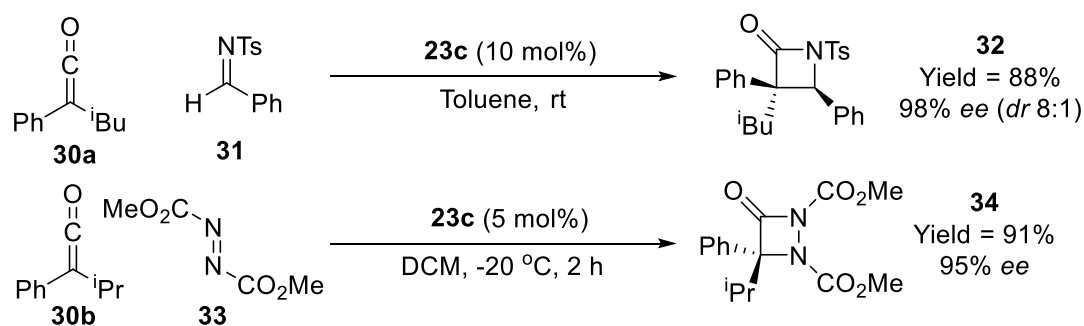
*Scheme 8 - Synthesis of Fu's planar chiral DMAP derivative 23a*

This family of catalysts has proven to be highly versatile, being used for the kinetic resolution of arylalkylcarbinols, propargylic and allylic alcohols, diols and amines (Scheme 9).<sup>38-39, 41-43</sup>



*Scheme 9 - Kinetic resolution of 1-ethanol derivatives and propargylic alcohols using planar chiral catalyst 23b*

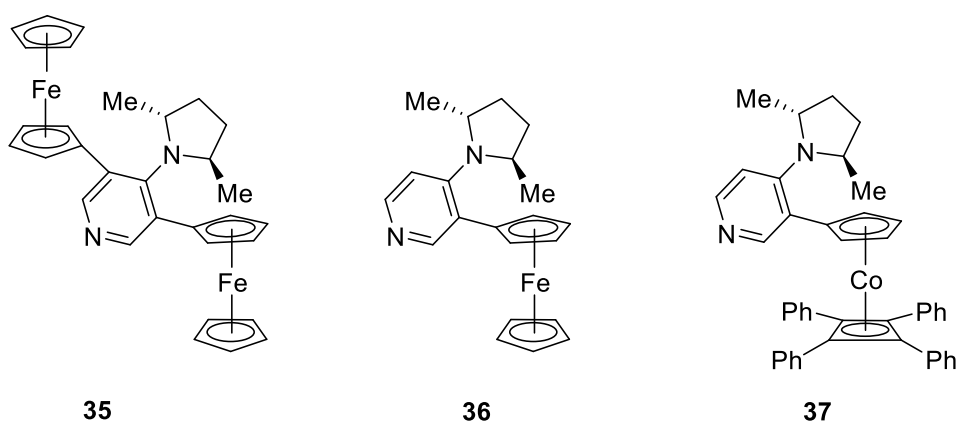
Although the preliminary report of this family of catalysts in 1996 reported a modest selectivity factor of 6.5 for the resolution of 2-phenylethanol the methodology was rapidly improved in several follow up reports.<sup>38</sup> Investigation into different catalyst designs, acylating agents and reaction conditions such as solvent and base meant that these reaction could obtain selectivity factors between 20 and 40 for a large number of substrates.<sup>39, 42-43</sup>



*Scheme 10 - Planar chiral catalyst 23c carrying out the Staudinger synthesis of  $\beta$ -lactams (top) and a [2+2] cycloaddition to form aza- $\beta$ -lactams (bottom)*

Additionally, they have proven effective for the Staudinger synthesis of  $\beta$ -lactams, [2+2] cycloadditions to form aza- $\beta$ -lactams, addition of amines to ketenes to form amines, Steglich rearrangements and the C-acylation of silyl ketene acetals, all of which were successfully carried out asymmetrically.<sup>16, 17, 28, 31</sup> This has meant that for the last decade the Fu catalysts have been used as the benchmark for most other asymmetric DMAP catalysts, however no other has yet to match the great versatility of this design in terms of reactivity.

### *Pseudo Planar Chiral*



First reported by Richards in the mid-2000s, this class of catalyst has its core based on Fu's catalyst design, where a ferrocene (or cobalt metallocene) unit is incorporated as a 3-position substituent of DMAP.<sup>44-45</sup> However, in these examples the ferrocene or cobalt metallocene has free rotation and its conformation is driven *via* relay of stereochemical information from the dimethylpyrrolidino substituent at the 4-position.<sup>44-45</sup>

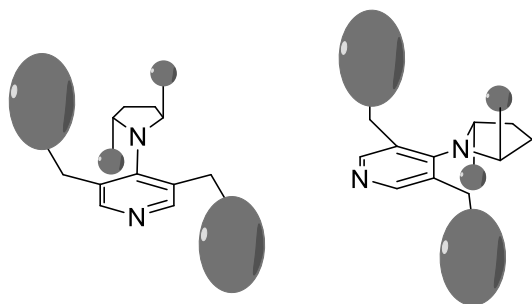
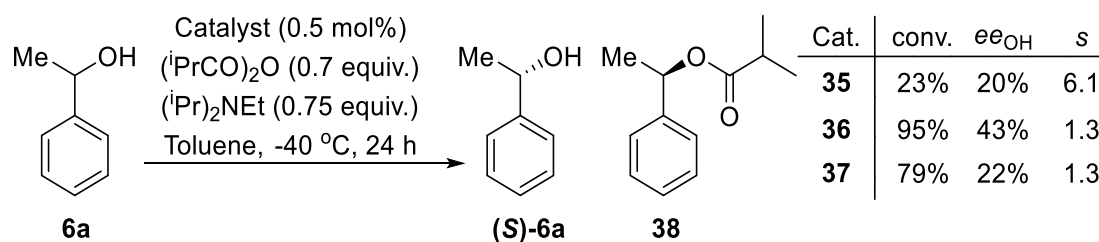


*Figure 7 - Minimal energy conformation of Me<sub>2</sub>PPY-Metallocene catalyst due to steric interactions*

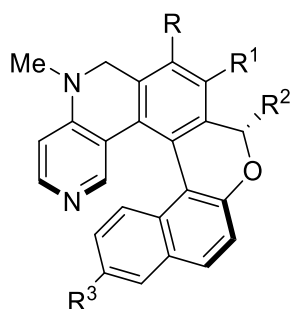
This relay of information is made possible by the steric clashes between the two methyl groups at the 4-position and the metallocene groups at the 3-position (Figure 7), this is interesting as the relatively small methyl group can induce a substantial chiral environment around the pyridine nitrogen.<sup>44-45</sup>



*Scheme 11 - Kinetic resolution of 1-phenylethanol using catalysts 35, 36 and 37*

Although **35**, **36** and **37** are related to Fu's design, they do not appear to be as successful in the kinetic resolution of secondary alcohols, where the C<sub>2</sub> symmetric catalyst **35** gave higher selectivity (*s* = 6.1) but low conversions (23%) for 1-phenylethanol.<sup>44-45</sup> On the other hand **36** gives high conversion (95%) but the selectivity of the catalyst is low (*s* = 1.3) rendering it unsuitable for kinetic resolutions. There have been some promising results when used for the Steglich rearrangement, but these are still not at the level of some of the other asymmetric DMAP catalysts.<sup>44-45</sup>

### Helical

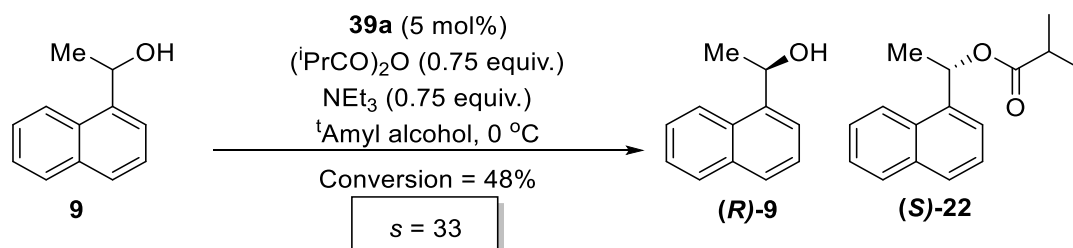


**39a** - R = Et, R<sup>1</sup> = Et, R<sup>2</sup> = H, R<sup>3</sup> = H

**39b** - R = Et, R<sup>1</sup> = Ph, R<sup>2</sup> = Me, R<sup>3</sup> = Br

Carbery reported catalysts composed of DMAP in helicene frameworks which were first reported in 2011 with further derivatisations reported in 2012.<sup>27, 46</sup> When synthesising **39a** the catalyst requires resolution, whilst due to **39b** containing a defined

stereocentre at R<sup>2</sup>, it can be synthesised with a *dr* of 95:5 favouring the above shown conformation.<sup>27, 46</sup> Additionally the incorporation of a bromide at R<sup>3</sup> allows for a great range of diversity to be installed using traditional cross-coupling techniques.<sup>27</sup>



*Scheme 12 - Kinetic resolution of 1-(1-naphthyl)ethanol using catalyst 39a*

To date these catalysts have only been used for the kinetic resolution of secondary alcohols, however the results from these reactions appear promising, achieving selectivity factors as high as 116 for 1-(9-anthryl)ethanol and activity using a large range of secondary alcohol substrates.<sup>27, 46</sup>

## Cation- $\pi$ interactions

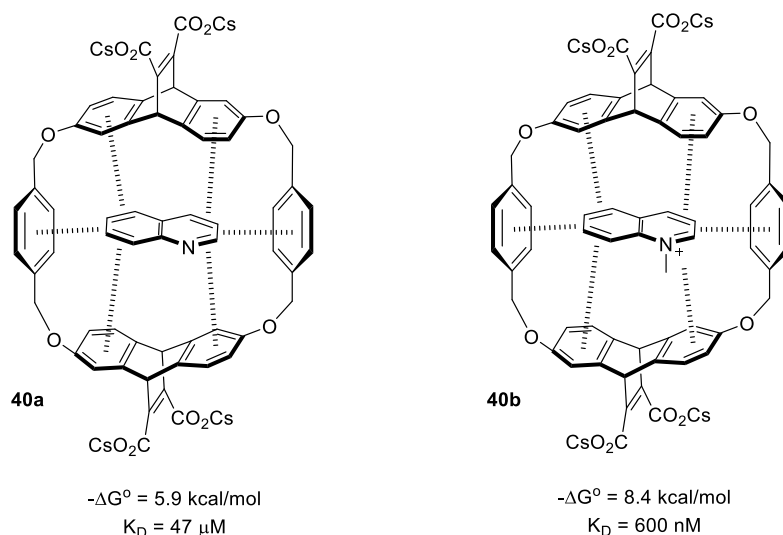


*Figure 8 - Host-guest system of quinoline and N-methylquinolinium with a host cyclophane*

The term 'cation- $\pi$ ' interaction was first introduced by Dougherty when discussing the interactions of quinolone (**40a**) and *N*-methylquinolinium (**40b**) guests with a host

cyclophane (Figure 8), or more generally the term describe the stabilisation of a positively charged species by an electron rich  $\pi$ -system.<sup>47-49</sup> He determined that, although the quinolinium species should be better solvated in aqueous media than quinoline, stronger binding was observed for the ammonium salt.<sup>49</sup> This therefore was not simply a hydrophobic effect, such as is observed with a pyrene guest, extra stabilisation was being gained due to the positive charge of the quinolinium.<sup>49</sup>

Dougherty's example was not the first observation of a cation- $\pi$  interaction, previous work has been carried out on gas phase measurements of the interaction of potassium with benzene recording a  $-\Delta G^0_{298}$  value of 11.9 kcal/mol ( $-\Delta H^0 = 19.2$  kcal/mol) compared to 11.5 kcal/mol for water ( $-\Delta H^0 = 17.9$  kcal/mol).<sup>50</sup> Later work also demonstrated that as the cation size decreased an increase in bind energies was observed.<sup>51-52</sup> Additionally, binding of ammonium species in the gas phase was investigated by Deakyne showing binding energies ( $-\Delta H^0$ ) in the region of 15 kcal/mol.<sup>53</sup> These tantalising results in the gas phase along with evidence of similar results in aqueous media have led to extensive investigations into cation- $\pi$  interactions in several areas of chemistry including asymmetric synthesis, catalysis, sensing and biomedical applications.<sup>47, 54-55</sup>

## Pre-organised Intramolecular Cation- $\pi$ Stacking

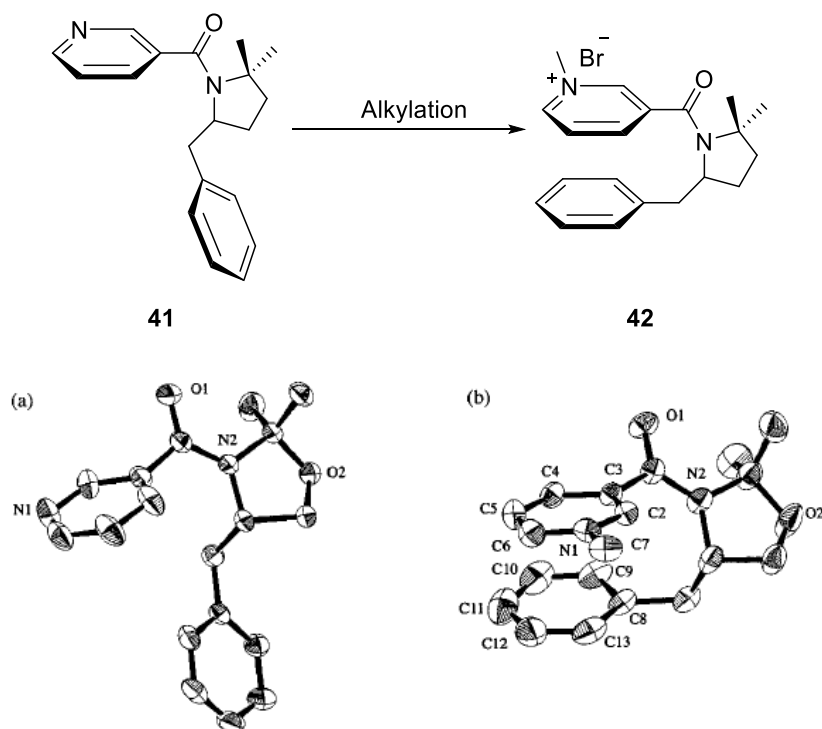


Figure 9 - Methylation of **41** leading to a cation- $\pi$  interaction in **42** including crystal structures of both compounds. Reprinted and adapted with permission from *J. Am. Chem. Soc.*, 2002, 124, 8184. Copyright 2016 American Chemical Society.

Over the past two decades Yamada has reported numerous applications of cation- $\pi$  interactions in organic synthesis, such as the example in Figure 9.<sup>54-62</sup> Pyridine **41** can be used for the stereoselective synthesis of 1,4-dihydropyridines, which are of interest for intermediates in alkaloid syntheses, as calcium agonists and as NADH models. This is achieved *via* a face-selective addition of a nucleophile to **42**. Due to the pseudo-planar chiral nature of the compound, introduced by the cation- $\pi$  interaction, facial selectivity is observed with *de* values greater than 99% and isolated yields up to 94%.<sup>61</sup> The conformation change can clearly be seen in the X-ray crystal structures in Figure 9 and has also been characterised using NMR and circular dichroism. Although this change is indicative of the formation of a cation- $\pi$  interaction it is also important to note that the amide bond in the linker placed the phenyl ring in close proximity to the pyridine before alkylation.<sup>55, 61</sup>



## Intramolecular Cation- $\pi$ Interactions in Non-Restricted Systems

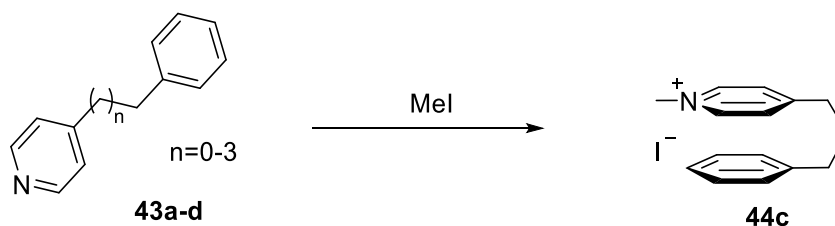


Figure 10 - Methylation of conformationally mobile 43a-d to afford a cation- $\pi$  interaction

Recent work by Fossey and co-workers has shown that cation- $\pi$  interactions can be observed in conformationally mobile pyridine systems.<sup>56, 63-64</sup> Studies into the linker length were conducted, where stacking interactions were probed using nOesy and fluorescence spectroscopy, which showed that in order to maximise a face-face cation- $\pi$  interaction (where the two  $\pi$ -surfaces are parallel) a linker length of 3 was optimal (Figure 10).<sup>64</sup>

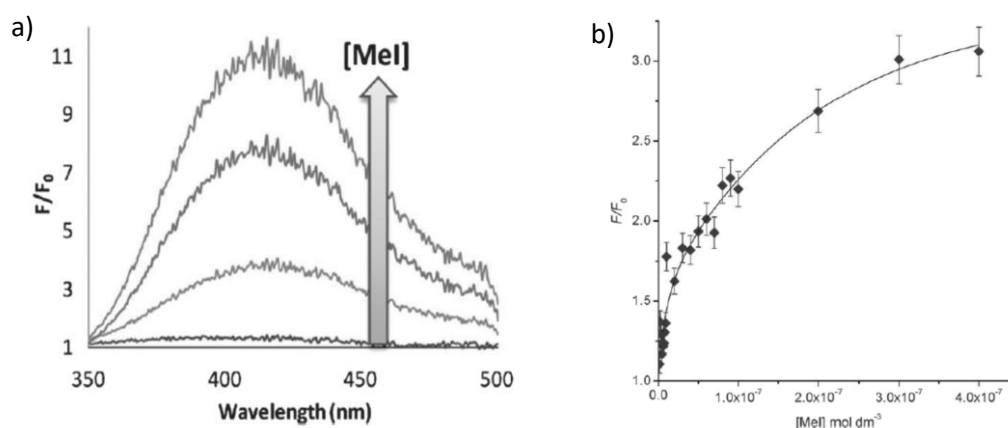


Figure 11 - a) Fluorescence excimer emission on addition of aliquots of MeI (0 to 0.6 mM) to a solution of 43 (1.0 mM) in  $\text{CH}_2\text{Cl}_2$  ( $\lambda_{\text{ex}} = 260 \text{ nm}$ ). b) Fluorescence  $F/F_0$  at 400 nm for addition of MeI (0-400 nM) to 43 (0.01 mM) in  $\text{CH}_2\text{Cl}_2$  ( $\lambda_{\text{ex}} = 260 \text{ nm}$ )<sup>56</sup>. Reprinted with permission.

Once the linker length had been optimised the fluorescence properties of **43** were investigated. Upon addition of millimolar quantities of methyl iodide to a 1.0 mM solution of **43** an excimer emission at approximately 400 nm was observed upon excitation at 260 nm (Figure 11a). This was then expanded to show that a significant fluorescence enhancement ( $F/F_0$ ) was obtained upon the addition of nanomolar levels of methyl iodide

to micromolar quantities of **17** lending itself to the detection of trace alkylating agents (Figure 11b).<sup>56</sup>

## Cation- $\pi$ Stacking in Catalysis with Chiral DMAP Derivatives

This section will briefly discuss two examples of the use of cation- $\pi$  interactions in DMAP catalysis. In both examples the interaction is used to exaggerate the chiral relay effect in order to induce an enhanced chiral environment around the pyridine nitrogen.<sup>35, 58, 65-66</sup> In contrast to the previous examples of cation- $\pi$  interactions, which use alkylation to form the pyridinium, the pyridinium species in the below examples use acylations. The key difference being that this is a dynamic process, meaning that due to sub-stoichiometric catalyst loading the pyridinium will constantly form and be quenched. Therefore, the cation- $\pi$  interaction must form quickly, in order to induce the chiral environment, leading to an enantioselective reaction. For this reason, pre-organisation can be seen as advantageous over a free arm system for catalysis.

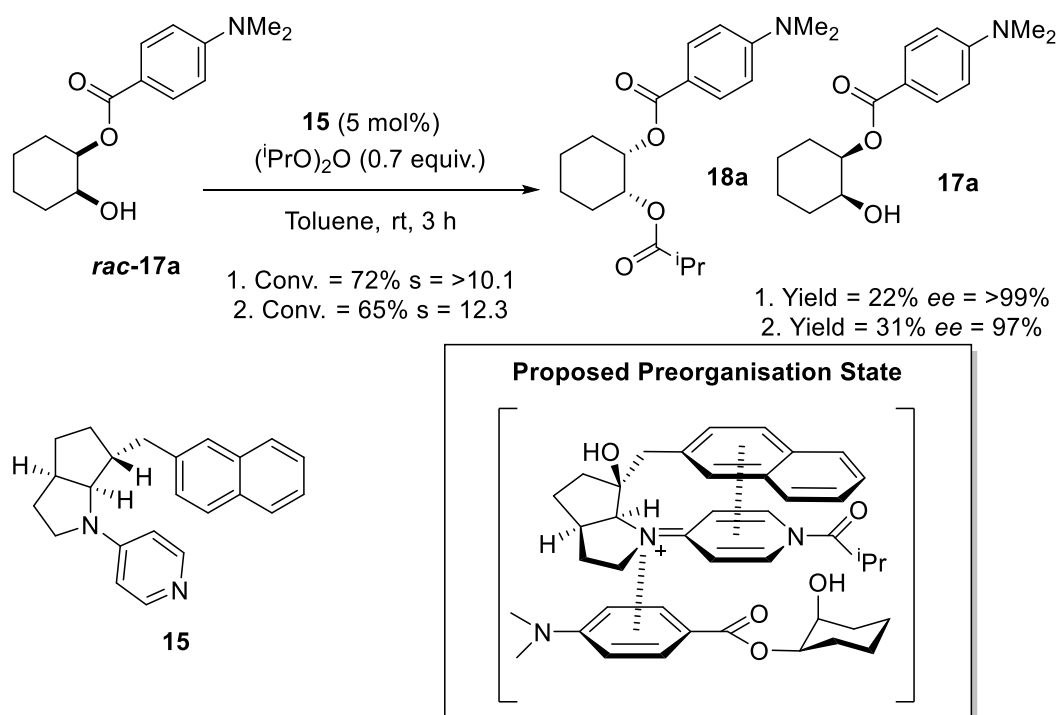
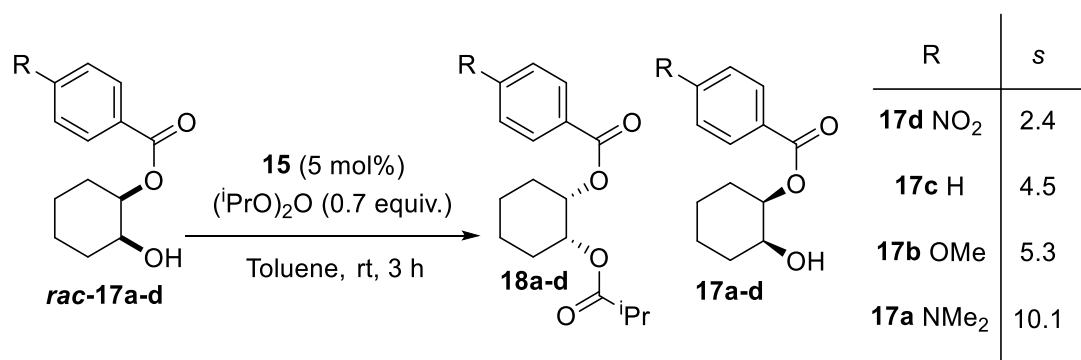


Figure 12 – Kinetic resolution of a cyclohexanediol derivative (**17a**) with Fuji's catalyst (**15**) including the proposed preorganisation state which contains both an exciplex and excimer cation- $\pi$  interaction

The kinetic resolution shown in Figure 12 was accomplished using **15**, which was reported by Fuji and co-workers and was first outlined in the section titled 'Pyridine 4-Position Derivatisation'. The reported mode of chiral induction for **15** is extremely interesting as two cation- $\pi$  interactions were proposed to be the key driving forces for chirality transfer.<sup>35</sup>

The interaction between the naphthalene unit and the pyridinium is called an exciplex interaction, a term used for a cation- $\pi$  interaction between two moieties within the same molecule. This interaction was studied with nOe spectroscopy where a comparison of spectra of the pyridine and acyl-pyridinium compounds was carried out. In **15** the protons at the 2- and 6-positions of the pyridine are equivalent by  $^1\text{H}$  NMR spectroscopic analysis and only show an nOe with protons in the pyrrolidine units. However, upon addition of an acylation agent all protons of the pyridinium become non-equivalent showing a loss of symmetry and a restriction in rotation. Additionally, an nOe is now detected between protons on the naphthalene unit and the pyridinium which was believed to be due to the naphthalene sitting parallel to the pyridinium in a 'closed conformation' such as the one shown in Figure 12.<sup>35</sup>



*Scheme 13 - Modification of the cycloheptanediol electronics and the effect on selectivity*

The second cation- $\pi$  interaction, which is called an excimer interaction, was not studied using spectroscopic techniques. Its existence was inferred from trends in reactivity and

catalysis results obtained. Electronic perturbation of the aromatic unit on the cyclohexanediol were modified in order to make it less electron rich, this was accomplished through either changing or removing the dimethylamino substituent. When these modified substrates were studied in a kinetic resolution reaction a reduction in selectivity was observed showing a clear trend between electronics and selectivity (Scheme 13). This was believed to be due to the weakening of the excimer interaction leading to a reduced directing effect on the substrate and thereby reducing selectivity.<sup>35</sup>

A second example was reported by Yamada and co-workers and again has a proposed cation- $\pi$  interaction within the transition state, however this interaction is between the acyl-pyridinium and a thiocarbonyl group (Figure 13). This interaction was inferred from study of the  $^1\text{H}$  NMR spectrum where upon acylation of the pyridine to form the acyl-pyridinium the  $\delta\text{ppm}$  between H-2, H-5 and H-6 on the pyridine ring were examined. Again, a large loss of symmetry was observed leading the authors to postulate that a cation- $\pi$  interaction was occurring.<sup>59</sup>

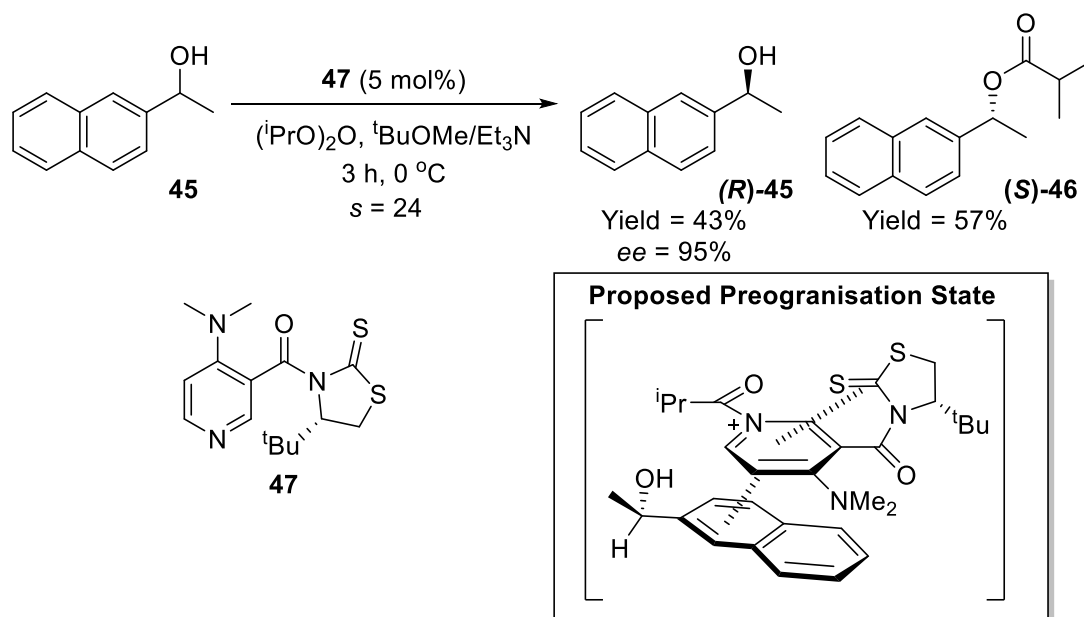


Figure 13 – Kinetic resolution of **45** with catalyst **47** and the proposed preorganisation state.

## Summary and Perspective

DMAP derived catalysts have proven themselves to be useful synthetic tools in asymmetric catalysis. A large number of chiral derivatives have been reported utilising a range of methods to introduce chirality into the structure with mixed success. Derivatising DMAP at the pyridine 2-position is widely reported to reduce catalytic activity despite exhibiting good chiral induction. On the other hand, 3- and 4-position derivatisation does not hinder activity but the chiral information must be relayed over a larger distance which can be challenging to overcome. Furthermore, the steric clash between the 4-position dialkylamino group and substituents at the 3-position of the pyridine is key to the success of numerous examples including work by Spivey, Richards and Kawabata.

The acyl-pyridinium intermediate, which is the main reason for the high activity of DMAP, has been successfully utilised to form cation- $\pi$  interactions in systems which have been preorganised to form the interactions, giving good selectivity in asymmetric catalysis. Although cation- $\pi$  interactions have been observed in flexible systems, for application other than asymmetric catalysis, this same degree of flexibility has not yet been achieved in organocatalysis. Furthermore, the sensing capabilities possible through the formation of a cation- $\pi$  complex have not yet been investigated in relation to a catalytic system.

## Concept & Aims

The hypothesis to be probed in this thesis is that cation- $\pi$  interactions can be utilised in catalysis for the relay of chiral information and this interaction be exploited in catalysis and sensing. To test the hypothesis chiral DMAP derivatives will be synthesised that incorporate a moiety capable of forming a cation- $\pi$  interaction with the acyl-pyridinium intermediate formed during catalysis, as seen in the catalytic cycle of DMAP (Figure 3).

The proposed catalysts will incorporate a unit capable of forming a cation- $\pi$  interaction which will provide the chiral relay effect and an opportunity for sensing. Kinetic resolution of secondary alcohols will be used as the benchmark reaction to test the utility of the systems as asymmetric catalysts. Furthermore, the presence of induced cation- $\pi$  interactions will be studied and the capability of the proposed catalysts to act as a sensor for catalytic efficiency and efficacy will be studied.

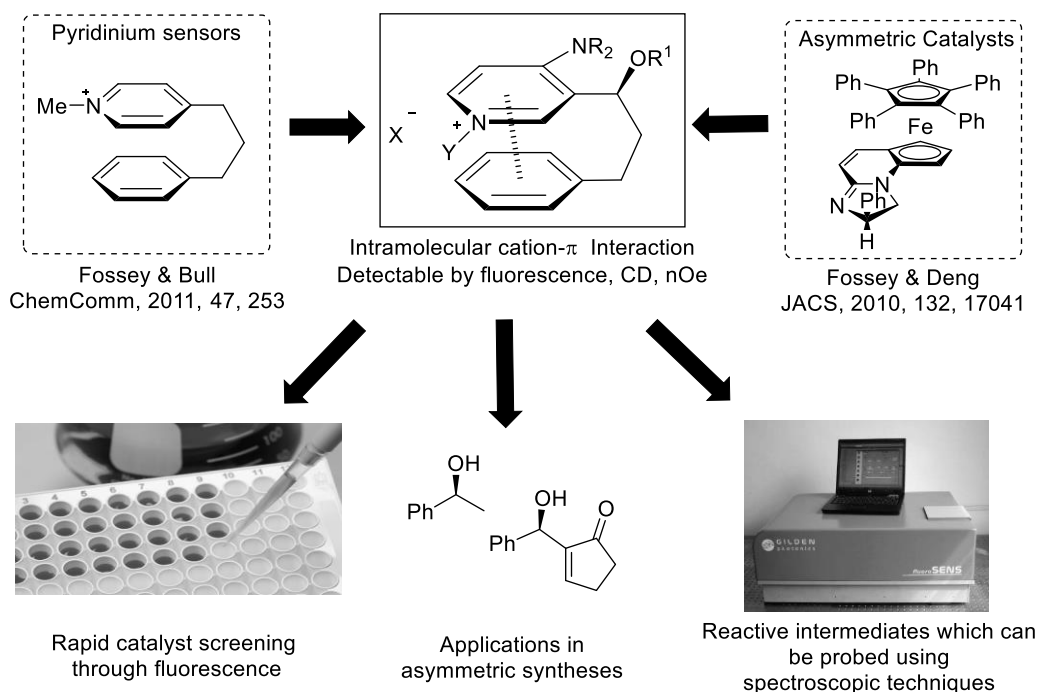


*Figure 14 - Combination of current research themes within the group*

This research aims to exploit synergies between catalysis and sensing by combining asymmetric nucleophilic catalysis and cation- $\pi$  interactions, in order to produce a DMAP based catalyst that is conformationally mobile and exhibits cation- $\pi$  stacking upon acylation (Figure 14).

Cation- $\pi$  interactions have been reported to relay chiral information, *via* a pre-installed stereogenic centre, around the catalytic site of a DMAP derivative for use as an asymmetric nucleophilic catalyst.<sup>54, 57</sup> This has only been achieved using rigid systems where the aromatic subunit has already been pre-organised to be in proximity to the acylpyridinium formed during the catalytic process.<sup>35, 58, 65-66</sup> Such catalysts have numerous potential applications including the kinetic resolution of chiral secondary alcohols<sup>1</sup> and the synthesis of  $\beta$ -lactams.<sup>17</sup>

However, Fossey and co-workers have demonstrated that cation- $\pi$  stacking interactions can occur in conformationally flexible phenyl-alkyl-pyridine systems and their alkylated pyridinium congeners that exhibit a fluorescence response, due to the exciplex formation, upon alkylation.<sup>56, 64</sup> These cation- $\pi$  interactions have been used as reporters for alkylating agents.<sup>56, 64</sup>

Fossey and co-workers have previously studied the linker length in non-rigid phenyl-alkyl-pyridine systems and found that a 3-carbon linker is optimal in order to maximise the cation- $\pi$  interaction observed in their system. Therefore, a 3 carbon alkyl chain has been appended to the 3-position of the pyridine of **50** and this linker will terminate in a phenyl group.<sup>56, 64</sup>

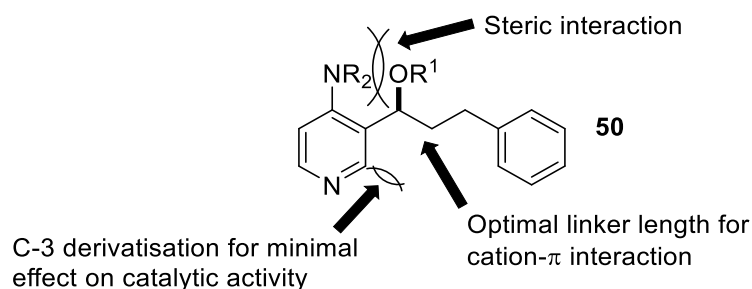


*Figure 15 - Design of catalyst core 50*

The core of the proposed catalyst (**50**, Figure 15) is analogous to the Vedejs style compounds, where a DMAP or PPY core is derivatised at the pyridine 3-position.<sup>31</sup> The 3-position was chosen over the 2-position in order to minimise effects on the rate of reaction due to steric interactions, and over 4-position as the transfer of chiral information would have to occur over a large distance which can be difficult to achieve.

The stereogenic centre is placed on the linker next to the pyridine core in order to impart a steric interaction between the dialkylamino group at the 4-position of the pyridine and the stereogenic centre. The effect of this steric interaction between the dialkylamino group and the stereogenic centre on the facial selectivity of the cation- $\pi$  interaction can be seen in Figure 16, conformation 1 will be favoured over conformation 2 due to a smaller steric clash being present. These steric interactions have been reported in numerous chiral DMAP derivatives for the relay of chiral information towards the catalyst's active site, such as the work by Richards, Spivey and Vedejs.<sup>29, 31, 45</sup> A protected secondary alcohol was chosen as the stereocentre because it can be easily synthesised by nucleophilic attack of an aldehyde and there is some literature precedent for its use.<sup>31</sup>



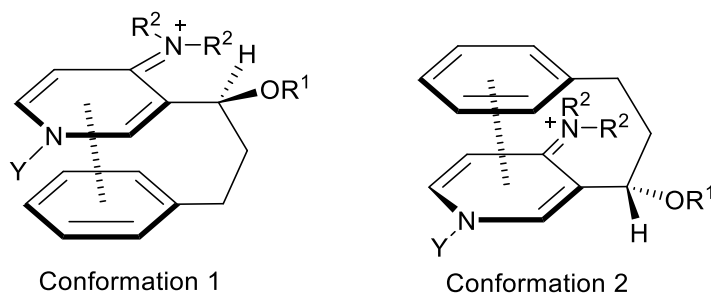


*Figure 16 - Two possible conformers displaying cation- $\pi$  interactions with the pyridinium of proposed catalyst 50*

Based on the proposed catalyst structure the objectives of this work are to:

1. Synthesise 3-position substituted DMAP derivatives, with the following structural variation, in order to investigate the relationship between structure and cation- $\pi$  interactions (Figure 17).
  - a. A three atom length chain at the pyridine 3-position terminating in an aromatic group.
  - b. A stereogenic centre on the three atom linker which has been resolved to obtain a single stereoisomer.
  - c. Variation in the electron, steric and  $\pi$ -surface properties of the terminal aromatic group.
  - d. Substitution of the three atom linker to effect stacking interactions.
  - e. Modifications of the pyridine 4-position to study rate and steric effects.

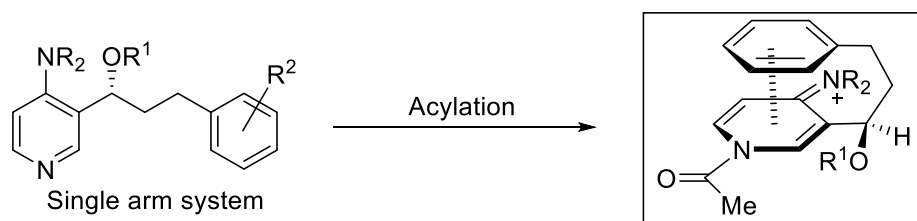


*Figure 17 - Design of single arm catalyst system demonstrating the acyl-pyridinium intermediate*

2. Test the synthesised 3-position substituted chiral DMAP derivatives in the kinetic resolution of secondary alcohols.
3. Synthesise 3,5-position di-substituted  $C_2$  symmetric DMAP derivatives (Figure 18), the design of which will be carried forward from knowledge gained from the 3-position substituted systems, predominantly based on their effectiveness as a catalyst.

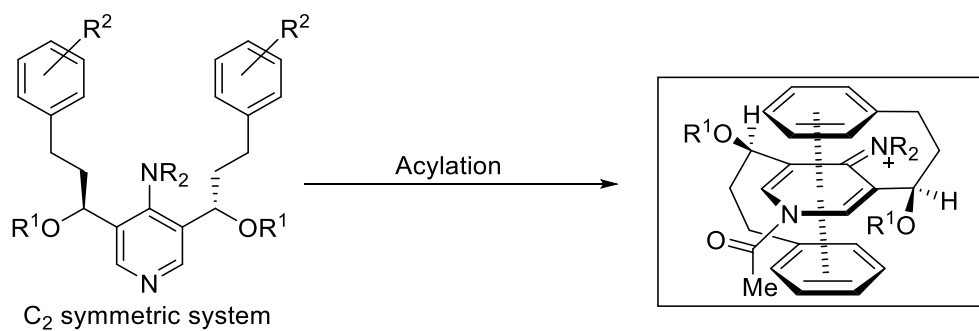


Figure 18 - Design of  $C_2$  symmetric system demonstrating the acyl-pyridinium intermediate

4. Test the synthesised 3,5-position di-substituted chiral DMAP derivatives in the kinetic resolution of secondary alcohols.
5. Study the synthesised compounds by fluorescence spectroscopy in order to detect if a cation- $\pi$  interaction is present.
6. Investigate if cation- $\pi$  interactions can reveal important information about intermediates utilising fluorescence spectroscopy which may inform the development of future catalysts.

## Synthesis of Catalyst Core Structure

This section will focus on the development of the synthetic route to obtain the core structure **50** outlined in the aims. In order to develop and optimise synthetic routes the primary synthetic target **50a** (Figure 19) was proposed, which attempts to keep structural complexity to a minimum.

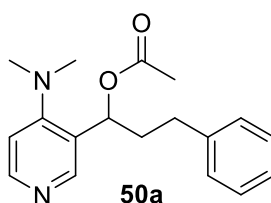


Figure 19 - Design of primary synthetic target **50a**

### Investigated Route 1

The successful synthesis of **50a** had previously been investigated within the group, however the desired compound had only been synthesised racemically utilising the retrosynthetic analysis outlined in Figure 20.<sup>67</sup>

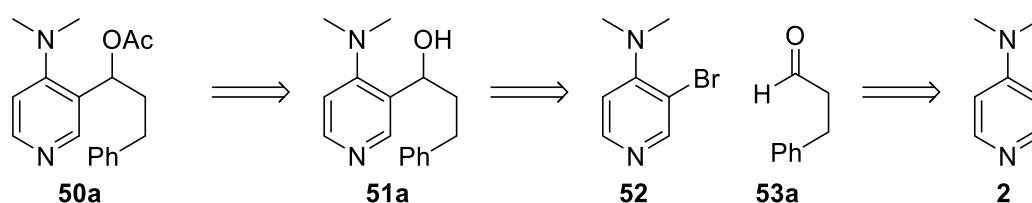


Figure 20 - Retrosynthetic analysis of **50a** based on research by A. Deeming

It was proposed that **50a** could be synthesised from the corresponding secondary alcohol **51a**, which would be synthesised from 3-bromo-4-dimethylaminopyridine (**52**) and hydrocinnamaldehyde (**53a**) utilising a lithium-halogen exchange process. 3-Bromo-4-dimethylaminopyridine (**52**) could be synthesised by carrying out the bromination of 4-dimethylaminopyridine (DMAP, **2**).

The synthesis of **rac-50a** was previously achieved,<sup>67</sup> however several synthetic challenges were still present. The bromination of DMAP gave variable and often low-yielding results (<20%). Only the racemate of **50a** had been synthesised during this previous research, which meant that the asymmetric approaches needed to be developed.

*Table 1 - Screening of bromination conditions for the synthesis of 52 from 2*

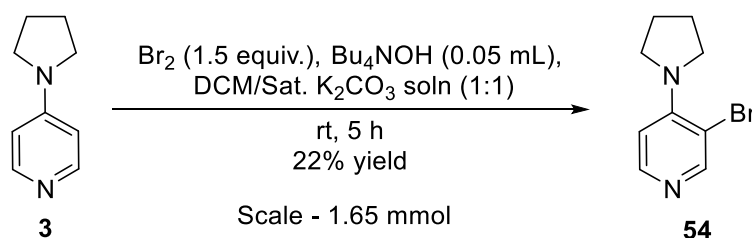
Reaction scheme: **2** (4-(dimethylamino)pyridine)  $\xrightarrow{\text{Conditions}}$  **52** (2-bromo-4-(dimethylamino)pyridine)

Entry	Conditions	Scale (mmol)	Yield (%)
1	Br <sub>2</sub> (2 equiv.), Bu <sub>4</sub> NOH (5 mL) <sup>a</sup> , DCM (125 mL), Sat. Aq. K <sub>2</sub> CO <sub>3</sub> (100 mL), 4.5 h <sup>68</sup>	41	11
2	Br <sub>2</sub> (3 equiv.), Bu <sub>4</sub> NOH (7.5 mL) <sup>a</sup> , DCM (125 mL), Aq. K <sub>2</sub> CO <sub>3</sub> (100 mL), 4.5 h <sup>68</sup>	41	20
3	Br <sub>2</sub> (2 equiv.), Bu <sub>4</sub> NOH (20 mL) <sup>a</sup> , DCM (500 mL), Sat. Aq. K <sub>2</sub> CO <sub>3</sub> (400 mL), 4.5 h <sup>68</sup>	164	10
4	NBS (1 equiv.), MeCN (200 mL), hν, 1 h <sup>69</sup>	41	21
5	Br <sub>2</sub> (2 equiv.), K <sub>2</sub> CO <sub>3</sub> (2 equiv.), DCM, 16 h <sup>70</sup>	41	-

<sup>a</sup>40% solution in H<sub>2</sub>O

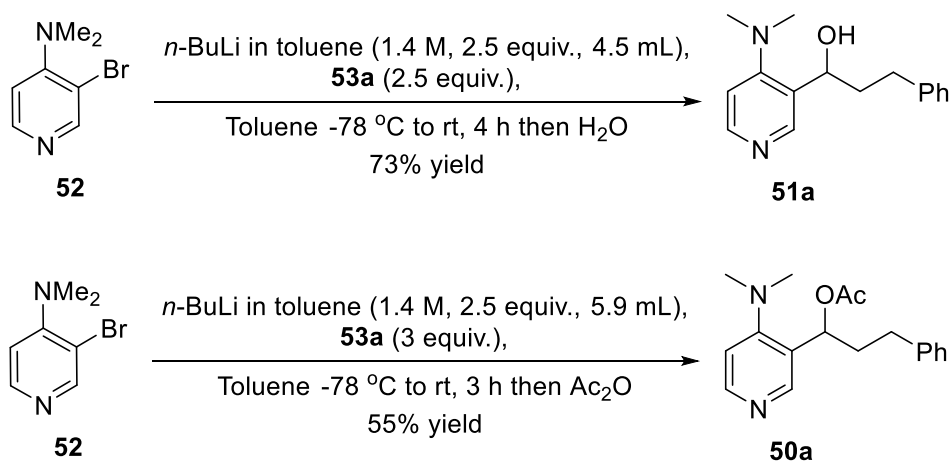
Initially the previous synthetic approach was repeated and evaluated. The bromination of **2** to afford **52** was carried out utilising literature methods, including those previously studied (Table 1).<sup>67-70</sup> Similar results were obtained to those within the group, none of which were in agreement with the reported literature, as the literature reported near quantitative yields for this transformation.<sup>67-70</sup> Upon further study of the available reported procedures, it was evident that the physical appearance of the compound varied greatly between reports, ranging from a colourless oil<sup>68</sup> to a yellow or dark orange solid,<sup>71</sup> observations of all outcomes were made in this study. Additionally, when an orange solid was obtained it could be distilled under reduced pressure, leaving a black residue, whilst the desired compound as a colourless oil was generated as the distillate. At this point it was assumed that the reported higher yielding procedures furnished impure compounds

which, by the analytical techniques employed, were indistinguishable. The same conditions for the synthesis of **52** were used for the synthesis of 3-bromo-4-pyrrolidinopyridine (**54**, Scheme 14) which was also obtained in low yield.



*Scheme 14 - Synthesis of 3-bromo-4-pyrrolidinopyridine via the bromination of PPY (**3**)*

The synthesis of **51a** from **52** and **53a** was achieved *via* a lithium-halogen exchange of **52** to give a carbon nucleophile which was reacted with hydrocinnamaldehyde (**53a**) to afford **51a** as a racemic mixture. If the reaction was quenched with acetic anhydride rather than water, target compound **50a** could be obtained (Scheme 15). The second step to synthesise **51a** and **50a** was robust and could be conducted on a multi-gram scale but the limitation of the bromination made this synthetic route undesirable.



*Scheme 15 - Synthesis of **51a** or **50a** from **52** utilising a lithium-halogen exchange*

## Investigated Route 2

Previous work by Fossey and co-workers reported the synthesis of phenyl-alkyl-pyridine based alkylating agents reporters which were synthesised by Grignard additions to

cyanopyridines.<sup>64</sup> This route was seen as advantageous, as the product of the Grignard addition is a ketone, which could potentially have been reduced asymmetrically to afford an enantio-enriched catalyst precursor.

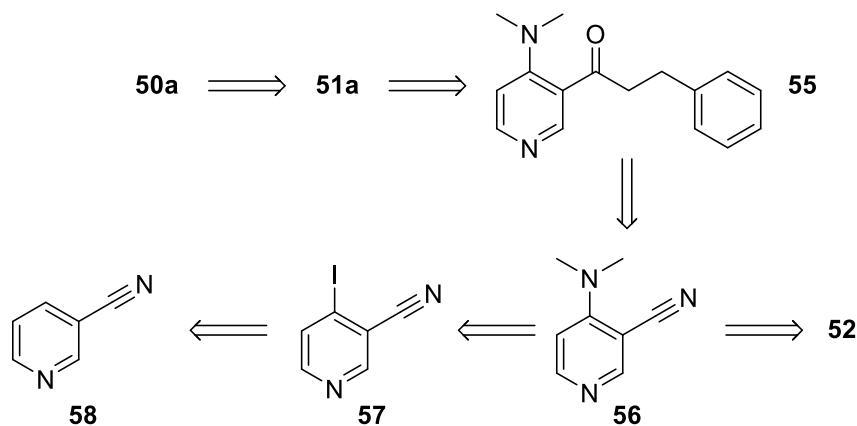


Figure 21 - Retrosynthetic analysis of 50a based on previous work reported by Fossey and co-workers

The retrosynthetic analysis of **50a**, based on a Grignard addition to cyanopyridine **56** to afford ketone **55** is shown in Figure 21. There has only been one reported synthesis of cyanopyridine **56**,<sup>72</sup> which was achieved using **52** as a starting material. Having previously observed that it was not possible to obtain **52** in an acceptable yield, this route was not attempted.

Nitrile **56** was inaccessible by the reported procedure because of the difficulty with accessing **52**, therefore a second possible route was devised *via* **57**, which had been reported in the literature and can be synthesised from **58**.<sup>73</sup> It was reported that over-iodination was possible, obtaining the desired compound (**57**) as well as 2,4-diiodo-3-cyanopyridine (**59**) in a 10:3 ratio in favour of the desired compound.<sup>73</sup> However, when the iodination was attempted, the corresponding di-iodo product **59** was difficult to separate from the desired mono-iodo compound **57**. Furthermore, when investigating the mono to di-iodo ratio by <sup>1</sup>H NMR spectroscopy it was found to be 3:13 in favour of the di-

iodinated compound (Figure 22). This procedure was therefore not taken any further due to the maximum yield of the first step being reduced to 19% based on this result.

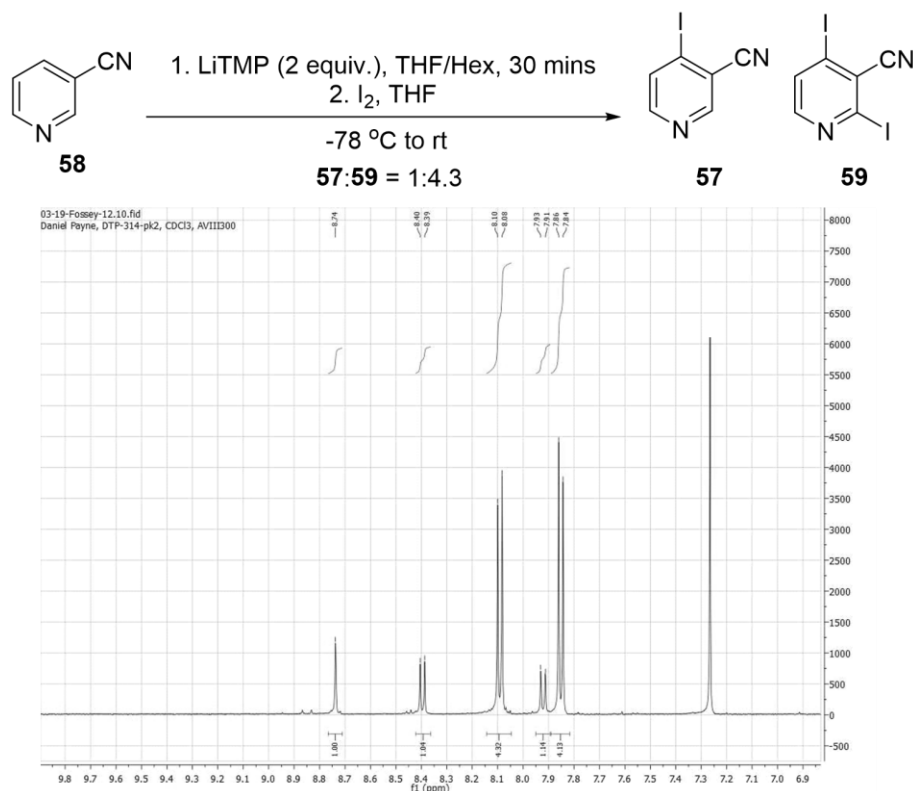


Figure 22 – Over-iodination of **58** to afford **57** and **59**

## Investigated Route 3

Due to the inaccessibility of 3-bromo- and 3-cyano-DMAP derivatives discussed in the first two synthetic routes, a previously reported preparation of 3-substituted DMAP derivatives was investigated.<sup>74</sup> This procedure used commercially available 4-chloropyridine (**61**) and employed a 3-position selective deprotonation which could then be used as a carbon nucleophile and reacted with benzaldehyde to afford secondary alcohol **62** in 90% yield (Figure 23).<sup>74</sup>

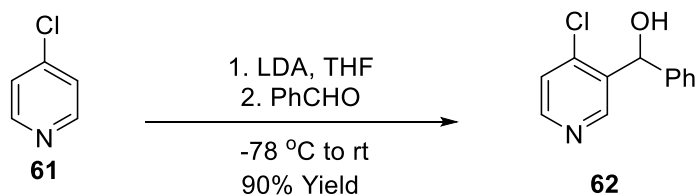


Figure 23 - 3-position derivatisation of 4-chloropyridine by Busto *et al.*<sup>74</sup>

Utilising the above transformation, it was proposed that **50a** could be synthesised from the corresponding secondary alcohol **51a**, which would be synthesised from the 4-chloropyridine derivative **60a** *via* an aromatic substitution. Pyridine **60a** could be synthesised from the regioselective deprotonation of **61** and subsequent reaction with hydrocinnamaldehyde (**53a**), as shown in Figure 6. The corresponding hydrochloride salt of **61** and aldehyde **53a** were commercially available.

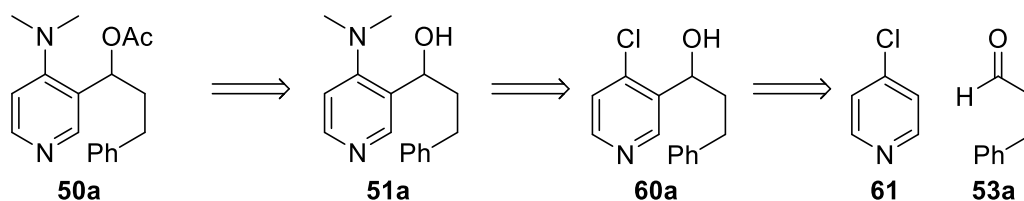
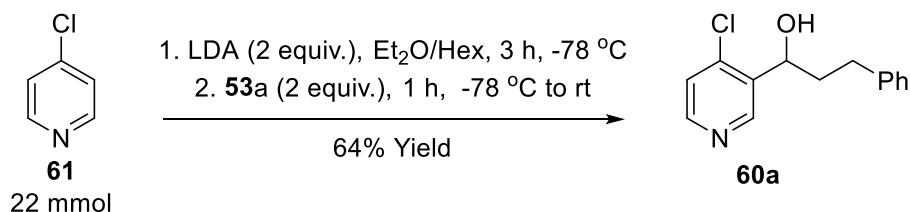


Figure 24 - Retrosynthetic analysis of **50a** utilising a regioselective deprotonation of 4-chloropyridine (**61**)

Employing the same condition as reported by Busto *et al.* **60a** was obtained in 64% yield from 4-chloropyridine (**61**), as shown in Scheme 16. This was a promising result, as it provided an expedient route to the core structure of **50a**. Additionally, a similar aromatic substitution as that needed to obtain **51a** from **60a** had been reported previously by Busto.<sup>74</sup>



Scheme 16 - Synthesis of **60a** from **61** via a regioselective deprotonation



It was noticed that **60a** underwent slow decomposition over a period of several weeks to an insoluble orange solid; this was overcome by storing **60a** as the hydrochloride salt. The crystal structure of the hydrochloride salt of **60a**·HCl was obtained from crystallisation from acetonitrile and can be seen in Figure 25. There are two key features that can be observed in the structure. Firstly, the steric interaction between the 4-position substituent of pyridine and the stereocentre are favourable for the chiral relay effect desired due to the oxygen being oriented towards the pyridine nitrogen. Secondly, there are no apparent intramolecular cation- $\pi$  or  $\pi$ - $\pi$  interactions or similar interactions between molecules within the packed structure. With a route to **60a**·HCl in hand, optimisation of the reaction was carried out in order to reduce the number of equivalents of aldehyde and LDA required, whilst maintaining or improving the yield of the reaction. The optimisation study is summarised in Table 2.

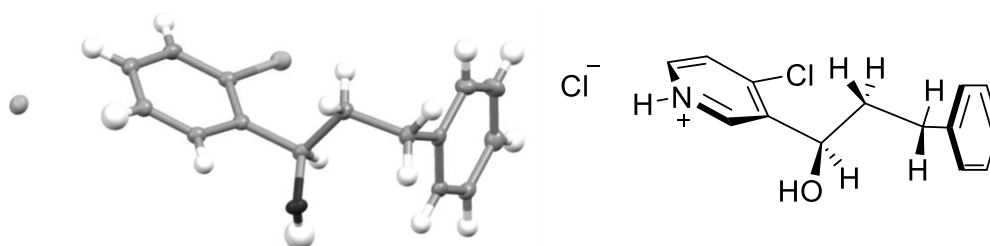
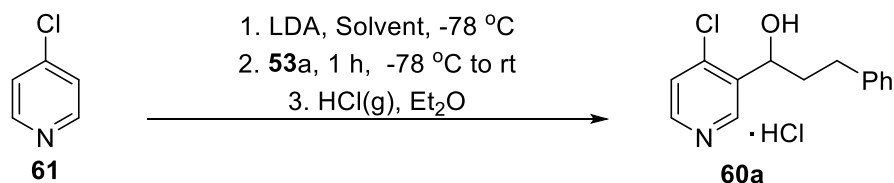


Figure 25 - Crystal structure of *rac*-**60a**·HCl with ellipsoids drawn at the 50 % probability level.

The optimisation of the synthesis of **60a** (Table 2) demonstrated that the number of LDA equivalents could be reduced to 1.5 without a considerable loss in yield (entries 1-4), and that the concentration of LDA was important, with an increase in molarity leading to a reduction in yield (entries 2 and 5-6). The time allowed for deprotonation also had an effect on yield, with 3 to 4 hours being optimal (entries 2 and 8-11). Finally, the number of aldehyde equivalents could be reduced to 1.5 with a 9% loss in yield, which may have been advantageous if the aldehyde were not commercially available, but for a commercially available compound such as **53a** this was not required.

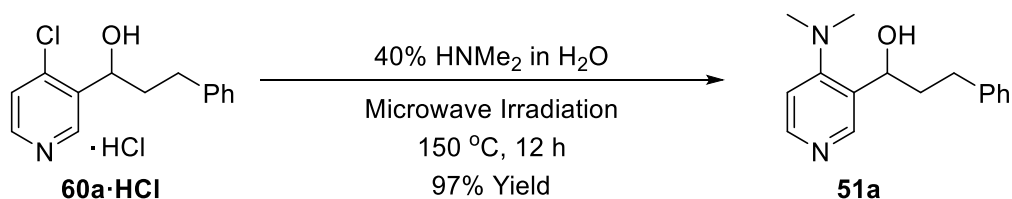
Table 2 - Optimisation of the synthesis of 60a



Entry	LDA Equiv.	LDA Conc. (M)	53a Equiv.	Solvent	Deprotonation time (h)	Yield (%)
1	1.2	0.1	2	Et <sub>2</sub> O	3	38
2	1.5	0.1	2	Et <sub>2</sub> O	3	58, 60, 56
3	2.0	0.1	2	Et <sub>2</sub> O	3	61
4	2.5	0.1	<b>2.5</b>	Et <sub>2</sub> O	3	67
5	1.5	<b>0.15</b>	2	Et <sub>2</sub> O	3	55
6	1.5	<b>0.25</b>	2	Et <sub>2</sub> O	3	48
7	1.5	<b>0.05</b>	2	Et <sub>2</sub> O	3	40
8	1.5	0.1	2	Et <sub>2</sub> O	<b>1</b>	8
9	1.5	0.1	2	Et <sub>2</sub> O	<b>2</b>	36
10	1.5	0.1	2	Et <sub>2</sub> O	<b>4</b>	63, 63
11	1.5	0.1	2	Et <sub>2</sub> O	<b>5</b>	57
12	1.5	0.1	<b>1.5</b>	Et <sub>2</sub> O	4	52
13	1.5	0.1	<b>1.75</b>	Et <sub>2</sub> O	4	56

Data shown in bold indicates the factor varied in the experiment.

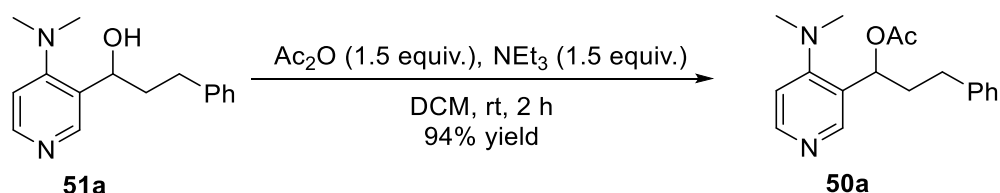
The nucleophilic aromatic substitution reaction to install the 4-dimethylamino substituent through displacement of the chloride of **60a**·HCl with dimethylamine was attempted in a sealed tube. However, a number of by-products were observed due to the long reaction times needed (>72 hours). A useful alternative to the sealed tube reactions was to use microwave irradiation, which yielded **51a** in a 97% yield in 12 hours (Scheme 17) without the need for purification by column chromatography.



Scheme 17 - Synthesis of 51a

With the DMAP moiety complete, the final synthetic step was derivatisation of the secondary alcohol. An acyl group was chosen, and the acylation of **51a** to afford **50a** was

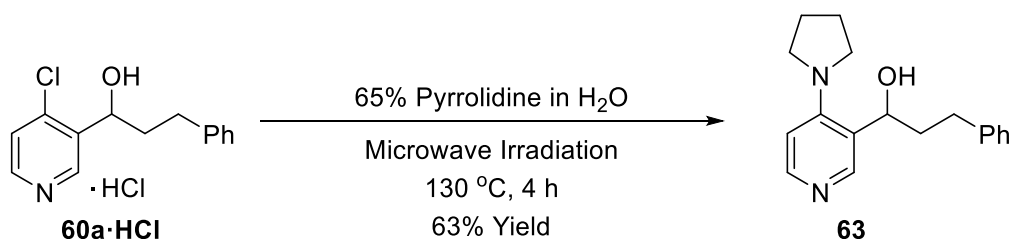
achieved in 94% yield (Scheme 18). Interestingly, no addition of an acylation catalyst was required due to the presence of stoichiometric DMAP in the catalyst, meaning that this transformation was 'self-catalysing'. This provided a 3-step synthesis of racemic core structure **50a** in a good overall yield of 57%.



*Scheme 18 - Acylation of 51a to synthesise 50a*

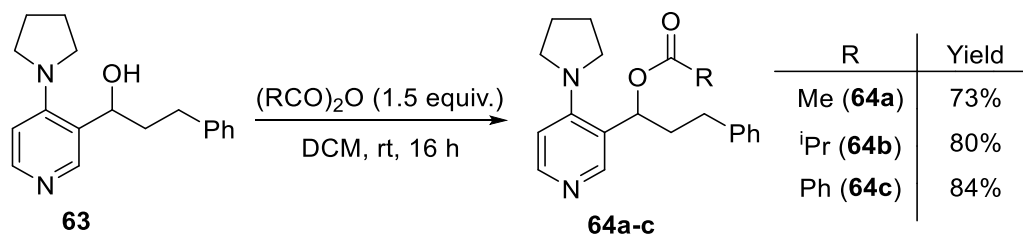
## Increasing Structural Diversity

With a synthetic route to **50a** developed, attempts were made to increase the structural diversity of the catalyst core. The 4-dimethylamino group was replaced for a 4-pyrrolidino group *via* the microwave-assisted aromatic substitution of **60a·HCl** with pyrrolidine in water to afford **63** in 63% yield (Scheme 19). It was not possible to introduce the 4-diethylamino group by the same method.



*Scheme 19 - Synthesis of 4-pyrrolidino derivative 63 from 60a·HCl*

The acylation of secondary alcohol **63** was self-catalysing to afford **64a** with acetic anhydride. Alternatively, *i*-propyl and phenyl groups were introduced as R by changing the anhydride to afford **64b** and **64c**, respectively (Scheme 20). The conditions differ slightly compared to those used for the synthesis of **50a**, as the base has been omitted because it was surplus to requirements in the presence of a stoichiometric DMAP-like catalyst.



*Scheme 20 - Protection of secondary alcohol 63 to afford 64a-c*

## Chiral HPLC Separation of Enantiomers of 60a

With **rac-60a·HCl** synthesised, a route was needed to obtain enantiopure materials. Efforts were focused on the chiral HPLC separation of **60a·HCl**, as this would allow for the largest number of enantiopure DMAP derivatives to be synthesised following a single separation.

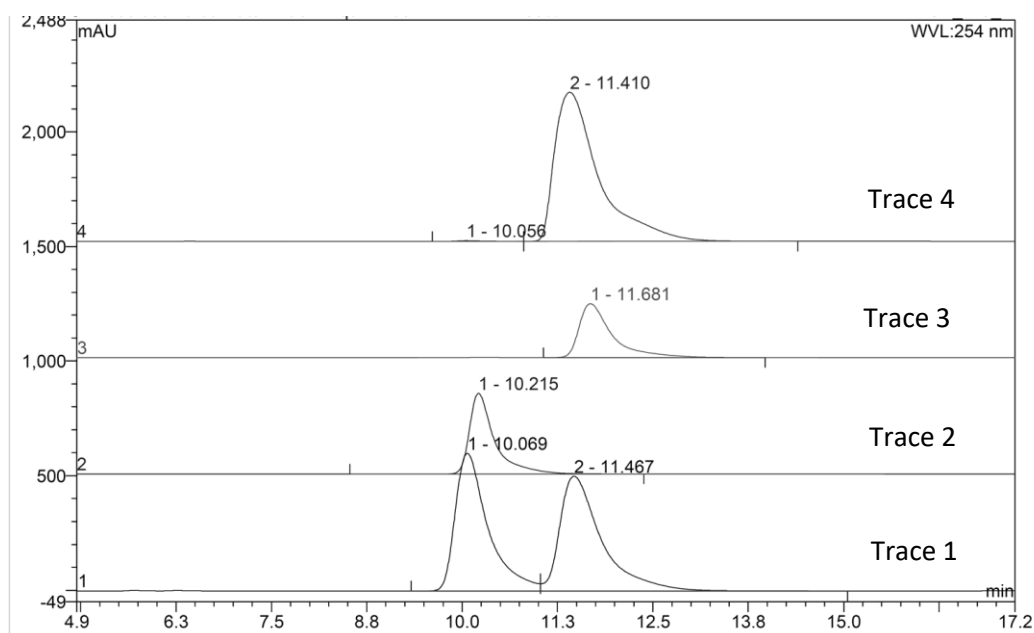
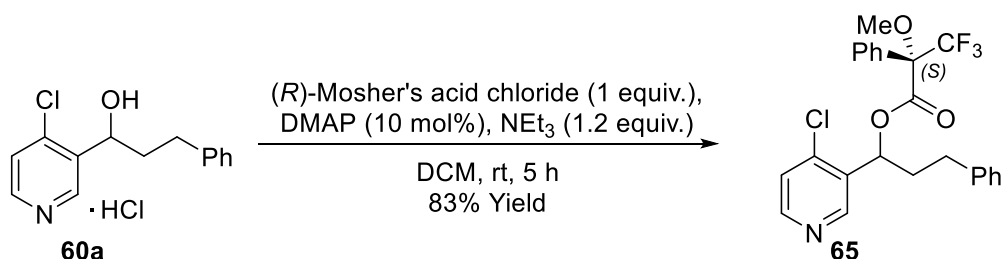


*Figure 26 - Chiral preparative HPLC separation of 60a·HCl*

The chiral resolution was achieved utilising a Phenomenex cellulose-1 preparative HPLC column with a mixture of acetonitrile and water as the mobile phase (Figure 26) to give 32% recovery of (**S**)-**60a** and 34% recovery of (**R**)-**60a**. Baseline separation was not achieved (Figure 26, trace 1), however the first eluting enantiomer could be obtained in greater than 99% *ee* (Figure 26, trace 2). The second eluting enantiomer of **60a·HCl** was

not obtained in enantiopure form upon first injection (Figure 26, trace 4) but was reinjected several times, affording this enantiomer in greater than 99% *ee* (Figure 26, trace 3).

In order to verify that **60a·HCl** was obtained in enantiopure form, the Meldrum's acid derivatives were synthesised (Scheme 21). Racemic **60a·HCl** was used in order to determine the chemical shifts of the diastereomeric CF<sub>3</sub> groups in the <sup>19</sup>F NMR spectrum, which were -70.9 ppm and -71.2 ppm.



*Scheme 21 - Meldrum's acid derivatisation of 60a·HCl to give 65*

The NMR analysis of the Meldrum's derivative of enantiopure **60a·HCl**, when combined with the HPLC data, appeared to confirm that it had been obtained in greater than 99% *ee* by the presence of only a single <sup>19</sup>F NMR signal at -70.9 ppm (Figure 27, bottom spectrum). A doping experiment was carried out in order to confirm the absence of the other enantiomer, where racemic **60a·HCl** was added to the NMR sample and the data was recorded again. Figure 27 (top spectra) shows that the second diastereoisomer can be seen in both the benzylic region of the <sup>1</sup>H NMR spectrum and a second CF<sub>3</sub> signal is present at -71.2 ppm in the <sup>19</sup>F NMR spectrum after doping.

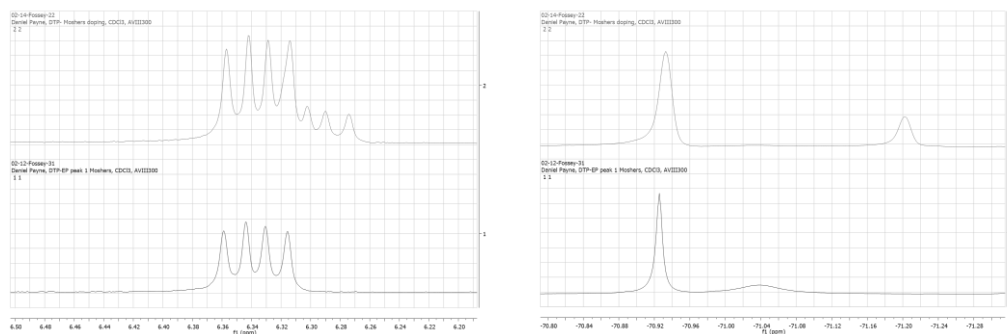


**Figure 27** – Mosher's derivatisation of enantiopure **60a·HCl**.  $^1\text{H}$  NMR (Left) before doping (bottom) and after addition of racemic **60a·HCl** (top).  $^{19}\text{F}$  NMR (right) before doping (bottom) and after addition of racemic **60a·HCl** (top).

The absolute configuration of **60a·HCl** was determined using crystal structure analysis.

The structure of **60a·HCl** is shown in Figure 28, from which the absolute configuration at C(6) was determined to be *S* with a Flack parameter of -0.006(9). The standard deviation on this value is acceptable for the absolute structure to have been determined from the diffraction data. Interestingly, (*S*)-**60a·HCl** crystallised as a different polymorph than the one observed in *rac*-**60a·HCl**.

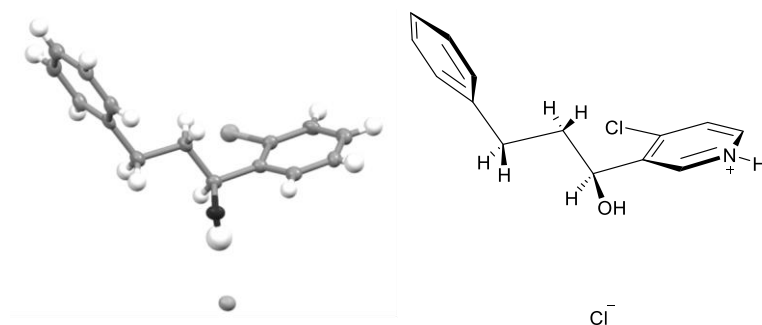
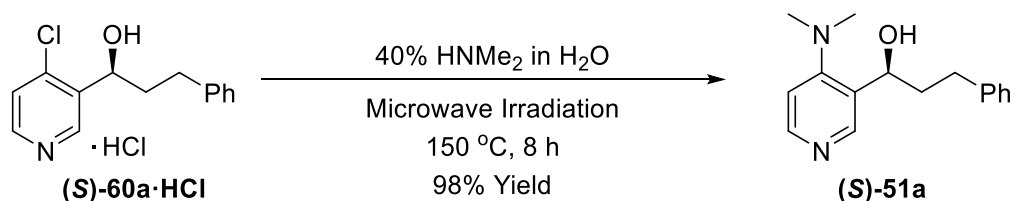


**Figure 28** - X-Ray crystal structure of **60a·HCl** with ellipsoids drawn at the 50 % probability level. Hydrogen bonding is shown using a dotted line. The absolute structure has been determined, with C(6) being *S* with a Flack parameter of -0.006(9).

With (*S*)-**60a·HCl** obtained through HPLC resolution using a chiral stationary phase, the same synthetic route as outlined for the racemic system was employed for the synthesis of (*S*)-**51a**, which is the microwave-promoted 4-position aromatic substitution reaction with dimethylamine (Scheme 22).



*Scheme 22 – Synthesis of (S)-51a from (S)-60a*

The crystal structure of **(S)-51a** was also obtained, but the Flack parameter (-0.02) was not within the limits of error to be able confirm the absolute configuration. Nevertheless, based on the data obtained for **(S)-60a·HCl** and the Flack parameter for **(S)-51a**, the most likely configuration is S.

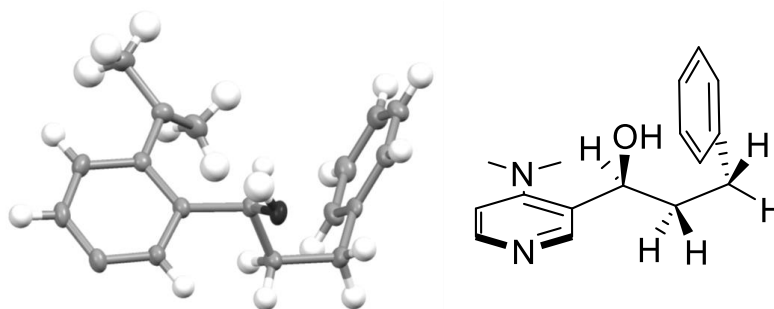
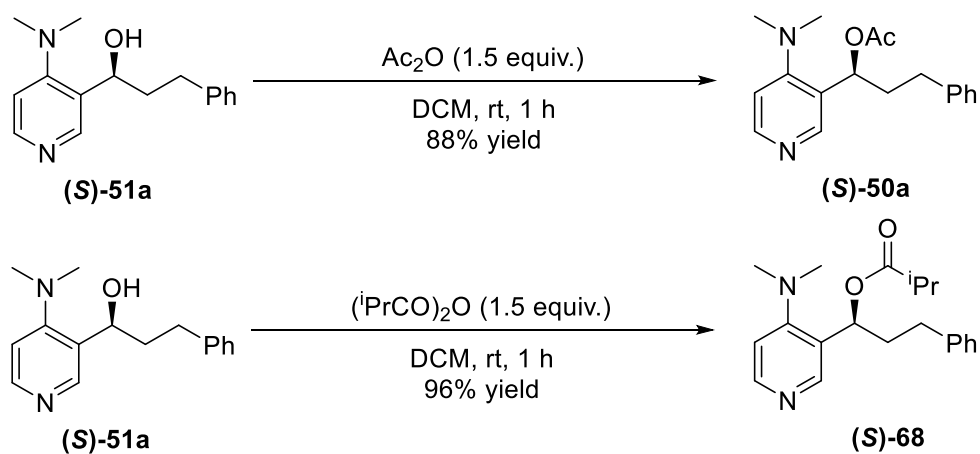


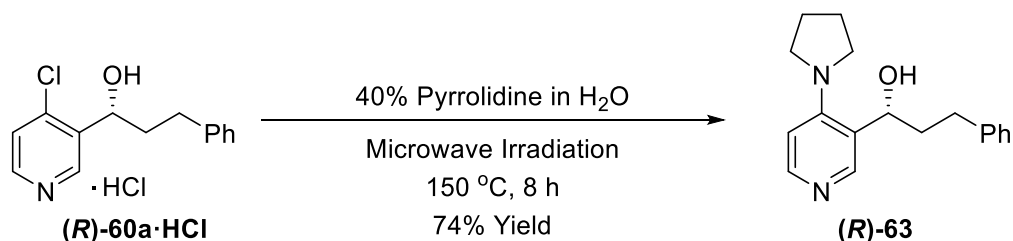
*Figure 29 - X-Ray crystal structure of (S)-51a·H<sub>2</sub>O with ellipsoids drawn at the 50% probability level and solvent molecules removed.*

The secondary alcohol protection of **(S)-51a** was carried out with acetic anhydride and isobutyric anhydride to give compounds **(S)-50a** and **(S)-68** in 88% and 96% yield, respectively (Scheme 23).



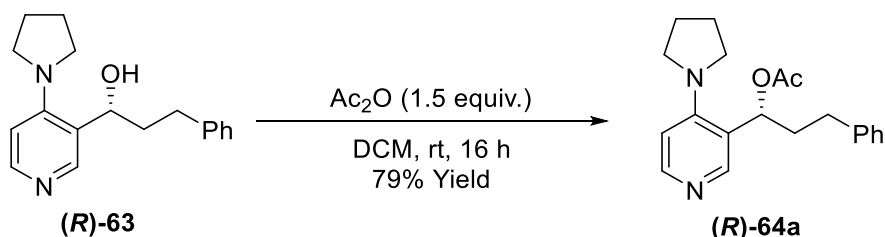
*Scheme 23 – Synthesis of (S)-50a and (S)-68 via secondary alcohol acylation of (S)-51a*

**(R)-60a·HCl** was used to synthesise the 4-pyrrolidino derivative **(R)-63**. The same conditions as used for the dimethylamine derivative were employed to afford **(R)-63** in 74% yield (Scheme 24).



*Scheme 24 - Synthesis of (R)-63 from (R)-60a·HCl*

DMAP derivative **(R)-64a** was obtained *via* acylation of **(R)-63** with acetic anhydride in 79% yield (Scheme 25).



*Scheme 25 - Acylation of (R)-63 to afford (R)-64a*

## Enantioenriched Catalyst using Asymmetric Synthesis

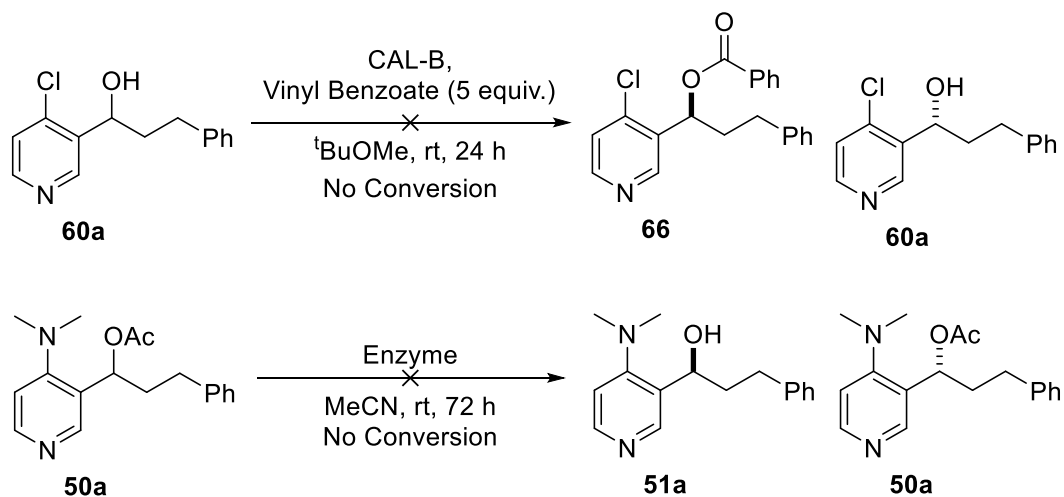
HPLC with a chiral stationary phase was able to provide enantiopure DMAP derivatives **(S)-50a**, **(S)-68** and **(R)-64a** in good yield. However, HPLC column containing a chiral stationary phase can be expensive (due to initial cost of the column) as well as time-consuming. For these reasons, attempts were made to synthesise these catalysts asymmetrically or, alternatively, resolve the enantiomers without chiral HPLC.

## Enzymatic Resolution

Enzymes have been proven to be effective at the kinetic resolution of secondary alcohols by either selective acylations or deacylations.<sup>74-75</sup> Additionally, Busto *et al.* have shown



that they can efficiently resolve a secondary alcohol DMAP derivative precursor (Figure 23) which has structural similarities to compound **60a**.<sup>74</sup>



*Scheme 26 – Attempts at enzymatic resolution to obtain non-racemic chiral DMAP derivatives*

Despite encouraging literature precedent on similar substrates, no conversion was observed by TLC in either of the reactions shown in Scheme 26. In the enzymatic deacylation of **50a**, both CAL and CAL-B were used, but neither was effective in the resolution reaction. Phosphate buffer solution was also used as solvent, but the substrate for resolution was not soluble in this medium, and no conversion was observed.

## Oxidation and Asymmetric Reduction

An oxidation and asymmetric reduction route was not initially considered to be the optimal route to investigate due to the introduction of two additional steps into the synthetic procedure. However, due to the lack of success with enzymatic resolutions, it was proposed that alcohol **60a** could be oxidised to ketone **67**, which could subsequently be reduced asymmetrically back to enantioenriched alcohol **60a** (Figure 30).

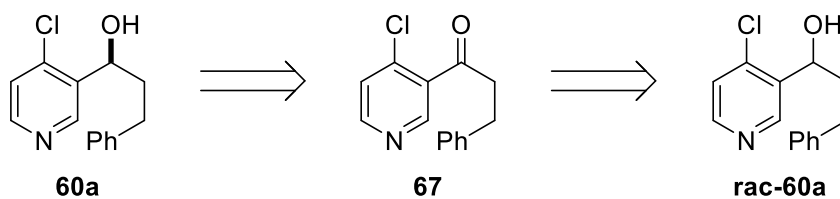
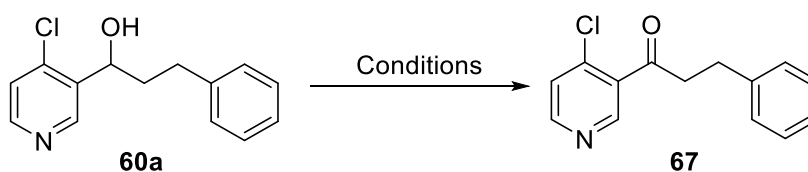


Figure 30 - Retrosynthetic analysis for the oxidation/reduction process to give non-racemic 60a

Oxidation conditions for the synthesis of ketone **67** from alcohol **rac-60a** were screened and the results are summarised in Table 3.

Table 3 - Conditions screening for the oxidation of alcohol 60a to ketone 67



Entry	Conditions	Scale	Yield
		(mmol)	(%)
1	CrO <sub>3</sub> (3 equiv.), acetone, 4 h <sup>74</sup>	5	14
2	CrO <sub>3</sub> (3 equiv.), acetone, 3 h <sup>74</sup>	5	18
3	PCC (1 equiv.), DCM, 15 min <sup>76</sup>	0.4	17
4	PCC (2 equiv.), DCM, 15 min <sup>76</sup>	0.4	40
5	PCC (2 equiv.), DCM, 2 h <sup>76</sup>	0.4	43
6	PCC (2 equiv.), DCM, 15 min <sup>76</sup>	2	36
7	PDC (2 equiv.), DCM, 2 h <sup>77</sup>	0.4	41
8	MnO <sub>2</sub> (5 equiv.), Dioxane, 24 h <sup>78</sup>	0.4	0 <sup>a</sup>
9	KMnO <sub>4</sub> (6 equiv.), CuSO <sub>4</sub> (2 equiv.), Benzene, 24 h <sup>79</sup>	0.4	0 <sup>a</sup>
10	1. DMSO (2.2 equiv.), Oxalyl chloride (1.1 equiv.), DCM, -78 °C, 30 mins. <sup>80</sup>	0.5	92
	2. NEt <sub>3</sub> (5 equiv.), DCM, -78 °C to rt, 30 mins		

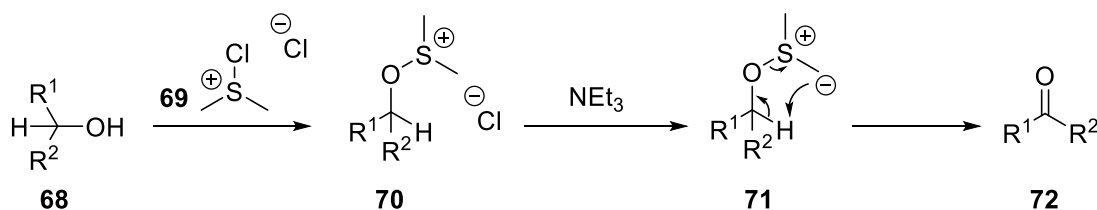
<sup>a</sup>No conversion observed by TLC

Chromium-based oxidants did give **67**, and an increase in yield was observed as chromium reagent acidity decreased from chromium oxide to PDC (Table 3, entries 1-7). An increase in reaction time when using chromium oxide led to a decrease in yield (Table 3, entries 1-2). Oxidations with potassium permanganate and manganese oxide were both unsuccessful, as no conversion was observed by TLC (Table 3, entries 9-10). A Swern oxidation provided a near-quantitative yield of the desired ketone **67**, and subsequent repeats of the reaction up to a 3 mmol scale showed that this was reproducible and scalable with no reduction in yield observed.

During the course of these experiments, it was noticed that upon concentration of ketone **67**, it would rapidly change from a colourless oil to a viscous dark orange semi-solid. It was believed that this was due to decomposition of the ketone, similar to that observed for 4-chloropyridine over several days, and for alcohol **60a** over several weeks, but the ketone decomposition took less than one hour. Storage conditions did not retard the decomposition either when stored at room temperature or at -20 °C, under either a nitrogen or air atmosphere. The route of decomposition of this compound is currently unknown due to the insolubility of the decomposition product in solvents used for NMR spectroscopy.

It is due to this rapid decomposition that the oxidation conditions are generally low-yielding, with the exception of a Swern Oxidation. Most oxidation reactions slowly produce the ketone over a period of time and it accumulates until the reaction reaches completion. For **67**, this means that it can decompose *in situ* over the course of the reaction, meaning that neither recovered starting material nor product would be isolated. This would also explain why increasing the reaction time reduced the yield obtained for the chromium oxidations as any **67** that forms has more time to decompose.

Consideration of the Swern mechanism (Scheme 27) shows that upon addition of DMSO and oxalyl chloride (which produces chloro(dimethyl)sulfonium chloride **69** *in situ*) to an alcohol **68**, an alkoxy-sulfonium intermediate **70** is formed. Intermediate **70** remains in the reaction mixture until the addition of base in the quenching step, which forms a sulfur ylide **71**, which decomposes to the ketone **72**.



*Scheme 27 - Mechanism of a Swern oxidation*

This means that, during the synthesis of **67** from **60a**, only during this quenching step is ketone **67** formed, and therefore **67** cannot decompose until this point. If a rapid workup and purification is used, then **67** can be obtained in good yield and taken rapidly to the reduction reaction. The decomposition of **67** made it difficult to obtain full characterisation data, but the crystal structure was obtained by making the hydrochloride salt, and the structure can be seen in Figure 31.

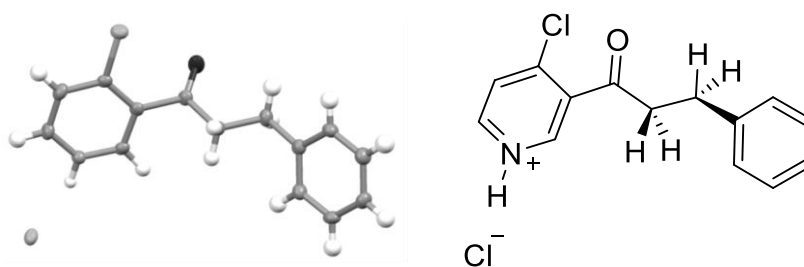


*Figure 31 - Crystal structure of 67·HCl with ellipsoids drawn at the 50% probability level.*

The first asymmetric reduction investigated was based on an asymmetric enzymatic reduction, the theory of which was based on previous literature.<sup>74</sup> This was utilising yeast, the limitations of which are that the reaction must be performed in an aqueous media within a specific pH range and at a temperature between 30 and 35 °C. The yeast must be

fed with D-glucose, which is digested to a range of smaller components, and the yeast can break down over a period of time so the reaction mixture can be highly complex with numerous components.

A yeast reduction of **67** was performed and a high ee was obtained using this method (>95%); however, the yield was low (2%), most likely due to the long reaction time (72 h) allowing the decomposition of **67**. Additionally, **67** was not soluble in the aqueous media and yeast cannot be used in organic solvents. Due to the low yield and problems with purification, this route was not investigated further.

Due to the limitations when using yeast, organocatalytic reductions were investigated, which overcome many of the limitations of yeast. Although DIP-chloride had been used in the synthesis of a similar compound,<sup>74</sup> it was not compatible with this system. This was due to the long reaction times required (72 h) which led to decomposition of the ketone before it could be reduced, therefore a more rapid asymmetric reduction was needed.

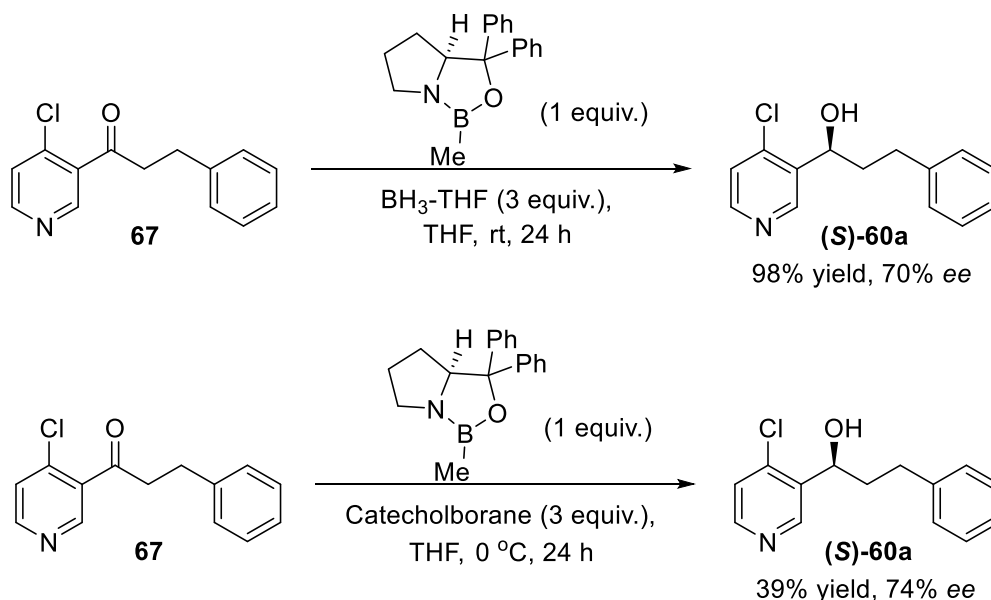


Figure 32- CBS reduction of **67** to afford (S)-**60a**

The proline-derived CBS catalyst was investigated due to its frequent use in the literature<sup>81</sup> and the conditions and reaction time appeared to be compatible with the

catalyst precursor (Figure 32). After optimisation, the highest yield obtained was 98% with an *ee* of 70% (determined by Mosher's ester derivatisation). Absolute stereochemistry was determined by comparison of the  $^{19}\text{F}$  NMR shifts of the Mosher's derivative to the previous enantiopure sample obtained from chiral HPLC purification. Use of catecholborane rather than borane-THF led to an increase in *ee* to 74% (determined by Mosher's ester derivatisation, Figure 32), however a reduction in yield to 39% was observed. The low *ee* values were due to a substantial background reduction reaction, determined by running the reaction without the catalyst present. This was most likely due to borane activation by **67**, which led to a non-stereoselective reduction to **60a**, eroding the *ee* of the reaction. Due to the low *ee* values obtained, despite the reaction being run with stoichiometric catalyst, this route was not used for the large-scale synthesis of enantioenriched **60a**.

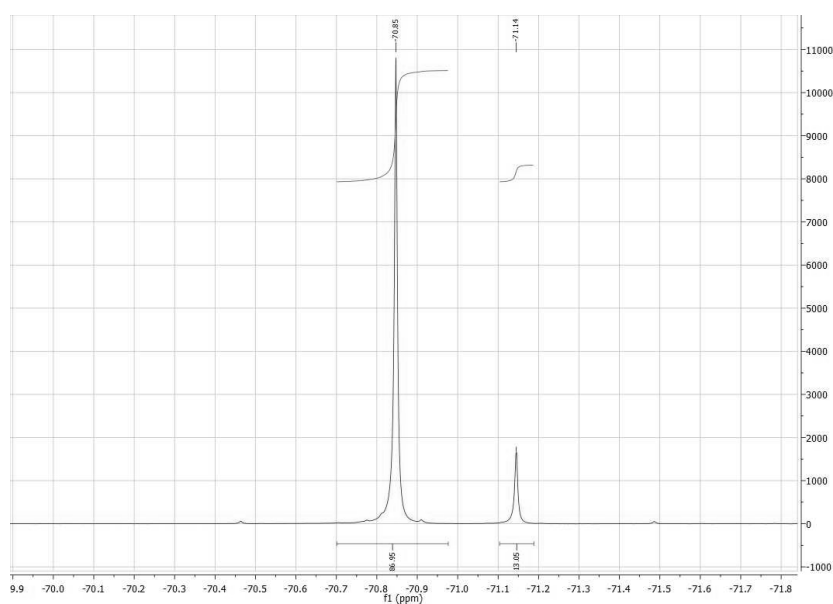


Figure 33 -  $^{19}\text{F}$  NMR spectrum of Mosher's ester of (S)-**60a** obtained through CBS reduction with catecholborane

## Section Summary

A three-step synthesis of **rac-50a** was developed with an overall yield of 57%. This route utilised a regioselective 3-position deprotonation of 4-chloropyridine with subsequent trapping with hydrocinnamaldehyde (**53a**) to afford secondary alcohol **60a·HCl**. An aromatic substitution of **60a·HCl** with dimethylamine gave DMAP derivative **51a**, which was acylated using acetic anhydride to afford the desired core structure **50a**.

Racemic **60a·HCl** was resolved to give **(S)-60a·HCl** and **(R)-60a·HCl**, both in greater than 99% *ee*, using preparative HPLC with a chiral stationary phase. These enantiopure compounds were then used in the synthesis of chiral DMAP derivatives **(S)-50a**, **(S)-68** and **(R)-64a**, which were obtained in 17%, 16% and 13% overall yield, respectively, including enantiomer separation (Figure 34).

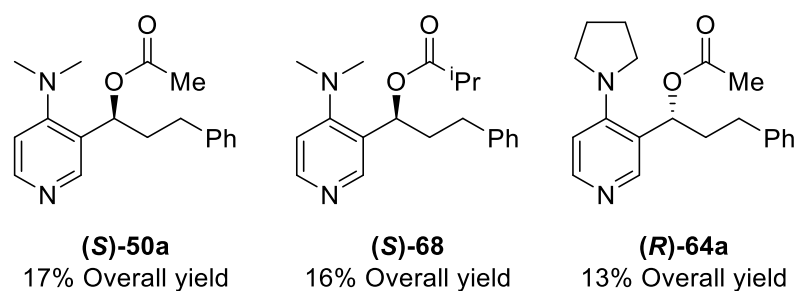


Figure 34 - Summary of catalysts synthesised

Attempts were made at the asymmetric synthesis of the DMAP derivatives shown in Figure 34 *via* enzymatic kinetic resolutions and oxidation/asymmetric reduction processes. The highest *ee* obtained was greater than 95%, but this was obtained in a 2% yield. A stoichiometric CBS reduction with catecholborane as the hydride source gave **60a** in 39% yield and 74% *ee*.

## Synthesis of Analogues

The synthesis of the catalyst core **50** can be achieved *via* a three-step synthetic procedure. Making modifications to the synthetic procedure means that diversity can be readily achieved at the pyridine 4-position. In order to achieve a greater level of diversity to allow for more parameters to be probed, a range of other structural modifications should be considered including variation in the aromatic stacking unit, linker substitution and alcohol derivatisation. The points of diversity desired (Figure 35) would require the following objectives to be achieved:

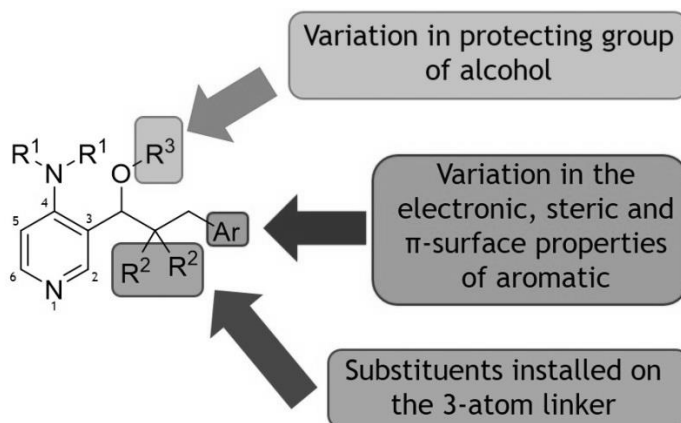


Figure 35 - Desired structural modification of DMAP core structure **50**

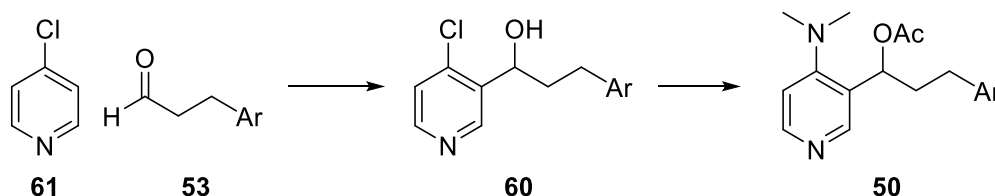
1. Synthesise 3-position substituted DMAP derivatives, with the following structural variations to probe the relationship between structure and cation- $\pi$  interactions
  - a. A three-atom length chain at the pyridine 3-position terminating in an aromatic group which includes variation in the electron, steric and  $\pi$ -surface properties.
  - b. A stereogenic centre on the three-atom linker which has been resolved to obtain a single stereoisomer and further variations in its protecting group.
  - c. Substitution of the three-atom linker to effect  $\pi$ -stacking interactions.



In order to meet these objectives a range of hydrocinnamaldehydes need to be synthesised to allow for variations to be introduced in the aromatic moiety and linker. A range of alcohol protecting groups could then be introduced.

## Linker Aromatic Unit Modification<sup>1</sup>

A synthetic route to the core structure **50** of the desired DMAP derivatives has been outlined (Scheme 28). However, in order to modify the aromatic moiety, essential for the stacking interaction, a range of hydrocinnamaldehyde derivatives first needed to be synthesised.



*Scheme 28 - Synthetic route to DMAP derivative core structure 50*

Several routes towards the synthesis of hydrocinnamaldehydes were investigated during this body of research and the results from these are outlined below. When considering synthetic routes, diversity of the aromatic group was key to the success of the synthesis, incorporating electron-donating, electron-withdrawing and extended  $\pi$ -surfaces into the system. This was in order to study the effects of  $\pi$ -surface and electronic properties on the formation of a cation- $\pi$  interaction.

In order to achieve the synthetic targets desired, a single route to all variations is preferable and key targets are anthryl, 4-nitrophenyl, 4-methoxyphenyl and 4-tolyl to

<sup>1</sup> Parts of this project were carried out in collaboration with Yiming Zhao as part of his studies towards a Masters degree in Chemistry. The contribution was steps towards the synthesis of (+)-**50d** and (+)-**50h**. These studies have previously been submitted as part of an MSc dissertation. They are included in this body of research for completeness of the narrative. All analytical data has been independently processed for this report.<sup>82</sup> Zhao, Y. Synthesis of chiral DMAP derivatives. The University of Birmingham, 2015.

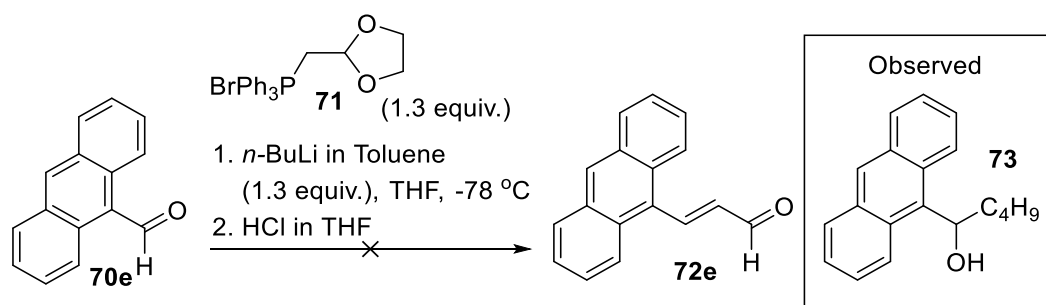
meet all the outlined criteria. Each hydrocinnamaldehyde derivative is required on a multi-gram scale in order to synthesise the required amount of each DMAP derivative. Therefore, cost effectiveness as well as scalability will be considered during the study of each synthetic route.

## Hydrocinnamaldehyde Derivatives Synthesis

Initial screening of synthetic routes to obtain hydrocinnamaldehydes was optimised for the 9-anthryl derivative, for which, at the time of writing, there have only been two reported syntheses.<sup>83-84</sup>

### *Wittig Approach*

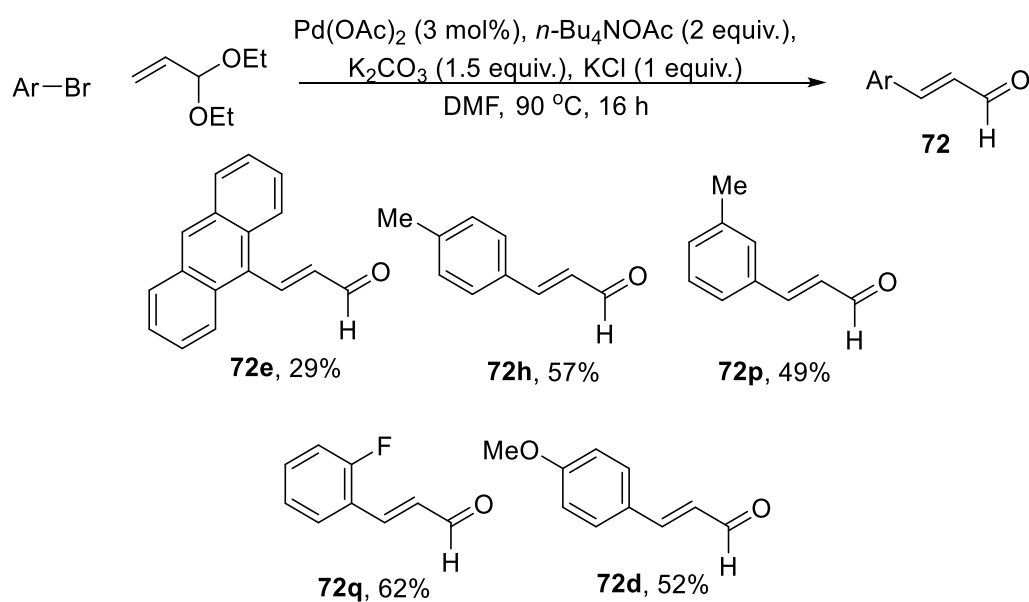
Hashizume *et al.* reported the synthesis of **72e** in 1994 utilising the Wittig reaction shown in Scheme 29 but this would then need to be chemoselectively reduced to provide the desired hydrocinnamaldehyde.<sup>83</sup> Phosphonium **71** is commercially available and the route would have allowed for a two-step synthesis to the desired compound. The reaction was initially attempted utilising lithium methoxide for the formation of the phosphorous ylide but only starting material was recovered. Therefore, the reaction was repeated with a stronger base (*n*-BuLi). This again did not provide the desired aldehyde, but instead secondary alcohol **73** was isolated in 63% yield. The observed product is most likely from the nucleophilic addition of the *n*-butyl anion to 9-anthraldehyde, which, based on the product observed and the yield obtained, suggests that the deprotonation did not occur and the ylide did not form.



*Scheme 29 – Attempt at the synthesis of 72e via a Wittig reaction*

Based on the unsuccessful attempt to synthesise **72e** via the above outlined Wittig approach, as well as the high cost of acetal phosphonium **71**, this route was not pursued further.

#### Heck Cross-Coupling Approach

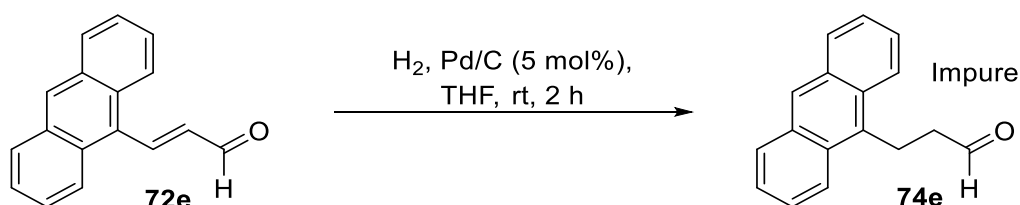


*Scheme 30 - Heck coupling to synthesise cinnamaldehyde derivatives 72d, e, h, p, q*

Several groups have reported the synthesis of compound **72e** through a Heck coupling of 9-bromoanthracene and acrolein diethyl acetal (Scheme 30), which would still require the olefin to be reduced chemoselectively.<sup>83, 85-89</sup> The palladium catalysed Heck cross-coupling was carried out and **72e** was obtained in 29% yield. The scope of the Heck reaction for the synthesis of cinnamaldehydes was then investigated, with a range of substituents studied.

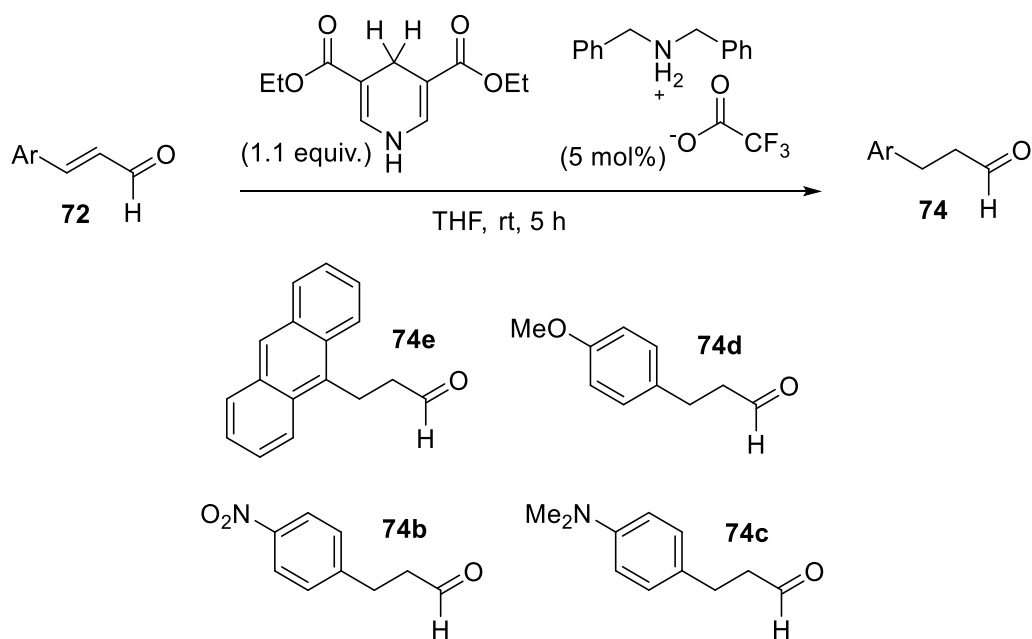
The reaction conditions were tolerant of both electron-rich (**72d**, **e**, **h**, **p**) and electron-poor (**72q**) aromatic bromides. The results obtained were in agreement with the literature report for electronic effects.<sup>85</sup>

With a range of cinnamaldehydes in hand, the reduction of their conjugated double bonds was the final task in the synthesis of the desired hydrocinnamaldehydes. Initially the procedure reported by Hashizume *et al.* was attempted using palladium on carbon to catalyse the olefin reduction by hydrogen.<sup>83</sup> Preliminary studies led to over-reduction of **72e** to obtain decomposition products and primary alcohol. When reaction times were reduced hydrocinnamaldehyde **72e** could be seen in the NMR spectrum of the crude material through the presence of two aldehyde signals and the appearance of aliphatic CH<sub>2</sub> signals. Despite numerous variations of the purification methods being attempted, including column chromatography and recrystallisation, aldehyde **74e** co-eluted with several by-products and could not be obtained with satisfactory purity.



*Scheme 31 - Hydrogenation of 9-anthrylcinnamaldehyde **72e** to give the corresponding hydrocinnamaldehyde **74e***

The palladium catalysed hydrogenation of cinnamaldehyde **72e** gave the desired compound (**74e**) in the presence of several co-eluting impurities, therefore an alternative method was investigated.



All products observed - coeluted with Hantzsch's pyridine

*Scheme 32 - Cinnamaldehyde olefin reduction with Hantzsch's pyridine*

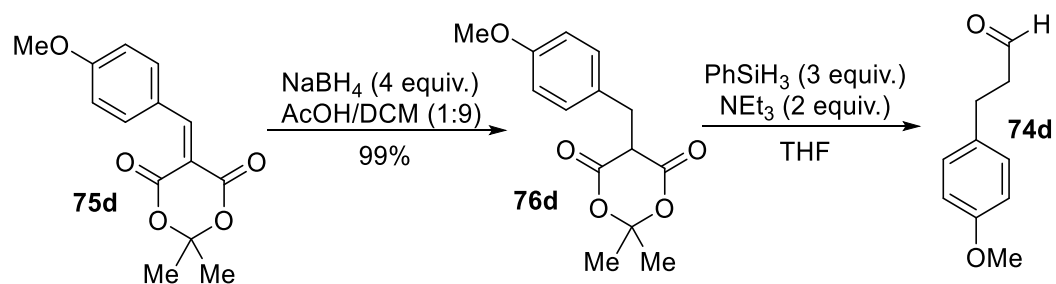
In 2004 List *et al.* reported the organocatalysed reduction of cinnamaldehydes, which utilised Hantzsch ester as the hydride source and an ammonium salt as the organocatalyst.<sup>90</sup> In their hands this route worked well, giving quantitative conversion to the desired product. However, when attempted as part of this study, it was found that the stoichiometric pyridine by-product from the reaction co-eluted with the hydrocinnamaldehydes formed, and several repetitions of purifications *via* column chromatography were needed to remove it. This route was therefore deemed less desirable due to the use of a palladium-catalysed cross coupling with variable yields, followed by an olefin reduction with products that were difficult to purify.

### *Meldrum's Acid Approach*

In 2007 Frost *et al.* reported the tandem molybdenum-catalysed hydrosilylation reaction outlined in Scheme 33.<sup>91</sup> This looked like a promising route, as Meldrum's acid derivatives (**75**) are readily synthesised from the Knoevenagel condensation of aldehydes with Meldrum's acid, meaning that this route affords hydrocinnamaldehydes in a two-step



Frost *et al.* also reported a second study two years later which overcame the low yields observed for electron-deficient substrates.<sup>92</sup> This required the reduction of a conjugated olefin followed by the hydrosilylation to afford the hydrocinnamaldehyde (Scheme 35). A key difference with this study was that although a second step was added into the sequence, it no longer required a molybdenum catalyst for the hydrosilylation.<sup>92</sup>

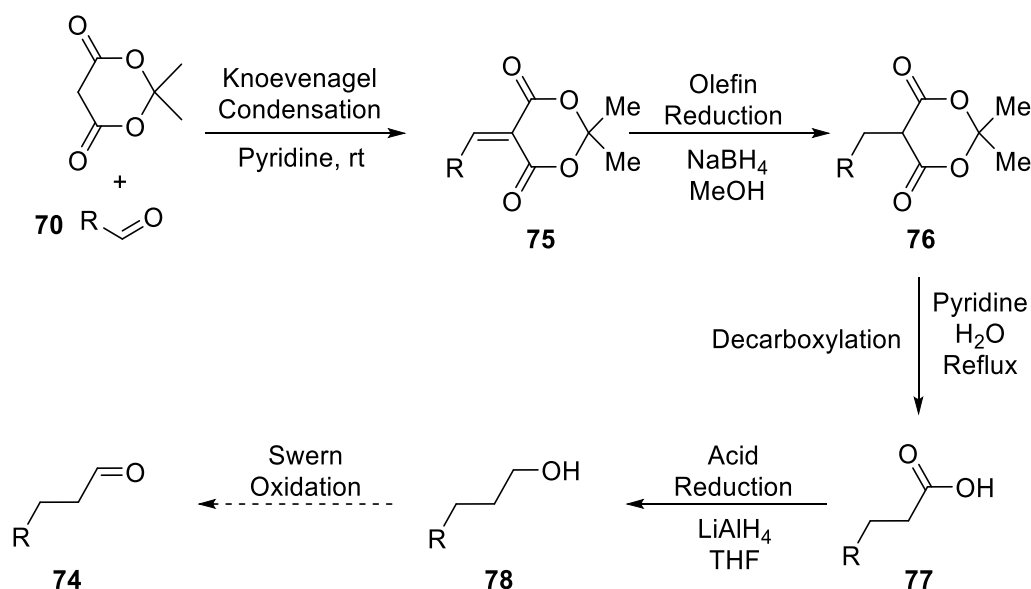


*Scheme 35 - Reduction of the Knoevenagel product conjugated double bond followed by hydrosilylation*

The two-step procedure in Scheme 35 was investigated with the 4-methoxyphenyl derivative **75b**, which had previously been used for the single-step process.<sup>92</sup> The olefin reduction was successful in quantitative yield with no need for purification beyond the reaction work-up. Additionally, the desired aldehyde could be observed in the  $^1\text{H}$  NMR spectrum of the crude material, apparently quantitatively. Even though promising results were obtained the relative cost of phenylsilane relative to the number of aldehydes and the quantities of each aldehyde required led to the search for a more economical approach.

In 2003 researchers at Glaxo-Smith-Kline (GSK) reported the synthesis of 3-(anthracen-9-yl)propan-1-ol (**78e**), which if oxidised would give an alternative route to the aldehyde (**74e**).<sup>93</sup> To obtain the desired hydrocinnamaldehydes, this would be a five-step synthesis in total (Scheme 36), four of which were published by GSK: a Knoevenagel condensation, olefin reduction, decarboxylation and a carboxylic acid reduction. With the addition of a Swern oxidation, the desired aldehydes would be obtained. Key points for this route are

that it was carried out on a 20-gram scale and no column chromatography was required during purification. Each step was well-established chemistry which has been proven to be efficient at the transformation required. However, the GSK route had only been carried out on a single substrate, starting with 9-anthraldehyde (**70e**) to afford 3-(anthracen-9-yl)propan-1-ol (**78e**) in an overall yield of 84% (4 steps). Therefore, a substrate scope study was embarked upon in an attempt to synthesise a range of hydrocinnamaldehyde derivatives utilising the GSK method to obtain the alcohol and then a Swern oxidation to obtain the desired aldehyde.<sup>94</sup>



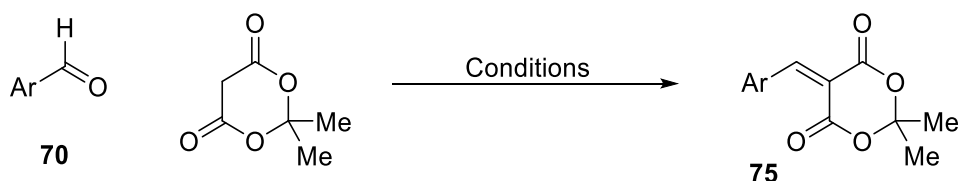
*Scheme 36 - General route for the synthesis of hydrocinnamaldehydes*

Synthesis of fourteen Meldrum's acid derivatives, encompassing a range of outlined desired properties, was carried out initially using the method by Frost *et al.* in water as solvent.<sup>91</sup> It was successful in the synthesis of *para*-nitro (**74b**), *para*-methoxy (**74d**) and *para*-dimethylamino (**74c**) derivatives, but it did not furnish the desired product when used with 9-anthraldehyde, most likely due to solvent incompatibility. At this stage the method by Andrews *et al.* (GSK) was investigated, which uses pyridine as the reaction solvent, and repeated with several of the previous substrates giving an increase in isolated



yield.<sup>93</sup> Furthermore, the anthryl Meldrum's acid derivative (**75e**) was obtained in 93% yield. This procedure was then applied to a range of substrates yielding the desired products in good to moderate yields (34-93%), except in the case of extremely electron-deficient substrates, such as *para*-trifluoromethyl. In this example, decomposition of the starting material was observed, with over 20 signals present in the <sup>19</sup>F NMR spectrum of the crude mixture, and no aldehyde remaining, judged by <sup>1</sup>H NMR spectroscopy. Dumas *et al.* reported a method which used an ammonium salt as a catalyst in benzene to yield the Knoevenagel condensation products in good yields with both electron-rich and electron-deficient substrates. This route was less than ideal as reported, due to the use of benzene. However, in this study benzene was substituted for toluene, obtaining similar conversions to that published. The same procedure also yielded the pentafluorophenyl derivative, which was not achievable with the initially studied sets of conditions. Both the *para*-trifluoromethyl (**75n**) and pentafluoro (**75o**) derivatives were not purified at this stage, due to some stability issues. Instead, when full conversion was determined to have been reached by <sup>1</sup>H NMR spectroscopic analysis of the crude reaction mixtures for these derivatives, they were taken forward to the next step.

Table 4 - Substrate scope for the Knoevenangel condensation of aromatic aldehydes with Meldrum's acid



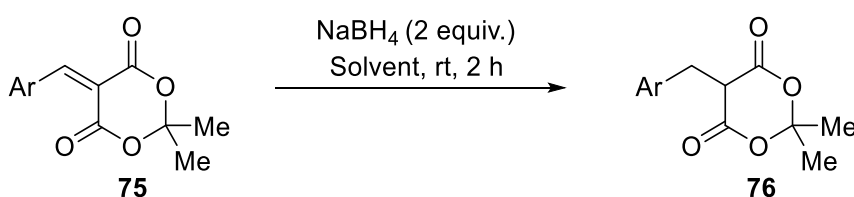
Entry	Substituent (Ar)	Conditions	Yield
1	4-NO <sub>2</sub> -C <sub>6</sub> H <sub>4</sub> - ( <b>75b</b> )	H <sub>2</sub> O, 75 °C, 2 h	79%
2	4-NO <sub>2</sub> -C <sub>6</sub> H <sub>4</sub> - ( <b>75b</b> )	Pyridine, rt, 15 h	74%
3	4-NMe <sub>2</sub> -C <sub>6</sub> H <sub>4</sub> - ( <b>75c</b> )	H <sub>2</sub> O, 75 °C, 2 h	87%
4	4-NMe <sub>2</sub> -C <sub>6</sub> H <sub>4</sub> - ( <b>75c</b> )	Pyridine, rt, 15 h	93%
5	4-OMe-C <sub>6</sub> H <sub>4</sub> - ( <b>75d</b> )	H <sub>2</sub> O, 75 °C, 2 h	75%
6	4-OMe-C <sub>6</sub> H <sub>4</sub> - ( <b>75d</b> )	Pyridine, rt, 15 h	91%
7	9-Anthryl ( <b>75e</b> )	H <sub>2</sub> O, 75 °C, 2 h	0%
8	9-Anthryl ( <b>75e</b> )	Pyridine, rt, 15 h	93%
9	2-Furyl ( <b>75f</b> )	Pyridine, rt, 15 h	91%
10	1-Pyrenyl ( <b>75g</b> )	Pyridine, rt, 15 h	88%
11	4-Me-C <sub>6</sub> H <sub>4</sub> - ( <b>75h</b> )	Pyridine, rt, 15 h	73%
12	4-OH-C <sub>6</sub> H <sub>4</sub> - ( <b>75i</b> )	Pyridine, rt, 15 h	67%
13	2-HCC-C <sub>6</sub> H <sub>4</sub> - ( <b>75j</b> )	Pyridine, rt, 15 h	56%
14	2-Br-C <sub>6</sub> H <sub>4</sub> - ( <b>75k</b> )	Pyridine, rt, 15 h	55%
15	3-Indole ( <b>75l</b> )	Pyridine, rt, 15 h	48%
16	2-Naphthyl ( <b>75m</b> )	Pyridine, rt, 15 h	34%
17	4-CF <sub>3</sub> -C <sub>6</sub> H <sub>4</sub> - ( <b>75n</b> )	Pyridine, rt, 15 h	0%
18	4-CF <sub>3</sub> -C <sub>6</sub> H <sub>4</sub> - ( <b>75n</b> )	Pyrollidinium acetate (10 mol%), Toluene, 50 °C, 36 h	N.D.*
19	C <sub>6</sub> F <sub>5</sub> - ( <b>75o</b> )	Pyrollidinium acetate (10 mol%), Toluene, 50 °C, 36 h	N.D.*

\*Compounds were taken to the next step without purification

With a range of condensation compounds synthesised, the next step was to reduce their conjugated double bonds. This was successfully carried out according to the method reported by Andrews *et al.*<sup>93</sup> giving high yields for all substrates with one exception. The 4-dimethylamino derivative gave a lower yield than expected (75%); however, this was

due to the work-up procedure of the reaction leading to a loss of material due to some minor decomposition. Additionally, it was found that for some substrates, the use of methanol as a solvent was not appropriate, as it caused the six membered malonate ring unit to open to the dimethyl malonate. Substituting ethanol for methanol stopped this transesterification reaction and furnished the desired compounds. For future repetition of these reactions, it would be advisable to use ethanol rather than methanol in all cases. The 2-furyl derivative proved to be problematic, showing limited solubility in numerous solvents including dichloromethane, chloroform, ethyl acetate and diethyl ether, making product isolation challenging. To obtain satisfactory mass spectrometry data and minimise fragmentation for **76**, some compounds were run in negative mode through the addition of ammonium salts.

*Table 5 - Reduction of Knoevenangel products to afford saturated Meldrum's derivatives 76b-h,j-l,n,o*

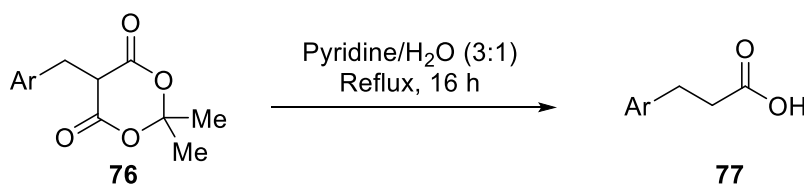


Entry	Substituent (Ar)	Solvent	Yield
1	4-NO <sub>2</sub> -C <sub>6</sub> H <sub>4</sub> - ( <b>76b</b> )	EtOH	99%
2	4-NMe <sub>2</sub> -C <sub>6</sub> H <sub>4</sub> - ( <b>76c</b> )	MeOH	75%
3	4-OMe-C <sub>6</sub> H <sub>4</sub> - ( <b>76d</b> )	EtOH	91%
4	9-Anthryl ( <b>76e</b> )	MeOH	N.D.
5	2-Furyl ( <b>76f</b> )	EtOH	87%
6	1-Pyrenyl ( <b>76g</b> )	MeOH	95%
7	4-Me-C <sub>6</sub> H <sub>4</sub> - ( <b>76h</b> )	EtOH	94%
8	2-HCC-C <sub>6</sub> H <sub>4</sub> - ( <b>76j</b> )	EtOH	88%
9	2-Br-C <sub>6</sub> H <sub>4</sub> - ( <b>76k</b> )	EtOH	88%
10	3-Indole ( <b>76l</b> )	EtOH	91%
11	4-CF <sub>3</sub> -C <sub>6</sub> H <sub>4</sub> - ( <b>76n</b> )	EtOH	98% (2 steps)
12	C <sub>6</sub> F <sub>5</sub> - ( <b>76o</b> )	EtOH	99% (2 Steps)

N.D. – Not determined and compound was taken to the next step containing residual water

Decarboxylation of derivatives **76** was carried out using the method reported by Andrews *et al.* and provided the desired compounds in acceptable to good yields, ranging from 48% to 98%.<sup>93</sup> Some unwanted by-products were observed for the *para*-methyl (**77h**) and *para*-methoxy (**77d**) derivatives. A small procedure modification, allowing the mixture to stir at room temperature for 1 hour before heating at reflux and reducing the reflux duration, yielded the compounds without requiring further purification. A minor impurity was also observed in the synthesis of the 2-furyl derivative **77f**, the desired compound again was poorly soluble in common laboratory solvents and therefore this impurity was taken through to the LiAlH<sub>4</sub> reduction. It was hoped that this impurity could then be removed utilising a technique such as column chromatography. The low yield for the 3-indole derivative **77i** was most likely due to product loss during reaction work-up, feasibly the compound may show some water solubility, especially at pH < 7.

Table 6 - Decarboxylation to synthesise hydrocinnamic acid derivatives **77b-h,j,l,n,o**



Entry	Substituent (Ar)	Yield
1	4-NO <sub>2</sub> -C <sub>6</sub> H <sub>4</sub> - ( <b>77b</b> )	65%
2	4-NMe <sub>2</sub> -C <sub>6</sub> H <sub>4</sub> - ( <b>77c</b> )	91%
3	4-OMe-C <sub>6</sub> H <sub>4</sub> - ( <b>77d</b> )	93% <sup>b</sup>
4	9-Anthryl ( <b>77e</b> )	80% (2 steps)
5	2-Furyl ( <b>77f</b> )	≤ 94% <sup>a</sup>
6	1-Pyrenyl ( <b>77g</b> )	98%
7	4-Me-C <sub>6</sub> H <sub>4</sub> - ( <b>77h</b> )	81% <sup>b</sup>
8	2-HCC-C <sub>6</sub> H <sub>4</sub> - ( <b>77j</b> )	86% <sup>a</sup>
9	3-Indole ( <b>77i</b> )	48%
10	4-CF <sub>3</sub> -C <sub>6</sub> H <sub>4</sub> - ( <b>77n</b> )	63%
11	C <sub>6</sub> F <sub>5</sub> - ( <b>77o</b> )	91%

<sup>a</sup>Compound taken forward containing impurities <sup>b</sup>Modified conditions: Pyridine/H<sub>2</sub>O (3:1), 1 h at rt followed by 4 h reflux

With a range of hydrocinnamic acid derivatives in hand, the penultimate synthetic transformation was the reduction of the carboxylic acid groups to primary alcohols to afford the hydrocinnamyl alcohol derivatives. This was achieved *via* a lithium aluminium hydride (LiAlH<sub>4</sub>) reduction in THF, which gave the corresponding alcohols in 83% to 99% yields, with the exception of the LiAlH<sub>4</sub> reduction of **77n** and **77o**.

Table 7 - Reduction of carboxylic acids to afford hydrocinnamyl alcohols **78c-e,g,h,j,l,n,o**

$$\text{Ar}-\text{CH}_2-\text{CH}_2-\text{COOH} \xrightarrow[\text{THF, } 0^\circ\text{C to rt, 16 h}]{\text{LiAlH}_4 (1.2 \text{ equiv.})} \text{Ar}-\text{CH}_2-\text{CH}_2-\text{CH}_2-\text{OH}$$

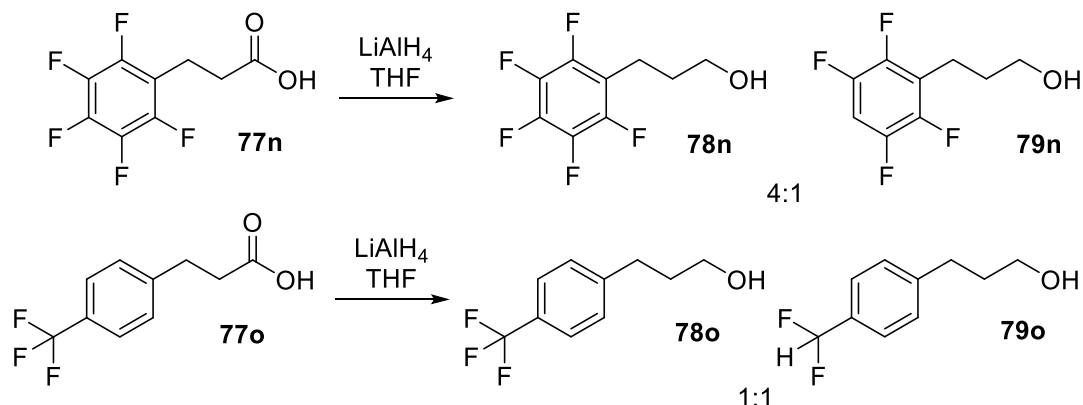
**77**  **78**

Entry	Substituent (Ar)	Yield
1	4-NMe <sub>2</sub> -C <sub>6</sub> H <sub>4</sub> - ( <b>78c</b> )	93%
2	4-OMe-C <sub>6</sub> H <sub>4</sub> - ( <b>78d</b> )	95%
3	9-Anthryl ( <b>78e</b> )	99%
4	1-Pyrenyl ( <b>78g</b> )	99%
5	4-Me-C <sub>6</sub> H <sub>4</sub> - ( <b>78h</b> )	83%
6	2-HCC-C <sub>6</sub> H <sub>4</sub> - ( <b>78j</b> )	53%
7	3-Indole ( <b>78l</b> )	66%
8	4-CF <sub>3</sub> -C <sub>6</sub> H <sub>4</sub> - ( <b>78n</b> )	N.D.*
9	C <sub>6</sub> F <sub>5</sub> - ( <b>78o</b> )	N.D.*

\*Reaction conditions led to partial fluorine substitution

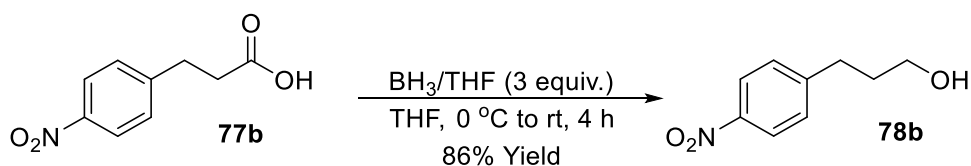
A major by-product was observed in the material isolated from the synthesis of fluorinated derivatives **78n** and **78o** which, by <sup>1</sup>H NMR spectroscopic analysis, appeared to have a similar structure to the desired compounds (Scheme 37). The pentafluoro derivative underwent a nucleophilic aromatic substitution (S<sub>N</sub>Ar) displacing one of the fluorine substituents to give **79n**. This was determined by GC mass spectrometry, where a mass of this by-product was found to be 208 m/z. additionally, an aromatic proton was observed in the <sup>1</sup>H NMR spectrum of the mixture. This had previously been demonstrated in the literature with similar substrates.<sup>95</sup> The *para*-trifluoromethyl derivative (**78n**) underwent a hydride-fluoride exchange to give the *para*-difluoromethyl compound **79o**

as a major impurity as determined by mass spectrometry and  $^1\text{H}$  NMR spectroscopy of the mixture, and has also previously been reported for similar compounds.<sup>96</sup>



*Scheme 37 - By-products formed during the lithium aluminium hydride reduction of fluorinated hydrocinnamic acids*

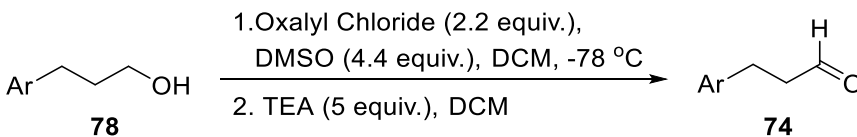
Due to the incompatibility of some substrates with  $\text{LiAlH}_4$ , an alternative and milder method to reduce carboxylic acids was investigated. Aromatic nitro compounds are also not compatible with  $\text{LiAlH}_4$  and have been shown to form diazo compounds upon exposure to  $\text{LiAlH}_4$ . Borane was found to be a suitable alternative, the reduction of the 4-nitro derivative **77b** was successfully carried out, obtaining a good yield of **78b** (86%) using borane in THF. This procedure should also be applicable to the fluorinated derivatives.



*Scheme 38 - Borane reduction of 4-nitro derivative 77b*

Hydrocinnamyl alcohol derivatives **78** obtained from the  $\text{LiAlH}_4$  reduction were then oxidised to the corresponding aldehydes **74** using a Swern oxidation. These reactions proceeded in 66-89% yield (Table 8).

Table 8 - Swern oxidation of cinnamoyl alcohols to give corresponding hydrocinnamaldehyde derivatives **74b,d,e,g,h,j**



Entry	Substituent (Ar)	Yield
1	4-NO <sub>2</sub> -C <sub>6</sub> H <sub>4</sub> - ( <b>74b</b> )	84%
3	4-OMe-C <sub>6</sub> H <sub>4</sub> - ( <b>74d</b> )	84%
4	9-Anthryl ( <b>74e</b> )	89%
5	1-Pyrenyl ( <b>74g</b> )	66%
6	4-Me-C <sub>6</sub> H <sub>4</sub> - ( <b>74h</b> )	83%
7	2-HCC-C <sub>6</sub> H <sub>4</sub> - ( <b>74j</b> )	77%

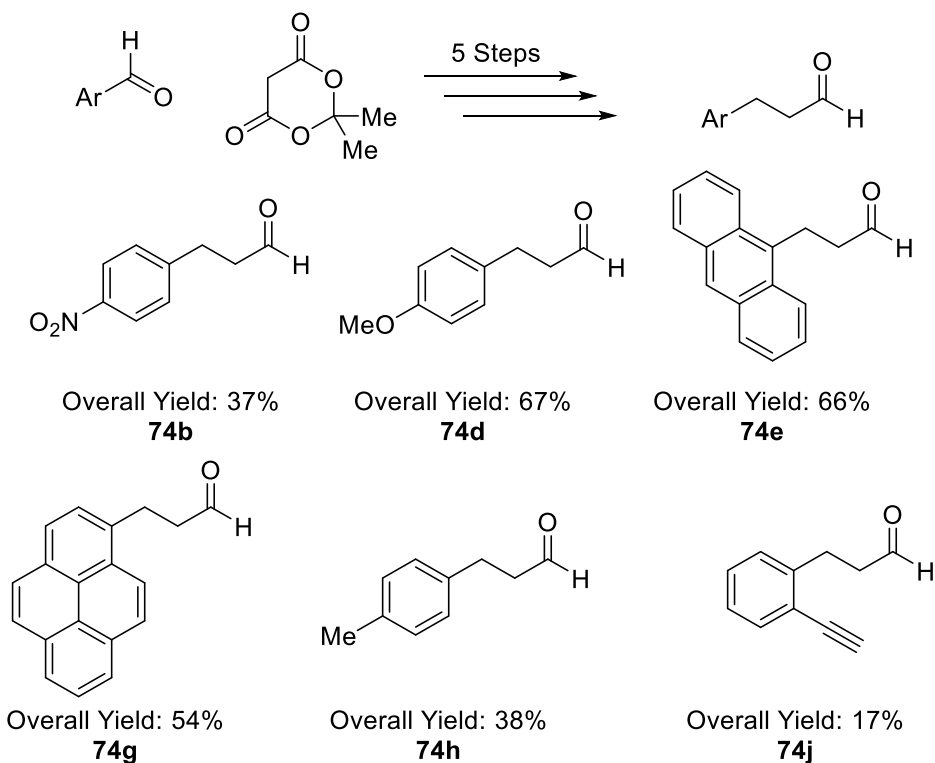


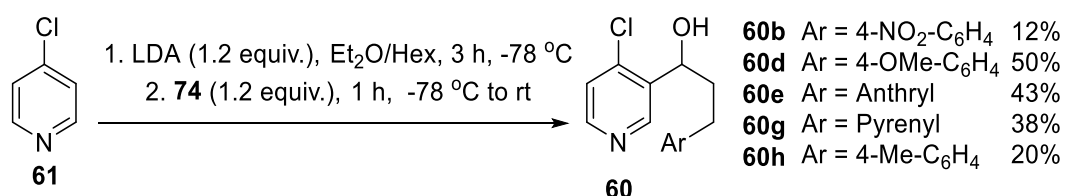
Figure 36 - summary of five step synthesis of hydrocinnamaldehyde derivatives with overall yields

The outlined five-step synthesis of aldehydes **74** was successful in providing a range of derivatives in acceptable yields (17-67%, Figure 36). A single set of conditions were not applicable to all substrates. By-products were observed in the LiAlH<sub>4</sub> reduction of **77n** and **77o**, the decarboxylation of **76d** and **76h** but modifications to the synthetic procedure can minimise their formation.

# Synthesis of DMAP Derivatives with Phenyl Modifications

Aldehydes **74b,d,e,g,h** were selected from those synthesised in order to probe the effects of the aromatic unit electronics and  $\pi$ -surface on the outcome of catalysis and the effects they may have had on the formation of cation- $\pi$  interactions. The derivatives chosen were 9-anthryl and 1-pyrenyl for their extended  $\pi$ -surface, 4-tolyl and 4-methoxyphenyl as electron rich aromatic moieties and 4-nitrophenyl as an electron deficient moiety.

Using the regioselective 3-position deprotonation with LDA methodology developed in the previous section 4-chloropyridine derivatives **60b,d,e,g,h** were synthesised in 20-50% yield from 4-chloropyridine (**61**). Attempts were also made to synthesise **60c** (4-NMe<sub>2</sub>-C<sub>6</sub>H<sub>4</sub>) however the product decomposed after isolation. The aldehyde equivalents were reduced from 1.5 equivalents to 1.2 equivalents in order to decrease the amount of waste.

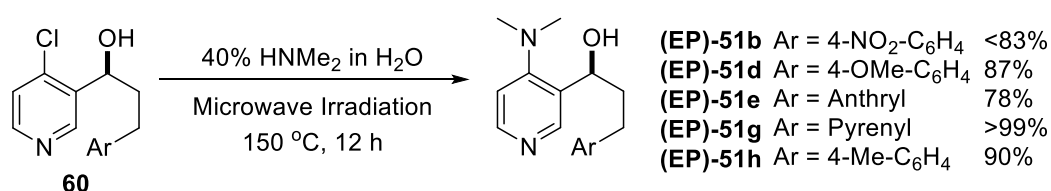


*Scheme 39 - 3-Position derivatisation of 4-chloropyridine with synthesised hydrocinnamaldehydes 74b,d,e,g,h*

With the five racemic 4-chloropyridine derivatives **60b,d,e,g,h** in hand attention focused on the separation of enantiomers by preparative HPLC with a chiral stationary phase. This was successfully achieved in all cases in greater than 99% *ee*, more information and HPLC traces can be found in the appendix. For reasons of clarity and simplicity, enantiopure compounds that are precursors (**60** and **51**) to the targets **50b,d,e,g,h** will be assigned the stereochemical descriptor '(EP)-', the final compound will be assigned a descriptor based on the optical rotation.

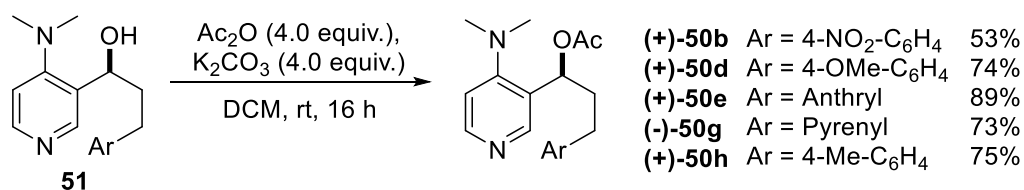


The nucleophilic aromatic substitution of 4-chloropyridine derivatives **(EP)-60b,d,e,g,h** was carried out in a microwave assisted manor to afford the desired DMAP derivatives **(EP)-51b,d,e,g,h** in 78-99% yield. A lower than expected yield (78%) was obtained for anthryl derivative **(EP)-51e**, this was most likely due to the limited solubility of the substrate in the reaction solvent. Nitro derivative **(EP)-51b** was isolated with a co-eluting decomposition by-product, which had not previously been observed for other derivatives. This compound was taken to the next step with the by-product still present.



*Scheme 40 - Aromatic substitution of 4-chloropyridine derivatives to afford DMAP derivatives (EP)-51b,d,e,g,h*

The acylation of the secondary alcohols **(EP)-51b,d,e,g,h** to give **(+)-50b,d,e,h** and **(-)-50g** was carried out with acetic anhydride and was self-catalysing. Acylation was successful for all five substrates with isolated yields ranging from 73-89% yield. This furnished five derivatives in eight steps from commercially available starting materials that contained a diverse range of aromatic groups suitable for probing cation- $\pi$  stacking in catalysis.

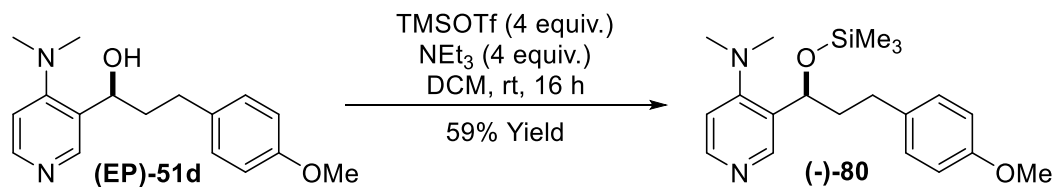


*Scheme 41 - Acylation of DMAP derivatives to afford (+)-50b,d,e,h and (-)-50g*

## Silylated Derivative

The silylation of secondary alcohol **(EP)-51d** can be carried out using DMAP catalysis. Therefore, similar to the acylation reactions for the synthesis of **(+)-50b,d,e,h** and **(-)-50g**, this process was self-catalysing and consequently only the addition of base was required

to aid catalyst turnover. Silylation of **(EP)-51d** was carried out affording DMAP derivative **(-)-80** in 59% yield.



*Scheme 42- Silylation of (EP)-51d to afford (-)-80*

## Substitution of Methylene Linker

Substitution on the linker, such as the example shown in Figure 37, cannot be achieved using the methodology previously developed as the quaternary carbon cannot be introduced using the developed Meldrum's acid approach. Fortunately, aldehyde **83** had previously been reported meaning that a similar modified procedure for the synthesis of DMAP derivative **83** could be employed.<sup>97</sup>

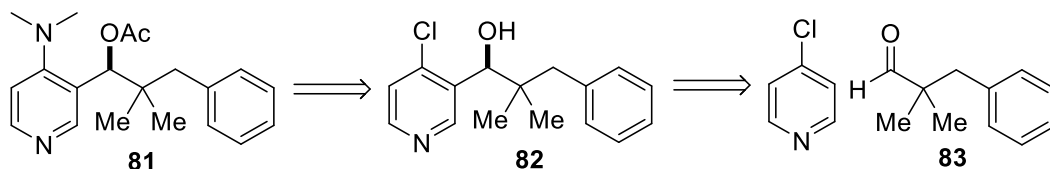
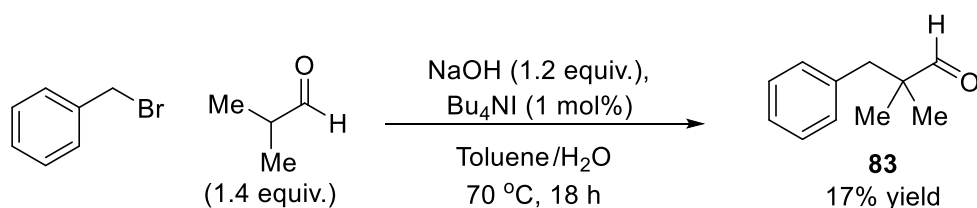


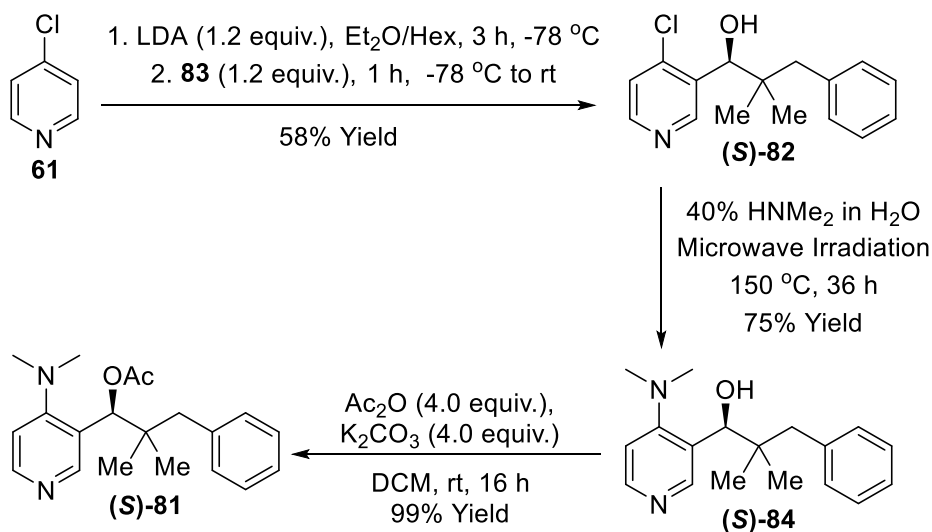
*Figure 37 - Retrosynthetic analysis of 81*

Aldehyde **83** was obtained *via* the substitution of benzyl bromide with the *in-situ* formed enolate of isobutyraldehyde in 17% yield after product purification by column chromatography and distillation (Scheme 43). A key point of this transformation was the distillation of the isobutyraldehyde immediately prior to performing the reaction in order to remove any of the carboxylic acid. Presence of the carboxylic acid lead to the ester formation which had a similar  $R_f$  to the desired compound.



*Scheme 43 - Synthesis of substituted aldehyde 83*

With aldehyde **83** in hand the synthetic route for the regioselective 3-position deprotonation of 4-chloropyridine previously developed could be utilised in the synthesis of DMAP derivative **81** (Scheme 44). The regioselective deprotonation of **61** was carried out in a 58% yield, which was higher than observed for aldehydes **74b,d,e,g,h** under the same conditions. The enantiomers of **82** were separated using preparative HPLC with a chiral stationary phase to afford the (*S*)-**82** as a single enantiomer in greater than 99% *ee*.



*Scheme 44 - Synthesis of linker substituted DMAP derivative (S)-81*

Crystals of (*S*)-**82** suitable for X-ray diffraction studies were obtained (Figure 38). The absolute stereochemistry was determined to be *S* with a Flack parameter of -0.003(3). It should be noted that  $\pi$ - $\pi$  stacking was not observed in the solid state between either the pyridine moiety or the aromatic side arm unit in either the single molecule or the packed structure.

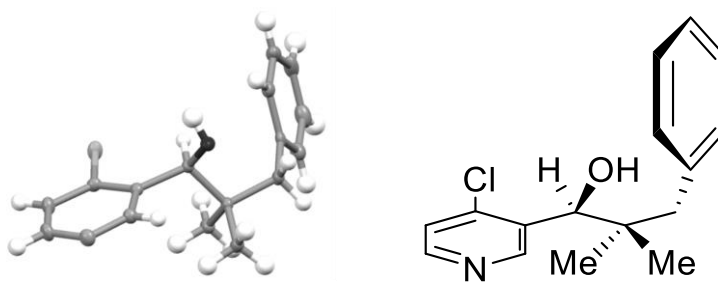


Figure 38 - Crystal structure of (S)-82 with ellipsoids drawn at the 50 % probability level. The absolute structure has been determined from the diffraction data, with the stereocentre being S

The aromatic substitution reaction of **(S)-82** to afford **(S)-84** was more troublesome, needing an extended reaction time (36 hours *versus* 12 hours) when compared to the unsubstituted derivatives. This may be due to the increased steric effect around the pyridine 4-position causing a retardation of the rate of reaction. Finally, the acylation of secondary alcohol **(S)-84** was carried out in near quantitative conversion to afford DMAP derivative **(S)-81**.

## Increasing Linker Rigidity

A design was sought that would increase linker rigidity to encourage the cation- $\pi$  interactions *via* pre-organisation of the aromatic moiety and DMAP core. When considering the system developed by Spivey<sup>29, 36-37</sup>, if a stereogenic centre was introduced in to the catalyst rather than using atropisomerism, then chiral induction may still occur. Additionally, if an extra  $sp^3$  carbon was inserted in-between the DMAP core and the aromatic sidearm then this would give a 3-atom linker which was less flexible than the systems previously outlined. The design of derivative **85** was conceived and the previously designed synthetic procedure utilising the regioselective 3-position deprotonation with LDA of 4-chloropyridine (**61**) was deemed to be applicable to its synthesis.

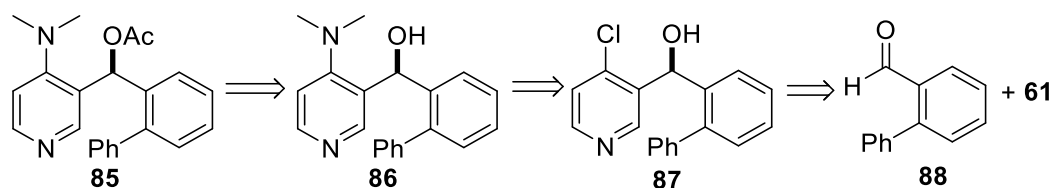
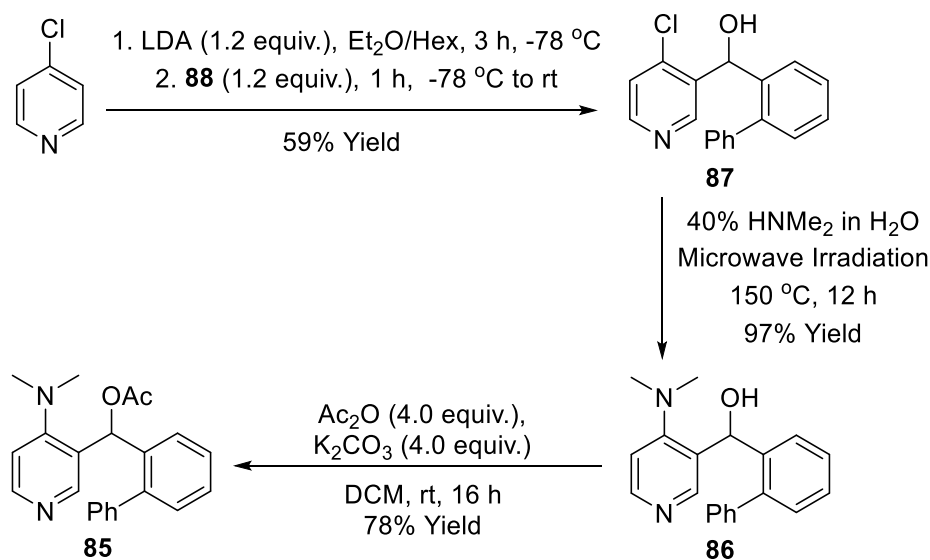


Figure 39 - Retrosynthetic analysis of derivative **85**

Commercially available aldehyde **88** would be converted to derivative **85** in a three-step process using the methodology developed for the synthesis of **50**. The 3-position deprotonation of pyridine **61** and subsequent reaction with aldehyde **88** was achieved in an acceptable 59% yield. 4-Aminopyridine derivative **86** was synthesised by the aromatic substitution of 4-chloropyridine **87** with dimethylamine, which was carried out in a 97% yield and alcohol acylation of **86** to give **85** was achieved in a 78% yield. Unfortunately, despite much effort none of the three racemic compounds could be enantiomerically resolved with preparative HPLC on the Phenomenex cellulose-1 preparative chiral column available.



Scheme 45 - Synthesis of DMAP derivative **85**

Crystals of **87** were obtained from slow evaporation of chloroform from the NMR sample. A structure was obtained from the data set collected however a large amount of disordered solvent was present in the crystals, therefore a SQUEEZE algorithm in

PLANTON was applied to the dataset in order to resolve the data successfully. Additionally, there were two crystallographically independent molecular conformations present in the crystals, one of which is shown in Figure 40, details of both conformations can be found in the appendix. It should be noted that  $\pi$ - $\pi$  stacking was not seen between either the pyridine moiety or the aromatic side arm unit in either of the conformations in the solid state.

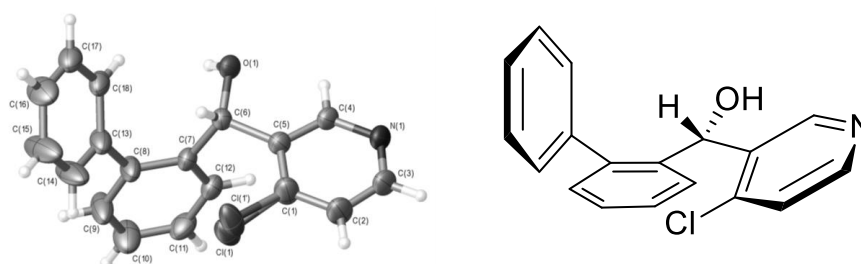


*Figure 40 - Crystal structure of Molecule 1 of 87 with ellipsoids drawn at the 50 % probability level. The structure contains two crystallographically-independent molecules of which only one is shown. The chlorine atom Cl(1)/Cl(1') is disordered over two*

An alternative route to the synthesis of **85** was developed due to the desire to use HPLC with a chiral stationary phase for the resolution of enantiomers (Figure 41). Carbon-carbon bonds between two aromatic units can be readily synthesised by a Suzuki cross-coupling, which would then allow for the installation of the phenyl unit. 2-Bromobenzaldehyde is commercially available and therefore the derivative could again be obtained using the previously designed methodology utilising the regioselective 3-position deprotonation with LDA of 4-chloropyridine (**61**).

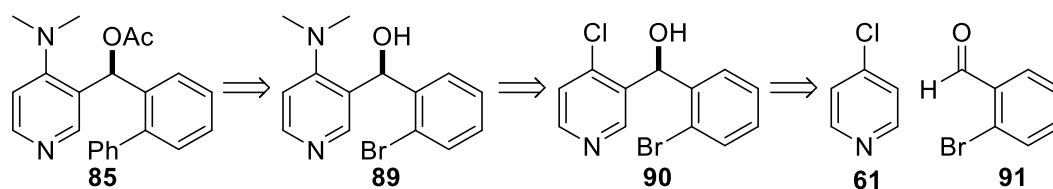
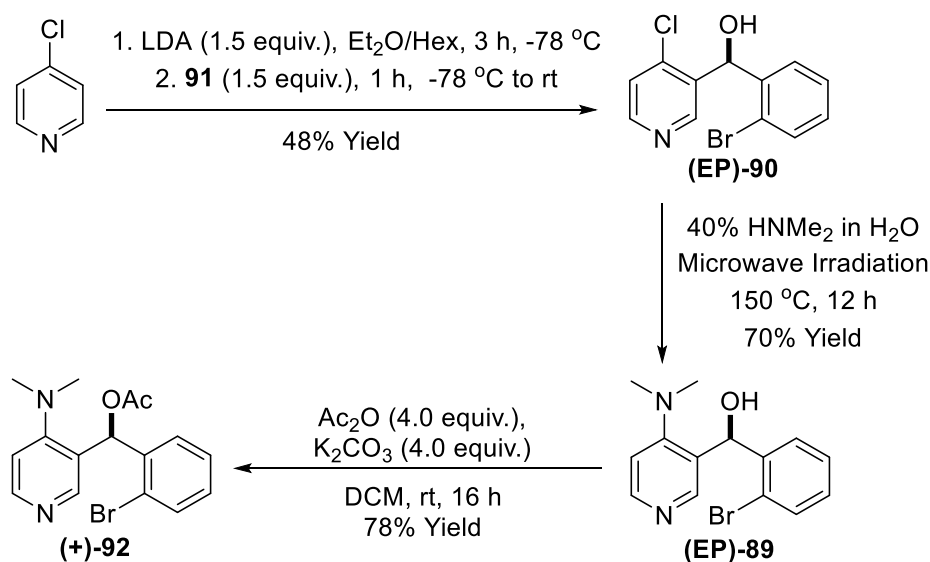


*Figure 41 - Alternative retrosynthetic analysis of 85*

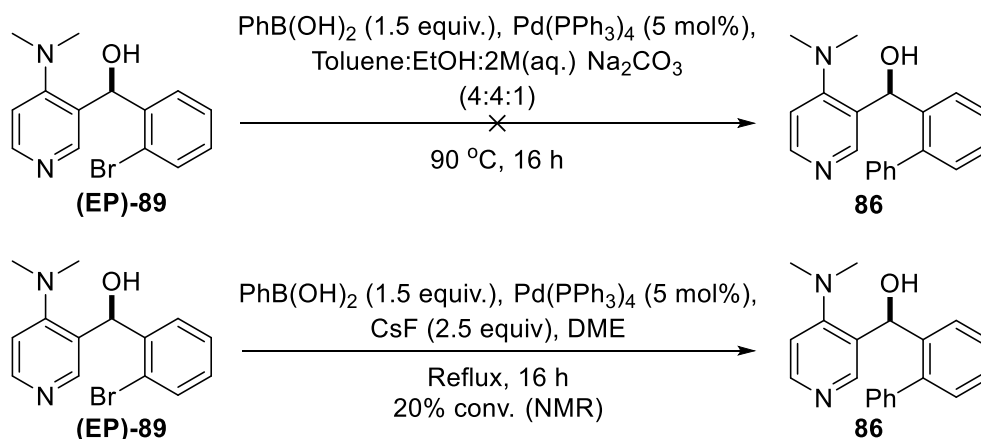
Deprotonation of pyridine **61** with LDA and subsequent reaction with 2-bromobenzaldehyde (**91**) was achieved in a 48% yield to give **90**. Derivative **90** was

resolved *via* preparative HPLC with a chiral stationary phase to obtain **(EP)-90** as a single enantiomer. The aromatic substitution of **(EP)-90** with dimethylamine to afford DMAP derivative **(EP)-89** was carried out in a 70% yield. The final step was the alcohol acylation of **(EP)-89** to give **(+)-92**, which was achieved in a 78% yield.



*Scheme 46 - Synthesis of bromophenyl derivative (+)-92*

Attempts were made to carry out the Suzuki coupling on secondary alcohol **(EP)-89**, however these were unsuccessful under two different sets of conditions (Scheme 47).<sup>36</sup> The first, which used a mixed reaction solvent system of toluene, ethanol and saturated aqueous sodium carbonate, led to quantitative recovery of the starting material. The failure of the reaction was most likely due to incompatible reaction conditions, where the starting materials were not soluble in the aqueous media. The second conditions, which used DME as solvent and CsF as an additive, did appear to give a small amount of the desired compound, as well as starting material and a large amount of an unidentifiable by-product in a 1:2:2 ratio respectively by <sup>1</sup>H NMR spectroscopic analysis of the reaction mixture. Due to time constraints this reaction was not investigated further.



*Scheme 47 - Suzuki cross-coupling to synthesise 86*

## Section Summary

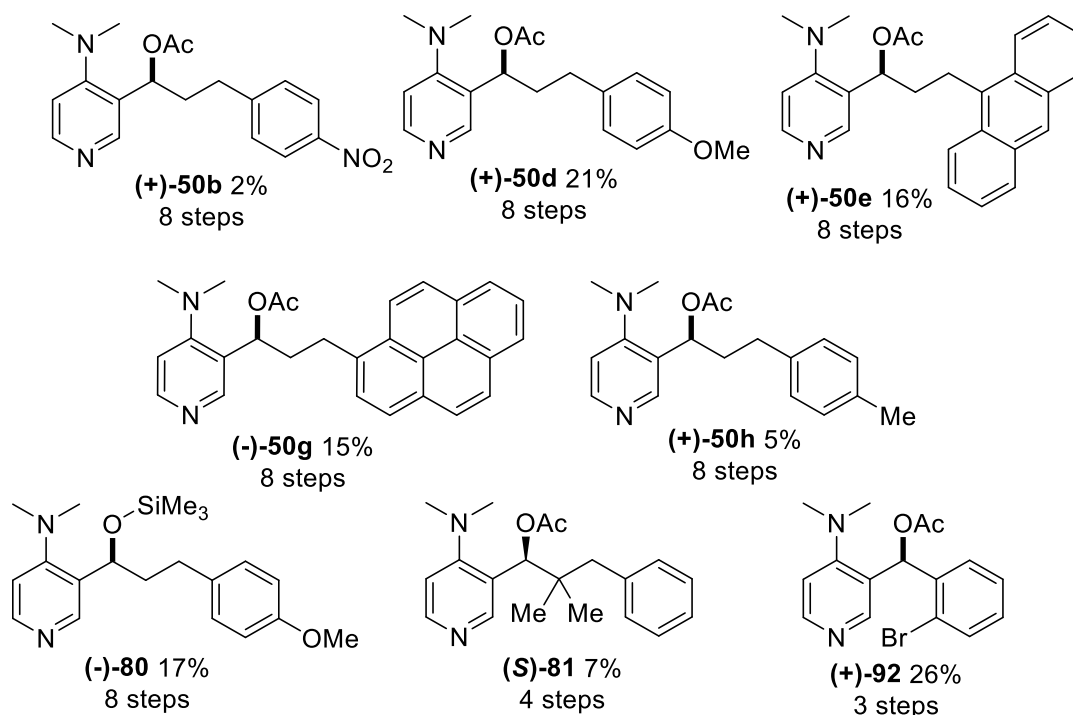


*Figure 42 - Summary of synthesised catalysts and their yields and total steps from commercially available starting materials*

A five-step synthesis to obtain a structurally diverse range of hydrocinnamaldehydes was developed, some of which were then in the synthesis of a range of DMAP derivatives using the methods developed in the previous chapter. In total, eight enantiopure (>99% ee) derivatives ((+)-**50b,d,e,h**, (-)-**50g**, (-)-**80**, (S)-**81** and (+)-**92**) were synthesised, which contain structural variations in the aromatic unit, the secondary alcohol derivatisation and



substitution on the three-atom linker. These were obtained in overall yields of between 7% and 26%. It should be noted that the overall yields do not include the percentage recovery from the separation of enantiomers and only includes the yields from synthetic transformations. The values for the percentage recovery of enantiomers can be found in the experimental section.

# Synthesis of 3,5-Disubstituted DMAP Derivatives

The synthesis of 3-substituted derivatives **50** has been outlined in the previous two sections, this was achieved through the synthesis of a library of hydrocinnamaldehyde derivatives. These were then utilised in the trapping of 3-position deprotonated 4-chloropyridine, which were subsequently used in the synthesis of a range of 3-derivatised DMAP derivatives.

As an addition to the catalyst library a selection of 3,5-disubstituted catalysts were also desired (Figure 43). This was in order to produce a comparable  $C_2$ -symmetric system to the single arm systems. It was felt that the  $C_2$ -symmetry would decrease complexity in the catalyst, specifically removing the challenge of controlling rotation of the pyridinium nitrogen-carbonyl bond though the introduction of symmetry. Therefore, facial selectivity for the approach of the nucleophile was no longer required as both faces of the DMAP core would be equivalent. The effects of the  $C_2$ -symmetry would be investigated through catalytic studies and comparisons to their single arm counterparts.

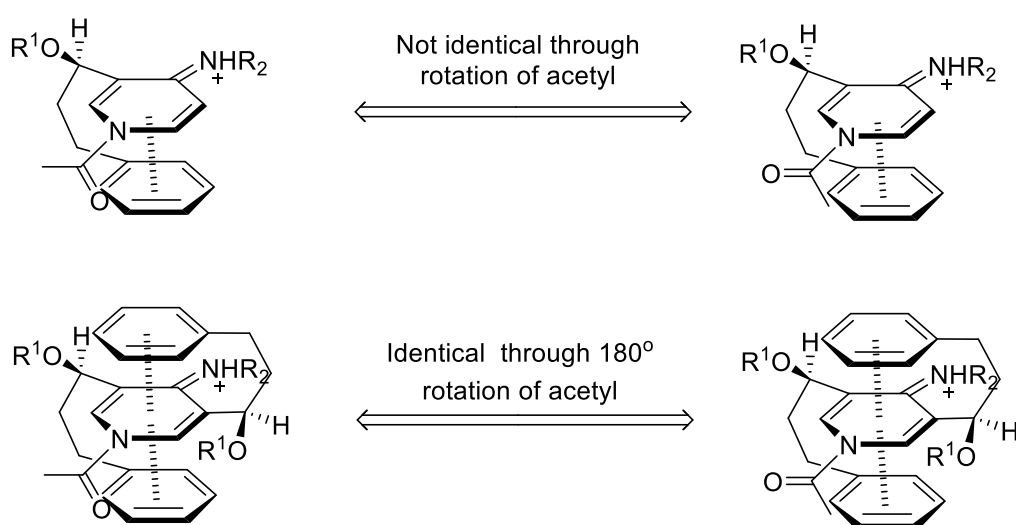
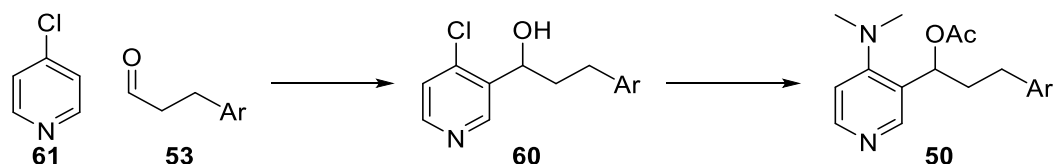


Figure 43 - Comparison of 3-substituted and 3,5-disubstituted DMAP derivatives

Based on the aims of this section the following objective needed to be met:

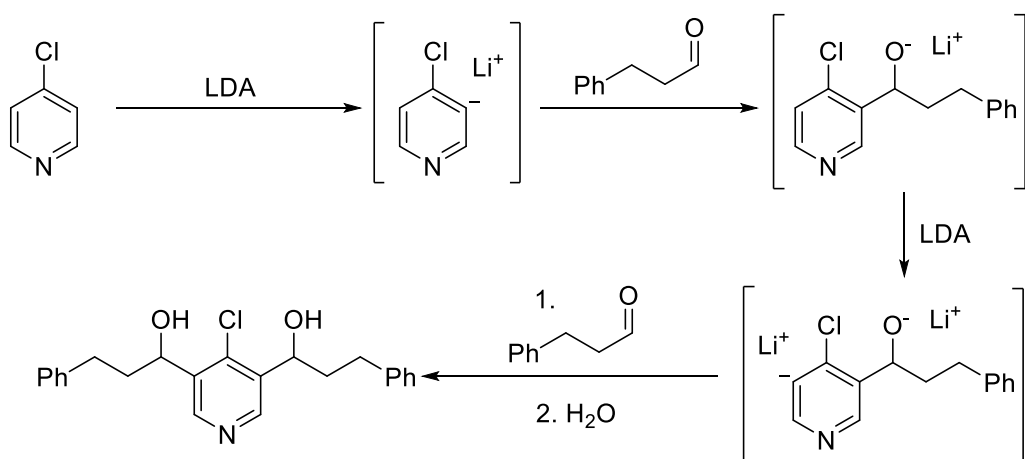
1. Synthesise 3,5-position di-substituted  $C_2$ -symmetric DMAP derivatives, the design of which will be carried forward from knowledge gained from the 3-substituted systems.

## Application of previously developed route



*Scheme 48 - synthetic route to DMAP derivative core structure*

In the previous two sections a synthetic route to the core structure of the desired single arm DMAP derivatives was outlined (Scheme 48). The key step was a regioselective 3-position deprotonation using LDA followed by trapping with hydrocinnamaldehydes. This proved to be effective in yielding the desired structures. Therefore, initial work focused on expanding this methodology to a double deprotonation process in a 3,5-position arrangement. This would be achieved *via* the sequential addition of LDA and aldehyde to yield the desired compounds.

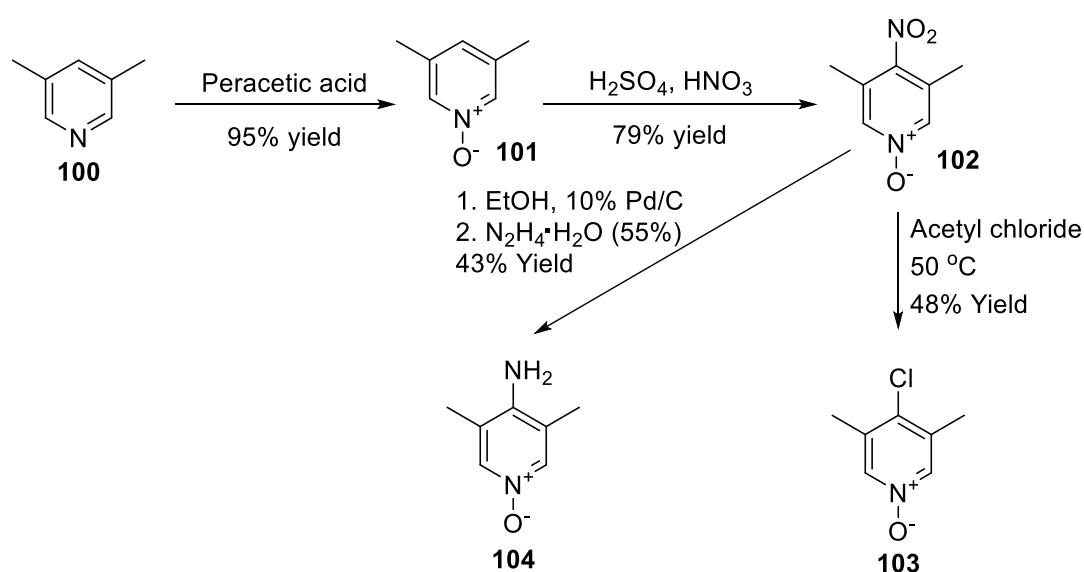


*Scheme 49 Sequential regioselective deprotonations to afford a 3,5-substituted DMAP derivative*

The route shown in Scheme 49 was attempted, which utilised the consecutive addition of LDA and aldehyde. It was observed that the first addition was successful, which had been previously shown for the single arm systems, however the second addition led to the formation of a mixture of several unidentifiable compounds. Therefore, a series of parallel different approaches were embarked upon. A new approach was needed in order to synthesise the desired structures.

## Lutidine Modifications

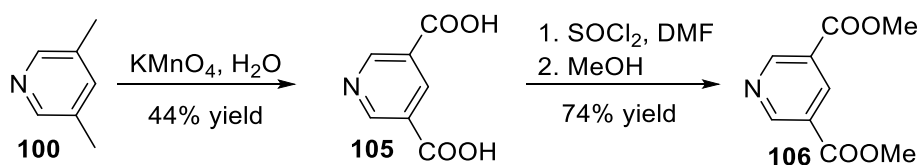
3,4,5-Substituted pyridines have previously been reported, having been synthesised through the modification of lutidine (3,5-dimethylpyridine). Although the most widely studied were simplistic systems, it was hoped that this methodology could be adapted to give compounds desired in this study.<sup>71, 98-99</sup> The most intriguing of these reports were from the 1950's and although the synthetic routes seem robust the analytical data was sparse compared to techniques now available, such as NMR. Therefore, some of this work was repeated to validate structure determination and investigate the usefulness of the transformations (Scheme 50).



*Scheme 50 - Lutidine N-Oxide formation and subsequent 4-position modifications*

3,5-Lutidine (**100**) can be readily converted to *N*-oxide **101** by reacting it with peracetic acid<sup>99</sup>, **101** can then be nitrated under standard conditions to give **102**.<sup>98</sup> Two further reactions were then carried out to give either 4-chloro derivative **103**<sup>71</sup> after an aromatic substitution reaction with acetyl chloride or 4-amino derivative **104**<sup>98</sup> after the nitro reduction was carried out with palladium.

Accessing **102-104** demonstrated that compounds could be obtained which could be implemented in synthetic procedures previously developed for the single-arm catalyst systems, such as the displacement of 4-chloropyridines to give the DMAP core. However, in order for the described pyridine 4-position transformations to be useful, derivatisation of the 3,5-methyl groups was required. There are only a few reports of the modification of 3,5-lutidine to afford symmetric pyridines, It was believed that the most synthetically useful transformation of those reported was the oxidation to afford the dicarboxylic acid **105** which was carried out with potassium permanganate.<sup>100</sup> Dicarboxylic acid **105** was converted to the corresponding diester **106** through *in situ* formation of the acid chloride followed by quenching with methanol to afford **106**.<sup>101</sup>

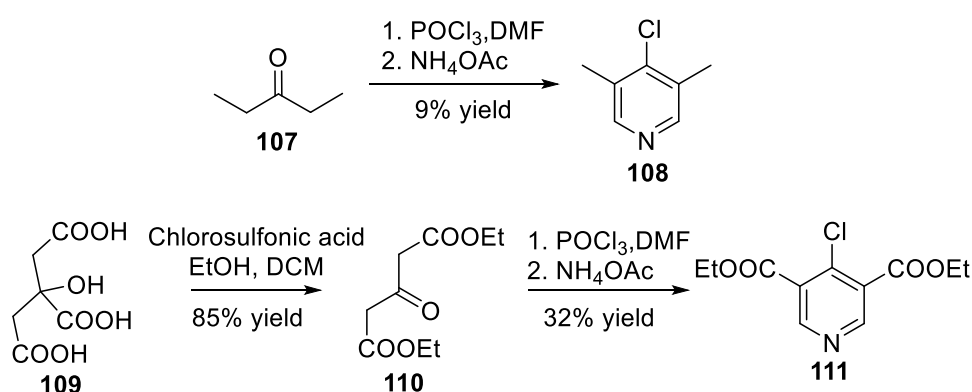


*Scheme 51 - Methyl oxidation of 3,5-lutidine*

Although the transformations were viable on model systems, the lack of literature precedent alongside the large number of synthetic steps required to build the level of complexity required in this project led to a search for viable alternatives.

## Vilsmeier-Haack Reaction

The Vilsmeier-Haack reaction had been reported to synthesise 4-chloro-3,5-diphenylpyridine, from 1,3-diphenylpropan-2-one and *in situ* formed Vilsmeier reagent (DMF and POCl<sub>3</sub>), as well as several other related non-symmetrical pyridines.<sup>102</sup> The reaction allows for the facile introduction of complexity, however, the reported compounds were not useful to obtain those desired in this study.



*Scheme 52 – Utilisation of the Vilsmeier-Haack reaction towards the synthesis of 3,4,5-substituted pyridines*

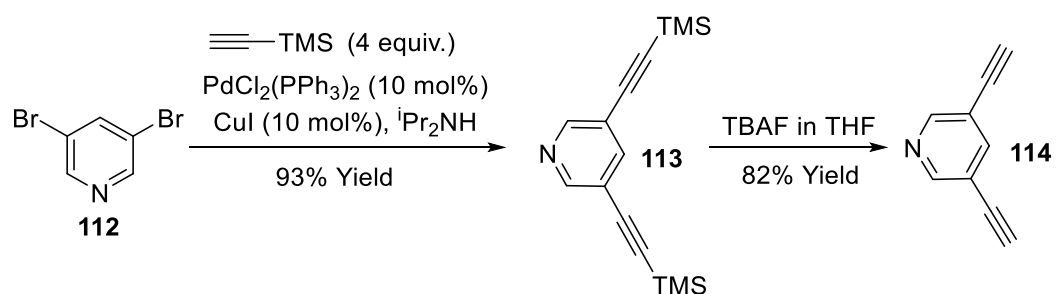
Precedent was not found for the installation of aliphatic or carbonyl substituents in the 3,5-positions of the synthesised pyridines, however if this were possible this would furnish an alternative route for similar compounds to those desired in a lower number of synthetic transformations than outlined above *via* the modification of 3,5-lutidine. The applicability of the synthetic procedure was probed initially through the synthesis of 3,5-dimethyl-4-chloropyridine (**108**), which was successfully carried out using the literature conditions in 9% overall yield (Scheme 52).<sup>102</sup> With the desired compound obtained from the first trial it was attempted to increase the complexity of the synthesised compounds. Esters in the 3- and 5- positions of pyridine would provide useful synthetic handles for the synthesis of the desired DMAP derivatives. Ketone **110** was readily synthesised from citric acid (**109**) in 85% yield. This was then successfully implemented in the Vilsmeier-Haack

reaction to afford diester **111** in 32% yield producing a core which could be derivatised to yield DMAP-like catalysts.

## Sonogashira Reaction

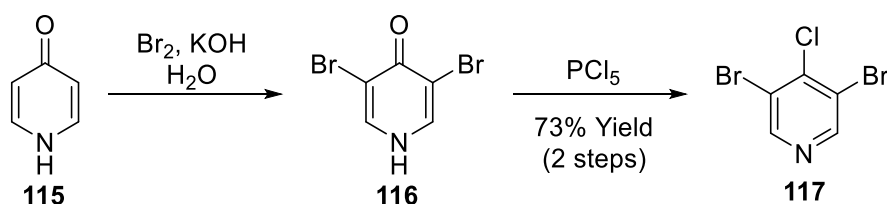
The Sonogashira reaction is an extensively studied palladium catalysed carbon-carbon bond forming transformation which allows for the introduction of alkynes into substrates by coupling the  $sp$  hybridised carbon of a terminal alkyne typically with the  $sp^2$  carbon of an aryl or vinyl halide or triflate.<sup>103</sup>

3,5-Dibromopyridine (**112**) is commercially available and the Sonogashira reaction can be used to afford **113** which can subsequently be deprotected with TBAF to afford bis-alkyne **114** in a 75% yield over two steps (Scheme 53).<sup>104</sup>



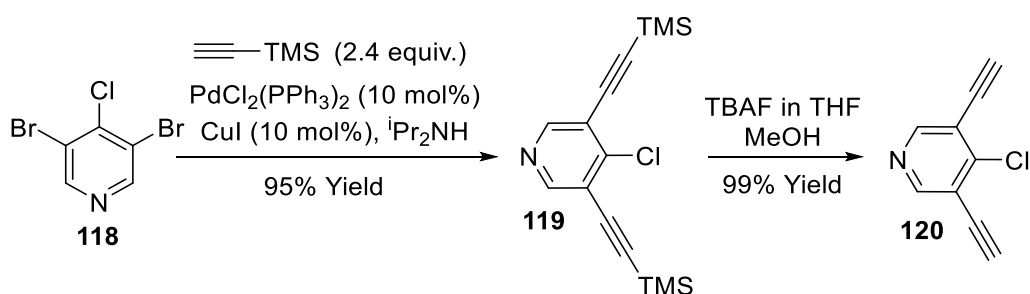
*Scheme 53 – Sonogashira reaction to synthesise dialkyne 114 from 3,5-dibromopyridine*

To apply the Sonogashira reaction to the synthesis of 3,4,5-substituted catalyst systems a 4-substituted pyridine was required with bromides in the 3- and 5-positions. In order to use methodology developed for the 3-substituted derivatives in subsequent steps, 4-chloro-3,5-dibromopyridine **117** was synthesised in 73% yield through the bromination of 4-pyridone followed by chlorination.<sup>105</sup>



Scheme 54 - Synthesis of 3,5-dibromo-4-chloropyridine (**117**) from 4-pyridone (**115**)

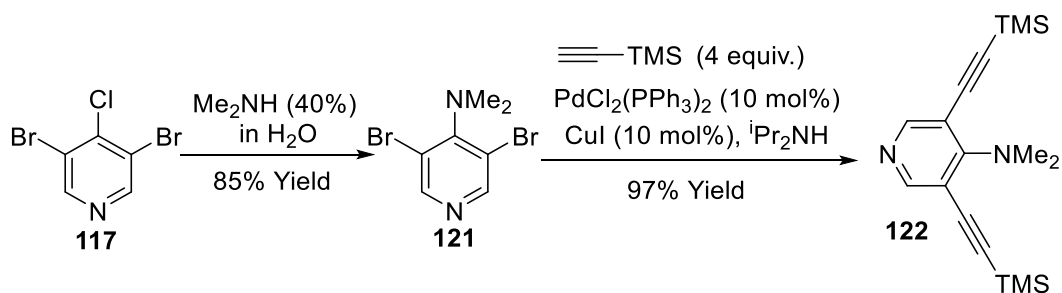
With pyridine **117** in hand, the Sonogashira reaction was carried out to afford **119** in 95% yield, which could be deprotected with TBAF in THF/Methanol to give the desired bis-alkyne **120**. The addition of methanol led to the *in situ* quenching of the carbanion formed from the TMS cleavage, this was required because when the deprotection was attempted without the addition of methanol decomposition was observed. Alternative deprotection conditions of potassium carbonate in methanol were also investigated, however 4-position substitution was observed to give the 4-methoxy ether due to the presence of *in situ* formed potassium methoxide.



Scheme 55 - Sonogashira reaction to synthesise dialkyne **120** from 3,5-dibromo-4-chloropyridine (**118**)

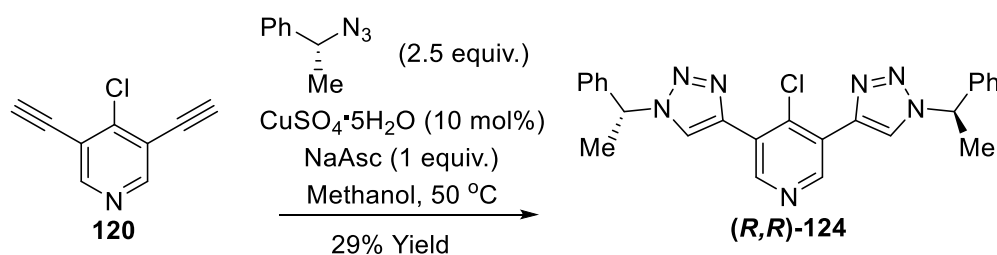
It is also possible to carry out the 4-position nucleophilic aromatic substitution of 3,5-dibromo-4-chloropyridine (**117**) with dimethylamine to synthesise DMAP derivative **121** in 85% yield (Scheme 56). The Sonogashira coupling remains high yielding furnishing dialkyne **122** in a 97% yield.





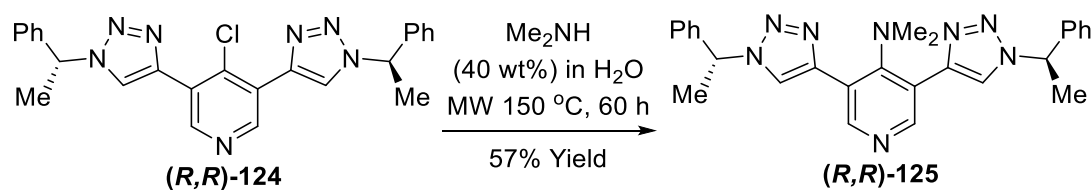
*Scheme 56 - Sonogashira reaction to synthesise dialkyne 122 from 3,5-dibromo-4-dimethylaminopyridine (121)*

With 3,5-dialkynes **120** in hand it was envisaged, in collaboration with William Brittain (doctoral research in Fossey group), that a 1,3-dipolar cycloaddition with a chiral azide would produce a chiral  $\text{C}_2$ -symmetric DMAP derivative. The copper catalysed azide-alkyne cycloaddition (CuAAC) is a quintessential reaction for the synthesis of 1,4-triazoles, which are versatile chemical entities for a wide range of applications.<sup>106-107</sup> The  $\text{C}_2$ -symmetric 4-chloropyridine derivative (***R,R***-**124**) can be synthesised through the CuAAC of dialkyne **120** with (*R*)-(1-azidoethyl)benzene, which can be synthesised from (*R*)-1-phenylethanol,<sup>108</sup> in 29% yield as an enantiopure single diastereoisomer (Scheme 57).



*Scheme 57 - Synthesis of (*R,R*)-124 via a Double CuAAC*

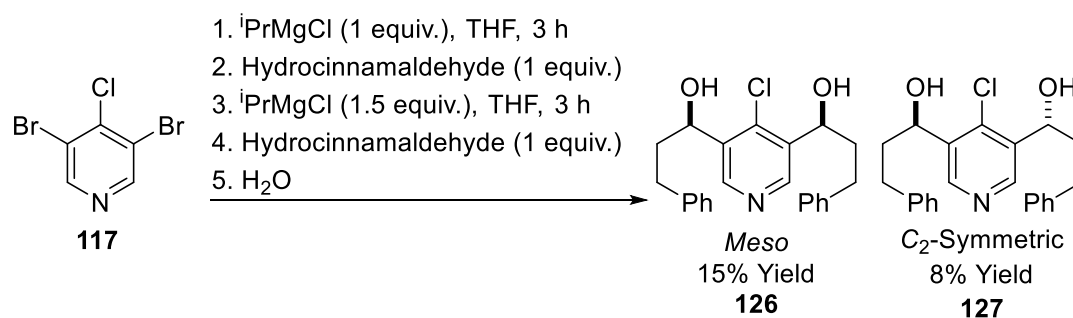
$\text{C}_2$ -Symmetric DMAP derivative (***R,R***-**125**) can be synthesised through the nucleophilic aromatic substitution of (***R,R***-**124**) with dimethylamine in 57% yield (Scheme 58). The reaction time need to be extended when compared to the 3-derivatised systems, it can be hypothesised that this was due to the increased sterics around the 4-position of pyridine.



*Scheme 58 - Synthesis of C<sub>2</sub>-symmetric DMAP catalyst (R,R)-125*

## Grignard Reaction

Grignard reagents are synthesised through the insertion of magnesium into a carbon-halogen bond. This is typically carried out in one of two ways, either through reacting organohalides with metallic magnesium or alternatively a transmetallation between an organohalide and a highly reactive Grignard reagent, such as isopropylmagnesium chloride.<sup>109</sup> 3,5-Dibromopyridines have been used in the formation of Grignard reagents through a transmetallation, the majority of reports show a single transmetallation and electrophilic trapping, however there were reports of a sequential process being performed.<sup>110</sup>



*Scheme 59 - Synthesis of C<sub>2</sub>-symmetric 4-chloropyridine 127 with a double Grignard transmetallation*

Dibromopyridine **117** was subjected to sequential addition process of isopropylmagnesium chloride and hydrocinnamaldehyde as an electrophile (Scheme 59) to afford a statistical mixture of *meso* and C<sub>2</sub>-symmetric diols **126** and **127**. Although a 1:1 ration of *Meso*:C<sub>2</sub> was observed in the crude reaction mixture, the desired C<sub>2</sub>-symmetric compound (**127**) was second to elute from the silica column and several fractions had co-eluted with the *meso* isomer (**126**) leading to a reduction in isolated yield. The two

diastereoisomers were distinguished by single crystal X-ray crystallography, crystals of **126** were successfully grown and determined to be *meso* (Figure 44), the relative stereochemistry of compound **127** was assigned by association.

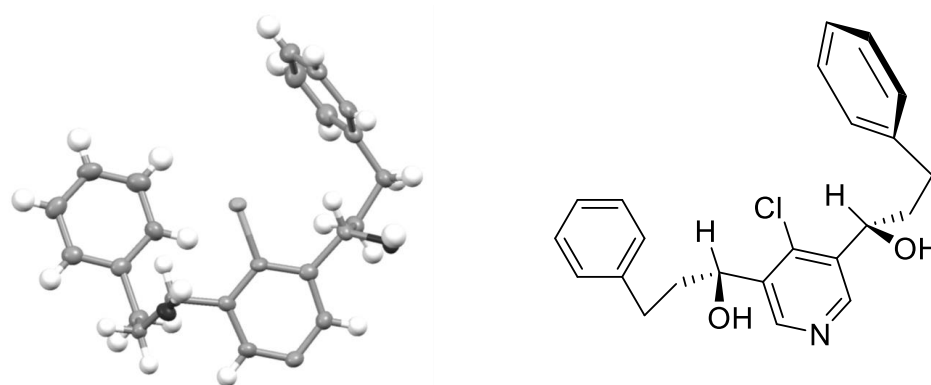
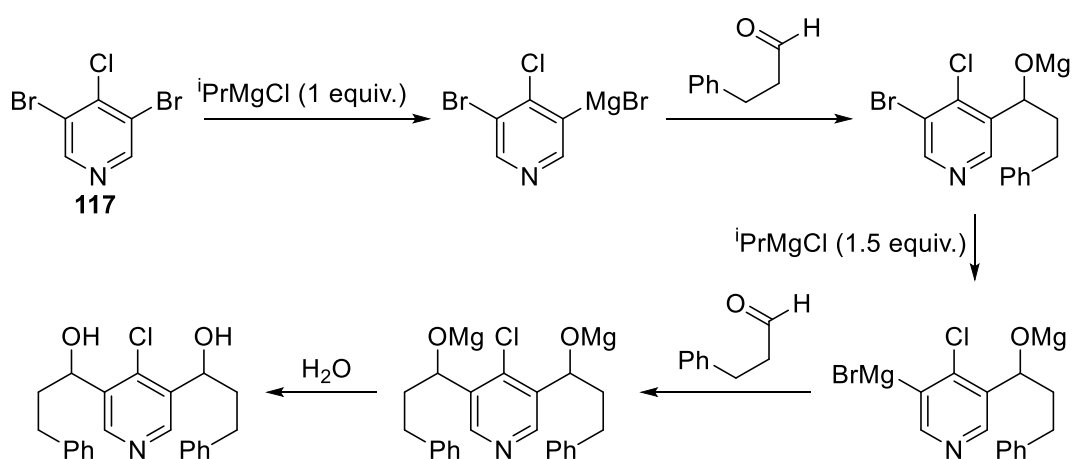


Figure 44 – X-Ray crystal structure of **126** (*Meso*) with ellipsoids drawn at the 50 % probability level.

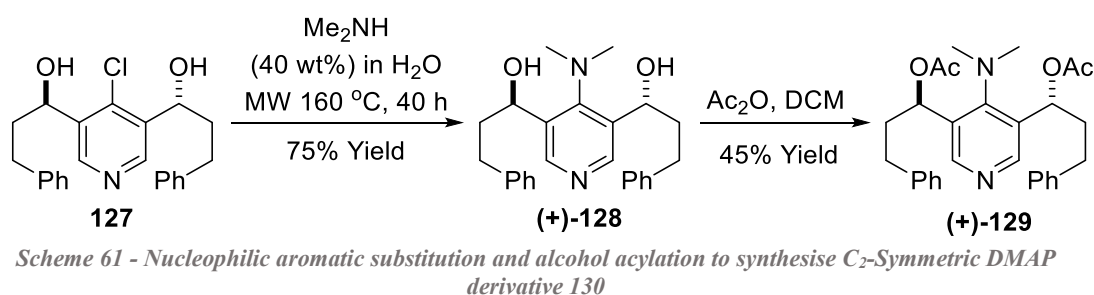
The stepwise scheme for this process can be seen in Scheme 60, where **117** is subjected to one equivalent of isopropylmagnesium chloride followed by quenching with hydrocinnamaldehyde as an electrophile. The resulting alkoxide is exposed to a second aliquot of Grignard reagent causing a second transmetallation of the remaining bromide, which is subsequently quenched with a second portion of hydrocinnamaldehyde affording the desired diol after aqueous workup.



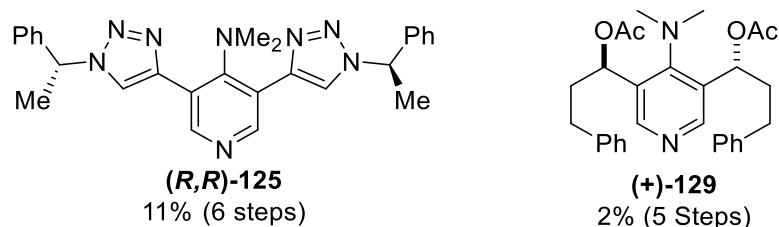
Scheme 60 - Double Grignard transmetallation to synthesise diols **126** (*Meso*) and **127** (*C<sub>2</sub>*)

4-Chloropyridine **127** was not separable by preparative chiral HPLC on the cellulose-1 column available, therefore the racemic compound was carried forward to the next step.

The nucleophilic aromatic substitution with dimethylamine was successfully carried out in acceptable yield (75%) after the reaction time was increased from 16 hours to 40 hours to afford DMAP derivative **128**. Diol **128** was separable by chiral preparative HPLC on cellulose 1 in greater than 99% *ee*, thus far the determination of the absolute configuration has not been achieved. Due to the small amount of sample obtained at this penultimate stage (10.1 mg), chiral derivatisation and enantiomer determination was not viable. Diol (**EP**)-**128** was acylated in a 45% yield to afford the enantiopure *C*<sub>2</sub>-symmetric DMAP derivative (**+**)-**129** in an overall yield of 2% over three steps.



## Section Summary



In this section two *C*<sub>2</sub>-symmetric DMAP catalysts were synthesised as single enantiomers. The first was synthesised *via* a double copper catalysed azide alkyne cycloaddition (CuAAC) with dialkyne **120**, which had been synthesised from dibromopyridine **117**, to afford DMAP derivative (***R,R***)-**125** in 11% overall yield. The second was synthesised *via* a sequential Grignard transmetalation, electrophile trapping process on dibromopyridine

**117** to afford, after substitution with dimethylamine and acylation, compound **(+)-129** in 2% overall yield.

# Catalysis

This section will address the following objectives:

1. Test the synthesised 3-position substituted chiral DMAP derivatives in the kinetic resolution of secondary alcohols.

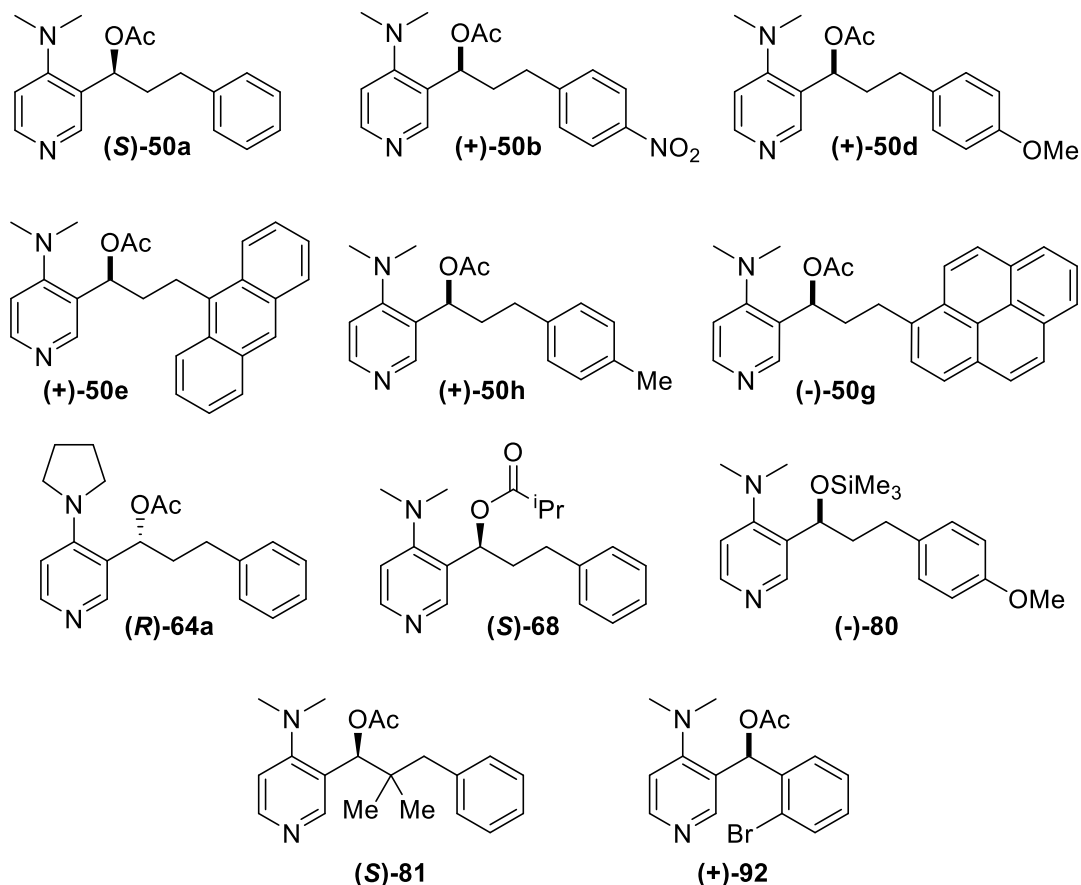


Figure 46 - Summary of 3-position DMAP derivatives synthesised as single enantiomers

2. Test the synthesised 3,5-position di-substituted chiral DMAP derivatives in the kinetic resolution of secondary alcohols.

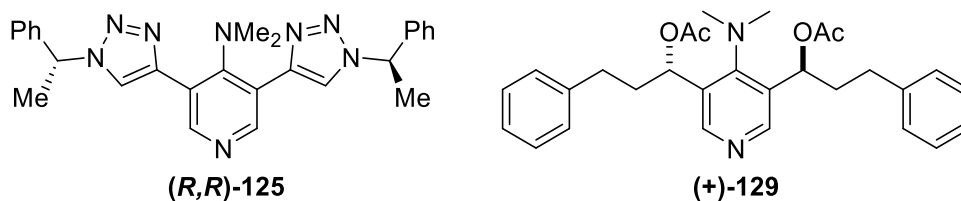
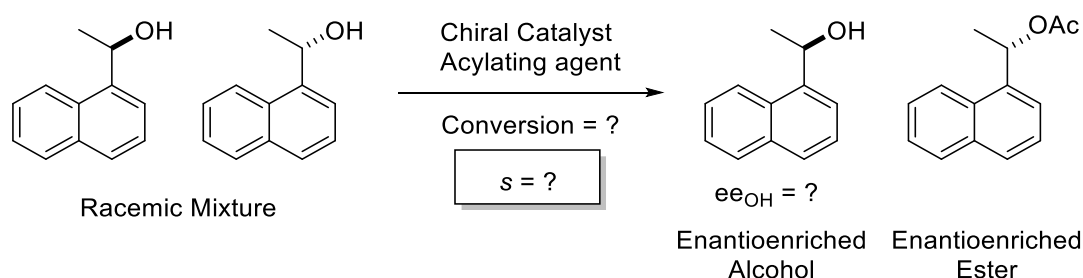


Figure 47 - Summary of 3,5-position DMAP derivatives synthesised as a single enantiomers and diastereoisomers

This will be achieved through the optimisation of reaction conditions using **(S)-50a** where choices of solvent, acylating reagent, base, substrate and temperature will be investigated. After condition optimisation all reactions will be screened in the same reaction, gas chromatography will be used to probe *ee* and conversion.

## Kinetic Resolution of Secondary Alcohols

The kinetic resolution of secondary alcohols can be viewed as the benchmark reaction for the effectiveness of asymmetric DMAP derivatives. The reaction takes a racemic mixture of a secondary alcohol and aims to use a catalyst to acylate one enantiomer of a racemic mixture faster than the other. A theoretical example of this reaction is shown in Scheme 62.<sup>19</sup>



*Scheme 62 - General scheme for the kinetic resolution of a secondary alcohol*

The effectiveness of a catalyst at carrying out this reaction is measured by a selectivity factor (*s*). The selectivity factor is the ratio of the rate constants for the reaction of each individual enantiomer (Equation 2) giving a number that must be greater than or equal to 1. If *s* is 1 then both enantiomers are reacting at the same rate and a number greater than one shows that the catalyst is reacting preferentially with one enantiomer.<sup>20</sup>

$$s = \frac{\text{Larger Rate Constant}}{\text{Smaller Rate Constant}} = \frac{\ln[(1 - ee_{OH})(1 - C)]}{\ln[(1 + ee_{OH})(1 - C)]}$$

*Equation 2 - Selectivity factor calculation<sup>20</sup>*

As the rate constant for each enantiomer can be troublesome to determine experimentally an equation has been derived by Kagan which relates the *ee* of the recovered alcohol and the conversion to the ester with selectivity factor (Equation 1) making the determination of *s* more rapid.<sup>20</sup>

## Optimisation of Catalysis Conditions

In order to optimise the conditions for the kinetic resolution of a secondary alcohol, catalyst **(S)-50a** was used. The effects of solvent, substrate, anhydride, base and temperature on the selectivity factor were probed. These are the three factors previously reported to have shown the greatest effect on selectivity factors (*s*).<sup>2, 39, 43, 63</sup>

Solvent screening (Table 9) demonstrated the importance of solvent choice for this reaction, as some give a near racemic product. Although a general trend is not immediately obvious and selectivity factors are low, so a hypothesis for the trend is tentative, it does appear that polar aprotic solvents give lower *s* values than non-polar aprotics. This is likely due to their strong stabilisation of the acyl-pyridinium intermediate, which may hinder cation- $\pi$  interactions. DCM appears to be an exception due to its higher dielectric constant and dipole moment when compared to chloroform. Chloroform's superiority in this reaction may be attributed to its ability to solvate the reagents without stabilising the positive charge of the acyl-pyridinium intermediate, thereby allowing the formation of the cation- $\pi$  stacked intermediate.



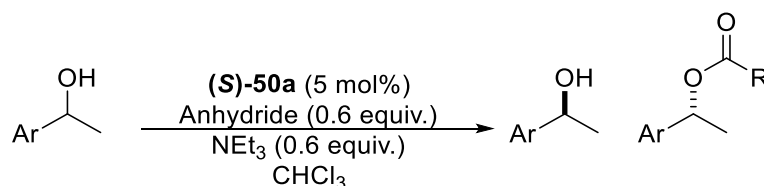
Table 9 - Solvent screen using catalyst (S)-50a

Entry	Solvent	$ee_{OH}^b$ (%)	$ee_{ester}^b$ (%)	Conversion <sup>b</sup> (%)	$S^c$
1	MeCN <sup>a</sup>	0.3	0.8	28	1.0
2	DMSO	0.1	0.8	11	1.0
3	Acetone <sup>a</sup>	0.5	3.3	19	1.1
4	EtOAc	0.7	4.4	18	1.1
5	1,4-Dioxane	0.7	4.5	12	1.1
6	DCM <sup>a</sup>	0.6	6.5	9	1.1
7	Et <sub>2</sub> O <sup>a</sup>	2.3	6.3	30	1.1
8	THF <sup>a</sup>	0.5	4.9	6	1.2
9	Ethyl Methyl Ketone	0.8	2.2	9	1.2
10	Toluene <sup>a</sup>	3.6	11.3	27	1.3
11	Hexane	5.4	13.3	33	1.3
12	CHCl <sub>3</sub>	6.8	12.5	39	1.3

<sup>a</sup> Solvents used were anhydrous, <sup>b</sup> conversion and ee determined by chiral GC after calibration correction factors applied, <sup>c</sup>  $S = \ln[(1 - C)(1 - ee_{SM})]/\ln[(1 - C)(1 + ee_{SM})]$

Once solvent was optimised, substrate effects and the acylation source were investigated (Table 10). The substrate effect was the same as reported in previous studies<sup>24</sup>, with the bulkier 1-(1-naphthyl)ethanol giving higher  $s$  values (2.61 vs, 1.32) than its phenyl counterpart. Alternative substrates were screened, however no increase in selectivity was observed, for 1-(2-methoxyphenyl)-1-ethanol the selectivity factor was 1.63 (conversion = 28%,  $ee_{OH}$  = 8%) and for menthol the selectivity factor was 1.12 (conversion = 28%,  $ee_{OH}$  = 2%).

Table 10 - Optimisation of substrate and acylating agent for (S)-50a



		Ar = Phenyl				
Entry	Anhydride	Compound number (OH/Ester)	ee <sub>OH</sub> <sup>a</sup> (%)	ee <sub>ester</sub> <sup>a</sup> (%)	C <sup>a</sup>	S <sup>b</sup>
1	Acetic	131/132	6.8	12.5	0.39	1.3
2	Propionic	131/133	7.3	8.9	0.56	1.2
3	Isobutyric	131/134	3.6	n.d. <sup>c</sup>	0.58	1.1
4	Benzoic	131/135	-0.5 <sup>d</sup>	n.d. <sup>c</sup>	0.33	1.0
		Ar = Naphthyl				
		Compound number (OH/Ester)	ee <sub>OH</sub> (%)	ee <sub>ester</sub> (%)	C <sup>b</sup>	S <sup>c</sup>
5	Acetic	136/137	33.2	n.d. <sup>c</sup>	0.51	2.6
6	Propionic	136/138	21.3	n.d. <sup>c</sup>	0.42	2.2
7	Isobutyric	136/139	13.2 <sup>e</sup>	n.d. <sup>c</sup>	n.d. <sup>e</sup>	n.d. <sup>e</sup>
8	Benzoic	136/140	3.4	n.d. <sup>c</sup>	n.d. <sup>f</sup>	n.d. <sup>f</sup>

<sup>a</sup> conversion and ee determined by chiral GC after calibration correction factors applied.

<sup>b</sup>  $S = \ln[(1 - C)(1 - ee_{SM})]/\ln[(1 - C)(1 + ee_{SM})]$ . <sup>c</sup> Not determined due to no ester separation by GC. <sup>d</sup> Favours other enantiomer. <sup>e</sup> Ester signal merged with alcohol enantiomer. <sup>f</sup> Calibration error too large to give values.

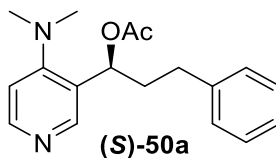
When the data for the anhydride source is considered it can be seen that on increasing the steric bulk of the anhydride erosion in selectivity is observed, to a point where benzoic anhydride gives a near racemic reaction. This is contrary to literature, where propionic anhydride has been reported to give superior results for secondary alcohol kinetic resolutions due to its increase steric bulk compared to acetic anhydride.<sup>24</sup>

Temperature effects were probed for the kinetic resolution of 1-(1-naphthyl)ethanol using acetic anhydride under the same conditions as the solvent and substrate screens. When the temperature was lowered to -20 °C a selectivity factor of 2.68 was observed (conversion = 52%, ee<sub>OH</sub> = 35%) and at -78 °C a selectivity factor of 1.81 was obtained

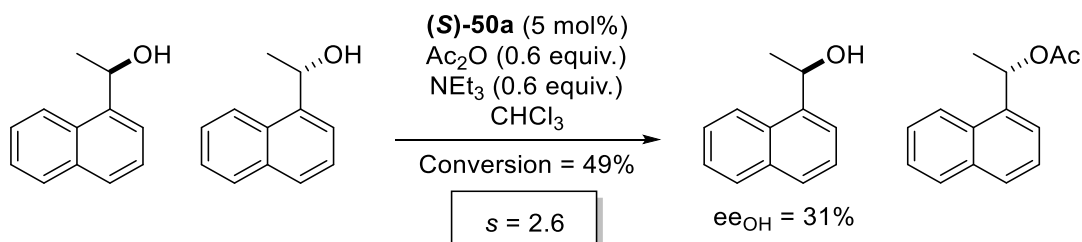
(conversion = 2%,  $ee_{OH} = <1\%$ ). This demonstrated that lowering the temperature had no noticeable effect on selectivity, however at very low temperatures the rate of reaction slowed, dramatically decreasing the conversion.

Finally, the effect of the omission of base was studied, the theory behind this was that the omission of base would slow down the rate of reaction, which may have aided the formation of the diastereomeric transition state. A selectivity factor of 2.70 was obtained (conversion = 42%,  $ee_{OH} = 35\%$ ), which means that this changes had no effect on the selectivity factor. Therefore, the optimisation conditions can be seen in Table 10, entry 5.

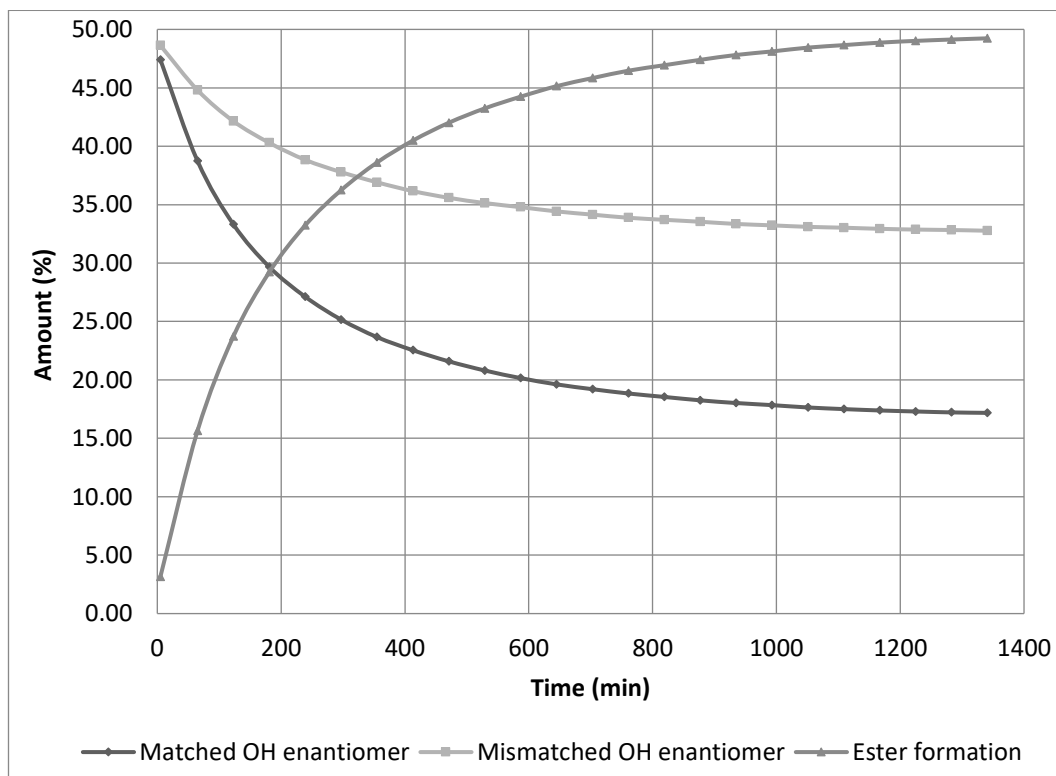
*(S)*-1-(4-(Dimethylamino)pyridin-3-yl)-3-phenylpropyl acetate ((*S*)-50a)



Catalyst **(S)-50a** was used in the kinetic resolution of 1-(1-naphthyl)ethanol using the conditions determined in Table 10, entry 5. These gave a selectivity factor of 2.6 which correlated to a conversion of 49% and an alcohol *ee* of 31%. This was determined *via* the monitoring of the reaction mixture using GC with a chiral stationary phase, the average selectivity factor over 17 timepoints (*t* = 413 mins to 1341 mins) was  $s = 2.57 \pm 0.02$ .

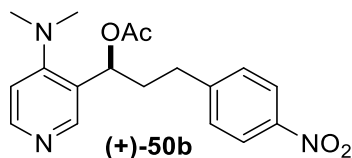


*Scheme 63- Kinetic resolution of 1-(1-naphthyl)ethanol using (S)-50a*

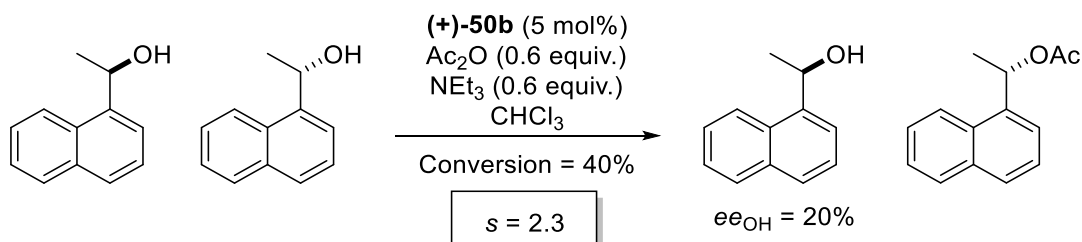


*Graph 1 - Real time monitoring of the kinetic resolution of 1-(1-naphthyl)ethanol using (S)-50a*

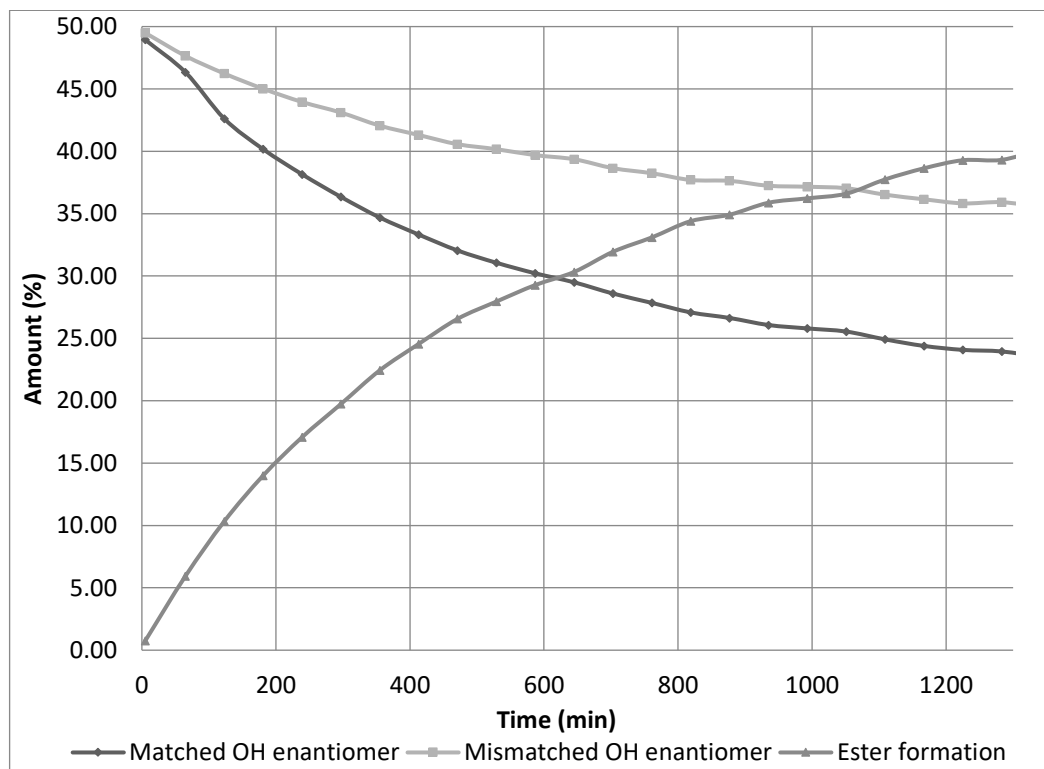
1-(4-(Dimethylamino)pyridin-3-yl)-3-(4-nitrophenyl)propyl acetate ((+)-50b)



Catalyst **(+)-50b** was used in the kinetic resolution of 1-(1-naphthyl)ethanol using the conditions determined in Table 10, entry 5. These gave a selectivity factor of 2.3 which correlated to a conversion of 40% and an alcohol *ee* of 20%. This was determined *via* the monitoring of the reaction mixture using GC with a chiral stationary phase, the average selectivity factor over 15 timepoints (*t* = 529 mins to 1341 mins) was *s* = 2.26±0.02.

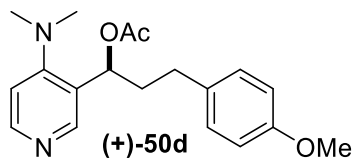


Scheme 64- Kinetic resolution of 1-(1-naphthyl)ethanol using (+)-50b

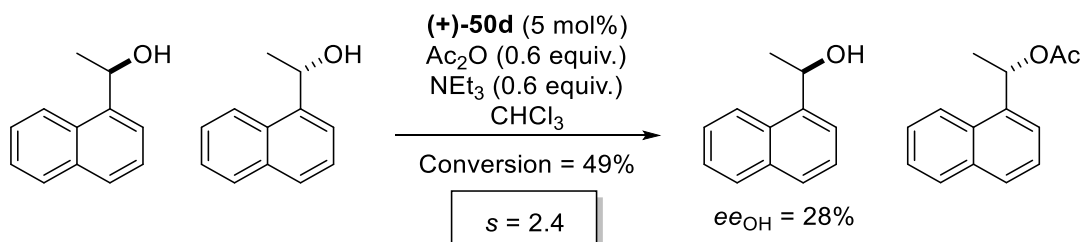


Graph 2 - Real time monitoring of the kinetic resolution of 1-(1-naphthyl)ethanol using (+)-50b

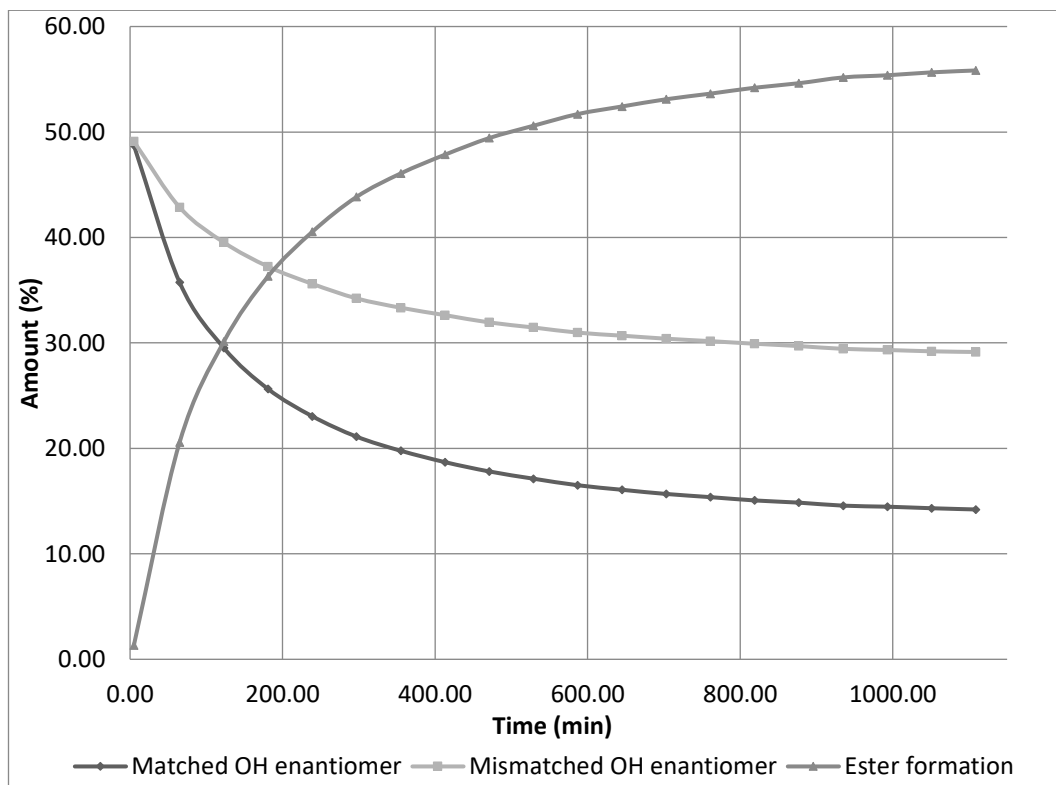
**1-(4-(Dimethylamino)pyridin-3-yl)-3-(4-methoxyphenyl)propyl acetate ((+)-50d)**



Catalyst **(+)-50d** was used in the kinetic resolution of 1-(1-naphthyl)ethanol using the conditions determined in Table 10, entry 5. These gave a selectivity factor of 2.4 which correlated to a conversion of 49% and an alcohol *ee* of 28%. This was determined *via* the monitoring of the reaction mixture using GC with a chiral stationary phase, the average selectivity factor over 16 timepoints (*t* = 239 mins to 1109 mins) was *s* = 2.36±0.02.

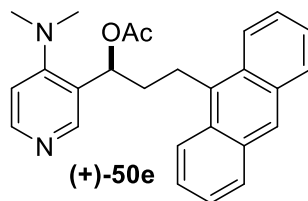


*Scheme 65- Kinetic resolution of 1-(1-naphthyl)ethanol using (+)-50d*

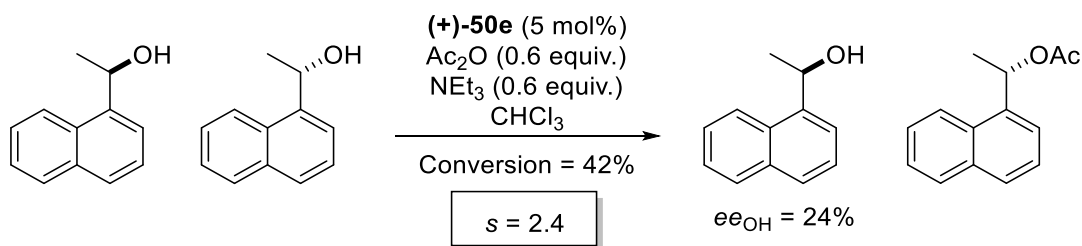


*Graph 3 - Real time monitoring of the kinetic resolution of 1-(1-naphthyl)ethanol using (+)-50d*

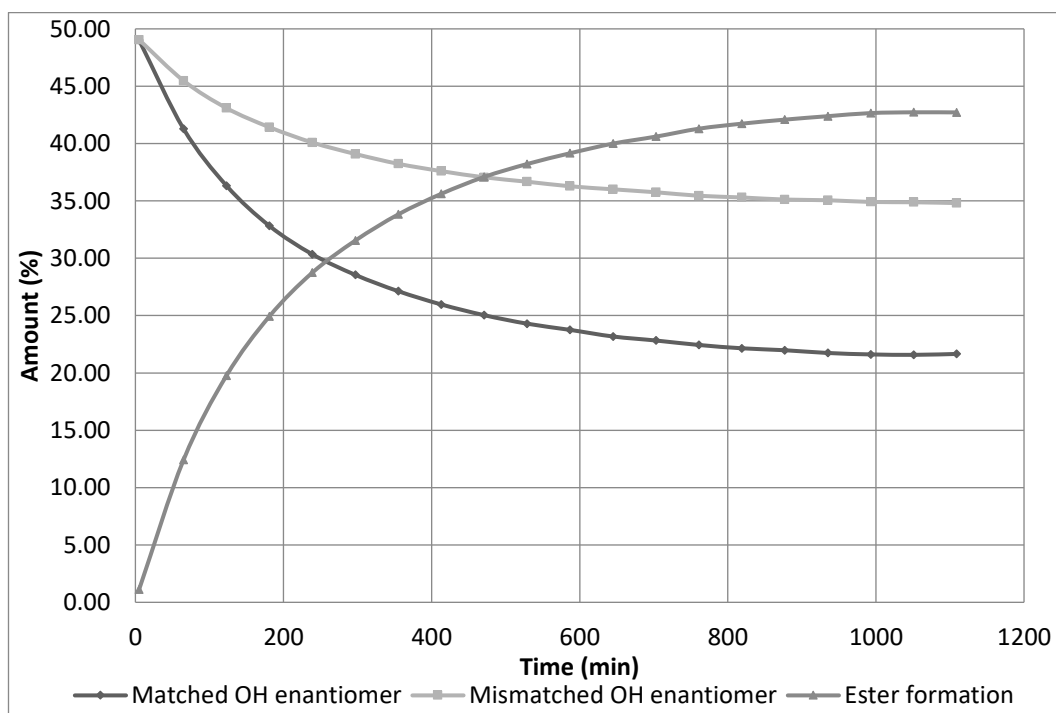
3-(Anthracen-9-yl)-1-(4-(dimethylamino)pyridin-3-yl)propyl acetate ((+)-50e)



Catalyst **(+)-50e** was used in the kinetic resolution of 1-(1-naphthyl)ethanol using the conditions determined in Table 10, entry 5. These gave a selectivity factor of 2.4 which correlated to a conversion of 42% and an alcohol *ee* of 24%. This was determined *via* the monitoring of the reaction mixture using GC with a chiral stationary phase, the average selectivity factor over 11 timepoints (*t* = 529 mins to 1109 mins) was *s* = 2.39±0.01.

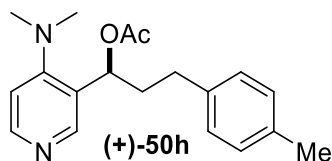


Scheme 66- Kinetic resolution of 1-(1-naphthyl)ethanol using (+)-50e

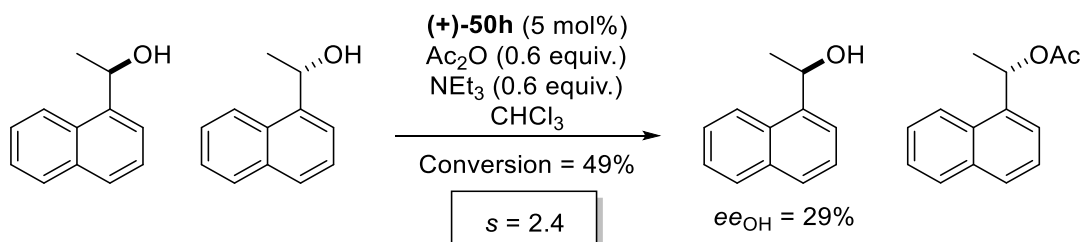


Graph 4 - Real time monitoring of the kinetic resolution of 1-(1-naphthyl)ethanol using (+)-50e

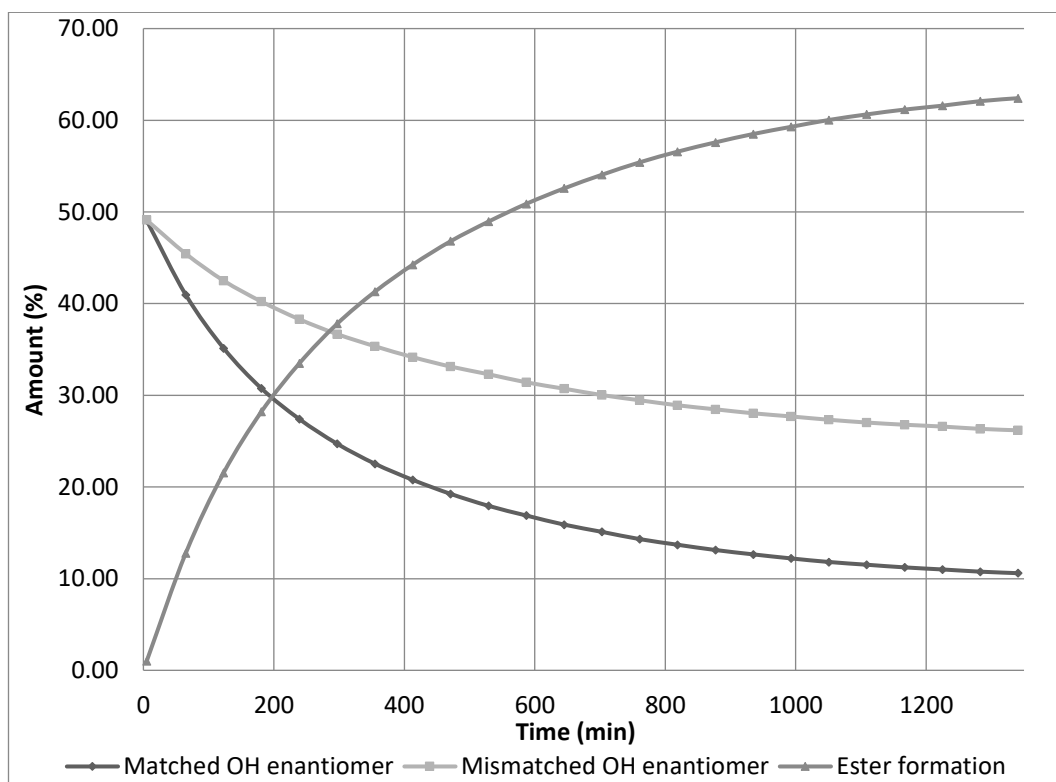
**1-(4-(Dimethylamino)pyridin-3-yl)-3-(p-tolyl)propyl acetate ((+)-50h)**



Catalyst **(+)-50h** was used in the kinetic resolution of 1-(1-naphthyl)ethanol using the conditions determined in Table 10, entry 5. These gave a selectivity factor of 2.4 which correlated to a conversion of 49% and an alcohol *ee* of 29%. This was determined *via* the monitoring of the reaction mixture using GC with a chiral stationary phase, the average selectivity factor over 15 timepoints (*t* = 529 mins to 1341 mins) was *s* = 2.42±0.02.



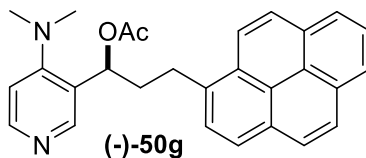
*Scheme 67- Kinetic resolution of 1-(1-naphthyl)ethanol using (+)-50h*



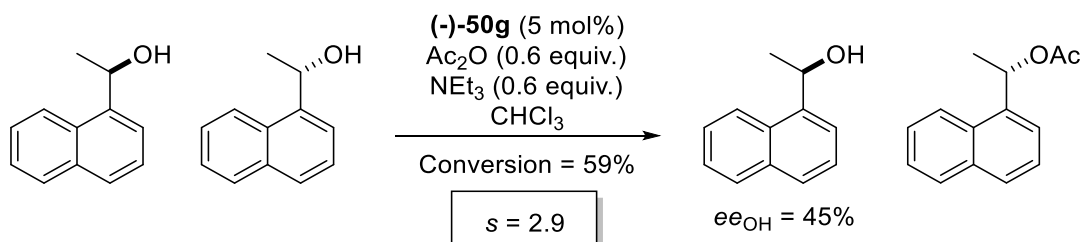
*Graph 5 - Real time monitoring of the kinetic resolution of 1-(1-naphthyl)ethanol using (+)-50h*



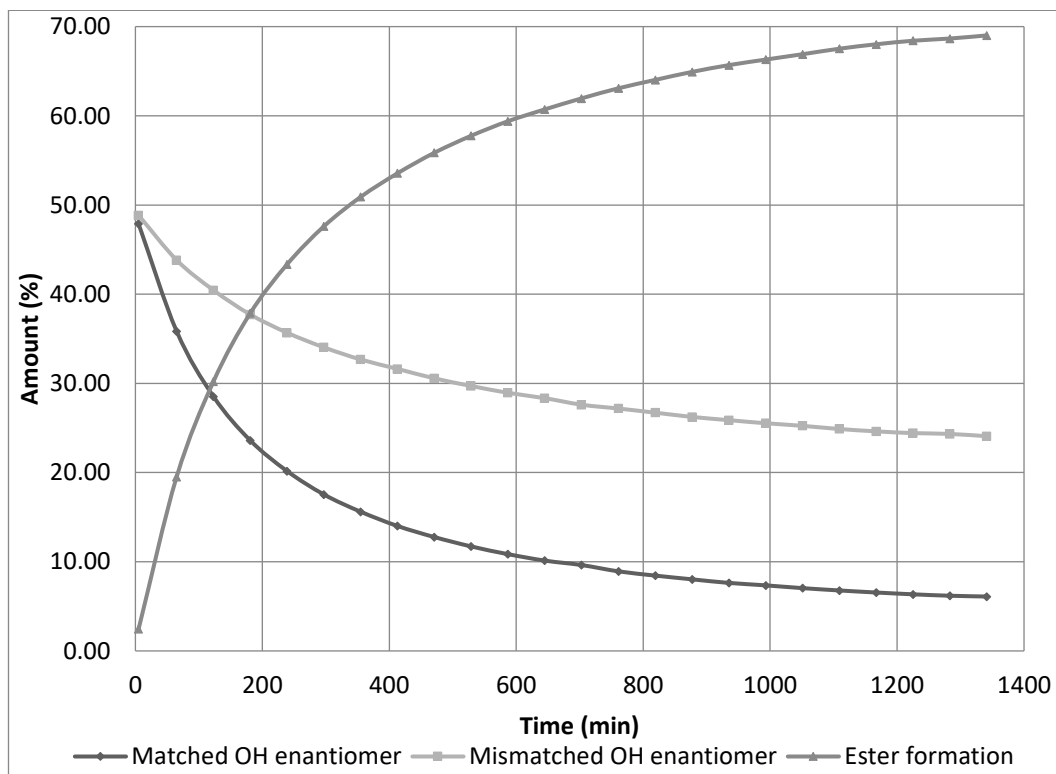
**1-(4-(Dimethylamino)pyridin-3-yl)-3-(pyren-1-yl)propyl acetate ((-)-50g)**



Catalyst **(-)-50g** was used in the kinetic resolution of 1-(1-naphthyl)ethanol using the conditions determined in Table 10, entry 5. These gave a selectivity factor of 2.9 which correlated to a conversion of 59% and an alcohol *ee* of 45%. This was determined *via* the monitoring of the reaction mixture using GC with a chiral stationary phase, the average selectivity factor over 17 timepoints (*t* = 413 mins to 1341 mins) was *s* = 2.90±0.04.

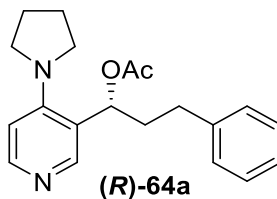


*Scheme 68- Kinetic resolution of 1-(1-naphthyl)ethanol using (-)-50g*

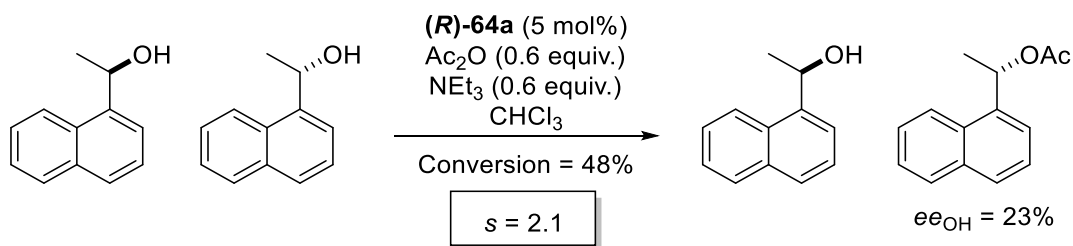


*Graph 6 - Real time monitoring of the kinetic resolution of 1-(1-naphthyl)ethanol using (-)-50g*

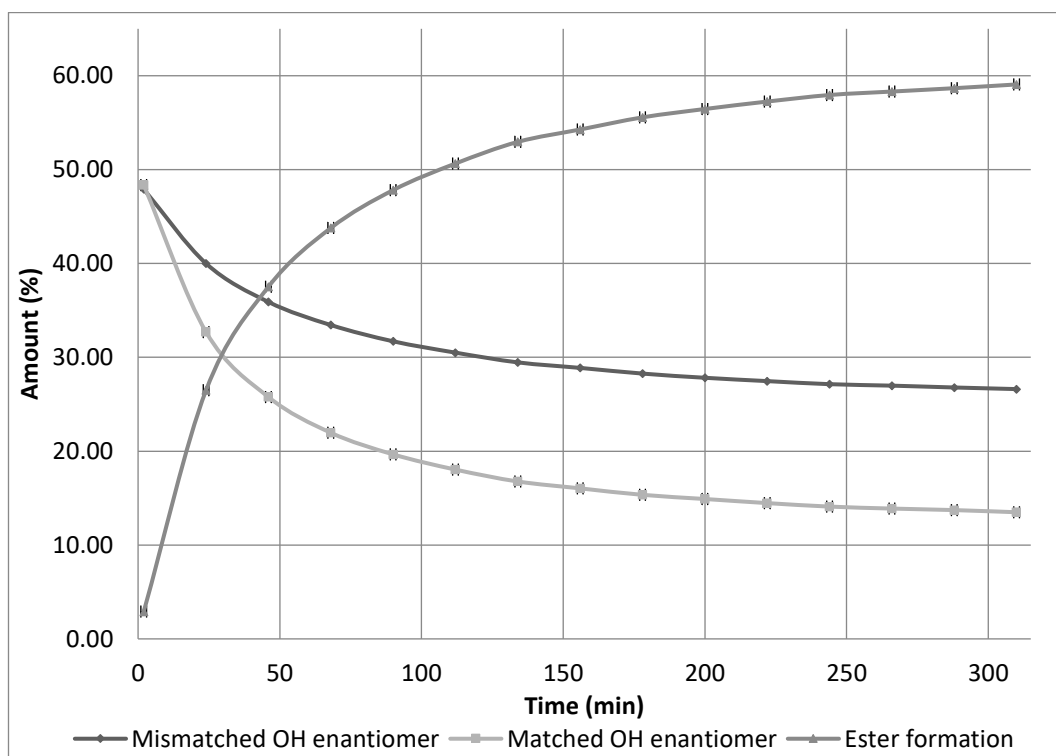
*(R)*-3-Phenyl-1-(4-(pyrrolidin-1-yl)pyridin-3-yl)propyl acetate (*(R)*-64a)



Catalyst **(R)-64a** was used in the kinetic resolution of 1-(1-naphthyl)ethanol using the conditions determined in Table 10, entry 5. These gave a selectivity factor of 2.1 which correlated to a conversion of 48% and an alcohol *ee* of 23%. This was determined *via* the monitoring of the reaction mixture using GC with a chiral stationary phase, the average selectivity factor over 13 timepoints (*t* = 46 mins to 310 mins) was *s* = 2.10±0.02.

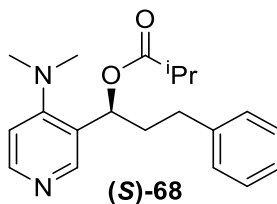


*Scheme 69- Kinetic resolution of 1-(1-naphthyl)ethanol using (R)-64a*

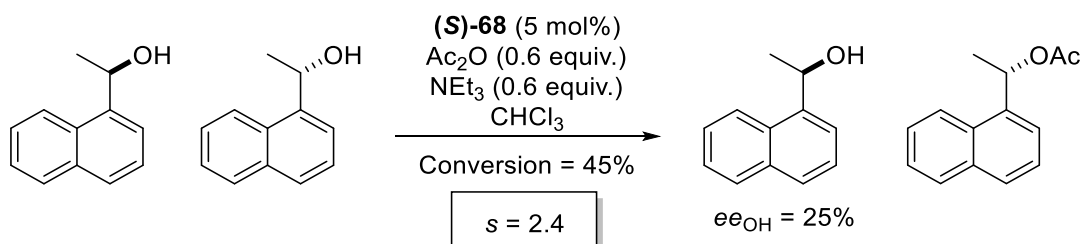


*Graph 7 - Real time monitoring of the kinetic resolution of 1-(1-naphthyl)ethanol using (R)-64a*

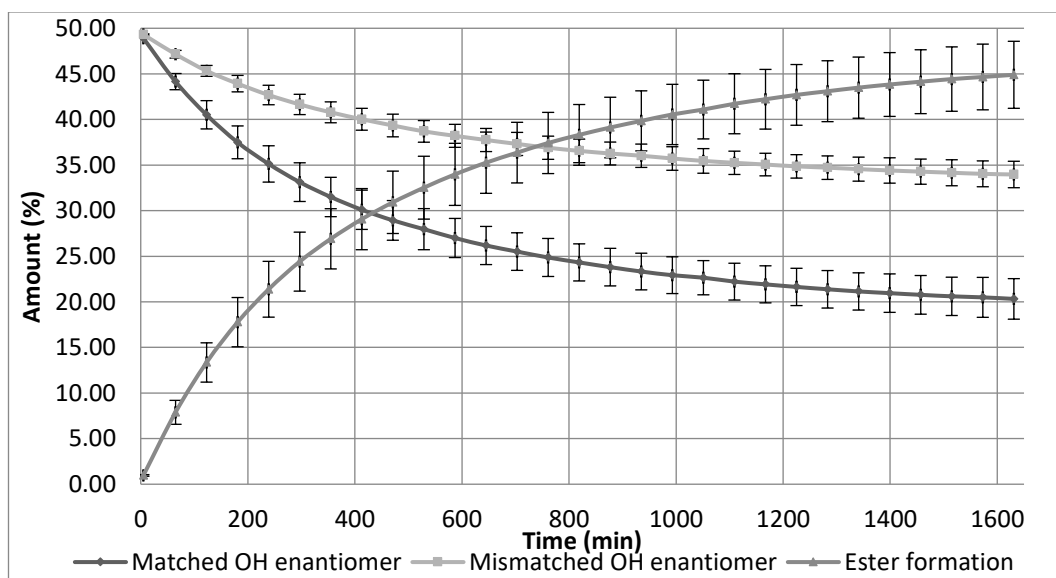
*(S)*-1-(4-(Dimethylamino)pyridin-3-yl)-3-phenylpropyl isobutyrate (*(S)*-68)



Catalyst **(S)-68** was used in the kinetic resolution of 1-(1-naphthyl)ethanol using the conditions determined in Table 10, entry 5. The experiment was run twice and the results detailed below are an average of the two data sets, this was done in order to ensure reproducibility. These gave a selectivity factor of 2.4 which correlated to a conversion of 45% and an alcohol *ee* of 25%. This was determined *via* the monitoring of the reaction mixture using GC with a chiral stationary phase, the average selectivity factor over 13 timepoints (*t* = 935 mins to 1631 mins) was  $s = 2.38 \pm 0.01$ .

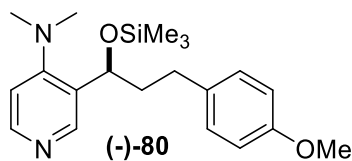


*Scheme 70- Kinetic resolution of 1-(1-naphthyl)ethanol using (S)-68*

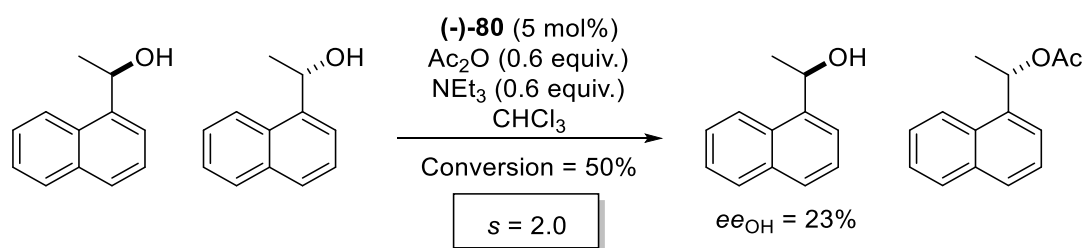


*Graph 8 - Real time monitoring of the kinetic resolution of 1-(1-naphthyl)ethanol using (S)-68*

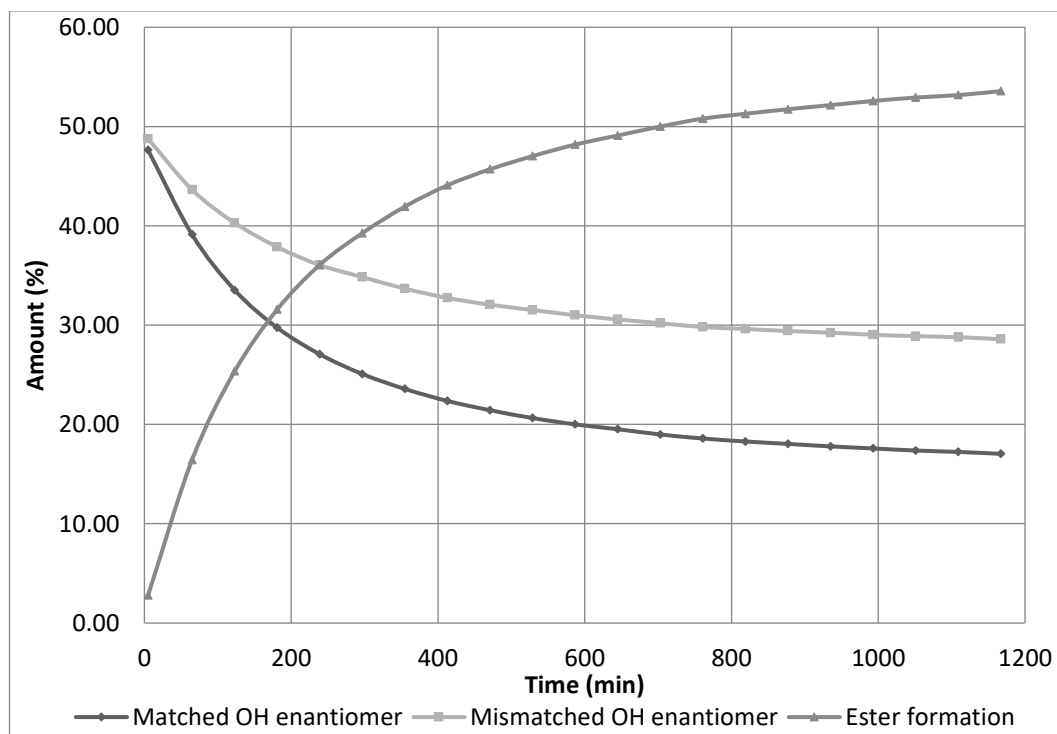
3-(3-(4-Methoxyphenyl)-1-((trimethylsilyl)oxy)propyl)-N,N-dimethylpyridin-4-amine  
(-)-80



Catalyst **(-)-80** was used in the kinetic resolution of 1-(1-naphthyl)ethanol using the conditions determined in Table 10, entry 5. These gave a selectivity factor of 2.0 which correlated to a conversion of 50% and an alcohol *ee* of 23%. This was determined *via* the monitoring of the reaction mixture using GC with a chiral stationary phase, the average selectivity factor over 15 timepoints (*t* = 355 mins to 1167 mins) was *s* = 1.95±0.01.

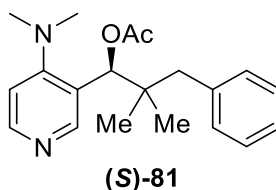


Scheme 71- Kinetic resolution of 1-(1-naphthyl)ethanol using (-)-80

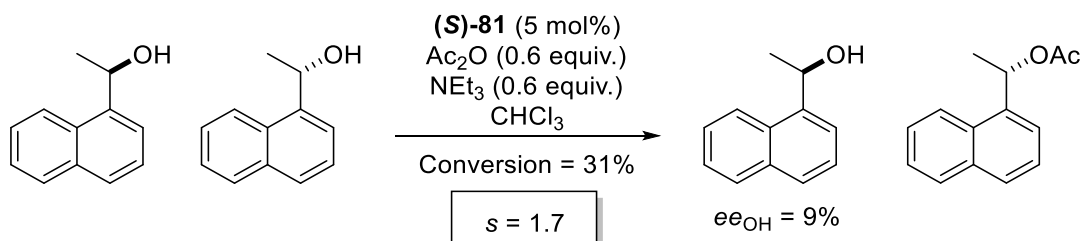


Graph 9 - Real time monitoring of the kinetic resolution of 1-(1-naphthyl)ethanol using (-)-80

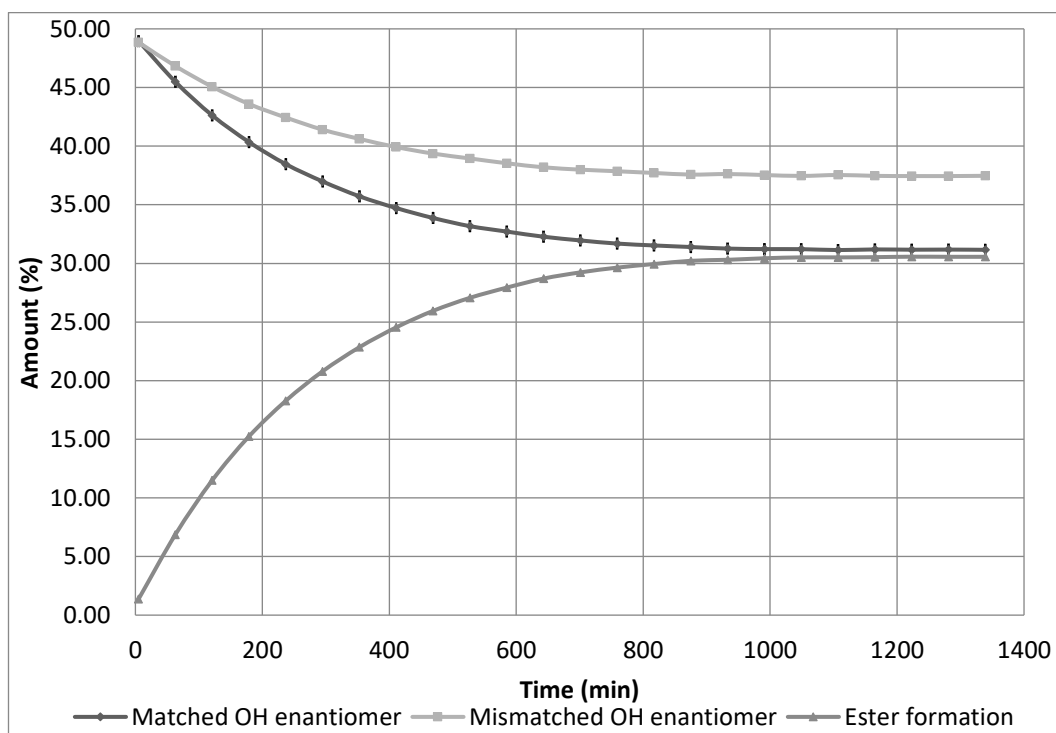
*(S)*-1-(4-(Dimethylamino)pyridin-3-yl)-2,2-dimethyl-3-phenylpropyl acetate (*(S)*-81)



Catalyst **(S)-81** was used in the kinetic resolution of 1-(1-naphthyl)ethanol using the conditions determined in Table 10, entry 5. These gave a selectivity factor of 1.7 which correlated to a conversion of 31% and an alcohol *ee* of 9%. This was determined *via* the monitoring of the reaction mixture using GC with a chiral stationary phase, the average selectivity factor over 18 timepoints (*t* = 353 mins to 1339 mins) was *s* = 1.66±0.01.

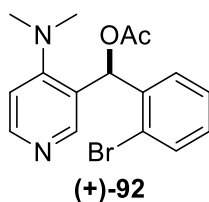


*Scheme 72- Kinetic resolution of 1-(1-naphthyl)ethanol using (S)-81*

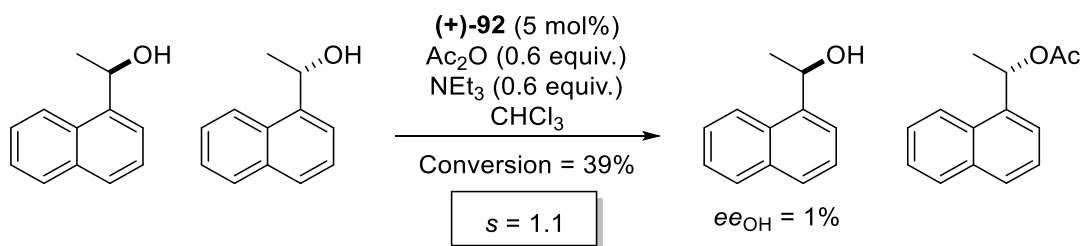


*Graph 10 - Real time monitoring of the kinetic resolution of 1-(1-naphthyl)ethanol using (S)-81*

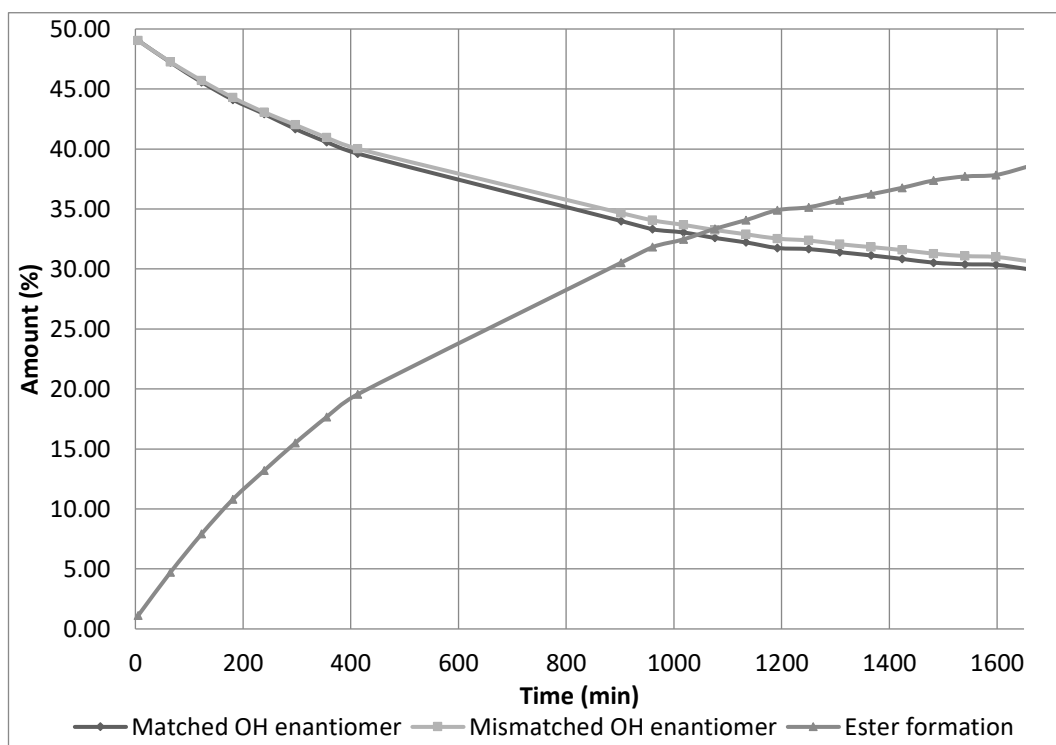
(2-Bromophenyl)(4-(dimethylamino)pyridin-3-yl)methyl acetate ((+)-92)



Catalyst **(+)-92** was used in the kinetic resolution of 1-(1-naphthyl)ethanol using the conditions determined in Table 10, entry 5. These gave a selectivity factor of 1.1 which correlated to a conversion of 39% and an alcohol *ee* of 1%. This was determined *via* the monitoring of the reaction mixture using GC with a chiral stationary phase, the average selectivity factor over 20 timepoints ( $t = 123$  mins to 1656 mins) was  $s = 1.05 \pm 0.01$ .

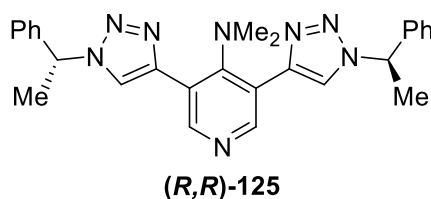


Scheme 73- Kinetic resolution of 1-(1-naphthyl)ethanol using (+)-92

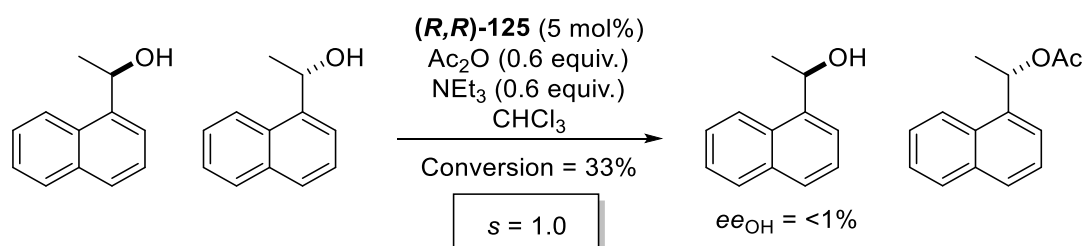


Graph 11 - Real time monitoring of the kinetic resolution of 1-(1-naphthyl)ethanol using (+)-92

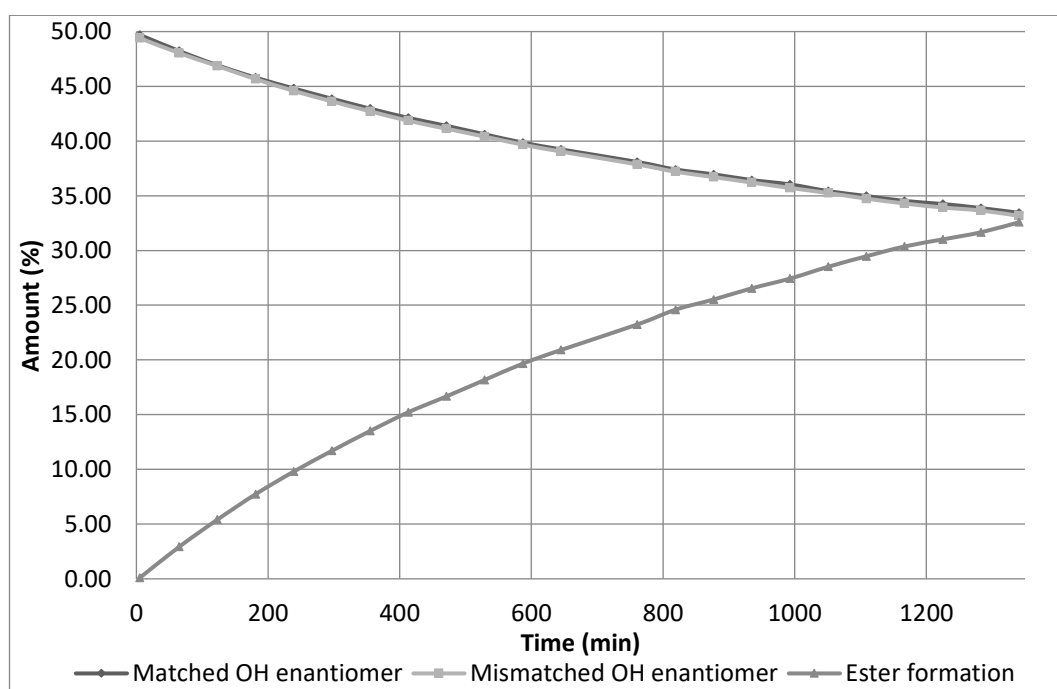
*N,N*-dimethyl-3,5-bis(1-((*R*)-1-phenylethyl)-1*H*-1,2,3-triazol-5-yl)pyridin-4-amine  
(*R,R*)-125



Catalyst **(*R,R*)-125** was used in the kinetic resolution of 1-(1-naphthyl)ethanol using the conditions determined in Table 10, entry 5. These gave a selectivity factor of 1.0 which correlated to a conversion of 33% and an alcohol *ee* of <1%. This was determined *via* the monitoring of the reaction mixture using GC with a chiral stationary phase, the average selectivity factor over 20 timepoints (*t* = 181 mins to 1341 mins) was *s* = 1.03±0.01.

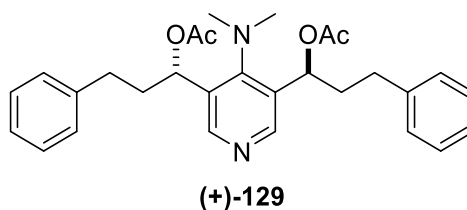


*Scheme 74- Kinetic resolution of 1-(1-naphthyl)ethanol using (*R,R*)-125*

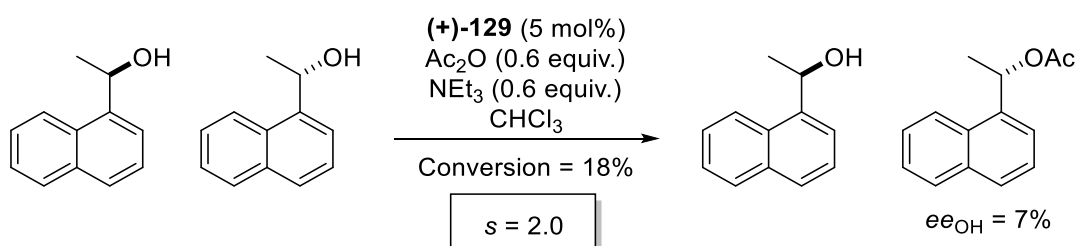


*Graph 12 - Real time monitoring of the kinetic resolution of 1-(1-naphthyl)ethanol using (*R,R*)-125*

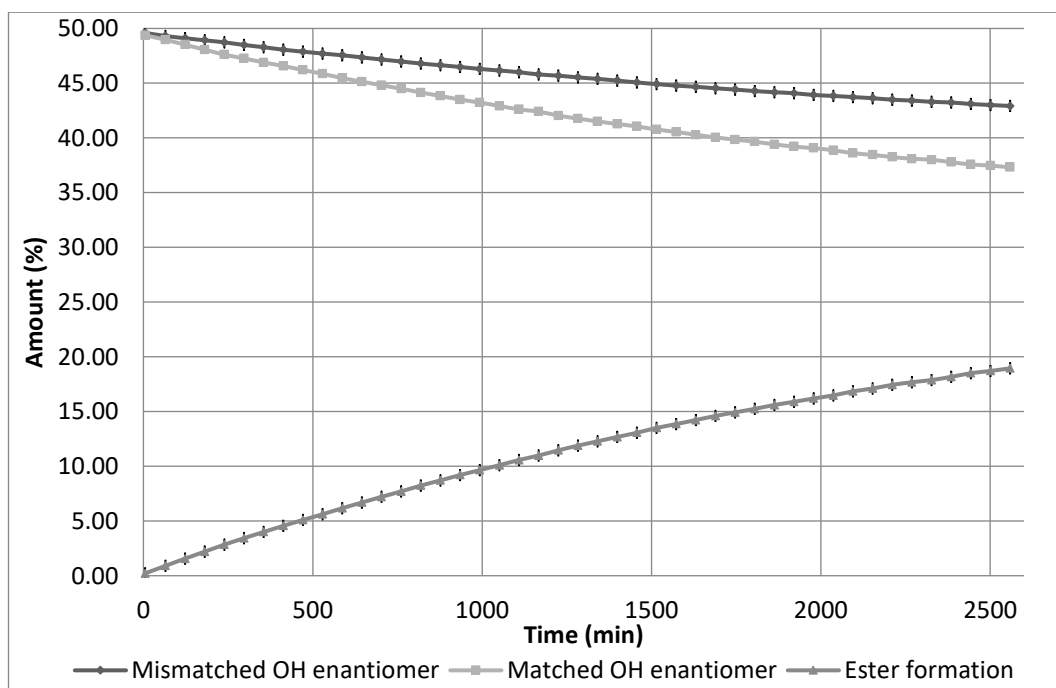
(4-(dimethylamino)pyridine-3,5-diyl)bis(3-phenylpropane-1,1-diyl) diacetate ((+)-129)



Catalyst **(+)-129** was used in the kinetic resolution of 1-(1-naphthyl)ethanol using conditions determined in Table 10, entry 5. These gave an *s* of 2.0 which correlated to a conversion of 19% and an alcohol *ee* of 7%. This was determined *via* the monitoring of the reaction mixture using GC with a chiral stationary phase, the average selectivity factor over 35 timepoints (*t* = 587 mins to 2559 mins) was *s* = 2.01±0.02.



Scheme 75- Kinetic resolution of 1-(1-naphthyl)ethanol using (+)-129



Graph 13 - Real time monitoring of the kinetic resolution of 1-(1-naphthyl)ethanol using (+)-129

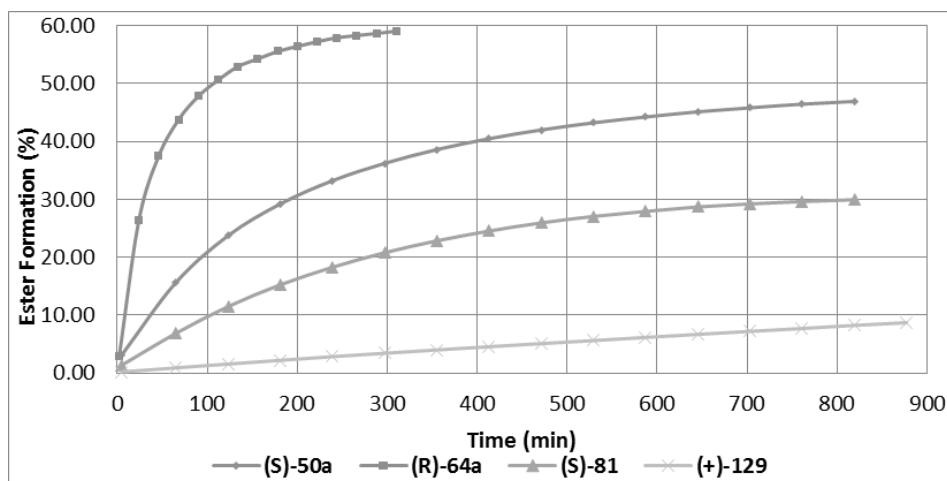


## Catalyst Comparison and Summary

*Table 11 - Summary of selectivity factors for the kinetic resolution of 1-(1-naphthyl)ethanol*

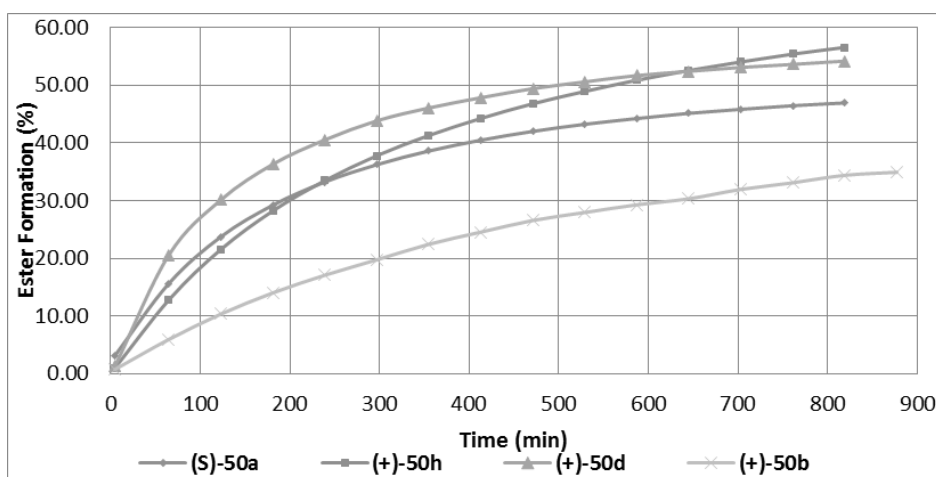
Entry	Catalyst	Conversion (%)	$ee_{OH}$ (%)	Selectivity factor (s)
1	(S)-50a	49	31	2.57±0.02
2	(+)-50b	40	20	2.26±0.02
3	(+)-50d	49	28	2.36±0.02
4	(+)-50e	42	24	2.39±0.01
5	(+)-50h	49	29	2.42±0.02
6	(-)-50g	59	45	2.90±0.04
7	(R)-64a	48	23	2.10±0.02
8	(S)-68	45	25	2.38±0.01
9	(-)-80	50	23	1.95±0.01
10	(S)-81	31	9	1.66±0.01
11	(+)-92	39	1	1.05±0.01
12	(R,R)-125	33	<1	1.03±0.01
13	(+)-129	19	7	2.01±0.02

A summary of the selectivity factors obtained can be seen in Table 11, all were between 2.90 and 1.03 with all standard deviations less than 0.05. For 3-position derivatised systems the conversions were high (30-60%) however when derivatised in the three and five positions the conversion and rate of reaction drops dramatically, most likely due to steric crowding around the active site of the catalyst. This theory is also supported by the observation that substitution of the linker leads to a drop in conversion of the alcohol to ester. This can be demonstrated by comparison of the rates of ester formation (Graph 14), (+)-129 gave the lowest rate of formation, followed by the dimethyl catalyst (S)-81, which was followed by catalyst (S)-50a and finally (R)-64a. The large rate increase caused by the installation of a pyrrolidino group at the 4-position of pyridine has previously been demonstrated for other DMAP derivatives<sup>10</sup>, this dramatic increase in rate led to a marginal decrease in the selectivity factor when compared to its dimethylamino equivalent (S)-50a (2.1 vs. 2.6).



Graph 14 - Comparison of the rate of ester formation for catalysts (S)-50a, (R)-64a, (S)-81 and 130

Variation of the aromatic unit electronics appeared to have no effect on the selectivity factor, however variation in the rate of conversion of alcohol is observed (Graph 15). From the limited derivatives available it appears that aromatic units with electron donating substituents (**50h** and **50d**) yield faster rates of conversion than those with electron withdrawing substituents (**50b**) when compared to unsubstituted derivative (**(S)-50a**).

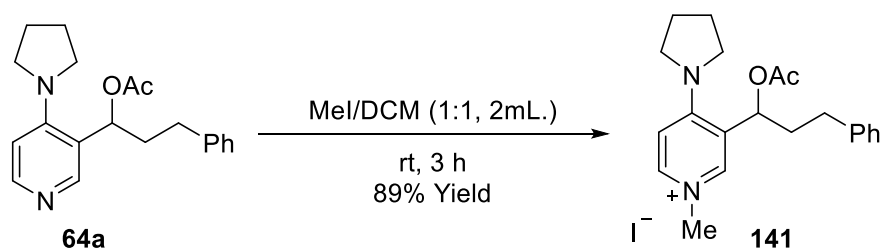


Graph 15 - Comparison of the rate of ester formation for catalysts (S)-50a, 50h, 50d and 50b

## Fluorescence

Fossey and co-workers have reported the use of fluorescence spectroscopy to determine the presence of cation- $\pi$  interaction in flexible systems for the detection of alkylating agents. A characteristic broad excimer emission was observed at approximately 400 nm upon excitation of the sample which was attributed to the presence of a cation- $\pi$  interaction.<sup>56, 64</sup>

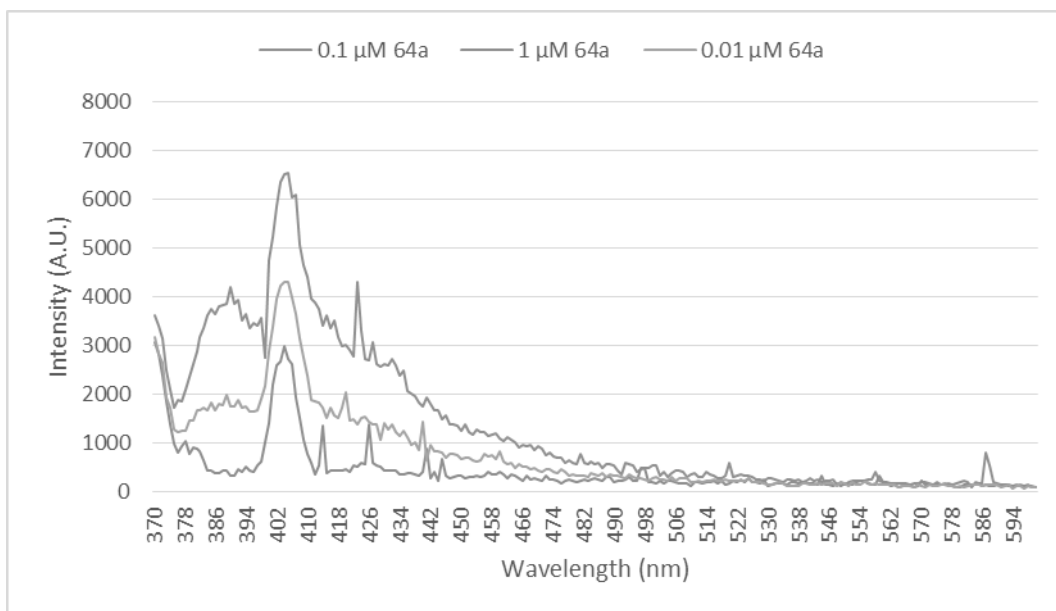
Initial studies focus on the determination of an appropriate excitation wavelength and concentration of analyte to observe the cation- $\pi$  interaction between the pyridinium and the aryl moiety. In order to do this the methylation of **64a** was carried out in DCM to synthesise **141**, which was achieved in 89% yield (Scheme 76).



*Scheme 76 - Synthesis of 141 by methylation of 64a*

With **141** in hand, a set of serial dilutions in DCM were made ranging in concentration from 0.01  $\mu$ M to 1.00 mM. The solutions were studied by recording excitation/emission spectra to determine the correct excitation wavelength to observe a fluorescence response which could be attributed to a cation- $\pi$  interaction. At an excitation wavelength of 340 nm a fluorescence response was observed with a  $\lambda_{\text{max}}$  around 405 nm. Interestingly, the response was very sensitive in terms of concentration dependency. A response was only observed at a 0.1  $\mu$ M concentration of **141**, if the concentration were adjusted by a factor of 10 (0.01  $\mu$ M or 1  $\mu$ M) the fluorescence intensity would decrease (Graph 16). The decrease in concentration could be attributed to the effects of dilution causing an

intensity loss, however the effect due to an increase in concentration cannot be attributed to a dilution effect. It may be due to the interruption of the cation- $\pi$  interaction due to increase intermolecular interactions, causing drop in fluorescence intensity.

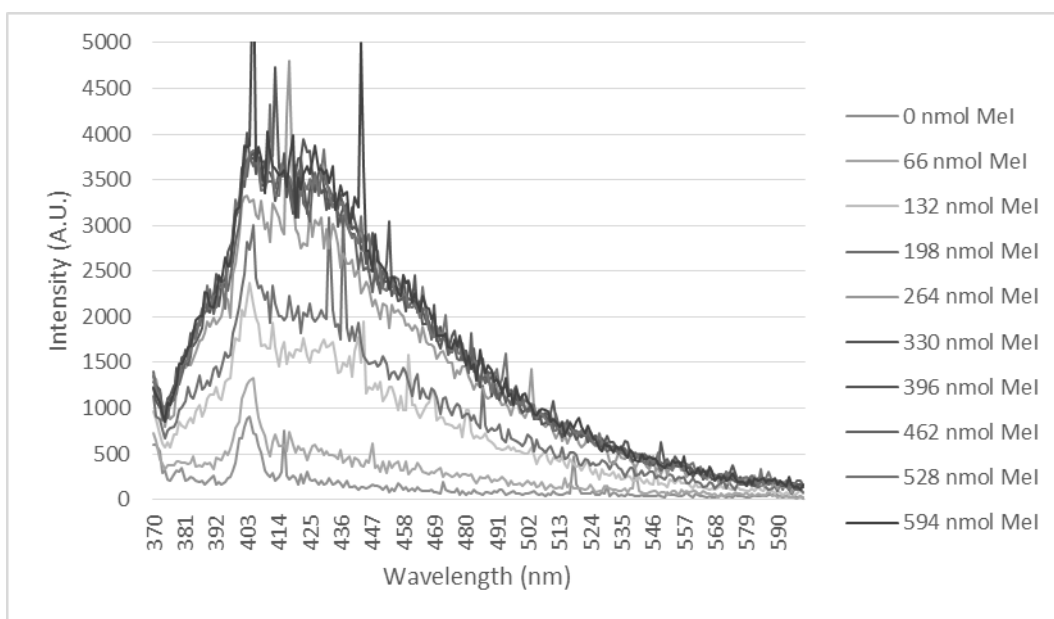


*Graph 16 - Relationship between concentration of 64a and the observed fluorescence response*

Upon determination of the correct excitation wavelength (340nm) a titration experiment was embarked upon. A solution of **64a** at a concentration of 0.1  $\mu$ M was monitored with fluorescence spectroscopy as aliquots of methyl iodide were added (Graph 17). A fluorescence increase was observed as each aliquot was added until a maximum intensity was reached, which was caused by full conversion of **64a** to **141**. The maximum intensity was reached after addition of 4 equivalents of methyl iodide, this was demonstrated by the addition of several subsequent additions of methyl iodide having no effect on fluorescence intensity.

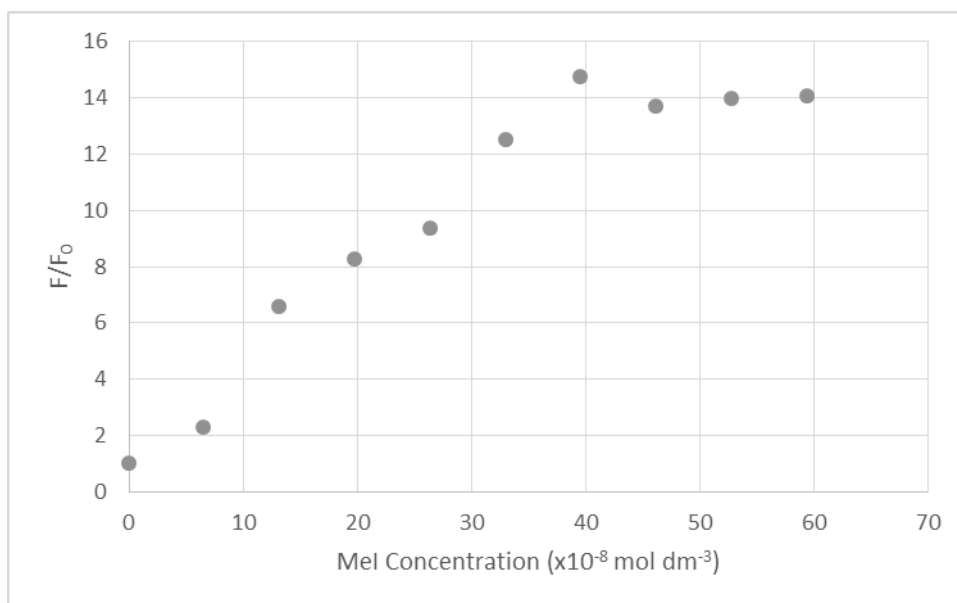
This work was then expanded to look at the response of the compounds to sub-stoichiometric amounts of alkylation agent and to compare these compounds to previous work by Fossey and co-workers. It was observed that the fluorescence enhancement ( $F/F_0$ ) was observed rapidly (shorter than the scan length) for all samples, which was an

improvement on reported systems that took up to 15 minutes to equilibrate.<sup>56, 64</sup> Upon titration of methyl iodide (0-600 nM) into a solution of **21** (0.1  $\mu$ M) a maximum fluorescence enhancement of 14 was observed reaching a maximum at 4 equivalents of methyl iodide.



Graph 17 - Fluorescence spectra ( $\lambda_{ex} = 340$  nm) of **64a** (0.1  $\mu$ M) upon titration with MeI (0-600 nM)

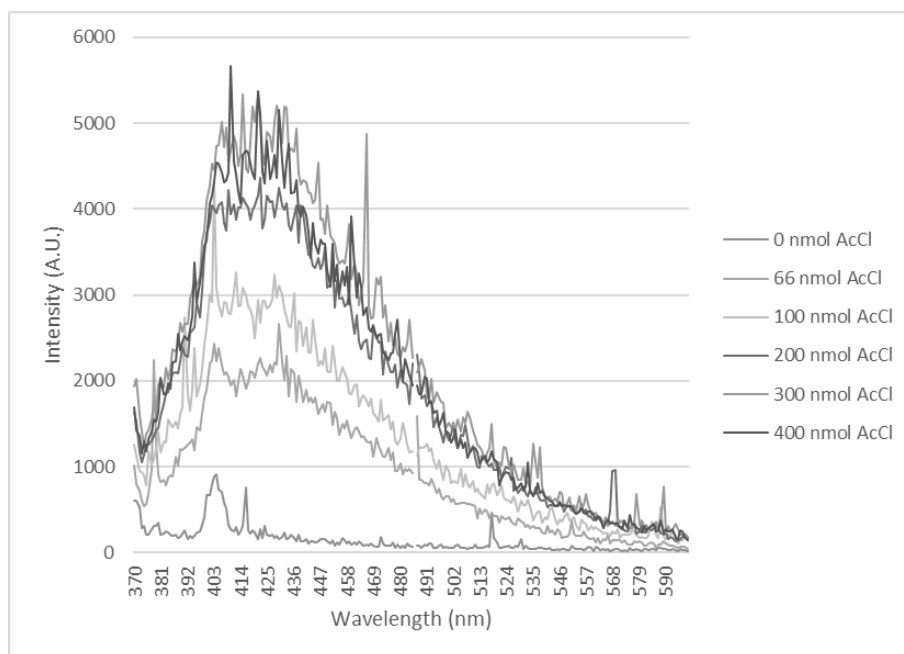
Due to the arbitrary values recorded for intensity the most useful measure of fluorescence response is fluorescence enhancement ( $F/F_0$ ), this is where the value at the  $\lambda_{max}$  of each spectrum is divided by the fluorescence response at the corresponding wavelength before methyl iodide has been added. When  $F/F_0$  is calculated for the data in Graph 17 a maximum enhancement value of 14 is obtained at the addition of approximately 4 equivalents of methyl iodide,  $F/F_0$  data can be seen in Graph 18. When compared to an example from the literature for alkylating agent sensors,<sup>56</sup> **64a** appears to be superior, showing not only a large fluorescence enhancement but also greater sensitivity as it is able to detect the same amounts of methyl iodide with a much smaller sensor loading (10  $\mu$ M vs. 0.1  $\mu$ M).



Graph 18 - Fluorescence enhancement for the titration of **64a** with methyl iodide (0-600 nmol)

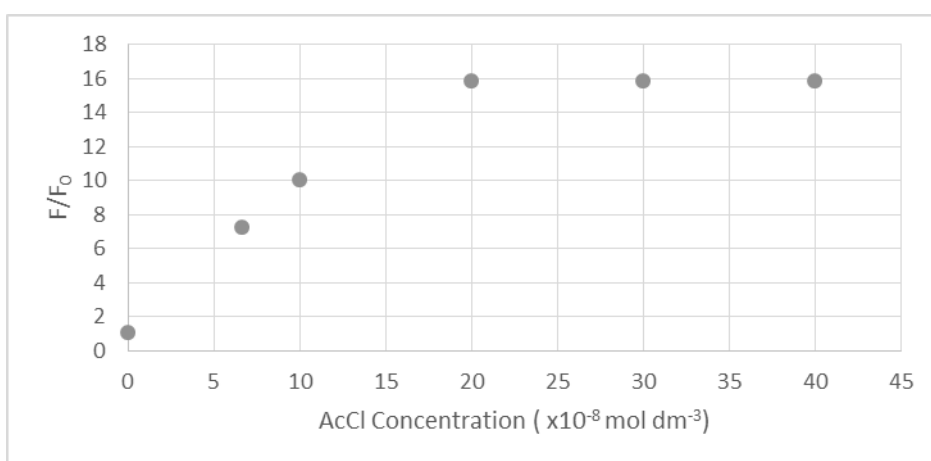
Although observing cation- $\pi$  stacking in the methylated structures is useful as proof of principle and it shows that these structures can be used as a sensor for alkylating agents, it does not give any information regarding the use of **64a** in catalysis because the reactive intermediate in catalysis is an acyl-pyridinium.

A second titration experiment was carried out where a solution of **64a** at a concentration of 0.1  $\mu\text{M}$  was monitored with fluorescence spectroscopy as aliquots of acetyl chloride were added (Graph 19). A fluorescence increase was observed as each aliquot was added until a maximum intensity was reached, which was caused by full conversion of **64a** to the acyl pyridinium. The maximum intensity was reached after addition of 2 equivalents of acetyl chloride, this was demonstrated by the addition of several subsequent additions of acetyl chloride having no effect on fluorescence intensity. When compared to methylation the equivalents need to reach complete conversion is lower (2 equivalents *versus* 4 equivalents).



Graph 19 - Fluorescence spectra ( $\lambda_{ex} = 340 \text{ nm}$ ) of **64a** ( $0.1 \mu\text{M}$ ) upon titration with AcCl (0-400 nM)

When  $F/F_0$  is calculated for the data in Graph 19 a maximum enhancement value of 16 is obtained at the addition of approximately 4 equivalents of acetyl chloride, fluorescence enhancement data can be seen in Graph 20. There do not appear to have been any previous reports of a cation- $\pi$  interaction being detected upon acylation of a pyridine compound in the literature available. Furthermore it is a promising advancement towards *in situ* monitoring of acylation reaction *via* cation- $\pi$  interactions.



Graph 20 - Fluorescence enhancement for the titration of **64a** with acetyl chloride (0-400 nM)

## Conclusion

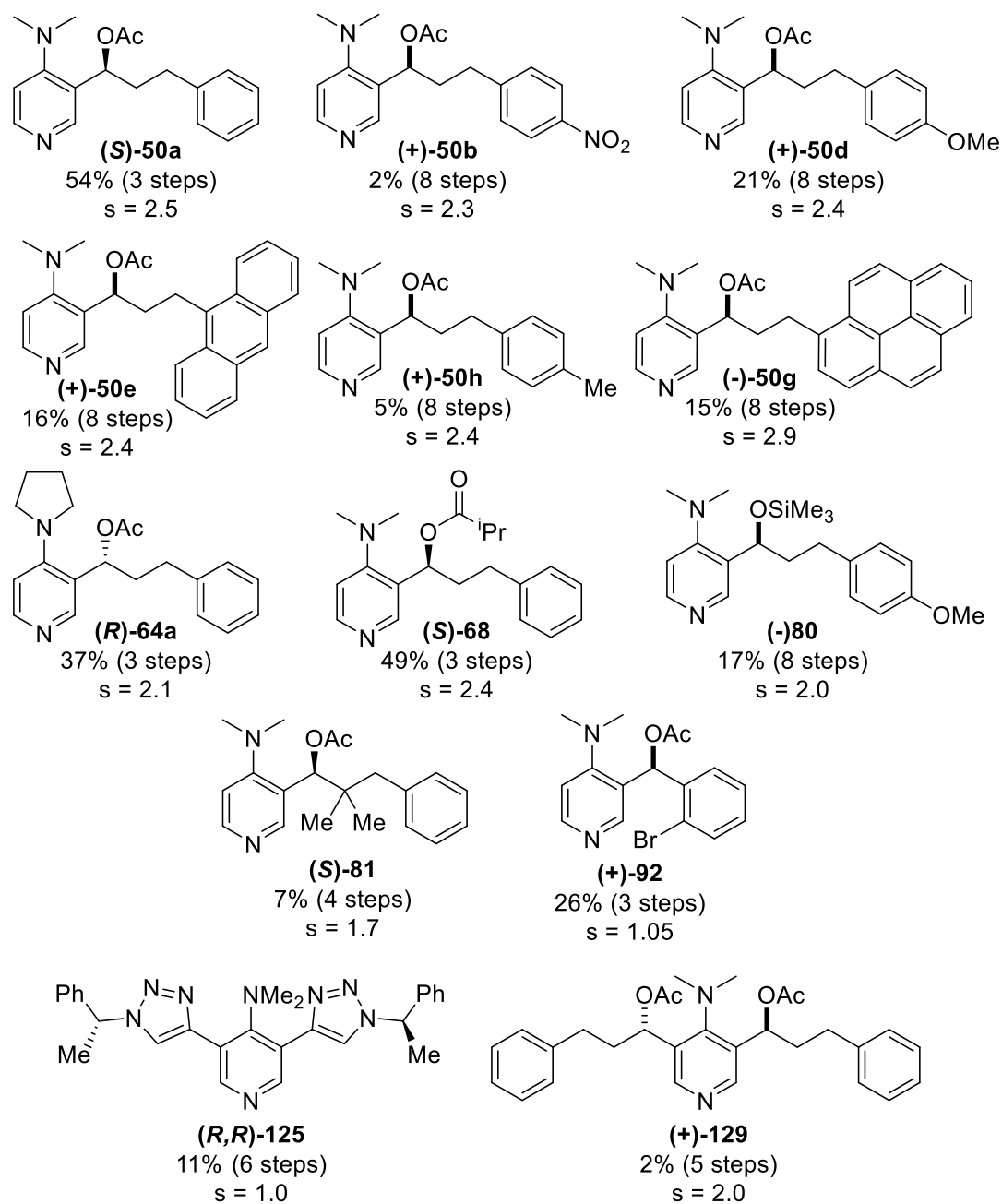


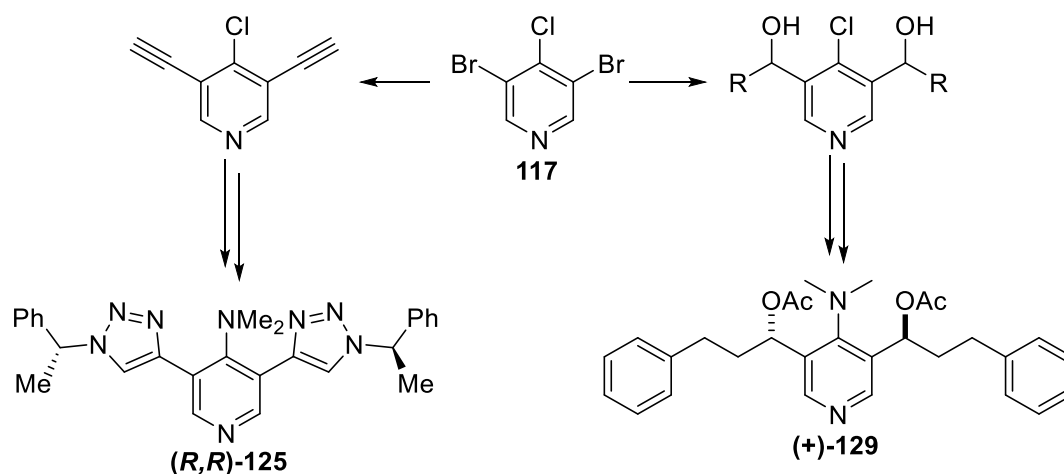
Figure 48 - Summary of catalysts synthesised with overall yields, step count and selectivity factors obtained in the kinetic resolution of 1-(1-naphthyl)ethanol

In this study the ability to utilise cation- $\pi$  interactions in chiral DMAP derivatives for the kinetic resolution of secondary alcohols has been probed. This was achieved through the synthesis of a library of 3- and 3,5-substituted DMAP derivatives (Figure 48). These catalysts contained a range of structural variations, including at the 4-position of pyridine,



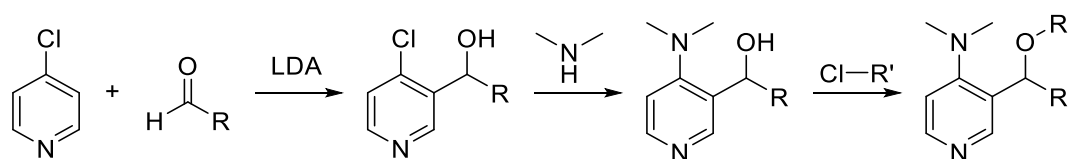
in the substituent of the alcohol, in the linker rigidity and in the electronics and  $\pi$ -surface of the aromatic moiety of the linker.

Both  $C_2$ -symmetric 3,5-disubstituted catalysts were synthesised from a common intermediate: 3,5-dibromo-4-chloropyridine (**117**). Catalyst **(*R,R*)-125** was synthesised *via* a double copper catalysed 'click' reaction with a chiral azide and a *bis*-alkyne obtained through a double Sonogashira reaction with 3,5-dialkyne **117**. Catalyst **130** was synthesised utilising a double transmetalation to the corresponding Grignard of **117** which was quenched with the corresponding aldehyde.



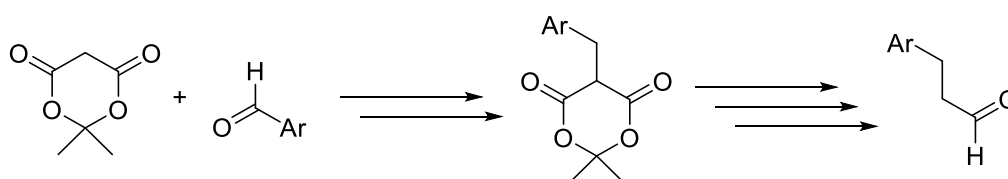
*Scheme 77 - General scheme for the synthesis of 3,5-positions substituted DMAP derivatives*

Three-position derivatisation was achieved, after optimisation, through a three-step synthesis from 4-chloropyridine and a range of aldehydes. Regioselective deprotonation of 4-chloropyridine was carried out with LDA, the resulting carbanion was quenched with an aldehyde to give a secondary alcohol. A nucleophilic aromatic substitution was used to exchange the 4-chloro group for a dimethylamino group and finally the alcohol was derivatised through either acylation or silylation (Scheme 78).



*Scheme 78 - General scheme for the synthesis of 3-positions substituted DMAP derivatives*

Although some aldehydes were commercially available, a number of the hydrocinnamaldehydes needed to be synthesised. This was achieved *via* a five-step synthesis from Meldrum's acid and an arylaldehyde (Scheme 79) *via* a Knoevenagel condensation, olefin reduction, decarboxylation, carboxylic acid reduction and alcohol oxidation. The outlined five-step synthesis was successful in providing a range of hydrocinnamaldehyde derivatives in acceptable yields but it was found that a single set of conditions were not applicable to all substrates.



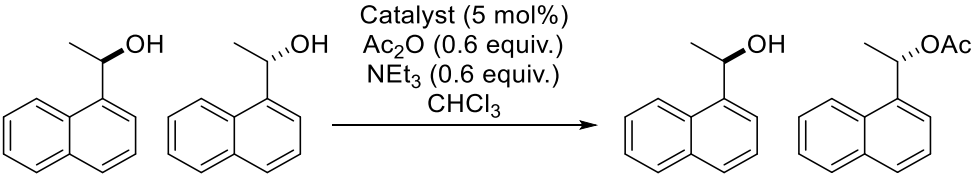
*Scheme 79 - Summary of the synthesis of hydrocinnamaldehydes with key intermediates shown*

The synthesised catalysts were screened for their effectiveness at the kinetic resolution of secondary alcohols with selectivity factors (*s*) between 1.0 and 2.9 obtained. This was achieved through *in situ* monitoring of the reaction mixture using gas chromatography with a column with a chiral stationary phase, this allowed for the comparison of relative rates as well as the determination of selectivity. The highest selectivity factor (2.9) was from the catalyst with a flexible linker terminating in a pyrene group. The lowest were for the triazole containing catalyst and the 2-bromophenyl catalyst which did not have a three-carbon linker. It was found that substitution of the linker caused a lowering of the selectivity factor and furthermore a  $C_2$ -symmetric system gave no benefit when compared to the mono-derivatised compounds.

With some selectivity obtained in the kinetic resolution of secondary alcohols, preliminary fluorescence studies were carried out to interrogate whether a cation- $\pi$  interaction was present. A fluorescence response was observed when catalyst **(S)-50a** was acylated or alkylated at very low concentrations. The response was however determined to be

concentration dependent and occurred at concentrations that were too low to validate the interaction by other techniques, such as nOe spectroscopy. Additionally, attempts to observe this interaction with other catalyst systems was unsuccessful.

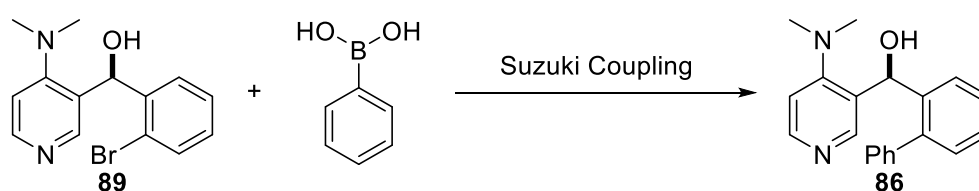
*Table 12 - Summary of the selectivity factors obtained for all catalysts*

				
Entry	Catalyst	Conversion (%)	$ee_{OH}$ (%)	Selectivity factor (s)
1	(S)-50a	49	31	2.57±0.02
2	(+)-50b	40	20	2.26±0.02
3	(+)-50d	49	28	2.36±0.02
4	(+)-50e	42	24	2.39±0.01
5	(+)-50h	49	29	2.42±0.02
6	(-)-50g	59	45	2.90±0.04
7	(R)-64a	48	23	2.10±0.02
8	(S)-68	45	25	2.38±0.01
9	(-)-80	50	23	1.95±0.01
10	(S)-81	31	9	1.66±0.01
11	(+)-92	39	1	1.05±0.01
12	(R,R)-125	33	<1	1.03±0.01
13	(+)-129	19	7	2.01±0.02

In conclusion, thirteen novel chiral DMAP derivatives were synthesised with synthetic routes optimised within this study. In order to achieve this, methodology was developed for the synthesis of a structurally diverse range of hydrocinnamaldehydes, which overcame a number of synthetic challenges. The synthesised catalysts were then studied in the kinetic resolution of secondary alcohols, with selectivity factors up to 2.9 obtained for the resolution of 1-(1-naphthyl)ethanol. Finally, the fluorescence properties of the catalysts were probed in an attempt to observe a cation- $\pi$  interaction from which the preliminary results appear promising.

In order to further progress this body of research there are several key DMAP derivatives which should be synthesised and tested in the kinetic resolution of secondary alcohols.

Further derivatisation of the 3-position modified DMAP derivatives is unlikely to yield the level of selectivity required for asymmetric catalysis. Therefore, initial studies should focus on the synthesis of enantiopure **86** due to its rigidity and preorganisation, the most likely route for this is the Suzuki cross-coupling of **89** with aryl boronic acids, the synthesis of enantiopure **89** has been detailed in this study. If this route were successful it would give rise to a rapid and diverse library of derivatives through modification of the aryl portion of the boronic acid.



*Scheme 80 - Synthesis of enantiopure 86 with a Suzuki cross-coupling*

The 1,4-triazole was synthesised and studied in the kinetic resolution of 1-(1-naphthyl)ethanol giving a selectivity factor of 1.0. Synthesis of the 1,5-triazole regioisomer would allow for the study of the effects of the regiochemistry. It can be hypothesised that the 1,5-isomer would bring the phenyl group and the stereocentre towards the active site of the DMAP core. This may give a higher level of selectivity in asymmetric catalysis. If favourable results were obtained, then the synthesis of enantiopure secondary azides can be achieved from enantiopure secondary alcohols allowing for a library of derivatives to be synthesised.

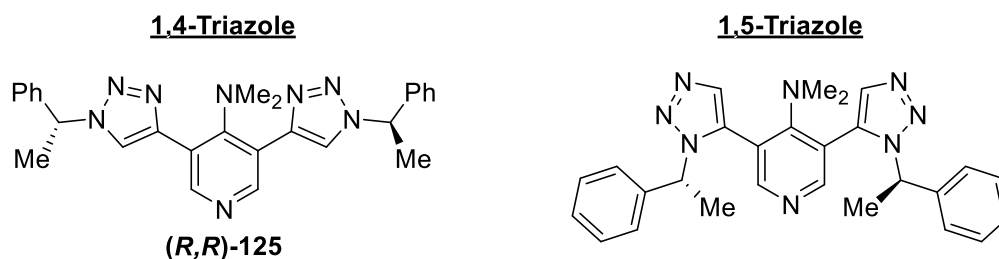


*Figure 49 - Comparison of triazole regioisomers*

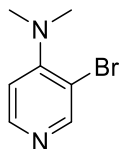
# Experimental

## General Information

Commercially available solvents and reagents were used without further purification.  $^1\text{H}$  and  $^{19}\text{F}$  NMR spectra were recorded on a Bruker AVIII300 NMR spectrometer at 300 MHz and 282 MHz, respectively.  $^1\text{H}$  NMR and  $^{13}\text{C}$  NMR were recorded at 400 MHz and 101 MHz, respectively, on a Bruker AVIII400 NMR spectrometer at room temperature. All 2D NMR spectra were recorded on a Bruker AVIII400 NMR spectrometer at room temperature. Data was processed on Mestrec version 10.0.2-15465 and Topspin 2.0 (version of Nov 9<sup>th</sup> 2006). Chemical shifts ( $\delta$ ) are reported in ppm relative to TMS for  $\text{CDCl}_3$  ( $\delta$  0.00) or the residual solvent peak for  $^1\text{H}$  NMR or relative to the solvent reported for  $^{13}\text{C}$  NMR, coupling constants ( $J$ ) are expressed in Hertz (Hz). Shift multiplicities are reported as singlet (s), Doublet (d), triplet (t), quartet (q), double doublet (dd), multiplet (m) and broad singlet (bs). Mass spectra were recorded with an electrospray MS Waters LCT time of flight Mass spectrometer or with an EI (GC/MS) Waters GCT Premier Time of Flight Mass Spectrometer. Infrared spectra were recorded on a PerkinElmer 100FT-IR spectrometer at room temperature using an ATR attachment. Fluorescence spectroscopy measurements were performed using a Gilden Photonics FluoroSENS SENS-9000 instrument, with Starna Silica (quartz) cuvettes with 10 mm path lengths and four polished faces and data was processed with the FluoroSENS 1.88.7 software package. Analytical HPLC was carried out on a Shimadzu Prominence system with diode array detection. Preparative HPLC was carried out on a Dionex Summit HPLC system with two wavelength detection. Gas chromatography was performed on a Varian 3900 GC with a Varian 8410 Autosampler.

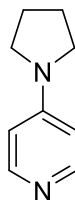
## Synthesis of Catalyst Core Structure

### 3-Bromo-4-dimethylaminopyridine (**52**)<sup>67-70</sup>



Bromine (6.35 mL, 123 mmol, 3.0 equiv.) in  $\text{CH}_2\text{Cl}_2$  (25 mL) was added dropwise over 30 mins to a vigorously stirred solution of dimethylaminopyridine (5.00 g, 41 mmol, 1.0 equiv.) and tetrabutylammonium hydroxide (40% in  $\text{H}_2\text{O}$ , 7.5 mL, 12 mmol, 0.3 equiv.) in  $\text{CH}_2\text{Cl}_2$  (100 mL) and saturated aqueous potassium carbonate solution (100 mL) for 4.5 hrs under ambient conditions. The organic phase was separated and washed with  $\text{H}_2\text{O}$  (3 x 150 mL), dried over  $\text{MgSO}_4$  and the solvent was removed under reduced pressure. The crude reaction mixture was purified by flash chromatography (silica, EtOAc) and vacuum distillation (lit<sup>68</sup>: 172 °C @ 1.5 mmHg) to afford **52** as a colourless oil (1.66 g, 20%);  $R_f$  = 0.5 (EtOAc);  $^1\text{H}$  NMR (300 MHz,  $\text{CDCl}_3$ )  $\delta$  8.51 (s, 1H, Py), 8.28 (d,  $J$  = 5.6 Hz, 1H, Py), 6.80 (d,  $J$  = 5.6 Hz, 1H, Py), 2.97 (s, 6H,  $\text{CH}_3$ );  $^{13}\text{C}$  NMR (101 MHz,  $\text{CDCl}_3$ )  $\delta$  157.9, 153.4, 148.8, 113.8, 112.5, 42.5; IR (neat)  $\nu$  ( $\text{cm}^{-1}$ ) 1577 (C=C), 952 (C-Br).

### 4-(Pyrrolidin-1-yl)pyridine (**3**)<sup>111</sup>

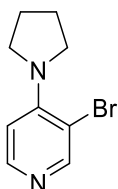


4-Chloropyridine (1.00 g, 6.67 mmol, 1.0 equiv.) was added to pyrrolidine (5.53 mL, 66.7 mmol, 10.0 equiv.) in  $\text{H}_2\text{O}$  (3 mL) and heated in a microwave reactor for 30 mins at 130 °C before being allowed to slowly reach room temperature. The solvent of the resulting reaction mixture was removed under reduced pressure and the solid residue was passed

through a SiO<sub>2</sub> plug (3 cm) with CH<sub>2</sub>Cl<sub>2</sub> as eluent. The CH<sub>2</sub>Cl<sub>2</sub> was removed under reduced pressure and the crude material was recrystallised from hexane/EtOAc to afford **3** as a white crystalline solid (0.63 g, 51%);\* R<sub>f</sub> = 0.3 (CH<sub>2</sub>Cl<sub>2</sub>/MeOH [19:1]); <sup>1</sup>H NMR (300 MHz, CDCl<sub>3</sub>) δ 8.07 (d, *J* = 6.8 Hz, 2H, Ar), 6.62 (d, *J* = 6.8 Hz, 2H, Ar), 3.49 (m, 4H, Pyr), 2.14 (m, 4H, Pyr); <sup>13</sup>C NMR (101 MHz, CDCl<sub>3</sub>) δ 139.1, 107.3, 48.4, 25.2; TOF MS ES+ *m/z*: 149.0 [M+H]<sup>+</sup>.

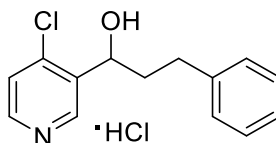
*\*Quaternary <sup>13</sup>C NMR shift not visible.*

### **3-Bromo-4-(pyrrolidin-1-yl)pyridine (**54**)<sup>36</sup>**

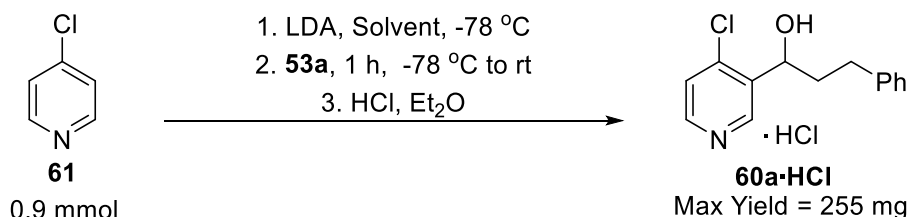


Bromine (0.13 mL, 2.46 mmol, 1.5 equiv.) and 1 drop of tetrabutylammonium hydroxide was added to a vigorously stirred solution of **3** (0.30 g, 1.64 mmol, 1.0 equiv.) in a biphasic solution of CH<sub>2</sub>Cl<sub>2</sub> (2.8 mL) and saturated aqueous potassium carbonate solution (2.8 mL) and stirred for 5 hrs at room temperature. The phases were separated and the aqueous was washed with CH<sub>2</sub>Cl<sub>2</sub> (3 x 10 mL). The resulting organic phase was evaporated under reduced pressure. EtOAc was added and the resulting precipitate was filtered and the filtrate purified by flash chromatography (silica, EtOAc) to afford the product as a yellow oil (94 mg, 22%); R<sub>f</sub> = 0.43 (EtOAc); <sup>1</sup>H NMR (300 MHz, CDCl<sub>3</sub>) δ 8.37 (s, 1H, Py), 8.08 (d, *J* = 5.6 Hz, 1H, Py), 6.47 (d, *J* = 5.6 Hz, 1H, Py), 3.68 – 3.50 (m, 4H, Pyr), 2.05 – 1.82 (m, 4H, Pyr); <sup>13</sup>C NMR (101 MHz, CDCl<sub>3</sub>) δ 153.7, 151.5, 147.9, 110.5, 105.0, 50.6, 25.7; TOF MS EI+ *m/z*: 226.0/228.0 [M]<sup>+</sup>.

**4-Chloro-3-(1-hydroxy-3-phenylpropyl)pyridin-1-ium chloride (60a-HCl)**



General Procedure for Synthesis of Racemate **rac-60a-HCl**:



Entry	LDA Equiv.	LDA Conc. (M)	53a Equiv.	Solvent	Deprotonation time (hrs)	Yield (%)
1	1.2	0.1	2	Et <sub>2</sub> O	3	38
2	1.5	0.1	2	Et <sub>2</sub> O	3	58, 60, 56
3	2.0	0.1	2	Et <sub>2</sub> O	3	61
4	2.5	0.1	<b>2.5</b>	Et <sub>2</sub> O	3	67
5	1.5	<b>0.15</b>	2	Et <sub>2</sub> O	3	55
6	1.5	<b>0.25</b>	2	Et <sub>2</sub> O	3	48
7	1.5	<b>0.05</b>	2	Et <sub>2</sub> O	3	40
8	1.5	0.1	2	Et <sub>2</sub> O	<b>1</b>	8
9	1.5	0.1	2	Et <sub>2</sub> O	<b>2</b>	36
10	1.5	0.1	2	Et <sub>2</sub> O	<b>4</b>	63, 63
11	1.5	0.1	2	Et <sub>2</sub> O	<b>5</b>	57
12	1.5	0.1	<b>1.5</b>	Et <sub>2</sub> O	4	52
13	1.5	0.1	<b>1.75</b>	Et <sub>2</sub> O	4	56

*Data shown in bold indicates the factor varied in the experiment.*

4-Chloropyridine (1.0 equiv., 100 mg/mL Et<sub>2</sub>O) was added dropwise to a solution of 0.1 M LDA in Et<sub>2</sub>O (1.5 equiv.) at -78 °C and stirred for 4 hrs. Hydrocinnamaldehyde (2 equiv.) was added dropwise and the reaction mixture was slowly allowed to reach room temperature over 1 hr before the addition of H<sub>2</sub>O (5 mL/mmol) and stirred for 15 mins. The phases were separated, the aqueous phase was extracted with Et<sub>2</sub>O (2x15 mL), organic phases were combined, dried over MgSO<sub>4</sub>, reduced onto silica and eluted through silica (4 cm) with 200 mL/mmol of EtOAc:hexane (1:1). The eluting solvent was removed under reduced pressure and the residue dissolved in Et<sub>2</sub>O (25 mL/mmol), to which 4 M



HCl in dioxane (1 mL/mmol) was added dropwise leading to the formation of a white precipitate. The solvent was removed under reduced pressure and the resulting solid recrystallised from MeCN to afford **rac-60a·HCl** as colourless needles after filtration.

#### CBS Reduction of ketone **67** with borane to give **(S)-60a·HCl**

Borane solution (1M in THF, 0.72 mL, 0.72 mmol, 1.0 equiv.) was added dropwise to a solution of (S)-CBS (200 mg, 0.72 mmol, 1.0 equiv.) in THF (10 mL) at 0 °C and stirred for 15 mins, to which ketone **67** (178 mg, 0.72 mmol, 1.0 equiv.) in THF (5 mL) was added dropwise over 30 mins and left to slowly reach room temperature for 1 hr. Two subsequent portions of borane solution (1M in THF, 0.72 mL, 1.0 equiv.) were added over the following 4 hrs and left to stir for an additional 12 hrs. The reaction mixture was evaporated under reduced pressure onto silica and purified by flash chromatography (Silica, 0-100% EtOAc/hexane). The resulting solid was dissolved in Et<sub>2</sub>O (5 mL), to which 4 M HCl in dioxane (1 mL) was added dropwise leading to the formation of a white precipitate. The solvent was removed under reduced pressure and the solid recrystallised from MeCN to afford **(S)-60a·HCl** as colourless needles after filtration (174 mg, 98%, 70% ee by Mosher's ester derivatisation).

#### CBS Reduction of ketone **67** with catecholborane to give **(S)-60a·HCl**

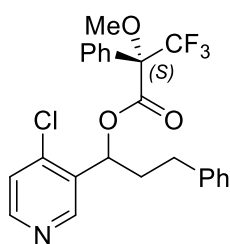
Catecholborane solution (1M in THF, 1.5 mL, 1.5 mmol, 3.0 equiv.) was added dropwise to a solution of (S)-CBS (130 mg, 0.5 mmol, 1.0 equiv.) in THF (10 mL) at 0 °C and stirred for 15 mins, to which ketone **67** (116 mg, 0.5 mmol, 1.0 equiv.) in THF (5 mL) was added dropwise over 30 mins and left to slowly reach room temperature for 18 hrs. The reaction mixture was evaporated under reduced pressure onto silica and purified by flash chromatography (silica, 0-100% EtOAc/hexane). The resulting solid was dissolved in Et<sub>2</sub>O (5 mL), to which 4 M HCl in dioxane (0.5 mL) was added dropwise leading to the formation

of a white precipitate. The solvent was removed under reduced pressure and the solid recrystallised from MeCN to afford **(S)-60a** as colourless needles after filtration (54 mg, 39%, 74% *ee* by Mosher's ester derivatisation).

Mp 154-156 °C;  $^1\text{H}$  NMR (400 MHz,  $\text{d}_3\text{-MeOD}$ )  $\delta$  8.96 (s, 1H, Py), 8.73 (d,  $J$  = 6.3 Hz, 1H, Py), 8.13 (d,  $J$  = 6.3 Hz, 1H, Py) 7.33 – 7.13 (m, 5H, Ph), 5.10 (dd,  $J$  = 8.7 3.1 Hz, 1H,  $\text{CHOH}$ ), 3.00 – 2.80 (m, 2H,  $\text{PhCH}_2$ ), 2.22 – 1.93 (m, 2H,  $\text{CH}_2\text{CH}$ );  $^{13}\text{C}$  NMR (101 MHz,  $\text{d}_3\text{-MeOD}$ )  $\delta$  151.5, 144.7, 141.0, 140.9, 140.5, 136.5, 128.2, 128.1, 125.7, 67.1, 37.9, 31.1; IR (neat)  $\nu$  ( $\text{cm}^{-1}$ ) 3209 (OH), 2717 ( $\text{N}^+\text{H}$ ); TOF MS ES+  $m/z$ : 248.1/250.1 [ $\text{M-Cl}$ ] $^+$ ; HR-MS calc. [ $\text{C}_{14}\text{H}_{15}\text{N}_2\text{O}^{35}\text{Cl}$ ] $^+$  248.0837, obs. 248.0763;

Preparative HPLC: Enantiomers were separated on a Phenomenex Cellulose 1 Preparative HPLC column eluting with acetonitrile:water [1:1] at a flow rate of 15 mL/min. A total of 400 mg of racemic compound was inject and 127 mg of **(R)-60a** (32%,  $[\alpha]^{293}_{\text{D}} -21.1^\circ$  (c 0.38,  $\text{CHCl}_3$ )) and 135 mg of **(S)-60a** (34%) was recovered.

**1-(4-Chloropyridin-3-yl)-3-phenylpropyl (2S)-3,3,3-trifluoro-2-methoxy-2-phenylpropanoate (65)**

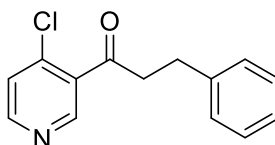


(*R*)-Mosher's acid chloride (0.023 mL, 0.12 mmol, 1.2 equiv.) was added to a stirring solution of 1-(4-(dimethylamino)pyridin-3-yl)-3-phenylpropan-1-ol (**51a**, 25 mg, 0.10 mmol, 1.0 equiv.),  $\text{NEt}_3$  (0.017 mL, 0.12 mmol, 1.2 equiv.) and DMAP (1.2 mg, 0.01 mmol, 0.1 equiv.) in  $\text{CH}_2\text{Cl}_2$  (2 mL) at room temperature for 5 hrs. The organic mixture was washed with  $\text{H}_2\text{O}$  (5 mL), dried over  $\text{MgSO}_4$ , the solvent was removed under reduced

pressure and the residue was purified by column chromatography (silica, 0-100% EtOAc/hexane) to afford **65** as a colourless oil (38 mg, 83%). *Characterisation data for 65 has been reported as an equimolar mixture of diastereoisomers.*

$R_f$  = 0.68 (Hexane/EtOAc [1:1]);  $^1\text{H}$  NMR (300 MHz,  $\text{CDCl}_3$ )  $\delta$  8.53 (s, 0.5H, Py), 8.44 (t,  $J$  = 5.3 Hz, 1H, Py), 8.33 (s, 0.5H, Py), 7.60 – 6.99 (m, 11H, Ph), 6.32 (ddd,  $J$  = 12.7, 8.4, 4.6 Hz, 1H,  $\text{CH}_2$ ), 3.61 (s, 1.5H,  $\text{CH}_3$ ), 3.50 (s, 1.5H,  $\text{CH}_3$ ), 2.87 – 2.46 (m, 2H,  $\text{CH}_2$ ), 2.43 – 2.02 (m, 2H,  $\text{CH}_2$ );  $^{19}\text{F}$  NMR (282 MHz,  $\text{CDCl}_3$ )  $\delta$  -70.85, -71.14;  $^{13}\text{C}$  NMR (101 MHz,  $\text{CDCl}_3$ )  $\delta$  165.9, 165.8, 150.1, 150.0, 149.0, 148.7, 142.2, 140.1, 140.0, 133.2, 133.1, 131.8, 131.7, 129.9, 128.6, 128.5, 128.2, 127.3, 127.2, 126.4, 126.3, 124.6, 124.5, 73.1, 72.9, 55.7, 55.6, 36.7, 36.6, 31.5, 31.2, 30.9; IR (neat)  $\nu$  ( $\text{cm}^{-1}$ ) 1750 (C=O); TOF MS ES+  $m/z$ : 464.2/466.1  $[\text{M}]^+$ .

#### 1-(4-Chloropyridin-3-yl)-3-phenylpropan-1-one (**67**)



General Procedure for Chromium Mediated Oxidations of **60a**:

Entry	Conditions	Scale (mmol)	Yield (%)
1	$\text{CrO}_3$ (3 equiv.), acetone, 4h	5	14
2	$\text{CrO}_3$ (3 equiv.), acetone, 3h	5	18
3	PCC (1 equiv.), DCM, 15 min	0.4	17
4	PCC (2 equiv.), DCM, 15 min	0.4	40
5	PCC (2 equiv.), DCM, 2 h	0.4	43
6	PCC (2 equiv.), DCM, 15 min	2	36
7	PDC (2 equiv.), DCM, 2h	0.4	41

1-(4-(Dimethylamino)pyridin-3-yl)-3-phenylpropan-1-ol in the relevant solvent (1 mL) was added dropwise to a solution of the chromium reagent in solvent at 0 °C before being allowed to reach room temperature, the reaction was allowed to stir under dry conditions until full conversion by TLC. The reaction mixture was diluted with  $\text{Et}_2\text{O}$ , filtered through

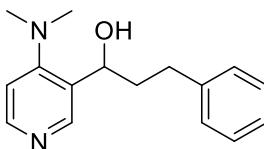
celite, the solvent was removed under reduced pressure and the residue purified by flash chromatography (silica, 0-100% EtOAc/hexane) to afford the desired compound.

#### General Procedure for Swern Oxidation of **60a**:

Dimethyl Sulfoxide (80  $\mu$ L, 1.2 mmol, 2.2 equiv.) in  $\text{CH}_2\text{Cl}_2$  (1 mL) was added dropwise to a solution of oxalyl chloride (50  $\mu$ L, 0.6 mmol, 1.1 equiv.) in  $\text{CH}_2\text{Cl}_2$  (1 mL) at  $-78^\circ\text{C}$  and stirred for 10 mins. 1-(4-(Dimethylamino)pyridin-3-yl)-3-phenylpropan-1-ol (130 mg, 0.5 mmol, 1.0 equiv.) in  $\text{CH}_2\text{Cl}_2$  (1 mL) was added dropwise and the reaction mixture was stirred for a further 30 mins. Triethylamine (0.37 mL, 2.1 mmol, 5.0 equiv.) was added dropwise to the solution and stirred at  $-78^\circ\text{C}$  for 5 mins before being allowed to reach room temperature over 25 mins. The reaction mixture was evaporated under reduced pressure onto silica and purified by flash chromatography (silica, 0-100% EtOAc/hexane) to afford **67** as a colourless oil. (120 mg, 92%).

$R_f$  = 0.52 (Hexane/EtOAc [1:1]);  $^1\text{H}$  NMR (300 MHz,  $\text{CDCl}_3$ )  $\delta$  8.67 (s, 1H, Py), 8.58 (d,  $J$  = 5.4 Hz, 1H, Py), 7.40 (d,  $J$  = 5.4 Hz, 1H, Py), 7.36 – 7.19 (m, 5H, Ph), 3.33 (t,  $J$  = 7.5 Hz, 2H,  $\text{CH}_2$ ), 3.09 (t,  $J$  = 7.5 Hz, 2H,  $\text{CH}_2$ );  $^{13}\text{C}$  NMR (101 MHz,  $\text{CDCl}_3$ )  $\delta$  200.0, 152.0, 149.8, 141.5, 140.3, 134.5, 128.6, 128.4, 126.4, 125.4, 44.7, 30.0; IR (neat)  $\nu$  ( $\text{cm}^{-1}$ ) 1699 (C=O); TOF MS EI+  $m/z$ : 245.1/247.1  $[\text{M}]^+$ , 210.1  $[\text{M}-\text{Cl}]^+$ , 140/142.0  $[\text{M}-\text{CH}_2\text{CH}_2\text{Ph}]^+$ ; HR-MS calc.  $[\text{C}_{14}\text{H}_{12}\text{NOCl}]^+$  245.0602, obs. 245.0607.

#### 1-(4-(Dimethylamino)pyridin-3-yl)-3-phenylpropan-1-ol (**51a**)



Procedure for lithium-halogen exchange of **52** to give **51a**:

3-Bromo-4-dimethylaminopyridine **52** (0.5 g, 2.5 mmol, 1.0 equiv.) in toluene (5 mL) was added dropwise over 10 mins to a stirred solution of <sup>n</sup>Butyl lithium (1.4 M in toluene, 4.45 mL, 6.2 mmol, 2.5 equiv.) in toluene (10 mL) at -78 °C and stirred for 20 mins. Hydrocinnamaldehyde (0.95 g, 6.2 mmol, 2.5 equiv.) was added dropwise over 10 mins and the reaction mixture was warmed to room temperature over 30 mins, quenched with H<sub>2</sub>O (30 mL) and the organic phase was washed with 1 M aqueous HCl (3 x 15mL). The aqueous extract was basified to pH >10 and extracted three times with EtOAc (3 x 100 mL). The organic extracts were combined, dried over MgSO<sub>4</sub> and the solvent was removed under reduced pressure to afford a pale yellow oil which was purified by column chromatography (silica, 0-10% MeOH/CH<sub>2</sub>Cl<sub>2</sub>) to afford **51a** as a colourless oil (0.47 g, 73%).

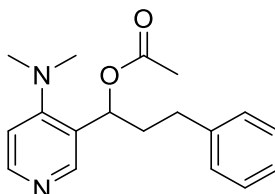
Procedure for aromatic substitution of **(S)-60a** to give **(S)-51a**:

4-Chloro-3-(1-hydroxy-3-phenylpropyl)pyridin-1-ium chloride (**(S)-60a·HCl**) (100 mg, 0.35 mmol, 1.0 equiv.) was added portionwise to a stirred solution of HNMe<sub>2</sub> (40% w/w in H<sub>2</sub>O, 3 mL) in a microwave reaction vessel and heated to 150 °C for 8 hrs. The solvent volume was reduced by 75%, basified with saturated aqueous NaHCO<sub>3</sub> (10 mL) and extracted with CH<sub>2</sub>Cl<sub>2</sub> (3 x 10 mL). The combined organic extracts were combined, dried over MgSO<sub>4</sub> and evaporated to dryness under reduced pressure to afford **(S)-51a** as a colourless oil (88 mg, 98%).

R<sub>f</sub> = 0.38 (CH<sub>2</sub>Cl<sub>2</sub>/MeOH [9:1]); <sup>1</sup>H NMR (400 MHz, CDCl<sub>3</sub>) δ 8.51 (s, 1H, Py), 8.35 (d, *J* = 5.6 Hz, 1H, Py), 7.36 – 7.17 (m, 5H, Ph), 6.90 (d, *J* = 5.6 Hz, 1H, Py), 4.98 (dd, *J* = 8.9, 4.2 Hz, 1H, CHOH), 2.99 – 2.66 (m, 8H, CH<sub>3</sub> & CH<sub>2</sub>), 2.31 – 2.04 (m, 2H, CH<sub>2</sub>); <sup>13</sup>C NMR (101 MHz, CDCl<sub>3</sub>) δ 158.3, 149.4, 149.2, 141.7, 132.1, 128.6, 128.4, 125.9, 113.8, 68.3, 44.1, 39.5,

32.5; IR (neat)  $\nu$  (cm<sup>-1</sup>) 3166 (OH), 1593.14 (C=C); TOF MS ES<sup>+</sup>  $m/z$ : 279.2 [M+Na]<sup>+</sup>, 257.2 [M+H]<sup>+</sup>; HR-MS calc. [C<sub>16</sub>H<sub>21</sub>N<sub>2</sub>O]<sup>+</sup> 257.1648, obs. 257.1655;

#### 1-(4-(Dimethylamino)pyridin-3-yl)-3-phenylpropyl acetate (**50a**)



Acylation of racemic **51a**:

Acetic anhydride (0.09 mL, 0.09 mmol, 1.3 equiv.) and triethylamine (0.11 mL, 0.80 mmol, 1.2 equiv.) were added to a solution of **51a** (0.16 g, 0.62 mmol, 1.0 equiv.) in CH<sub>2</sub>Cl<sub>2</sub> (10 mL) and stirred for 26 hrs at room temperature. The reaction mixture was washed with H<sub>2</sub>O (2 x 20 mL), dried over MgSO<sub>4</sub>, filtered and the solvent was removed under reduced pressure to afford **50a** (0.174 g, 94%) as a colourless oil.

Acylation of (**S**)-**51a**:

Acetic anhydride (36  $\mu$ L, 0.38 mmol, 1.2 equiv.) was added to a stirring solution of (**S**)-1-(4-(dimethylamino)pyridin-3-yl)-3-phenylpropan-1-ol ((**S**)-**51a**) (83 mg, 0.32 mmol, 1.0 equiv.) in CH<sub>2</sub>Cl<sub>2</sub> (2 mL) at room temperature for 1 hr. The organic mixture was washed with saturated aqueous NaHCO<sub>3</sub> (5 mL), dried over MgSO<sub>4</sub>, filtered and evaporated to dryness under reduced pressure to afford (**S**)-**50a** as a colourless oil (84 mg, 88%).

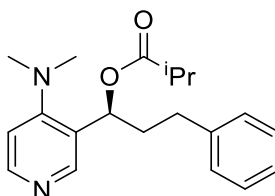
Synthesis of racemic **50a** from **52** via a lithium-halogen exchange:

Bromide **52** (1.5g, 7.5 mmol, 1.0 equiv.) in toluene (5 mL) was added dropwise over 10 mins to a stirred solution of <sup>n</sup>Butyl lithium (1.4 M in toluene, 13.4 mL, 18.7 mmol, 2.5 equiv.) in toluene (130 mL) at -78 °C and stirred for 1 hr. Hydrocinnamaldehyde (2.5 mL, 18.7 mmol, 2.5 equiv.) was added dropwise over 10 mins and the reaction mixture was

slowly warmed to room temperature over 30 mins. Acetic anhydride (1.8 mL, 18.7 mmol, 2.5 equiv.) was added dropwise and stirred for 10 mins. Brine (100 mL) was added and the phases were separated, the organic phase was dried over MgSO<sub>4</sub> and the solvent was removed under reduced pressure to afford a pale yellow oil which was purified by column chromatography (silica, 0-5% MeOH/CH<sub>2</sub>Cl<sub>2</sub>) to afford **50a** as a yellow oil (1.23 g, 55%).

$R_f = 0.47$  (CH<sub>2</sub>Cl<sub>2</sub>/MeOH [9:1]); <sup>1</sup>H NMR (400 MHz, CDCl<sub>3</sub>)  $\delta$  8.49 (s, 1H, Py), 8.33 (d,  $J = 5.6$  Hz, 1H, Py), 7.33 – 7.15 (m, 5H, Ph), 6.81 (d,  $J = 5.6$  Hz, 1H, Py), 6.11 (dd,  $J = 8.9, 4.3$  Hz, 1H, CHOH), 2.83 – 2.56 (m, 8H, CH<sub>3</sub> & CH<sub>2</sub>), 2.35 – 2.01 (m, 5H, CH<sub>2</sub>Ph); <sup>13</sup>C NMR (101 MHz, CDCl<sub>3</sub>)  $\delta$  170.5, 157.7, 149.6, 148.8, 141.0, 128.6, 128.4, 128.4, 126.0, 112.9, 70.3, 43.5, 37.7, 32.1, 21.2; IR (neat)  $\nu$  (cm<sup>-1</sup>) 1734 (C=O), 1588 (C=C Ar); TOF MS ES+  $m/z$ : 321.2 [M+Na]<sup>+</sup>, 299.2 [M+H]<sup>+</sup>; HR-MS calc. [C<sub>18</sub>H<sub>23</sub>N<sub>2</sub>O<sub>2</sub>]<sup>+</sup> 299.1754, obs. 299.1764.

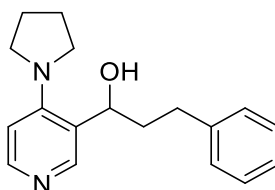
**(S)-1-(4-(Dimethylamino)pyridin-3-yl)-3-phenylpropyl isobutyrate ((S)-68)**



Isobutyric anhydride (36  $\mu$ L, 0.22 mmol, 1.5 equiv.) was added to a solution of **(S)-51a** (37 mg, 0.14 mmol, 1.0 equiv.) in CH<sub>2</sub>Cl<sub>2</sub> (2 mL) and stirred for 1 hr at room temperature. The reaction mixture was washed with water (2 x 20 mL), dried over MgSO<sub>4</sub>, filtered and the solvent was removed under reduced pressure. The residue was purified by column chromatography (silica, 0-10% MeOH/CH<sub>2</sub>Cl<sub>2</sub>) to afford **(S)-68** (45 mg, 96%) as a colourless oil;  $[\alpha]^{293}_D$  11.1° (c 0.18, CHCl<sub>3</sub>); <sup>1</sup>H NMR (400 MHz, CDCl<sub>3</sub>)  $\delta$  8.45 (s, 1H, Py), 8.30 (d,  $J = 5.6$  Hz, 1H, Py), 7.32 – 7.25 (m, 2H, Ph), 7.25 – 7.11 (m, 3H, Ph), 6.78 (d,  $J = 5.6$  Hz, 1H, Py), 6.04 (dd,  $J = 9.1, 4.1$  Hz, 1H, CHOH), 2.83 – 2.72 (m, 1H, CH<sub>2</sub>), 2.72 (s, 7H, CH<sub>2</sub> & N(CH<sub>3</sub>)<sub>2</sub>), 2.71 – 2.55 (m, 1H, CH<sub>2</sub>), 2.31 – 2.17 (m, 1H, CH<sub>2</sub>), 2.12 – 1.98 (m, 1H, CH<sub>2</sub>), 1.23 (d,  $J = 7.0$

Hz, 3H, CHCH<sub>3</sub>), 1.19 (d, *J* = 7.0 Hz, 3H, CHCH<sub>3</sub>); <sup>13</sup>C NMR (101 MHz, CDCl<sub>3</sub>) δ 176.5, 157.7, 149.4, 148.4, 141.0, 128.8, 128.4, 126.1, 112.8, 70.0, 43.4, 37.8, 34.1, 32.1, 19.0, 18.9; IR (neat) ν (cm<sup>-1</sup>) 1731 (C=O); TOF MS ES+ *m/z*: 327.2 [M+H]<sup>+</sup>; HR-MS calc. [C<sub>20</sub>H<sub>27</sub>N<sub>2</sub>O<sub>2</sub>]<sup>+</sup> 327.2067, obs. 327.2072.

### 3-Phenyl-1-(4-(pyrrolidin-1-yl)pyridin-3-yl)propan-1-ol (**63**)



Synthesis of racemic **63**:

**60a** (0.5 g, 3.0 mmol) was dissolved in pyrrolidine (4 mL) and H<sub>2</sub>O (2 mL) and heated in a microwave reactor at 130 °C for 4 hrs before being allowed to reach room temperature. The solvent was removed under reduced pressure and purified by flash chromatography (silica, 0-10% MeOH/CH<sub>2</sub>Cl<sub>2</sub>) and recrystallised from CH<sub>2</sub>Cl<sub>2</sub>/EtOAc to afford **63** as an off-white solid (360 mg, 63%)

Enantiopure product:

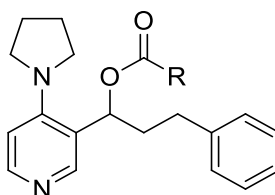
**(R)-60a** (0.11 g, 0.66 mmol) was dissolved in pyrrolidine (1.2 mL) and H<sub>2</sub>O (2.0 mL) and heated in a microwave reactor at 150 °C for 8 hrs before being allowed to reach room temperature. The solvent was removed under reduced pressure and the residue was purified by flash chromatography (silica, 0-10% MeOH/CH<sub>2</sub>Cl<sub>2</sub>) and recrystallised from CH<sub>2</sub>Cl<sub>2</sub>/EtOAc to afford **(R)-63** as an off-white solid (96 mg, 74%);

*R<sub>f</sub>* = 0.1 (CH<sub>2</sub>Cl<sub>2</sub>/MeOH [9:1]); <sup>1</sup>H NMR (300 MHz, CDCl<sub>3</sub>) δ 8.51 (s, 1H, Py), 7.85 (d, *J* = 7.1 Hz, 1H, Py), 7.41 – 7.12 (m, 5H, Ph), 6.54 (d, *J* = 7.1 Hz, 1H, Py), 5.32 (dd, *J* = 8.3, 3.7 Hz, 1H, CHOH), 3.52 (m, 2H, Pyr), 3.17 (m, *J* = 8.9 Hz, 2H, Pyr), 3.03 – 2.74 (m, 2H, CH<sub>2</sub>), 2.06 –



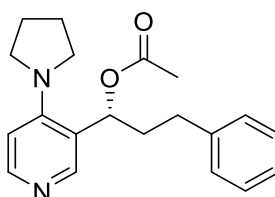
1.69 (m, 6H, Pyr & CH<sub>2</sub>); <sup>13</sup>C NMR (101 MHz, CDCl<sub>3</sub>) δ 154.5, 141.7, 138.3, 136.2, 128.9, 128.5, 128.3, 126.0, 108.7, 65.4, 51.5, 40.1, 31.7, 25.5; IR (neat) ν (cm<sup>-1</sup>) 3215.5 (OH); TOF MS ES+ m/z: 321.2 [M+Na]<sup>+</sup>, 283.2 [M+H]<sup>+</sup>; HR-MS calc. [C<sub>18</sub>H<sub>23</sub>N<sub>2</sub>O]<sup>+</sup> 283.1805, obs. 283.1810.

General Procedure for the Acylation of **63** to form **64a-c**



The corresponding anhydride (1.5 equiv.) was added to a stirred solution of **60a** (0.1 g, 0.35 mmol, 1.0 equiv.) in CH<sub>2</sub>Cl<sub>2</sub> (5 mL) for 16 hrs. The reaction mixture was washed with saturated aqueous NaHCO<sub>3</sub> solution, the organic phase was dried over MgSO<sub>4</sub>, filtered and the solvent was removed under reduced pressure to afford the crude compound which was purified by flash chromatography (silica, 0-10% MeOH/CH<sub>2</sub>Cl<sub>2</sub>) to afford the product.

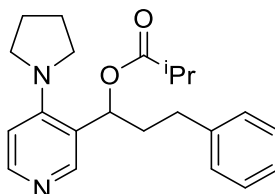
**(R)-3-Phenyl-1-(4-(pyrrolidin-1-yl)pyridin-3-yl)propyl acetate ((R)-64a)**



Colourless oil (83 mg, 73%); [α]<sub>D</sub><sup>293</sup> -12.0° (c 0.1, CHCl<sub>3</sub>); R<sub>f</sub> = 0.44 (CH<sub>2</sub>Cl<sub>2</sub>/MeOH [9:1]); <sup>1</sup>H NMR (300 MHz, CDCl<sub>3</sub>) δ 8.39 (s, 1H, Py), 8.12 (d, *J* = 6.0 Hz, 1H, Py), 7.25 (m, 5H, Ph), 6.44 (d, *J* = 6.0 Hz, 1H, Py), 6.24 (dd, *J* = 9.4, 3.9 Hz, 1H, CHOH), 3.39 – 3.00 (m, 4H, Pyr), 2.87 – 2.55 (m, 2H, CH<sub>2</sub>), 2.39 – 1.96 (m, 5H, CH<sub>3</sub> & CH<sub>2</sub>), 1.96 – 1.74 (m, 4H, Pyr); <sup>13</sup>C NMR (101 MHz, CDCl<sub>3</sub>) δ 170.6, 151.1, 149.3, 148.7, 141.0, 128.6, 128.5, 126.1, 121.8, 109.0, 70.2,

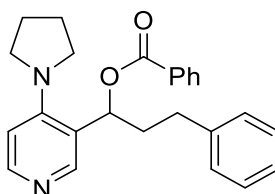
50.5, 38.5, 32.0, 25.7, 21.2; IR (neat)  $\nu$  ( $\text{cm}^{-1}$ ) 1735 (C=O), 1648 (C=C); TOF MS AP+  $m/z$ : 325.2  $[\text{M}+\text{H}]^+$ , 283.2  $[\text{M}-\text{Ac}]^+$ ; HR-MS calc.  $[\text{C}_{20}\text{H}_{25}\text{N}_2\text{O}_2]^+$  325.1911, obs. 325.1905.

**3-Phenyl-1-(4-(pyrrolidin-1-yl)pyridin-3-yl)propyl isobutyrate (64b)**



Colourless oil (98 mg, 80%);  $R_f$  = 0.47 ( $\text{CH}_2\text{Cl}_2/\text{MeOH}$  [9:1]);  $^1\text{H}$  NMR (300 MHz,  $\text{CDCl}_3$ )  $\delta$  8.38 (s, 1H, Py), 8.11 (d,  $J$  = 5.8 Hz, 1H, Py), 7.43 – 7.01 (m, 5H, Ph), 6.44 (d,  $J$  = 5.8 Hz, 1H, Py), 6.22 (dd,  $J$  = 9.6, 3.7 Hz, 1H,  $\text{CH}_2\text{OH}$ ), 3.40 – 2.99 (m, 4H, Pyr), 2.85 – 2.54 (m, 3H,  $\text{CH}_2$  &  $\text{CH}(\text{iPr})$ ), 2.42 – 1.95 (m, 2H,  $\text{CH}_2$ ), 1.94 – 1.64 (m, 4H, Pyr), 1.28 (d,  $J$  = 7.0 Hz, 3H,  $\text{CH}_3$ ), 1.17 (d,  $J$  = 7.0 Hz, 3H,  $\text{CH}_3$ );  $^{13}\text{C}$  NMR (101 MHz,  $\text{CDCl}_3$ )  $\delta$  176.7, 151.1, 149.0, 148.5, 140.1, 128.6, 128.5, 126.1, 122.0, 109.0, 69.8, 50.5, 38.8, 34.1, 32.0, 25.7, 19.0, 18.9; IR (neat)  $\nu$  ( $\text{cm}^{-1}$ ) 1730 (C=O), 1649 (C=C Ar); TOF MS AP+  $m/z$ : 353.2  $[\text{M}+\text{H}]^+$ , 283.2  $[\text{M}-\text{CO}(\text{iPr})]^+$ ; HR-MS calc.  $[\text{C}_{22}\text{H}_{29}\text{N}_2\text{O}_2]^+$  353.2224, obs. 353.2224.

**3-Phenyl-1-(4-(pyrrolidin-1-yl)pyridin-3-yl)propyl benzoate (64c)**



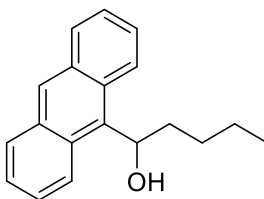
Colourless oil (114 mg, 84%);  $R_f$  = 0.50 ( $\text{CH}_2\text{Cl}_2/\text{MeOH}$  [9:1]);  $^1\text{H}$  NMR (300 MHz,  $\text{CDCl}_3$ )  $\delta$  8.51 (s, 1H, Py), 8.24 – 7.93 (m, 3H, Ar), 7.73 – 7.37 (m, 3H, Ph), 7.35 – 7.08 (m, 4H, Ph), 6.66 – 6.31 (m, 2H, Ar &  $\text{CHOH}$ ), 3.50 – 3.25 (m, 2H, Pyr), 3.26 – 2.99 (m, 2H, Pyr), 2.96 – 2.61 (m, 2H,  $\text{CH}_2$ ), 2.60 – 2.34 (m, 1H,  $\text{CH}_2$ ), 2.31 – 2.02 (m, 1H,  $\text{CH}_2$ ), 1.98 – 1.72 (m, 4H, Pyr);  $^{13}\text{C}$  NMR (101 MHz,  $\text{CDCl}_3$ )  $\delta$  166.1, 151.2, 149.4, 148.7, 140.9, 133.1, 130.1, 129.7, 128.6, 128.5, 128.5, 126.1, 121.8, 109.1, 70.8, 50.6, 38.7, 32.0, 25.7; IR (neat)  $\nu$  ( $\text{cm}^{-1}$ ) 1714

(C=O), 1649 (C=C); TOF MS AP+  $m/z$ : 387.2 [M+H]<sup>+</sup>, 283.2 [M-Bz]<sup>+</sup>, 265.2 [M-BzOH]<sup>+</sup> HR-MS calc. [C<sub>25</sub>H<sub>27</sub>N<sub>2</sub>O<sub>2</sub>]<sup>+</sup> 387.2067, obs. 387.2069.

## Synthesis of Analogues

### Witting By-Product

#### 1-(Anthracen-9-yl)pentan-1-ol (73)



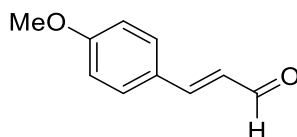
Yellow solid (0.3 g, 63%); <sup>1</sup>H NMR (400 MHz, CDCl<sub>3</sub>) δ 8.66 (s, 2H, Anth-*H*), 8.38 (s, 1H, Anth-*H*), 8.03 – 7.95 (m, 2H, Anth-*H*), 7.51 – 7.41 (m, 4H, Anth-*H*), 6.24 (ddd, *J* = 8.1, 6.1, 2.1 Hz, 1H, *CHOH*), 2.51 – 2.37 (m, 1H, *CHCH*<sub>2</sub>), 2.25 (d, *J* = 2.1 Hz, 1H, *OH*), 2.19 – 2.07 (m, 1H, *CHCH*<sub>2</sub>), 1.70 – 1.57 (m, 1H, *CHCH*<sub>2</sub>*CH*<sub>2</sub>), 1.42 – 1.22 (m, 3H, *CHCH*<sub>2</sub>*CH*<sub>2</sub> & *CH*<sub>2</sub>*CH*<sub>3</sub>), 0.92 – 0.84 (m, 3H, *CH*<sub>3</sub>); <sup>13</sup>C NMR (101 MHz, CDCl<sub>3</sub>) δ 135.3, 134.1, 131.7, 129.3, 129.3, 128.0, 125.4, 124.8, 71.2, 37.5, 29.1, 22.7, 14.0; IR (neat)  $\nu$  (cm<sup>-1</sup>) 3225 (*OH*); TOF MS ES+  $m/z$ : 271.1 [M+Li]<sup>+</sup>.

### Heck Cross-Coupling to Synthesise Cinnamaldehydes 72d,e,h,p,q

Palladium acetate (0.03 equiv.), tetrabutylammonium acetate (2.00 equiv.), potassium carbonate (1.50 equiv.), potassium chloride (1.00 equiv.) and acrolein diethyl acetal (3.00 equiv.) were added to a flame dried flask charged with DMF (0.2M) under argon. Aryl bromide (0.1 equiv.) was added and the reaction mixture was heated to 90 °C for 21 hrs, the reaction was then cooled to room temperature and 2M aqueous HCL (2.5 mL/mmol) was added and stirred for 30 mins. The resulting mixture was diluted with water (15 mL/mmol), extracted with EtOAc (3 x 10 mL/mmol) and the combined organic phases

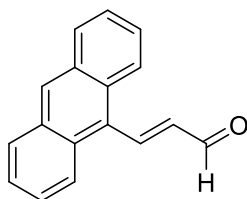
were washed with water (3 x 20 mL/mmol) and brine (3 x 10 mL/mmol) and the solvent was removed under reduced pressure. The residue was purified by column chromatography (silica, 0-10% EtOAc/hexane) to give the desired compound.

**(E)-3-(4-Methoxyphenyl)acrylaldehyde (72d)<sup>88</sup>**



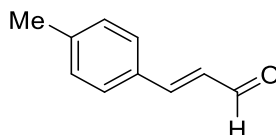
White Solid (170 mg, 52%);  $R_f$  = 0.33 (Hexane/EtOAc [9:1]);  $^1\text{H}$  NMR (300 MHz,  $\text{CDCl}_3$ )  $\delta$  9.66 (d,  $J$  = 7.8 Hz, 1H, CHO), 7.57 – 7.50 (m, 2H, Ar), 7.43 (d,  $J$  = 15.9 Hz, 1H, CHCHCHO), 7.05 – 6.90 (m, 2H, Ar), 6.62 (dd,  $J$  = 15.9, 7.8 Hz, 1H, CHCHO), 3.87 (s, 3H,  $\text{CH}_3$ );  $^{13}\text{C}$  NMR (101 MHz,  $\text{CDCl}_3$ )  $\delta$  193.7, 162.2, 152.7, 130.4, 126.8, 126.5, 114.6, 55.5; IR (neat)  $\nu$  ( $\text{cm}^{-1}$ ) 1662 (C=O), 1598 (C=C); TOF MS EI+  $m/z$ : 162.1  $[\text{M}]^+$ , 131.0  $[\text{M}-\text{CHO}]^+$ .

**(E)-3-(Anthracen-9-yl)acrylaldehyde (72e)<sup>89</sup>**



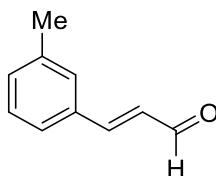
Yellow Solid ([135 mg, 29%]; TLC:  $R_f$  = 0.33 (Hexane/EtOAc [9:1]);  $^1\text{H}$  NMR (400 MHz,  $\text{CDCl}_3$ )  $\delta$  10.03 (d,  $J$  = 7.8 Hz, 1H, CHO), 8.58 – 8.44 (m, 2H, CHCHCHO & Ar), 8.26 – 8.15 (m, 2H, Ar), 8.08 – 8.01 (m, 2H, Ar), 7.61 – 7.47 (m, 4H, Ar), 6.77 (dd,  $J$  = 16.3, 7.8 Hz, 1H, CHCHO);  $^{13}\text{C}$  NMR (101 MHz,  $\text{CDCl}_3$ )  $\delta$  193.4, 149.9, 137.5, 131.2, 129.4, 129.2, 129.1, 128.2, 126.9, 125.5, 124.7; IR (neat)  $\nu$  ( $\text{cm}^{-1}$ ) 1677 (C=O), 1663 (C=C); TOF MS EI+  $m/z$ : 232.1  $[\text{M}]^+$ , 203.1  $[\text{M}-\text{CHO}]^+$ .

**(E)-3-(p-Tolyl)acrylaldehyde (72h)<sup>112</sup>**



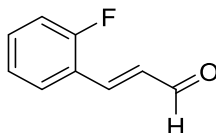
White solid (209 mg, 57%);  $R_f = 0.2$  (Hexane/EtOAc [9:1]);  $^1\text{H}$  NMR (300 MHz,  $\text{CDCl}_3$ )  $\delta$  9.69 (d,  $J = 7.8$  Hz, 1H, CHO), 7.52 – 7.42 (m, 3H, CHCHCHO & Ar), 7.25 (d,  $J = 7.9$  Hz, 2H, Ar), 6.69 (dd,  $J = 15.9, 7.8$  Hz, 1H, CHCHO), 2.40 (s, 3H,  $\text{CH}_3$ );  $^{13}\text{C}$  NMR (101 MHz,  $\text{CDCl}_3$ )  $\delta$  193.8, 153.0, 142.0, 131.3, 129.9, 128.5, 127.7, 21.6; TOF MS EI+  $m/z$ : 146.1  $[\text{M}]^+$ , 131.0  $[\text{M-Me}]^+$ .

**(E)-3-(m-Tolyl)acrylaldehyde (72p)<sup>85</sup>**



Colourless oil (195 mg, 49%);  $R_f = 0.39$  (Hexane/EtOAc [9:1]);  $^1\text{H}$  NMR (300 MHz,  $\text{CDCl}_3$ )  $\delta$  9.70 (d,  $J = 7.7$  Hz, 1H, CHO), 7.46 (d,  $J = 16.0$  Hz, 1H, CHCHCHO), 7.41 – 7.22 (m, 4H, Ar), 6.72 (dd,  $J = 16.0, 7.7$  Hz, 1H, CHCHO), 2.40 (s, 3H,  $\text{CH}_3$ );  $^{13}\text{C}$  NMR (101 MHz,  $\text{CDCl}_3$ )  $\delta$  193.8, 153.1, 138.8, 134.0, 132.2, 129.1, 129.0, 128.5, 125.7, 21.3; IR (neat)  $\nu$  ( $\text{cm}^{-1}$ ) 1673 (C=O), 1627 (C=C); TOF MS EI+  $m/z$ : 146.1  $[\text{M}]^+$ , 131.0  $[\text{M-Me}]^+$ .

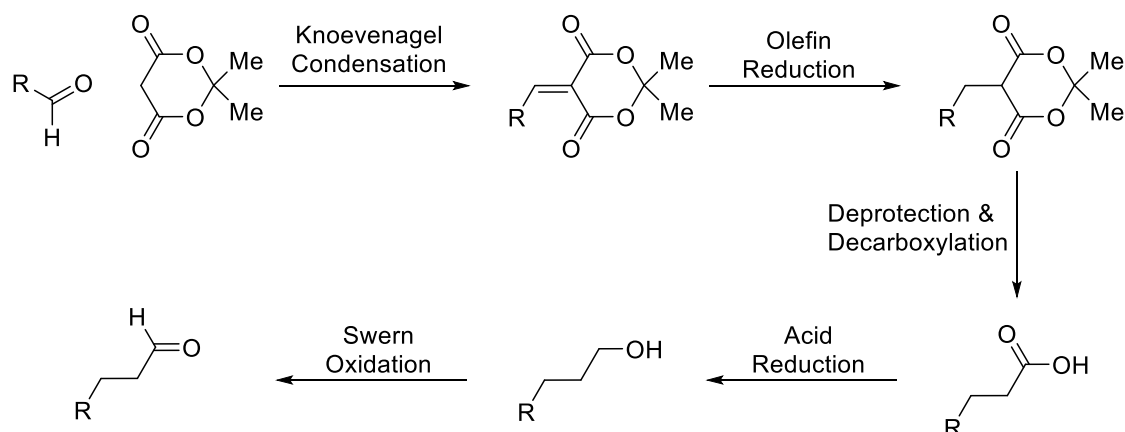
**(E)-3-(2-Fluorophenyl)acrylaldehyde (72q)<sup>85</sup>**



Yellow Oil (186 mg, 62%);  $R_f = 0.21$  (Hexane/EtOAc [9:1]);  $^1\text{H}$  NMR (300 MHz,  $\text{CDCl}_3$ )  $\delta$  9.73 (d,  $J = 7.7$  Hz, 1H, CHO), 7.67 (d,  $J = 16.2$  Hz, 1H, CHCHCHO), 7.60 (td,  $J = 7.6, 1.8$  Hz, 1H, Ar), 7.48 – 7.39 (m, 1H, Ar), 7.26 – 7.11 (m, 2H, Ar), 6.79 (dd,  $J = 16.2, 7.7$  Hz, 1H, CHCHO);

$^{19}\text{F}$  NMR (282 MHz,  $\text{CDCl}_3$ )  $\delta$  -114.3 (ddd,  $J$  = 10.7, 7.5, 5.4 Hz); IR (neat)  $\nu$  ( $\text{cm}^{-1}$ ) 1680 (C=O), 1627 (C=C); TOF MS EI+  $m/z$ : 150.1  $[\text{M}]^+$ , 121.0  $[\text{M}-\text{CHO}]^+$ .

## Synthesis of hydrocinnamaldehyde derivatives<sup>94</sup>



*Scheme 81 - General scheme for the synthesis of hydrocinnamaldehyde derivatives from Meldrum's Acid*

### Knoevenagel Condensation to Synthesise 75b-o

#### *Knoevenagel General Method 1*

Aldehyde (1.0 equiv.) and Meldrum's acid (1.0 equiv.) were suspended in water (0.5 M) and stirred at 75 °C for 2 hrs. The resulting reaction mixture was filtered and the solid residue was washed with water (20 mL/mmol) and petroleum ether (20 mL/mmol) to give the desired compound.

#### *Knoevenagel General Method 2*

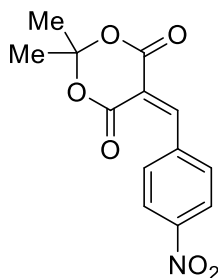
Aldehyde (1.0 equiv.) and Meldrum's acid (1.0 equiv.) were dissolved in Pyridine (0.1 M) and stirred at room temperature overnight under  $\text{N}_2$ . The resulting reaction mixture was reduced to dryness and the resulting solids were either used without further purification or recrystallised.

#### *Knoevenagel General Method 3*

Aldehyde (1.1 equiv.) and Meldrum's acid (1.0 equiv.) were added to a stirred solution of pyrrolidine (0.1 equiv.) and acetic acid (0.1 equiv.) in anhydrous toluene (0.2M) and stirred

at 50 °C for 30 hrs under argon. The solvent was removed under reduced pressure to give the desired compounds which were taken to the next step without purification.

**2,2-Dimethyl-5-(4-nitrobenzylidene)-1,3-dioxane-4,6-dione (75b)<sup>92</sup>**

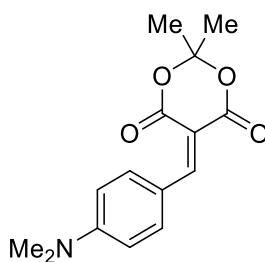


Knoevenagel General Method 1: White solid (1.34 g, 79%);

Knoevenagel General Method 2: White solid (2.05 g, 74%);

Mp 219-220 °C; <sup>1</sup>H NMR (400 MHz, d<sub>6</sub>-DMSO) δ 8.51 (s, 1H, C=CH), 8.30 (d, *J* = 8.8 Hz, 2H, Ar), 8.07 (d, *J* = 8.8 Hz, 2H, Ar), 1.79 (s, 6H, CH<sub>3</sub>); <sup>13</sup>C NMR (101 MHz, d<sub>6</sub>-DMSO) δ 162.1, 159.5, 154.3, 149.1, 139.0, 132.9, 123.6, 119.6, 105.6, 27.7; IR (neat) ν (cm<sup>-1</sup>) 1756 (C=O), 1723 (C=O), 1629 (C=C); TOF MS ES+ *m/z*: 322.0 [M+2Na-H]<sup>+</sup>, 278.0 [M+H]<sup>+</sup>.

**5-(4-(Dimethylamino)benzylidene)-2,2-dimethyl-1,3-dioxane-4,6-dione (75c)<sup>92</sup>**



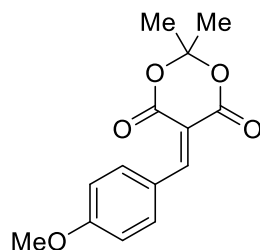
Knoevenagel General Method 1: Orange solid (2.39 g, 87%);

Knoevenagel General Method 2: Orange solid (5.14 g, 93%);

Mp 169-171 °C (EtOH); <sup>1</sup>H NMR (300 MHz, CDCl<sub>3</sub>) δ 8.30 (s, 1H, C=CH), 8.25 (d, *J* = 9.3 Hz, 2H, Ar), 6.69 (d, *J* = 9.3 Hz, 2H, Ar), 3.15 (s, 6H, N(CH<sub>3</sub>)<sub>2</sub>), 1.77 (s, 6H, CH<sub>3</sub>); <sup>13</sup>C NMR (101

MHz, CDCl<sub>3</sub>)  $\delta$  165.2, 161.5, 158.1, 154.5, 139.0, 120.1, 111.2, 105.0, 103.4, 40.1, 27.3; IR (neat)  $\nu$  (cm<sup>-1</sup>) 1724 (C=O), 1692 (C=O), 1609 (C=C); TOF MS ES+  $m/z$ : 298.1 [M+Na]<sup>+</sup>, 232.1 [M- C<sub>3</sub>H<sub>6</sub>]<sup>+</sup>.

**5-(4-Methoxybenzylidene)-2,2-dimethyl-1,3-dioxane-4,6-dione (75d)<sup>92</sup>**

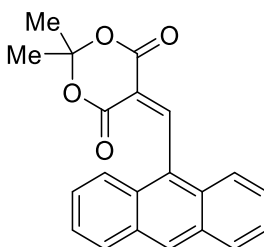


Knoevenagel General Method 1: Yellow solid (2.73 g, 75%);

Knoevenagel General Method 2: Yellow solid (5.14 g, 91%);

Mp 129-131 °C; <sup>1</sup>H NMR (300 MHz, CDCl<sub>3</sub>)  $\delta$  8.38 (s, 1H, C=CH), 8.23 (d,  $J$  = 8.9 Hz, 1H, Ar), 6.99 (d,  $J$  = 8.9 Hz, 2H, Ar), 3.91 (s, 3H, OCH<sub>3</sub>), 1.79 (s, 6H, CH<sub>3</sub>); <sup>13</sup>C NMR (101 MHz, CDCl<sub>3</sub>)  $\delta$  164.7, 164.1, 160.5, 157.9, 137.7, 124.7, 114.4, 110.8, 104.2, 55.7, 27.5; IR (neat)  $\nu$  (cm<sup>-1</sup>) 1745 (C=O), 1710 (C=O), 1598 (C=C); TOF MS ES-  $m/z$ : 278.3 [M+NH<sub>2</sub>]<sup>-</sup>, 176.2 [C<sub>10</sub>H<sub>8</sub>O<sub>3</sub>]<sup>-</sup>; HR-MS calc. [C<sub>14</sub>H<sub>16</sub>O<sub>5</sub>N]<sup>-</sup> 278.1034, obs. 278.1027.

**5-(Anthracen-9-ylmethylene)-2,2-dimethyl-1,3-dioxane-4,6-dione (75e)<sup>93</sup>**

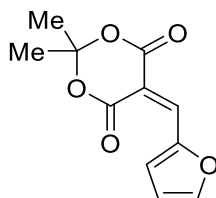


Knoevenagel General Method 2. Orange solid (8.50 g, 93%); Mp 191-192 °C; <sup>1</sup>H NMR (300 MHz, CDCl<sub>3</sub>)  $\delta$  9.45 (s, 1H, C=CH), 8.53 (s, 1H, Ar), 8.10 – 7.99 (m, 2H, Ar), 7.90 – 7.75 (m, 2H, Ar), 7.60 – 7.40 (m, 4H, Ar), 1.89 (s, 6H, CH<sub>3</sub>); <sup>13</sup>C NMR (101 MHz, CDCl<sub>3</sub>)  $\delta$  161.9, 157.9, 157.7, 130.9, 130.3, 129.3, 128.6, 127.1, 126.8, 125.6, 124.5, 121.0, 105.0, 28.2; IR (neat)



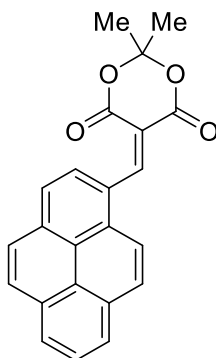
$\nu$  (cm<sup>-1</sup>) 1766 (C=O), 1731 (C=O), 1621 (C=C); TOF MS ES+  $m/z$ : 355.1 [M+Na]<sup>+</sup>, 329.1 [M+Li]<sup>+</sup>, 289.1 [M-C<sub>3</sub>H<sub>6</sub>]<sup>+</sup>; HR-MS calc. [C<sub>21</sub>H<sub>16</sub>O<sub>4</sub>Na]<sup>+</sup> 355.0941, obs. 355.0937.

**5-(Furan-2-ylmethylene)-2,2-dimethyl-1,3-dioxane-4,6-dione (75f)<sup>113</sup>**



Knoevenagel General Method 2. Black solid (1.12 g, 91%); <sup>1</sup>H NMR (400 MHz, CDCl<sub>3</sub>)  $\delta$  8.47 (d,  $J$  = 3.9 Hz, 1H, OCH=CH), 8.36 (s, 1H, C=CH), 7.86 (dd,  $J$  = 1.7, 0.7 Hz, 1H, OCCH), 6.76 (ddd,  $J$  = 3.9, 1.7, 0.7 Hz, 1H, OCHCH), 1.78 (s, 6H, CH<sub>3</sub>); <sup>13</sup>C NMR (101 MHz, CDCl<sub>3</sub>)  $\delta$  163.2, 160.2, 150.4, 150.2, 141.2, 128.1, 115.3, 107.5, 104.5, 27.6; IR (neat)  $\nu$  (cm<sup>-1</sup>) 1742 (C=O), 1706 (C=O), 1584 (C=C); TOF MS ES-  $m/z$ : 238.3 [M+NH<sub>2</sub>]<sup>-</sup>; HR-MS calc. [C<sub>11</sub>H<sub>12</sub>O<sub>5</sub>N]<sup>-</sup> 238.0721, obs. 238.0712.

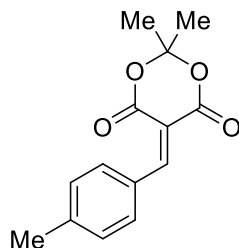
**2,2-Dimethyl-5-(pyren-1-ylmethylene)-1,3-dioxane-4,6-dione (75g)**



Knoevenagel General Method 2. Orange solid (3.16 g, 88%); Mp 205-206 °C; <sup>1</sup>H NMR (300 MHz, CDCl<sub>3</sub>)  $\delta$  9.54 (s, 1H, C=CH), 8.50 (d,  $J$  = 7.6 Hz, 1H, Ar), 8.35 – 8.03 (m, 8H, Ar), 1.92 (s, 6H, CH<sub>3</sub>); <sup>13</sup>C NMR (101 MHz, CDCl<sub>3</sub>)  $\delta$  163.2, 160.0, 156.3, 135.0, 131.8, 131.0, 130.4, 130.3, 129.9, 128.8, 127.3, 127.1, 127.0, 126.6, 125.6, 124.5, 124.2, 122.7, 115.2, 104.7,

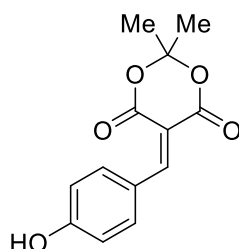
27.9; IR (neat)  $\nu$  ( $\text{cm}^{-1}$ ) 1763 (C=O), 1731 (C=O), 1603 (C=C), 1592 (C=C); TOF MS ES+  $m/z$ : 395.3  $[\text{M}+\text{K}]^+$ , 379.3  $[\text{M}+\text{Na}]^+$ . One quaternary  $^{13}\text{C}$  signal is not visible in the  $^{13}\text{C}$  NMR.

**2,2-Dimethyl-5-(4-methylbenzylidene)-1,3-dioxane-4,6-dione (75h)<sup>92</sup>**



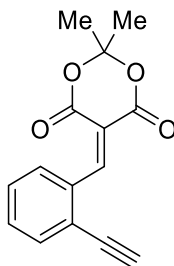
Knoevenagel General Method 2. White solid (0.32 g, 94%); Mp 126-128 °C;  $^1\text{H}$  NMR (300 MHz,  $\text{CDCl}_3$ )  $\delta$  8.40 (s, 1H, C=CH), 8.01 (d,  $J$  = 8.2 Hz, 2H, Ar), 7.30 (d,  $J$  = 8.2 Hz, 2H, Ar), 2.44 (s, 3H,  $\text{PhCH}_3$ ), 1.80 (s, 6H,  $\text{CH}_3$ );  $^{13}\text{C}$  NMR (101 MHz,  $\text{CDCl}_3$ )  $\delta$  163.6, 160.0, 158.3, 145.5, 134.2, 129.6, 129.1, 113.4, 104.4, 27.6, 22.0; IR (neat)  $\nu$  ( $\text{cm}^{-1}$ ) 1764 (C=O), 1726 (C=O), 1601 (C=C); TOF MS ES-  $m/z$ : 262.3  $[\text{M}+\text{NH}_2]^-$ , 160.2  $[\text{C}_{10}\text{H}_8\text{O}_2]^-$ ; HR-MS calc.  $[\text{C}_{14}\text{H}_{16}\text{O}_4\text{N}]^-$  262.1085, obs. 262.1082.

**5-(4-Hydroxybenzylidene)-2,2-dimethyl-1,3-dioxane-4,6-dione (75i)<sup>113</sup>**



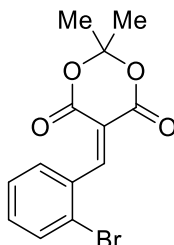
Knoevenagel General Method 2. Pale yellow solid (0.58 g, 67%); Mp 204-209 °C;  $^1\text{H}$  NMR (400 MHz,  $\text{d}_3\text{-MeOD}$ )  $\delta$  8.35 (s, 1H, C=CH), 8.20 (d,  $J$  = 8.9 Hz, 2H, Ar), 6.90 (d,  $J$  = 8.9 Hz, 2H, Ar), 1.78 (s, 6H,  $\text{CH}_3$ );  $^{13}\text{C}$  NMR (101 MHz,  $\text{d}_3\text{-MeOD}$ )  $\delta$  164.4, 164.0, 160.8, 157.8, 137.9, 123.6, 115.4, 109.6, 104.0, 26.0; IR (neat)  $\nu$  ( $\text{cm}^{-1}$ ) 3276 (OH), 1745 (C=O), 1692 (C=O), 1615 (C=C); TOF MS ES-  $m/z$ : 247.3  $[\text{M}-\text{H}]^-$ ; HR-MS calc.  $[\text{C}_{13}\text{H}_{11}\text{O}_5]^-$  247.0612, obs. 247.0604.

**5-(2-Ethynylbenzylidene)-2,2-dimethyl-1,3-dioxane-4,6-dione (75j)**



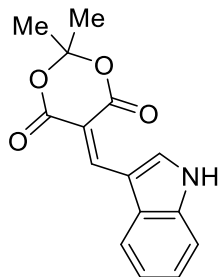
Knoevenagel General Method 2. Orange solid (0.50 g, 56%); Mp 136-137 °C;  $^1\text{H}$  NMR (400 MHz,  $\text{CDCl}_3$ )  $\delta$  8.86 (s, 1H, C=CH), 7.99 (dd,  $J$  = 7.9, 1.4 Hz, 1H, Ar), 7.61 (dd,  $J$  = 7.4, 1.4 Hz, 1H, Ar), 7.47 (ddd,  $J$  = 7.9, 7.4, 1.4 Hz, 1H, Ar), 7.43 (ddd,  $J$  = 7.9, 7.4, 1.4 Hz, 1H, Ar), 3.50 (s, 1H C $\equiv$ CH), 1.83 (s, 6H,  $\text{CH}_3$ );  $^{13}\text{C}$  NMR (101 MHz,  $\text{CDCl}_3$ )  $\delta$  162.5, 159.3, 156.0, 134.2, 133.2, 132.0, 130.8, 128.6, 124.6, 117.1, 104.8, 85.1, 80.9, 27.8; IR (neat)  $\nu$  ( $\text{cm}^{-1}$ ) 3260 (C $\equiv$ C), 1757 (C=O), 1724 (C=O), 1607 (C=C); TOF MS ES-  $m/z$ : 272.3 [ $\text{M}+\text{NH}_2$ ] $^-$ ; HR-MS calc. [ $\text{C}_{15}\text{H}_{14}\text{O}_4\text{N}$ ] $^-$  272.0928, obs. 272.0921.

**5-(2-Bromobenzylidene)-2,2-dimethyl-1,3-dioxane-4,6-dione (75k)<sup>114</sup>**



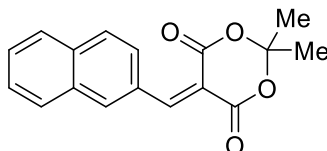
Knoevenagel General Method 2. White solid (0.59 g, 55%); Mp 139-142 °C;  $^1\text{H}$  NMR (400 MHz,  $\text{CDCl}_3$ )  $\delta$  8.61 (s, 1H, C=CH), 7.75 (dd,  $J$  = 7.8, 2.1 Hz, 1H, Ar), 7.67 (dd,  $J$  = 7.8, 1.6 Hz, 1H, Ar), 7.39 (ddd,  $J$  = 7.9, 7.6, 1.6 Hz, 1H, Ar), 7.34 (ddd,  $J$  = 7.9, 7.6, 2.1 Hz, 1H, Ar), 1.83 (s, 6H,  $\text{CH}_3$ );  $^{13}\text{C}$  NMR (101 MHz,  $\text{CDCl}_3$ )  $\delta$  162.1, 158.9, 156.6, 132.9, 132.8, 131.7, 127.0, 125.0, 117.8, 105.0, 27.8; IR (neat)  $\nu$  ( $\text{cm}^{-1}$ ) 1763 (C=O), 1729 (C=O), 1619 (C=C); TOF MS ES-  $m/z$ : 326.3/328.3 [ $\text{M}+\text{NH}_2$ ] $^-$ , 224.2/226.2 [ $\text{C}_9\text{H}_5\text{O}_2\text{Br}^{79}$ ] $^-$ ; HR-MS calc. [ $\text{C}_{13}\text{H}_{13}\text{O}_4\text{NBr}^{79}$ ] $^-$  326.0033, obs. 326.0029. One quaternary  $^{13}\text{C}$  signal is not visible in the  $^{13}\text{C}$  NMR.

**5-((1H-Indol-3-yl)methylene)-2,2-dimethyl-1,3-dioxane-4,6-dione (75l)<sup>115</sup>**



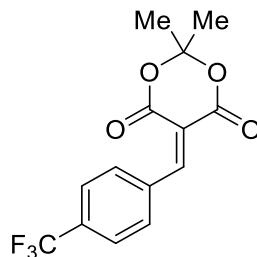
Knoevenagel General Method 2. Yellow solid (0.45 g, 48%); Mp 254-257 °C (Decomposition at 240 °C); <sup>1</sup>H NMR (400 MHz, d<sub>6</sub>-DMSO) δ 12.90 (s, 1H, NH), 9.33 (s, 1H, C=CH), 8.74 (s, 1H, NHCH), 8.06 – 7.84 (m, 1H, Ar), 7.75 – 7.54 (m, 1H, Ar), 7.45 – 7.22 (m, 2H, Ar), 1.71 (s, 6H, CH<sub>3</sub>); <sup>13</sup>C NMR (101 MHz, d<sub>6</sub>-DMSO) δ 164.4, 161.9, 146.6, 140.5, 136.9, 129.3, 124.4, 123.4, 118.4, 113.8, 111.7, 103.9, 103.5, 27.2; IR (neat) ν (cm<sup>-1</sup>) 3160 (NH), 1730 (C=O), 1675 (C=O), 1600 (C=C); TOF MS ES<sup>-</sup> m/z: 270.3 [M-H]<sup>-</sup>; HR-MS calc. [C<sub>15</sub>H<sub>12</sub>O<sub>4</sub>N]<sup>-</sup> 270.0772, obs. 270.0765.

**2,2-Dimethyl-5-(naphthalen-2-ylmethylene)-1,3-dioxane-4,6-dione (75m)<sup>114</sup>**



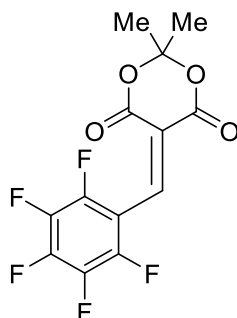
Knoevenagel General Method 2. White solid (0.11 g, 34%); Mp 151-153 °C; <sup>1</sup>H NMR (300 MHz, CDCl<sub>3</sub>) δ 8.59 (s, 1H, C=CH), 8.56 (s, 1H, Ar), 8.13 (dd, *J* = 8.8, 1.5 Hz, 1H, Ar), 7.95 (d, *J* = 8.1 Hz, 1H, Ar), 7.88 (d, *J* = 8.8 Hz, 1H, Ar), 7.87 (d, *J* = 8.1 Hz, 1H, Ar), 7.64 (ddd, *J* = 8.1, 6.9, 1.5 Hz, 1H, Ar), 7.56 (ddd, *J* = 8.1, 6.9, 1.5 Hz, 1H, Ar), 1.84 (s, 6H, CH<sub>3</sub>); <sup>13</sup>C NMR (101 MHz, CDCl<sub>3</sub>) δ 163.4, 160.0, 158.2, 137.0, 135.7, 132.7, 129.8, 129.4, 129.4, 128.3, 128.1, 127.8, 127.0, 114.4, 104.6, 27.7; IR (neat) ν (cm<sup>-1</sup>) 1758 (C=O), 1722 (C=O), 1593 (C=C); TOF MS ES<sup>-</sup> m/z: 298.4 [M+NH<sub>2</sub>]<sup>-</sup>, 196.2 [C<sub>13</sub>H<sub>8</sub>O<sub>2</sub>]<sup>-</sup>; HR-MS calc. [C<sub>17</sub>H<sub>16</sub>O<sub>4</sub>N]<sup>-</sup> 298.1085, obs. 298.1082.

### 2,2-Dimethyl-5-(4-(trifluoromethyl)benzylidene)-1,3-dioxane-4,6-dione (**75n**)<sup>114</sup>



Knoevenagel General Method 3; Cream solid; Mp 126-129 °C; <sup>1</sup>H NMR (300 MHz, CDCl<sub>3</sub>) δ 8.44 (s, 1H, C=CH), 8.06 (d, *J* = 8.3 Hz, 2H, Ar), 7.73 (d, *J* = 8.3 Hz, 2H, Ar), 1.83 (s, 6H, CH<sub>3</sub>); <sup>19</sup>F NMR (282 MHz, CDCl<sub>3</sub>) δ -63.32; <sup>13</sup>C NMR (101 MHz, CDCl<sub>3</sub>) δ 162.5, 159.2, 155.8, 134.8, 132.9, 129.0, 126.2, 125.5, 125.5, 105.0, 27.8; TOF MS ES- *m/z*: 316.4 [M+NH<sub>2</sub>]<sup>+</sup>, 214.2 [C<sub>10</sub>H<sub>5</sub>O<sub>2</sub>F<sub>3</sub>]<sup>+</sup>; HR-MS calc. [C<sub>14</sub>H<sub>13</sub>O<sub>4</sub>NF<sub>3</sub>]<sup>+</sup> 316.0802, obs. 316.0798.

### 2,2-Dimethyl-5-((perfluorophenyl)methylene)-1,3-dioxane-4,6-dione (**75o**)



Knoevenagel General Method 3. <sup>1</sup>H NMR (300 MHz, CDCl<sub>3</sub>) δ 8.16 (q, *J* = 1.5 Hz, 1H, C=CH), 1.85 (s, 6H, CH<sub>3</sub>); <sup>19</sup>F NMR (282 MHz, CDCl<sub>3</sub>) δ -134.92, -148.31, -161.07; <sup>13</sup>C NMR (101 MHz, CDCl<sub>3</sub>) δ 160.3, 158.5, 138.9, 123.0, 105.7, 27.6. *Signals for Carbons of the aromatic ring could not be assigned in the <sup>13</sup>C NMR spectrum due to fluorine coupling.*

### Olefin Reduction to Synthesise **76b-h,j-l,n,o**

Sodium borohydride (4.0 equiv.) was added portionwise over 2 hrs a stirred solution of the Knoevenagel products (**76**, 1.0 equiv.) suspended in either methanol or ethanol (0.1 M). Upon completion, determined by TLC, the reaction was quenched with 1M aqueous

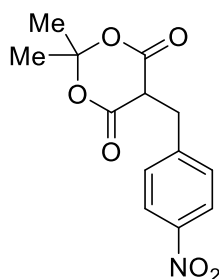
HCl (15 mL/mmol) and the precipitate was filtered, washed with water and dried at the pump to afford the desired compound without further purification.

*Table 13 - Summary of solvents and yields for the synthesis of 76b-h,j-l,n,o*

Entry	Substituent (Ar)	Solvent	Yield
1	4-NO <sub>2</sub> -C <sub>6</sub> H <sub>4</sub> - ( <b>76b</b> )	EtOH	99%
2	4-NMe <sub>2</sub> -C <sub>6</sub> H <sub>4</sub> - ( <b>76c</b> )	MeOH	75%
3	4-OMe-C <sub>6</sub> H <sub>4</sub> - ( <b>76d</b> )	EtOH	99%
4	9-Anthryl ( <b>76e</b> )	MeOH	N.D. *
5	2-Furyl ( <b>76f</b> )	EtOH	87%
6	1-Pyrenyl ( <b>76g</b> )	MeOH	95%
7	4-Me-C <sub>6</sub> H <sub>4</sub> - ( <b>76h</b> )	EtOH	94%
8	2-HCC-C <sub>6</sub> H <sub>4</sub> - ( <b>76j</b> )	EtOH	88%
9	2-Br-C <sub>6</sub> H <sub>4</sub> - ( <b>76k</b> )	EtOH	88%
10	3-Indole ( <b>76l</b> )	EtOH	91%
11	4-CF <sub>3</sub> -C <sub>6</sub> H <sub>4</sub> - ( <b>76n</b> )	EtOH	98% (2 steps)
12	C <sub>6</sub> F <sub>5</sub> - ( <b>76o</b> )	EtOH	99% (2 Steps)

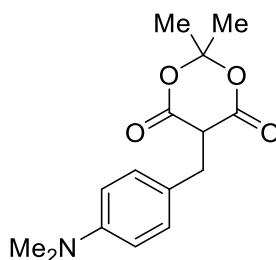
\*Compound was taken to the next step containing residual water

**2,2-dimethyl-5-(4-nitrobenzyl)-1,3-dioxane-4,6-dione (**76b**)**<sup>92</sup>



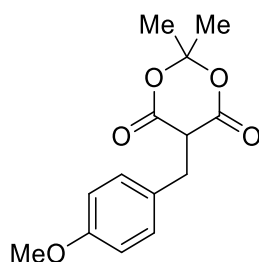
White solid (1.52 g, 99%); Mp 142-144 °C; <sup>1</sup>H NMR (400 MHz, d<sub>6</sub>-DMSO) δ 8.15 (d, *J* = 8.5 Hz, 2H, Ar), 7.59 (d, *J* = 8.5 Hz, 2H, Ar), 4.91 (t, *J* = 5.5 Hz, 1H, CHCH<sub>2</sub>), 3.40 (d, *J* = 5.5 Hz, 2H, CH<sub>2</sub>), 1.85 (s, 3H, CH<sub>3</sub>), 1.66 (s, 3H, CH<sub>3</sub>); <sup>13</sup>C NMR (101 MHz, CDCl<sub>3</sub>) δ 170.4, 165.8, 147.3, 146.6, 130.9, 123.6, 105.6, 47.0, 31.4, 28.4, 26.3; IR (neat) ν (cm<sup>-1</sup>) 1776 (C=O), 1730 (C=O); TOF MS ES- *m/z*: 278.3 [M-H]<sup>-</sup>; HR-MS calc. [C<sub>13</sub>H<sub>12</sub>O<sub>6</sub>N]<sup>-</sup> 278.0670, obs. 278.0667.

**5-(4-(Dimethylamino)benzyl)-2,2-dimethyl-1,3-dioxane-4,6-dione (76c)**



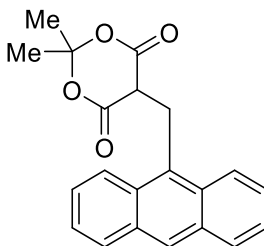
yellow solid (2.39 g, 87%); Mp 110-112 °C;  $^1\text{H}$  NMR (300 MHz,  $\text{CDCl}_3$ )  $\delta$  7.18 (d,  $J$  = 8.8 Hz, 2H, Ar), 6.65 (d,  $J$  = 8.8 Hz, 2H, Ar), 3.71 (t,  $J$  = 4.8 Hz, 1H,  $\text{CHCH}_2$ ), 3.41 (d,  $J$  = 4.8 Hz, 2H,  $\text{CH}_2$ ), 2.91 (s, 6H,  $\text{N}(\text{CH}_3)_2$ ), 1.71 (s, 3H,  $\text{CH}_3$ ), 1.45 (s, 3H,  $\text{CH}_3$ );  $^{13}\text{C}$  NMR (101 MHz,  $\text{CDCl}_3$ )  $\delta$  165.7, 149.8, 130.6, 124.8, 112.7, 105.2, 48.4, 40.6, 31.6, 28.5, 27.4; IR (neat)  $\nu$  ( $\text{cm}^{-1}$ ) 1791 (C=O), 1749 (C=O), 1612 (C=C); TOF MS ES+  $m/z$ : 278.3  $[\text{M}+\text{H}]^+$ , 220.2  $[\text{M}-\text{OC}_3\text{H}_6]^+$ .

**5-(4-Methoxybenzyl)-2,2-dimethyl-1,3-dioxane-4,6-dione (76d)<sup>92</sup>**



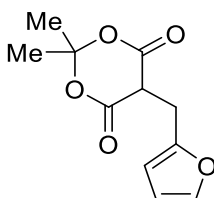
White solid (4.80 g, 91%);  $R_f$  = 0.56 (Hexane/EtOAc = 3:4); Mp 83-85 °C;  $^1\text{H}$  NMR (300 MHz,  $\text{CDCl}_3$ )  $\delta$  7.24 (d,  $J$  = 8.7 Hz, 2H, Ar), 6.82 (d,  $J$  = 8.7 Hz, 2H, Ar), 3.77 (s, 3H,  $\text{OCH}_3$ ), 3.73 (t,  $J$  = 4.9 Hz, 1H,  $\text{CHCH}_2$ ), 3.44 (d,  $J$  = 4.9 Hz, 2H,  $\text{CH}_2$ ), 1.72 (s, 3H,  $\text{CH}_3$ ), 1.48 (s, 3H,  $\text{CH}_3$ );  $^{13}\text{C}$  NMR (101 MHz,  $\text{CDCl}_3$ )  $\delta$  165.4, 158.7, 131.0, 129.0, 113.9, 105.2, 55.2, 48.3, 31.5, 28.5, 27.4; IR (neat)  $\nu$  ( $\text{cm}^{-1}$ ) 1785 (C=O), 1744 (C=O); TOF MS ES+  $m/z$ : 287.2  $[\text{M}+\text{Na}]^+$ ; HR-MS calc.  $[\text{C}_{14}\text{H}_{16}\text{O}_5\text{Na}]^+$  287.0890, obs. 287.0891.

**5-(Anthracen-9-ylmethyl)-2,2-dimethyl-1,3-dioxane-4,6-dione (76e)<sup>93</sup>**



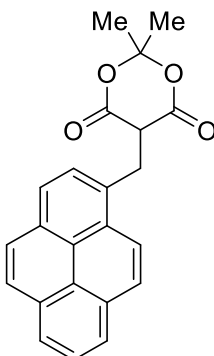
Yellow solid;  $^1\text{H}$  NMR (300 MHz,  $\text{CDCl}_3$ )  $\delta$  8.58 – 8.35 (m, 3H, Ar), 8.12 – 7.94 (m, 2H, Ar), 7.63 – 7.38 (m, 4H, Ar), 4.47 (d,  $J$  = 5.2 Hz, 2H,  $\text{CH}_2$ ), 3.95 (t,  $J$  = 5.2 Hz, 1H,  $\text{CHCH}_2$ ), 1.75 (s, 3H,  $\text{CH}_3$ ), 1.61 (s, 3H,  $\text{CH}_3$ );  $^{13}\text{C}$  NMR (101 MHz,  $\text{CDCl}_3$ )  $\delta$  165.3, 131.6, 130.5, 130.0, 129.4, 127.5, 126.3, 125.0, 124.3, 105.1, 49.1, 28.8, 26.3, 23.9.

**5-(Furan-2-ylmethyl)-2,2-dimethyl-1,3-dioxane-4,6-dione (76f)<sup>116</sup>**



Black solid (1.12 g, 91%);  $^1\text{H}$  NMR (300 MHz,  $\text{CDCl}_3$ )  $\delta$  7.30 – 7.29 (m, 1H,  $\text{HC=CH}$ ), 6.29 (dd,  $J$  = 3.2, 1.9 Hz, 1H,  $\text{HC=CH}$ ), 6.16 (dd,  $J$  = 3.2, 0.9 Hz, 1H,  $\text{HC=CH}$ ), 3.89 (t,  $J$  = 5.1 Hz, 1H,  $\text{CHCH}_2$ ), 3.50 (d,  $J$  = 5.1 Hz, 2H,  $\text{CH}_2$ ), 1.79 (s, 3H,  $\text{CH}_3$ ), 1.67 (s, 3H,  $\text{CH}_3$ );  $^{13}\text{C}$  NMR (101 MHz,  $\text{CDCl}_3$ )  $\delta$  164.9, 150.6, 141.5, 110.6, 107.7, 105.2, 45.4, 28.4, 26.9, 24.9; TOF MS ES-  $m/z$ : 223.2  $[\text{M-H}]^-$ ; HR-MS calc.  $[\text{C}_{11}\text{H}_{11}\text{O}_5]^-$  223.0612, obs. 223.0608.

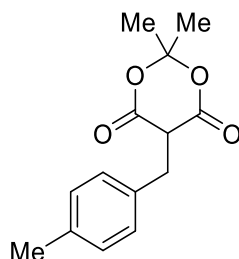
**2,2-Dimethyl-5-(pyren-1-ylmethyl)-1,3-dioxane-4,6-dione (76g)**





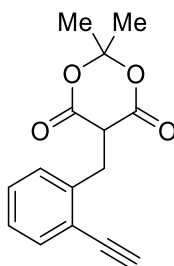
Cream solid (3.16 g, 88%); Mp 171-173 °C;  $^1\text{H}$  NMR (300 MHz,  $\text{CDCl}_3$ )  $\delta$  8.33 (d,  $J$  = 9.3 Hz, 1H, Ar), 8.23 – 8.12 (m, 5H, Ar), 8.09 – 7.97 (d,  $J$  = 11.4 Hz, 3H, Ar), 4.21 (d,  $J$  = 5.1 Hz, 2H,  $\text{CH}_2$ ), 3.91 (t,  $J$  = 5.1 Hz, 1H,  $\text{CHCH}_2$ ), 1.67 (s, 6H,  $\text{CH}_3$ );  $^{13}\text{C}$  NMR (101 MHz,  $\text{CDCl}_3$ )  $\delta$  165.4, 132.2, 131.3, 130.7, 128.9, 128.5, 128.4, 127.5, 127.2, 126.0, 125.4, 125.2, 125.1, 124.9, 124.8, 122.3, 105.2, 94.8, 48.8, 29.3, 28.6, 26.5; IR (neat)  $\nu$  ( $\text{cm}^{-1}$ ) 1790 (C=O) 1738 (C=O) 1612 (C=C) 1592 (C=C); TOF MS ES-  $m/z$ : 357.4  $[\text{M-H}]^-$ , 255.3  $[\text{M-C}_4\text{H}_7\text{O}_3]^-$ ; HR-MS calc.  $[\text{C}_{23}\text{H}_{17}\text{O}_4]^-$  357.1132, obs. 357.1125.

**2,2-Dimethyl-5-(4-methylbenzyl)-1,3-dioxane-4,6-dione (76h)<sup>116</sup>**



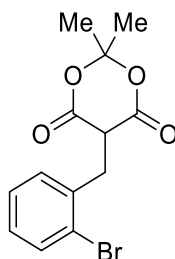
White solid (3.12 g, 94%);  $R_f$  = 0.53 (Hexane/EtOAc = 1:1); Mp 170-171 °C;  $^1\text{H}$  NMR (300 MHz,  $\text{CDCl}_3$ )  $\delta$  7.20 (d,  $J$  = 7.7 Hz, 2H, Ar), 7.09 (d,  $J$  = 7.7 Hz, 2H, Ar), 3.74 (t,  $J$  = 4.9 Hz, 1H, CH), 3.45 (d,  $J$  = 4.9 Hz, 2H,  $\text{CH}_2$ ), 2.30 (s, 3H,  $\text{PhCH}_3$ ), 1.73 (s, 3H,  $\text{CH}_3$ ), 1.50 (s, 3H,  $\text{CH}_3$ );  $^{13}\text{C}$  NMR (101 MHz,  $\text{CDCl}_3$ )  $\delta$  165.4, 136.8, 134.1, 129.6, 129.3, 105.2, 48.3, 31.8, 28.5, 27.3, 21.0; IR (neat)  $\nu$  ( $\text{cm}^{-1}$ ) 1785 (C=O), 1745 (C=O); TOF MS AP-  $m/z$ : 247.1  $[\text{M-H}]^-$ ; HR-MS calc.  $[\text{C}_{14}\text{H}_{15}\text{O}_4]^-$  247.0976, obs. 247.0968.

**5-(2-Ethynylbenzyl)-2,2-dimethyl-1,3-dioxane-4,6-dione (76j)<sup>117</sup>**



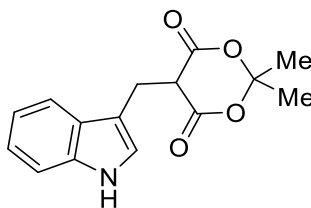
Orange solid (0.50 g, 56%); Mp 119-121 °C;  $^1\text{H}$  NMR (400 MHz,  $\text{CDCl}_3$ )  $\delta$  7.51 (dd,  $J$  = 2.9, 1.4 Hz, 1H, Ar), 7.49 (dd,  $J$  = 2.9, 1.4 Hz, 1H, Ar), 7.34 (td,  $J$  = 7.6, 1.4 Hz, 1H, Ar), 7.24 (td,  $J$  = 7.6, 1.4 Hz, 1H, Ar), 4.21 (t,  $J$  = 6.0 Hz, 1H,  $\text{CHCH}_2$ ), 3.55 (d,  $J$  = 6.0 Hz, 2H,  $\text{CH}_2$ ), 3.38 (s, 1H,  $\text{C}\equiv\text{CH}$ ), 1.80 (s, 3H,  $\text{CH}_3$ ), 1.76 (s, 3H,  $\text{CH}_3$ );  $^{13}\text{C}$  NMR (101 MHz,  $\text{CDCl}_3$ )  $\delta$  164.8, 140.7, 133.0, 131.2, 129.1, 127.0, 121.1, 105.0, 82.8, 81.6, 47.3, 30.6, 28.7, 26.1; IR (neat)  $\nu$  ( $\text{cm}^{-1}$ ) 3280 (CH), 1782 (C=O), 1738 (C=O); TOF MS ES-  $m/z$ : 257.3  $[\text{M}-\text{H}]^-$ ; HR-MS calc.  $[\text{C}_{15}\text{H}_{13}\text{O}_4]^-$  257.0819, obs. 257.0809.

**5-(2-Bromobenzyl)-2,2-dimethyl-1,3-dioxane-4,6-dione (76k)<sup>118</sup>**



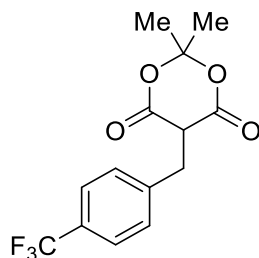
White solid (0.31 g, 88%);  $^1\text{H}$  NMR (300 MHz,  $\text{CDCl}_3$ )  $\delta$  7.57 (dd,  $J$  = 3.5, 1.5 Hz, 1H, Ar), 7.54 (dd,  $J$  = 3.5, 1.5 Hz, 1H, Ar), 7.29 (td,  $J$  = 7.7, 1.5 Hz, 1H, Ar), 7.14 (td,  $J$  = 7.7, 1.5 Hz, 1H, Ar), 4.06 (t,  $J$  = 5.9 Hz, 1H,  $\text{CHCH}_2$ ), 3.50 (d,  $J$  = 5.9 Hz, 2H,  $\text{CH}_2$ ), 1.82 (s, 3H,  $\text{CH}_3$ ), 1.77 (s, 3H,  $\text{CH}_3$ );  $^{13}\text{C}$  NMR (101 MHz,  $\text{CDCl}_3$ )  $\delta$  164.6, 137.0, 133.2, 132.8, 128.8, 127.5, 124.1, 105.2, 46.7, 32.1, 28.7, 26.2; IR (neat)  $\nu$  ( $\text{cm}^{-1}$ ) 1791 (C=O), 1744 (C=O); TOF MS ES-  $m/z$ : 311.2/313.2  $[\text{M}-\text{H}]^-$ , 209.1/211.1  $[\text{M}-\text{C}_4\text{H}_6\text{O}_3]^-$ ; HR-MS calc.  $[\text{C}_{13}\text{H}_{12}\text{O}_4\text{Br}]^-$  310.9924, obs. 310.9916.

**5-((1H-Indol-3-yl)methyl)-2,2-dimethyl-1,3-dioxane-4,6-dione (76l)<sup>119</sup>**



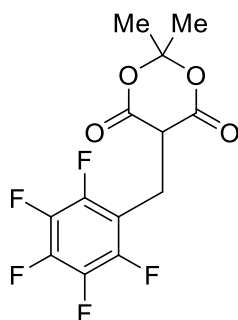
White solid (0.45 g, 48%); Mp 115-117 °C;  $^1\text{H}$  NMR (400 MHz,  $\text{CDCl}_3$ )  $\delta$  8.07 (s, 1H, NH), 7.73 (d,  $J$  = 7.8 Hz, 1H, Ar), 7.34 (d,  $J$  = 7.8 Hz, 1H, Ar), 7.23 – 7.11 (m, 3H, Ar), 3.78 (t,  $J$  = 4.7 Hz, 1H,  $\text{CHCH}_2$ ), 3.67 (d,  $J$  = 4.7 Hz, 2H,  $\text{CH}_2$ ), 1.70 (s, 3H,  $\text{CH}_3$ ), 1.46 (s, 3H,  $\text{CH}_3$ );  $^{13}\text{C}$  NMR (101 MHz,  $\text{CDCl}_3$ )  $\delta$  165.9, 135.8, 127.1, 124.3, 122.2, 119.8, 119.1, 111.5, 111.0, 105.1, 47.8, 28.4, 27.3, 22.2; IR (neat)  $\nu$  ( $\text{cm}^{-1}$ ) 3419 (NH), 1786 (C=O), 1741 (C=O); TOF MS ES-  $m/z$ : 272.3  $[\text{M}-\text{H}]^-$ ; HR-MS calc.  $[\text{C}_{15}\text{H}_{14}\text{O}_4\text{N}]^-$  272.0928, obs. 272.0920.

**2,2-Dimethyl-5-(4-(trifluoromethyl)benzyl)-1,3-dioxane-4,6-dione (76n)<sup>120</sup>**



White solid (0.85 g, 98%); Mp 147-149 °C;  $^1\text{H}$  NMR (300 MHz,  $\text{CDCl}_3$ )  $\delta$  7.56 (d,  $J$  = 8.2 Hz, 2H, Ar), 7.47 (d,  $J$  = 8.2 Hz, 2H, Ar), 3.79 (t,  $J$  = 5.0 Hz, 1H,  $\text{CHCH}_2$ ), 3.54 (d,  $J$  = 5.0 Hz, 2H,  $\text{CH}_2$ ), 1.76 (s, 3H,  $\text{CH}_3$ ), 1.63 (s, 3H,  $\text{CH}_3$ );  $^{19}\text{F}$  NMR (282 MHz,  $\text{CDCl}_3$ )  $\delta$  -62.58;  $^{13}\text{C}$  NMR (101 MHz,  $\text{CDCl}_3$ )  $\delta$  164.9, 141.2, 130.2, 125.5, 125.5, 105.3, 47.9, 31.5, 28.4, 27.0; IR (neat)  $\nu$  ( $\text{cm}^{-1}$ ) 1767 (C=O), 1729 (C=O), 1630 (C=C); TOF MS ES-  $m/z$ : 301.3  $[\text{M}-\text{H}]^-$ , 199.2  $[\text{M}-\text{C}_4\text{H}_7\text{O}_3]^-$ ; HR-MS calc.  $[\text{C}_{14}\text{H}_{12}\text{O}_4\text{F}_3]^-$  301.0693, obs. 301.0689. *One carbon signal attributed to the  $\text{CF}_3$  was not visible in the  $^{13}\text{C}$  NMR spectrum.*

**2,2-Dimethyl-5-((perfluorophenyl)methyl)-1,3-dioxane-4,6-dione (76o)**



White solid (1.65 g, >99%); Mp 120-123 °C;  $^1\text{H}$  NMR (300 MHz,  $\text{CDCl}_3$ )  $\delta$  3.92 (t,  $J$  = 6.9 Hz, 1H,  $\text{CHCH}_2$ ), 3.45 (dq,  $J$  = 6.9, 1.2 Hz, 2H,  $\text{CH}_2$ ), 1.84 (s, 3H,  $\text{CH}_3$ ), 1.80 (s, 3H,  $\text{CH}_3$ );  $^{19}\text{F}$  NMR (282 MHz,  $\text{CDCl}_3$ )  $\delta$  -142.08 (m), -155.83 (t,  $J$  = 20.8 Hz), -162.21 (m);  $^{13}\text{C}$  NMR (101 MHz,  $\text{CDCl}_3$ )  $\delta$  163.95, 105.57, 28.53, 26.53, 19.86; IR (neat)  $\nu$  ( $\text{cm}^{-1}$ ) 1802 (C=C), 1790 (C=O), 1747 (C=O); TOF MS ES+  $m/z$ : 347.2  $[\text{M}+\text{Na}]^+$ . Carbons of the aromatic ring were not visible in the  $^{13}\text{C}$  NMR spectrum due to fluorine coupling.

## Hydrolysis & Decarboxylation to Synthesise 76b-h,j,l,n,o

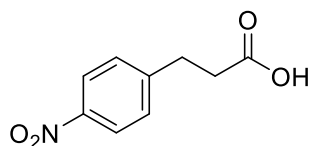
### Hydrolysis & Decarboxylation General Method 1

The reduced Meldrum's derivative (**76**) was dissolved in pyridine/water (5:2, 0.5 mmol/mL) and refluxed overnight. The reaction mixture was acidified with 1 M aqueous HCl (2 mL/mmol) and the resulting precipitate was filtered, washed with water and dried at the pump to afford the propionic acid derivatives without further purification.

### Hydrolysis & Decarboxylation General Method 2

The reduced Meldrum's derivative (**76**) was dissolved in pyridine/water (5:2, 0.5 mmol/mL), stirred at room temperature for 1 hr and refluxed for 4 hrs. The reaction mixture was acidified with 1M aqueous HCl (2 mL/mmol) and the resulting precipitate was filtered, washed with water and dried at the pump to afford the propionic acid derivatives without further purification.

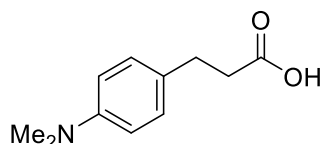
### 3-(4-Nitrophenyl)propanoic acid (**77b**)<sup>121</sup>



Hydrolysis & Decarboxylation General Method 1. White solid (0.63 g, 65%); Mp 169-172 °C;  $^1\text{H}$  NMR (300 MHz,  $d_6$ -DMSO)  $\delta$  12.23 (s, 1H, OH), 8.15 (d,  $J$  = 8.6 Hz, 2H, Ar), 7.53 (d,  $J$  = 8.6 Hz, 2H, Ar), 2.96 (t,  $J$  = 7.5 Hz, 2H,  $\text{CH}_2$ ), 2.62 (t,  $J$  = 7.5 Hz, 2H,  $\text{CH}_2$ );  $^{13}\text{C}$  NMR (101

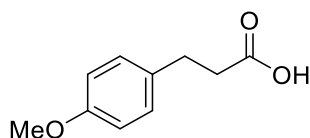
MHz, d<sub>6</sub>-DMSO)  $\delta$  173.9, 149.8, 146.4, 130.1, 123.9, 34.8, 30.5; IR (neat)  $\nu$  (cm<sup>-1</sup>) 2915 (OH), 1696 (C=O); TOF MS EI+  $m/z$ : 195.0 [M]<sup>+</sup>, 149.0 [C<sub>8</sub>H<sub>7</sub>NO<sub>2</sub>]<sup>+</sup>.

**3-(4-(Dimethylamino)phenyl)propanoic acid (77c)<sup>122</sup>**



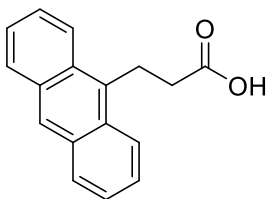
Hydrolysis & Decarboxylation General Method 1. Orange solid (1.52 g, 62%); Mp 102-103 °C; <sup>1</sup>H NMR (300 MHz, CDCl<sub>3</sub>)  $\delta$  7.09 (d,  $J$  = 8.7 Hz, 2H, Ar), 6.71 (d,  $J$  = 8.7 Hz, 2H, Ar), 2.93 – 2.83 (m, 8H, CH<sub>3</sub> & CH<sub>2</sub>), 2.68 – 2.59 (m, 2H, CH<sub>2</sub>); <sup>13</sup>C NMR (101 MHz, CDCl<sub>3</sub>)  $\delta$  179.1, 149.2, 129.1, 113.4, 113.0, 41.1, 36.1, 29.8; IR (neat)  $\nu$  (cm<sup>-1</sup>) 2970 (OH), 1699 (C=O); TOF MS EI+  $m/z$ : 193.1 [M+H]<sup>+</sup>, 134.1 [M-O<sub>2</sub>C<sub>2</sub>H<sub>3</sub>]<sup>+</sup>.

**3-(4-Methoxyphenyl)propanoic acid (77d)<sup>122</sup>**



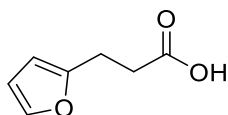
Hydrolysis & Decarboxylation General Method 2. White solid (2.47 g, 93%); Mp 99-100 °C; <sup>1</sup>H NMR (300 MHz, CDCl<sub>3</sub>)  $\delta$  7.13 (d,  $J$  = 8.6 Hz, 2H, Ar), 6.84 (d,  $J$  = 8.6 Hz, 2H, Ar), 3.79 (s, 3H, CH<sub>3</sub>), 2.90 (d,  $J$  = 7.9 Hz, 2H, CH<sub>2</sub>), 2.65 (d,  $J$  = 7.9 Hz, 2H, CH<sub>2</sub>); <sup>13</sup>C NMR (101 MHz, CDCl<sub>3</sub>)  $\delta$  179.2, 158.1, 132.2, 129.2, 114.0, 55.3, 35.9, 29.7; IR (neat)  $\nu$  (cm<sup>-1</sup>) 2930 (OH), 1699 (C=O); TOF MS ES-  $m/z$ : 179.1 [M-H]<sup>-</sup>; HR-MS calc. [C<sub>10</sub>H<sub>11</sub>O<sub>3</sub>]<sup>-</sup> 179.0714, obs. 179.0711.

**3-(Anthracen-9-yl)propanoic acid (77e)<sup>93</sup>**



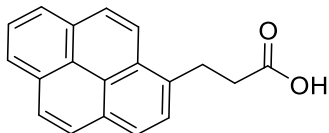
Hydrolysis & Decarboxylation General Method 1. Orange solid (1.48 g, 80%); Mp 193-195 °C;  $^1\text{H}$  NMR (300 MHz,  $\text{d}_6$ -DMSO)  $\delta$  8.51 (s, 1H, Ar), 8.33 (dd,  $J$  = 8.5, 1.4, 2H, Ar), 8.10 (dd,  $J$  = 8.5, 1.4, 2H, Ar), 7.74 – 7.37 (m, 4H, Ar), 4.01 – 3.78 (m, 2H,  $\text{ArCH}_2$ ), 3.38 (s, 1H, OH), 2.78 – 2.58 (m, 2H,  $\text{CH}_2\text{COOH}$ );  $^{13}\text{C}$  NMR (101 MHz,  $\text{d}_6$ -DMSO)  $\delta$  174.2, 133.4, 131.6, 129.5, 129.5, 126.5, 126.4, 125.6, 124.5, 35.7, 23.2; IR (neat)  $\nu$  ( $\text{cm}^{-1}$ ) 3050 (OH), 1688 (C=O); Scan ES-  $m/z$ : 249.1  $[\text{M}-\text{H}]^-$ .

### 3-(Furan-2-yl)propanoic acid (77f)<sup>123</sup>



Hydrolysis & Decarboxylation General Method 1. Black solid (0.58 g,  $\leq 94\%$ );  $^1\text{H}$  NMR (300 MHz,  $\text{CDCl}_3$ )  $\delta$  10.91 (s, 1H, OH), 7.31 (dd,  $J$  = 1.9, 1.0 Hz, 1H,  $\text{HC}=\text{CH}$ ), 6.28 (dd,  $J$  = 3.2, 1.9 Hz, 1H,  $\text{HC}=\text{CH}$ ), 6.04 (dd,  $J$  = 3.2, 1.0 Hz, 1H,  $\text{HC}=\text{CH}$ ), 2.97 (d,  $J$  = 7.6 Hz, 2H,  $\text{CH}_2$ ), 2.72 (t,  $J$  = 7.6 Hz, 2H,  $\text{CH}_2$ ); IR (neat)  $\nu$  ( $\text{cm}^{-1}$ ) 3030 (OH), 1705 (C=O); TOF MS EI+  $m/z$ : 140.1  $[\text{M}]^+$ .

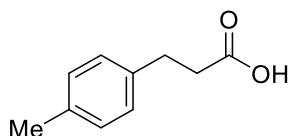
### 3-(Pyren-1-yl)propanoic acid (77g)<sup>124</sup>



Hydrolysis & Decarboxylation General Method 1. Ochre solid (1.12 g, 92%); Mp 163-167 °C;  $^1\text{H}$  NMR (300 MHz,  $\text{d}_3$ -MeOD)  $\delta$  8.30 (d,  $J$  = 9.5 Hz, 1H, Ar), 8.22 – 8.07 (m, 6H, Ar), 8.01 (d,  $J$  = 9.5 Hz, 1H, Ar), 7.92 (d,  $J$  = 7.9 Hz, 1H, Ar), 3.65 (t,  $J$  = 8.0 Hz, 2H,  $\text{CH}_2$ ), 2.83 (t,  $J$  = 8.0 Hz, 2H,  $\text{CH}_2$ );  $^{13}\text{C}$  NMR (101 MHz,  $\text{d}_3$ -MeOD)  $\delta$  175.2, 134.7, 131.4, 130.8, 130.1, 128.3,

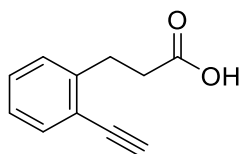
127.2, 127.1, 126.7, 126.4, 125.6, 124.8, 124.6, 124.5, 124.5, 123.1, 122.6, 35.5, 28.2; IR (neat)  $\nu$  ( $\text{cm}^{-1}$ ) 2903 (OH), 1690 (C=O); TOF MS ES-  $m/z$ : 273.3  $[\text{M-H}]^-$ .

### 3-(*p*-Tolyl)propanoic acid (77h)<sup>122</sup>



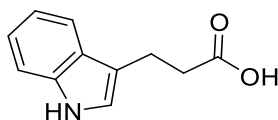
Hydrolysis & Decarboxylation General Method 2. White solid (1.54 g, 81%); Mp 116-118 °C;  $^1\text{H}$  NMR (300 MHz,  $\text{CDCl}_3$ )  $\delta$  10.67 (s, 1H, OH), 7.10 (s, 4H, Ar), 2.92 (t,  $J$  = 7.8 Hz, 2H,  $\text{CH}_2$ ), 2.67 (d,  $J$  = 7.8 Hz, 2H,  $\text{CH}_2$ ), 2.32 (s, 3H,  $\text{CH}_3$ );  $^{13}\text{C}$  NMR (101 MHz,  $\text{CDCl}_3$ )  $\delta$  179.2, 137.1, 135.9, 129.2, 128.1, 35.7, 30.2, 21.0; IR (neat)  $\nu$  ( $\text{cm}^{-1}$ ) 2919 (OH), 1698 (C=O); TOF MS ES-  $m/z$ : 163.0  $[\text{M-H}]^-$ ; HR-MS calc.  $[\text{C}_{10}\text{H}_{11}\text{O}_2]^-$  163.0765, obs. 163.0758.

### 3-(2-Ethynylphenyl)propanoic acid (77j)



Hydrolysis & Decarboxylation General Method 1. White solid (0.14 g,  $\leq 86\%$ );  $^1\text{H}$  NMR (400 MHz,  $\text{CDCl}_3$ )  $\delta$  7.49 (dd,  $J$  = 7.6, 1.4 Hz, 1H, Ar), 7.33 – 7.16 (m, 3H, Ar), 3.29 (s, 1H,  $\text{C}\equiv\text{CH}$ ), 3.14 (d,  $J$  = 8.1 Hz, 2H,  $\text{CH}_2$ ), 2.75 (d,  $J$  = 8.1 Hz, 2H,  $\text{CH}_2$ ); IR (neat)  $\nu$  ( $\text{cm}^{-1}$ ) 3287 ( $\text{C}\equiv\text{CH}$ ), 2919 (OH), 1704 (C=O); TOF MS AP+  $m/z$ : 175.1  $[\text{M+H}]^+$ .

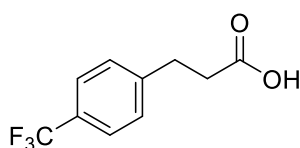
### 3-(1H-Indol-3-yl)propanoic acid (77l)<sup>125</sup>



Hydrolysis & Decarboxylation General Method 1. Red solid (66 mg, 48%); Mp 122-124 °C;  $^1\text{H}$  NMR (400 MHz,  $\text{d}_3$ -MeOD)  $\delta$  7.52 (dt,  $J$  = 7.8, 1.0 Hz, 1H, Ar), 7.31 (dt,  $J$  = 8.1, 1.0 Hz,

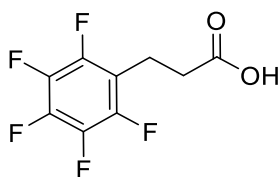
$^1\text{H}$ , Ar), 7.10 – 6.96 (m, 3H, Ar), 3.05 (t,  $J = 7.4$  Hz, 2H,  $\text{CH}_2$ ), 2.67 (t,  $J = 7.4$  Hz, 2H,  $\text{CH}_2$ );  $^{13}\text{C}$  NMR (101 MHz,  $\text{d}_3\text{-MeOD}$ )  $\delta$  176.0, 136.7, 127.1, 121.4, 120.9, 118.1, 117.7, 113.6, 110.8, 34.7, 20.4; IR (neat)  $\nu$  ( $\text{cm}^{-1}$ ) 3392 (NH), 3053 (OH), 1687 (C=O); TOF MS ES-  $m/z$ : 188.1  $[\text{M-H}]^-$ .

### 3-(4-(Trifluoromethyl)phenyl)propanoic acid (77n)<sup>122</sup>



Hydrolysis & Decarboxylation General Method 1. Viscous oil (0.34 g, 63%);  $^1\text{H}$  NMR (300 MHz,  $\text{d}_3\text{-MeOD}$ )  $\delta$  7.59 (d,  $J = 8.0$  Hz, 2H, Ar), 7.45 (d,  $J = 8.0$  Hz, 2H, Ar), 3.02 (t,  $J = 7.6$  Hz, 3H,  $\text{ArCH}_2$ ), 2.67 (t,  $J = 7.6$  Hz, 2H,  $\text{CH}_2\text{COOH}$ );  $^{19}\text{F}$  NMR (282 MHz,  $\text{d}_3\text{-MeOD}$ )  $\delta$  -63.90;  $^{13}\text{C}$  NMR (101 MHz,  $\text{d}_3\text{-MeOD}$ )  $\delta$  174.8, 145.5, 128.6, 124.9, 124.8, 34.7, 30.3; IR (neat)  $\nu$  ( $\text{cm}^{-1}$ ) 2901 (OH), 1707 (C=O); TOF MS EI+  $m/z$ : 218.1  $[\text{M}]^+$ , 172.1  $[\text{M-CH}_2\text{O}_2]^+$ , 159.1  $[\text{M-C}_2\text{H}_3\text{O}_2]^+$ . One carbon signal attributed to the  $\text{CF}_3$  was not visible in the  $^{13}\text{C}$  NMR spectrum.

### 3-(Perfluorophenyl)propanoic acid (77o)



Hydrolysis & Decarboxylation General Method 1. solid (0.45 g, 48%);  $^1\text{H}$  NMR (300 MHz,  $\text{d}_3\text{-MeOD}$ )  $\delta$  3.05 (t,  $J = 7.7$  Hz, 2H,  $\text{ArCH}_2$ ), 2.63 (t,  $J = 7.7$  Hz, 2H,  $\text{CH}_2\text{COOH}$ );  $^{19}\text{F}$  NMR (282 MHz,  $\text{d}_3\text{-MeOD}$ )  $\delta$  -145.65 – -146.12 (m), -160.81 (t,  $J = 20.0$  Hz), -165.89 – -166.27 (m);  $^{13}\text{C}$  NMR (101 MHz,  $\text{d}_3\text{-MeOD}$ )  $\delta$  173.8, 144.1 (m), 138.9 (m), 137.3 (m), 114.1 (m), 32.4, 17.5; IR (neat)  $\nu$  ( $\text{cm}^{-1}$ ) 2866 (OH), 1700 (C=O); TOF MS EI+  $m/z$ : 240.1  $[\text{M}]^+$ , 194.1  $[\text{M-CHO}_2]^+$ , 181.0  $[\text{M-C}_2\text{H}_3\text{O}_2]^+$ .



## Carboxylic Acid Reduction to Synthesise 78b-e,g,h,j,l

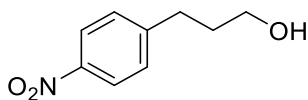
### *Carboxylic Acid Reduction General Method 1*

Lithium aluminium hydride (1.2 equiv.) was added slowly to a solution of 3-propionic acid derivative (1.0 equiv.) in THF (0.2 M) at 0 °C, the reaction was allowed to reach room temperature and stirred for 16 hrs and quenched by the sequential addition of water (1 mL/mg LiAlH<sub>4</sub>), 2M aqueous NaOH (1 mL/mg LiAlH<sub>4</sub>) and a second portion of water (1 mL/mg LiAlH<sub>4</sub>) and allowed to stir for 30 mins after which a white precipitate formed. The reaction mixture was dried over MgSO<sub>4</sub>, filtered and evaporated under reduced pressure to afford the desired 3-propanol derivatives without further purification.

### *Carboxylic Acid Reduction General Method 2*

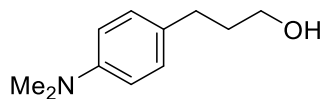
Borane in THF (7.7 mL, 7.7 mmol, 3.0 equiv.) was added dropwise to a solution of 3-propionic acid (1.0 equiv.) in THF (0.5 M) at 0 °C, warmed to room temperature and stirred for 4 hrs. The reaction mixture was quenched with 1 M aqueous HCl (20 mL/mmol), extracted with Et<sub>2</sub>O (2 x 100mL) and the combined organic phases were dried over MgSO<sub>4</sub>, filtered and the solvent was removed under reduced pressure. The residue was purified by column chromatography (silica, 0-100% EtOAc/hexane) to give the title compound.

### **3-(4-Nitrophenyl)propan-1-ol (78b)**<sup>126</sup>



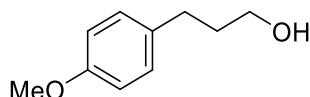
Carboxylic Acid Reduction General Method 2. Pale yellow oil (0.40 g, 86%); <sup>1</sup>H NMR (400 MHz, CDCl<sub>3</sub>) δ 8.15 (d, *J* = 8.6 Hz, 2H, Ar), 7.37 (d, *J* = 8.6 Hz, 2H, Ar), 3.70 (t, *J* = 6.2 Hz, 2H, CH<sub>2</sub>), 2.84 (t, *J* = 7.8 Hz, 2H, CH<sub>2</sub>), 1.98 – 1.86 (m, 2H, CH<sub>2</sub>), 1.65 (s, 1H, OH); <sup>13</sup>C NMR (101 MHz, CDCl<sub>3</sub>) δ 149.9, 146.4, 129.3, 123.7, 61.7, 33.6, 32.0; IR (neat) ν (cm<sup>-1</sup>) 3346 (OH); TOF MS EI+ *m/z*: 181.1 [M]<sup>+</sup>, 163.1 [M-H<sub>2</sub>O]<sup>+</sup>.

### 3-(4-(Dimethylamino)phenyl)propan-1-ol (78c)<sup>127</sup>



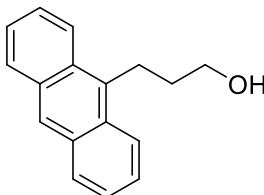
Carboxylic Acid Reduction General Method 1. Brown oil (1.30 g, 93%); <sup>1</sup>H NMR (300 MHz, CDCl<sub>3</sub>) δ 7.08 (d, *J* = 8.6 Hz, 2H, Ar), 6.70 (d, *J* = 8.6 Hz, 2H, Ar), 3.67 (t, *J* = 6.4 Hz, 2H, CH<sub>2</sub>), 2.91 (s, 6H, N(CH<sub>3</sub>)<sub>2</sub>), 2.61 (dd, *J* = 8.6, 6.4 Hz, 2H, CH<sub>2</sub>), 1.93 – 1.79 (m, 2H, CH<sub>2</sub>), 1.64 (s, 1H, OH); <sup>13</sup>C NMR (101 MHz, CDCl<sub>3</sub>) δ 149.1, 129.9, 129.0, 113.1, 62.5, 40.9, 34.5, 31.0; IR (neat) ν (cm<sup>-1</sup>) 3310 (OH); TOF MS EI+ *m/z*: 179.2 [M]<sup>+</sup>, 134.1 [M- C<sub>2</sub>H<sub>5</sub>O]<sup>+</sup>.

### 3-(4-Methoxyphenyl)propan-1-ol (78d)<sup>128</sup>



Carboxylic Acid Reduction General Method 1. Yellow oil (1.80 g, 95%); <sup>1</sup>H NMR (300 MHz, CDCl<sub>3</sub>) δ 7.11 (d, *J* = 8.7 Hz, 2H, Ar), 6.84 (d, *J* = 8.7 Hz, 2H, Ar), 3.78 (s, 3H, CH<sub>3</sub>), 3.65 (t, *J* = 6.4 Hz, 2H, CH<sub>2</sub>), 2.64 (d, *J* = 8.7 Hz, 2H, CH<sub>2</sub>), 1.95 – 1.70 (m, 3H, CH<sub>2</sub> & OH); <sup>13</sup>C NMR (101 MHz, CDCl<sub>3</sub>) δ 157.8, 133.9, 129.3, 113.8, 62.2, 55.3, 34.4, 31.1; IR (neat) ν (cm<sup>-1</sup>) 3352 (OH); TOF MS EI+ *m/z*: 166.1 [M]<sup>+</sup>; HR-MS calc. [C<sub>10</sub>H<sub>14</sub>O<sub>2</sub>]<sup>+</sup> 166.0988, obs. 166.0995.

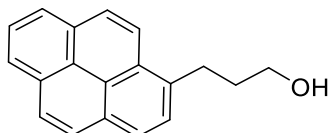
### 3-(Anthracen-9-yl)propan-1-ol (78e)<sup>93</sup>



Carboxylic Acid Reduction General Method 1. Pale yellow solid (1.39 g, 99%); Mp 93-94 °C; <sup>1</sup>H NMR (300 MHz, CDCl<sub>3</sub>) δ 8.44 – 8.20 (m, 3H, Ar), 8.11 – 7.89 (m, 2H, Ar), 7.66 – 7.35 (m, 4H, Ar), 3.82 (t, *J* = 6.2 Hz, 2H, CH<sub>2</sub>), 3.77 – 3.68 (m, 2H, CH<sub>2</sub>), 2.23 – 1.98 (m, 2H, CH<sub>2</sub>),

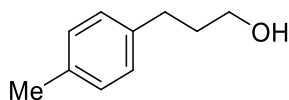
1.58 (s, 1H, OH);  $^{13}\text{C}$  NMR (101 MHz,  $\text{CDCl}_3$ )  $\delta$  134.3, 131.6, 129.7, 129.2, 125.8, 125.6, 124.9, 124.3, 62.7, 34.0, 24.1; IR (neat)  $\nu$  ( $\text{cm}^{-1}$ ) 3323 (OH); Scan ES+  $m/z$ : 259.4  $[\text{M}+\text{H}]^+$ .

**3-(Pyren-1-yl)propan-1-ol (78g)<sup>129</sup>**



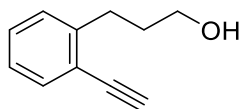
Carboxylic Acid Reduction General Method 1. Brown oil (1.03 g, 99%);  $^1\text{H}$  NMR (300 MHz,  $\text{CDCl}_3$ )  $\delta$  8.15 (d,  $J$  = 9.3 Hz, 1H, Ar), 8.09 – 8.01 (m, 2H, Ar), 8.01 – 7.83 (m, 5H, Ar), 7.73 (d,  $J$  = 7.8 Hz, 1H, Ar), 3.64 (t,  $J$  = 6.3 Hz, 2H,  $\text{CH}_2$ ), 3.40 – 3.16 (m, 2H,  $\text{CH}_2$ ), 2.71 (s, 1H, OH), 1.99 (m, 2H,  $\text{CH}_2$ );  $^{13}\text{C}$  NMR (101 MHz,  $\text{CDCl}_3$ )  $\delta$  136.1, 131.4, 130.9, 129.9, 128.7, 127.8, 127.5, 127.3, 127.2, 126.7, 125.9, 125.3, 124.9, 124.9, 124.8, 123.3, 62.4, 34.5, 29.6; IR (neat)  $\nu$  ( $\text{cm}^{-1}$ ) 3299 (OH); TOF MS ES+  $m/z$ : 283.3  $[\text{M}+\text{Na}]^+$ .

**3-(p-Tolyl)propan-1-ol (78h)<sup>130</sup>**



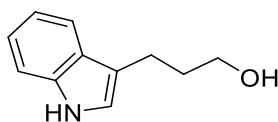
Carboxylic Acid Reduction General Method 1. Yellow oil (1.23 g, 83%);  $^1\text{H}$  NMR (300 MHz,  $\text{CDCl}_3$ )  $\delta$  7.07 (s, 4H, Ar), 3.62 (t,  $J$  = 6.5 Hz, 2H,  $\text{CH}_2$ ), 2.69 – 2.57 (m, 2H,  $\text{CH}_2$ ), 2.30 (s, 3H,  $\text{CH}_3$ ), 1.92 – 1.76 (m, 2H,  $\text{CH}_2$ );  $^{13}\text{C}$  NMR (101 MHz,  $\text{CDCl}_3$ )  $\delta$  138.8, 135.3, 129.1, 128.4, 62.1, 34.4, 31.7, 21.0; IR (neat)  $\nu$  ( $\text{cm}^{-1}$ ) 3324 (OH); TOF MS EI+  $m/z$ : 150.1  $[\text{M}]^+$ , 132.1  $[\text{M}-\text{H}_2\text{O}]^+$ ; HR-MS calc.  $[\text{C}_{10}\text{H}_{14}\text{O}]^+$  150.1039, obs. 150.1043.

**3-(2-Ethynylphenyl)propan-1-ol (78j)<sup>131</sup>**



Carboxylic Acid Reduction General Method 1. Colourless oil (63 mg, 53%);  $^1\text{H}$  NMR (400 MHz,  $\text{CDCl}_3$ )  $\delta$  7.48 (dd,  $J = 7.6, 1.5$  Hz, 1H, Ar), 7.30 – 7.20 (m, 2H, Ar), 7.16 (td,  $J = 7.6, 1.5$  Hz, 1H, Ar), 3.66 (t,  $J = 6.4$  Hz, 2H,  $\text{CH}_2$ ), 3.27 (s, 1H,  $\text{C}\equiv\text{CH}$ ), 2.89 (t,  $J = 7.6$  Hz, 2H,  $\text{CH}_2$ ), 1.97 – 1.86 (m, 2H,  $\text{CH}_2$ ), 1.78 (s, 1H, OH);  $^{13}\text{C}$  NMR (101 MHz,  $\text{CDCl}_3$ )  $\delta$  144.4, 133.0, 129.0, 128.9, 125.9, 121.5, 82.4, 80.8, 62.1, 33.4, 30.5; IR (neat)  $\nu$  ( $\text{cm}^{-1}$ ) 3291 (OH); TOF MS EI+  $m/z$ : 260.1  $[\text{M}]^+$ , 141.1  $[\text{M}-\text{H}_2\text{O}]^+$ .

### 3-(1H-Indol-3-yl)propan-1-ol (78l)<sup>132</sup>

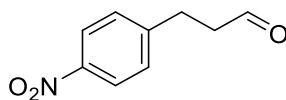


Carboxylic Acid Reduction General Method 1. Orange oil (30 mg, 66%);  $^1\text{H}$  NMR (400 MHz,  $\text{CDCl}_3$ )  $\delta$  8.01 (s, 1H, NH), 7.60 (dd,  $J = 7.8, 1.1$  Hz, 1H, Ar), 7.33 (dt,  $J = 8.1, 1.1$  Hz, 1H, Ar), 7.23 – 7.14 (m, 1H, Ar), 7.15 – 7.06 (m, 1H, Ar), 6.97 – 6.92 (m, 1H, Ar), 3.70 (t,  $J = 6.4$  Hz, 2H,  $\text{CH}_2$ ), 2.84 (t,  $J = 7.0$  Hz, 2H,  $\text{CH}_2$ ), 2.03 – 1.91 (m, 2H,  $\text{CH}_2$ ), 1.66 (s, 1H, OH);  $^{13}\text{C}$  NMR (101 MHz,  $\text{CDCl}_3$ )  $\delta$  136.0, 127.5, 122.0, 121.6, 119.2, 118.9, 115.9, 111.2, 62.6, 32.9, 21.4; IR (neat)  $\nu$  ( $\text{cm}^{-1}$ ) 3320 (OH); TOF MS AP+  $m/z$ : 176.1  $[\text{M}+\text{H}]^+$ , 158.1  $[\text{M}-\text{H}_2\text{O}]^+$ .

### Swern Oxidation to Synthesise 74b,d,e,g,h,j

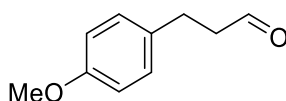
DMSO (4.4 equiv.) in  $\text{CH}_2\text{Cl}_2$  (0.2 M) was added dropwise to oxalyl chloride (2.2 equiv.) in  $\text{CH}_2\text{Cl}_2$  (1 M) at  $-78^\circ\text{C}$  and stirred for 15 mins. Alcohol (1.0 equiv.) in  $\text{CH}_2\text{Cl}_2$  (1 M) was added dropwise to the DMSO/oxalyl chloride solution and stirred for 1 hr at  $-78^\circ\text{C}$ . Triethylamine (5.0 equiv.) was added dropwise to the reaction mixture, stirred for 15 mins then slowly warmed to room temperature over 1 hr. Silica was added to the reaction mixture, the solvent evaporated under reduced pressure and the residue was purified by column chromatography (silica, 0-50% EtOAc/hexane) to give the aldehydes.

### 3-(4-Nitrophenyl)propanal (74b)<sup>92</sup>



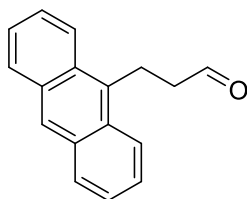
White solid (307 mg, 84%);  $^1\text{H}$  NMR (400 MHz,  $\text{CDCl}_3$ )  $\delta$  9.84 (s, 1H, CHO), 8.15 (d,  $J$  = 8.7 Hz, 2H, Ar), 7.37 (d,  $J$  = 8.7 Hz, 2H, Ar), 3.07 (t,  $J$  = 7.4 Hz, 2H,  $\text{ArCH}_2$ ), 2.87 (t,  $J$  = 7.4 Hz, 2H,  $\text{CH}_2\text{CHO}$ );  $^{13}\text{C}$  NMR (101 MHz,  $\text{CDCl}_3$ )  $\delta$  200.1, 148.3, 146.6, 129.3, 123.8, 44.5, 27.8; IR (neat)  $\nu$  ( $\text{cm}^{-1}$ ) 1713 (C=O); TOF MS EI+  $m/z$ : 179.0  $[\text{M}]^+$ .

### 3-(4-Methoxyphenyl)propanal (74d)<sup>92</sup>



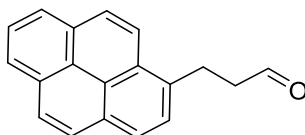
Yellow oil (1.33 g, 83%);  $^1\text{H}$  NMR (300 MHz,  $\text{CDCl}_3$ )  $\delta$  9.81 (t,  $J$  = 1.5 Hz, 1H, CHO), 7.11 (d,  $J$  = 8.8 Hz, 2H, Ar), 6.83 (d,  $J$  = 8.8 Hz, 2H, Ar), 3.78 (s, 3H,  $\text{CH}_3$ ), 2.97 – 2.85 (m, 2H,  $\text{CH}_2$ ), 2.87 – 2.65 (m, 2H,  $\text{CH}_2$ );  $^{13}\text{C}$  NMR (101 MHz,  $\text{CDCl}_3$ )  $\delta$  201.8, 158.1, 132.3, 129.2, 114.0, 55.3, 45.6, 27.3; IR (neat)  $\nu$  ( $\text{cm}^{-1}$ ) 1721 (C=O); TOF MS EI+  $m/z$ : 164.1  $[\text{M}]^+$ ; HR-MS calc.  $[\text{C}_{10}\text{H}_{12}\text{O}_2]^+$  164.0832, obs. 164.0836.

### 3-(Anthracen-9-yl)propanal (74e)<sup>83</sup>



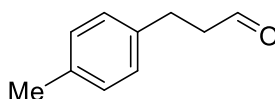
Yellow solid (2.34 g, 89%); Mp 84-86 °C;  $^1\text{H}$  NMR (300 MHz,  $\text{CDCl}_3$ )  $\delta$  9.87 (s, 1H, CHO), 8.31 (s, 1H, Ar), 8.17 – 8.08 (m, 2H, Ar), 8.00 – 7.92 (m, 2H, Ar), 7.56 – 7.35 (m, 4H, Ar), 3.95 – 3.82 (m, 2H,  $\text{ArCH}_2$ ), 2.93 – 2.80 (m, 2H,  $\text{CH}_2\text{CHO}$ );  $^{13}\text{C}$  NMR (101 MHz,  $\text{CDCl}_3$ )  $\delta$  201.4, 134.0, 132.4, 131.6, 129.5, 126.4, 126.0, 125.0, 123.8, 44.9, 20.0; IR (neat)  $\nu$  ( $\text{cm}^{-1}$ ) 1730 (C=O); TOF MS EI+  $m/z$ : 234.1  $[\text{M}]^+$ , 191.1  $[\text{M}-\text{CH}_2\text{CHO}]^+$ .

### 3-(Pyren-1-yl)propanal (74g)<sup>133</sup>



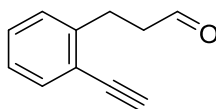
Yellow oil (0.60 g, 66%);  $^1\text{H}$  NMR (300 MHz,  $\text{CDCl}_3$ )  $\delta$  9.84 (t,  $J = 1.3$  Hz, 1H, CHO), 8.16 – 8.10 (m, 3H, Ar), 8.08 – 8.02 (m, 2H, Ar), 8.00 – 7.92 (m, 3H, Ar), 7.79 (d,  $J = 7.8$  Hz, 1H, Ar), 3.59 (t,  $J = 7.7$  Hz, 2H,  $\text{ArCH}_2$ ), 2.92 (td,  $J = 7.7, 1.3$  Hz, 2H,  $\text{CH}_2\text{CHO}$ );  $^{13}\text{C}$  NMR (101 MHz,  $\text{CDCl}_3$ )  $\delta$  201.4, 134.3, 131.4, 130.8, 130.2, 128.5, 127.7, 127.5, 127.0, 126.9, 126.0, 125.2, 125.2, 125.0, 124.5, 123.5, 122.7, 45.5, 25.7; IR (neat)  $\nu$  ( $\text{cm}^{-1}$ ) 1621 (C=O); TOF MS  $\text{AP}^+$   $m/z$ : 258.1  $[\text{M}]^+$ , 241.1  $[\text{M}-\text{OH}]^+$ ; HR-MS calc.  $[\text{C}_{19}\text{H}_{14}\text{O}]^+$  258.1045, obs. 258.1050.

### 3-(*p*-Tolyl)propanal (74h)<sup>134</sup>



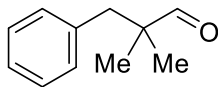
Colourless oil (0.92 g, 83%);  $^1\text{H}$  NMR (300 MHz,  $\text{CDCl}_3$ )  $\delta$  9.81 (t,  $J = 1.5$  Hz, 1H, CHO), 7.09 (t,  $J = 2.3$  Hz, 4H, Ar), 3.01 – 2.86 (m, 2H,  $\text{CH}_2$ ), 2.81 – 2.69 (m, 2H,  $\text{CH}_2$ ), 2.31 (s, 3H,  $\text{CH}_3$ );  $^{13}\text{C}$  NMR (101 MHz,  $\text{CDCl}_3$ )  $\delta$  201.7, 137.2, 135.8, 129.3, 128.2, 45.4, 27.7, 21.0; IR (neat)  $\nu$  ( $\text{cm}^{-1}$ ) 1723 (C=O); TOF MS  $\text{E}^+$   $m/z$ : 148.1  $[\text{M}]^+$ ; HR-MS calc.  $[\text{C}_{10}\text{H}_{12}\text{O}]^+$  148.0883, obs. 148.0886.

### 3-(2-Ethynylphenyl)propanal (74j)



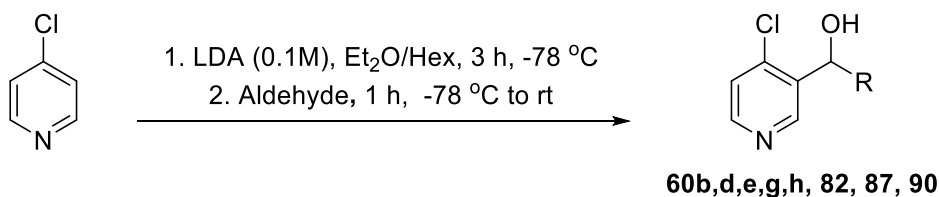
Colourless oil (46 mg, 77%);  $^1\text{H}$  NMR (400 MHz,  $\text{CDCl}_3$ )  $\delta$  9.83 (t,  $J = 1.4$  Hz, 1H, CHO), 7.49 (dd,  $J = 7.6, 1.4$  Hz, 1H, Ar), 7.29 (td,  $J = 7.6, 1.4$  Hz, 1H, Ar), 7.26 – 7.14 (m, 2H, Ar), 3.29 (s, 1H,  $\text{C}\equiv\text{CH}$ ), 3.13 (t,  $J = 7.7$  Hz, 2H,  $\text{ArCH}_2$ ), 2.82 (td,  $J = 7.7, 1.4$  Hz, 2H,  $\text{CH}_2\text{CHO}$ );  $^{13}\text{C}$  NMR (101 MHz,  $\text{CDCl}_3$ )  $\delta$  201.5, 143.0, 133.1, 129.2, 128.9, 126.4, 121.5, 81.9, 81.4, 44.4, 27.0; IR (neat)  $\nu$  ( $\text{cm}^{-1}$ ) 3285 (CCH), 1718 (C=O); TOF MS  $\text{EI}^+$   $m/z$ : 158.1  $[\text{M}]^+$ , 130.1  $[\text{M}-\text{H}_2\text{O}]^+$ .

### 2,2-Dimethyl-3-phenylpropanal (**83**)<sup>97</sup>



Benzyl bromide (3.8 mL, 32.0 mmol, 1.00 equiv.) was added to a solution of distilled isobutyraldehyde (4.0 mL, 43.8 mmol, 1.38 equiv.), tetrabutylammonium iodide (0.16 g, 0.4 mmol, 0.01 equiv.) and sodium hydroxide (1.5 g, 37.5 mmol, 1.17 equiv.) in a biphasic mixture of water (1.8 mL) and toluene (2.5 mL) and heated to 70 °C for 18 hrs. After cooling, the phases were separated and the aqueous was washed with ethyl acetate (3 x 20 mL), the combined organic extracts were dried over MgSO<sub>4</sub>, filtered and the solvent was removed under reduced pressure. The residue was purified by column chromatography (silica, 0-10% EtOAc/hexane) followed by vacuum distillation (81 °C at 10 mbar) to give **83** as a colourless oil (900 mg, 17%); <sup>1</sup>H NMR (300 MHz, CDCl<sub>3</sub>) δ 9.59 (s, 1H, CHO), 7.31 – 7.17 (m, 3H, Ar), 7.12 – 7.06 (m, 2H, Ar), 2.78 (s, 2H, CH<sub>2</sub>), 1.05 (s, 6H, CH<sub>3</sub>); – <sup>13</sup>C NMR (101 MHz, CDCl<sub>3</sub>) δ 206.0, 136.9, 130.2, 128.2, 126.5, 47.0, 43.2, 21.4; IR (neat) ν (cm<sup>-1</sup>) 1722 (C=O); TOF MS EI+ m/z: 162.1 [M]<sup>+</sup>, 147.1 [M- Me]<sup>+</sup>.

### Synthesis of **60b,d,e,g,h**, **82**, **87** and **90**



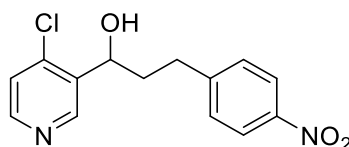
4-Chloropyridine (1.0 equiv.) in Et<sub>2</sub>O (1 mmol/mL) was added dropwise to a solution of 0.1 M LDA (Table 14) in Et<sub>2</sub>O at -78 °C under argon and stirred for 3 hrs. Aldehyde (Table 14) was added dropwise and stirred for 10 mins after which the reaction mixture was warmed to room temperature over 1 hr and quenched by addition of water (10 ml/mmol). The phases were separated and the aqueous was extracted with Et<sub>2</sub>O (2 x 10 mL/mmol)

and the combined organic extracts were washed with brine (20 mL/mmol), dried over  $\text{MgSO}_4$ , filtered and the solvent was removed under reduced pressure. The residue was purified by column chromatography (silica, 0-100% EtOAc/hexane) to give the title compounds.

*Table 14 - Summary of reagent equivalents and yields for the synthesis of 60b,d,e,g,h, 82, 87 and 90*

Entry	Product	Aldehyde	Scale (mmol)	LDA equivalents	Aldehyde equivalents	Yield (%)
1	60b	74b	1.18	1.5	1.5	12
2	60d	74d	6.10	1.2	1.2	50
3	60e	74e	1.50	1.2	1.2	43
4	60g	74g	1.94	1.2	1.2	38
5	60h	74h	3.93	1.2	1.2	19
6	82	83	3.90	1.2	1.2	58
7	87	91	5.76	1.2	1.2	59
8	90	88	1.37	1.5	1.5	48

#### 1-(4-Chloropyridin-3-yl)-3-(4-nitrophenyl)propan-1-ol (60b)



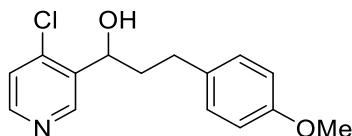
Colourless oil (40 mg, 12%);  $^1\text{H}$  NMR (300 MHz,  $\text{CDCl}_3$ )  $\delta$  8.79 (s, 1H, Py), 8.39 (d,  $J$  = 5.3 Hz, 1H, Py), 8.16 (d,  $J$  = 8.7 Hz, 2H, Ar), 7.38 (d,  $J$  = 8.7 Hz, 2H, Ar), 7.26 (d,  $J$  = 5.3 Hz, 1H, Py), 5.12 (t,  $J$  = 8.2, 5.3 Hz, 1H,  $\text{CHOH}$ ), 3.08 – 2.83 (m, 2H,  $\text{CH}_2$ ), 2.63 (s, 1H, OH), 2.23 – 2.01 (m, 2H,  $\text{CH}_2$ );  $^{13}\text{C}$  NMR (101 MHz,  $\text{CDCl}_3$ )  $\delta$  149.3, 149.1, 149.0, 146.5, 141.6, 137.7, 129.3, 124.5, 123.7, 68.5, 38.1, 31.8; IR (neat)  $\nu$  ( $\text{cm}^{-1}$ ) 3194 (OH); TOF MS AP+  $m/z$ : 293.1/295.1  $[\text{M}]^+$ ; HR-MS calc.  $[\text{C}_{14}\text{H}_{14}\text{O}_3\text{N}_2\text{Cl}^{35}]^+$  293.0687, obs. 293.0695.

Preparative HPLC: Enantiomers were separated on a Phenomenex Cellulose 1 Preparative HPLC column eluting with acetonitrile:water [1:1] at a flow rate of 15 mL/min. A total of



68 mg of racemic compound was inject and 18 mg (26%) of the first eluting enantiomer and 22 mg (32%) of the second eluting enantiomer were recovered.

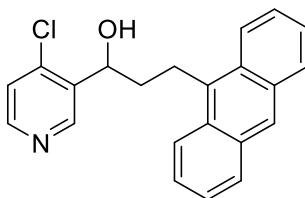
**1-(4-Chloropyridin-3-yl)-3-(4-methoxyphenyl)propan-1-ol (60d)**



Yellow solid (852 mg, 50%);  $R_f = 0.23$  (hexane/EtOAc = [1:1]); Mp: 59-61 °C;  $^1\text{H}$  NMR (400 MHz,  $\text{CDCl}_3$ )  $\delta$  8.72 (s, 1H, Py), 8.28 (d,  $J = 5.4$  Hz, 1H, Py), 7.21 (d,  $J = 5.3$  Hz, 1H, Py), 7.11 (d,  $J = 8.8$  Hz, 2H, Ar), 6.81 (d,  $J = 8.8$  Hz, 2H, Ar), 5.08 (dd,  $J = 8.4, 4.0$  Hz, 1H,  $\text{CHOH}$ ), 3.88 (s, 1H, OH), 3.77 (s, 3H,  $\text{CH}_3$ ), 2.86 – 2.64 (m, 2H,  $\text{CH}_2$ ), 2.13 – 1.92 (m, 2H,  $\text{CH}_2$ );  $^{13}\text{C}$  NMR (101 MHz,  $\text{CDCl}_3$ )  $\delta$  157.8, 148.9, 148.7, 141.8, 138.3, 133.3, 129.4, 124.3, 113.8, 68.6, 55.3, 39.1, 31.1; IR (neat)  $\nu$  ( $\text{cm}^{-1}$ ) 3148 (OH); TOF MS ES+  $m/z$ : 278.1/280.1  $[\text{M}+\text{H}]^+$ ; HR-MS calc.  $[\text{C}_{15}\text{H}_{17}\text{O}_2\text{NCl}]^{35+}$  278.0942, obs. 278.0950.

Preparative HPLC: Enantiomers were separated on a Phenomenex Cellulose 1 Preparative HPLC column eluting with acetonitrile:water [7:3] at a flow rate of 15 mL/min. The retention times of the enantiomers were 71.4 min and 80.8 min. A total of 380 mg of racemic compound was inject and 134 mg (35%) of the first eluting enantiomer was isolated. The second eluting enantiomer was not isolated.

**3-(Anthracen-9-yl)-1-(4-chloropyridin-3-yl)propan-1-ol (60e)**

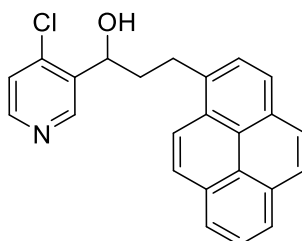


Yellow solid (220 mg, 43%);  $R_f = 0.55$  (EtOAc); Mp: 170-173 °C;  $^1\text{H}$  NMR (300 MHz,  $d_6$ -Acetone)  $\delta$  8.78 (s, 1H, Py), 8.34 – 8.26 (m, 2H, Ar), 8.25 – 8.17 (m, 2H, Ar), 7.92 (dd,  $J =$

7.8, 1.8 Hz, 2H, Ar), 7.46 – 7.29 (m, 4H, Ar), 7.25 (d,  $J$  = 5.3 Hz, 1H, Py), 5.25 (dd,  $J$  = 8.4, 3.3 Hz, 1H, CHOH), 5.01 (s, 1H, OH), 3.81 – 3.62 (m, 2H, CH<sub>2</sub>), 2.23 – 1.90 (m, 2H, CH<sub>2</sub>); <sup>13</sup>C NMR (101 MHz, d<sub>6</sub>-Acetone)  $\delta$  149.4, 149.3, 149.2, 140.7, 138.3, 134.1, 131.8, 129.6, 129.1, 127.3, 127.2, 125.7, 125.7, 124.9, 124.2, 123.9, 123.5, 121.4, 121.3, 68.6, 38.8, 23.9; IR (neat)  $\nu$  (cm<sup>-1</sup>) 3153 (OH); TOF MS ES<sup>+</sup>  $m/z$ : 348.1/350.1 [M+H]<sup>+</sup>; HR-MS calc. [C<sub>22</sub>H<sub>19</sub>ONCl<sup>35</sup>]<sup>+</sup> 348.1150, obs. 348.1151.

Preparative HPLC: Enantiomers were separated on a Phenomenex Cellulose 1 Preparative HPLC column eluting with acetonitrile at a flow rate of 10 mL/min. The retention times of the enantiomers were 18.9 min and 24.1 min. A total of 150 mg of racemic compound was inject and 83 mg (>50%, [ $\alpha$ ]<sub>D</sub><sup>293</sup> -1.3° (c 0.3, CHCl<sub>3</sub>)) of the first eluting enantiomer was isolated. The second eluting enantiomer was not isolated.

#### 1-(4-Chloropyridin-3-yl)-3-(pyren-1-yl)propan-1-ol (60g)

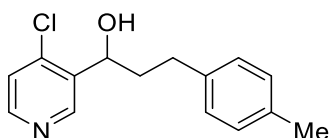


Orange solid (270 mg, 38%);  $R_f$  = 0.25 (hexane/EtOAc = [1:1]); <sup>1</sup>H NMR (400 MHz, CDCl<sub>3</sub>)  $\delta$  8.82 (s, 1H, Py), 8.34 (d,  $J$  = 5.3 Hz, 1H, Py), 8.26 (d,  $J$  = 9.3 Hz, 1H, Ar), 8.15 (d,  $J$  = 7.6 Hz, 2H, Ar), 8.13 – 8.04 (m, 2H, Ar), 8.01 (s, 2H, Ar), 7.97 (dd,  $J$  = 8.0, 7.2 Hz, 1H, Ar), 7.88 (d,  $J$  = 7.8 Hz, 1H, Ar), 7.19 (d,  $J$  = 5.3 Hz, 1H, Py), 5.20 (dd,  $J$  = 8.5, 3.8 Hz, 1H, CHOH), 3.66 – 3.44 (m, 2H, CH<sub>2</sub>), 2.80 (s, 1H, OH), 2.40 – 2.18 (m, 2H, CH<sub>2</sub>); <sup>13</sup>C NMR (101 MHz, CDCl<sub>3</sub>)  $\delta$  149.1, 149.0, 141.7, 137.7, 135.4, 131.4, 130.9, 130.0, 128.7, 127.5, 127.5, 127.2, 126.7, 125.9, 125.1, 125.0, 124.9, 124.8, 124.3, 123.2, 69.2, 39.1, 29.6; IR (neat)  $\nu$  (cm<sup>-1</sup>) 3183

(OH); TOF MS ES+ m/z: 372.1/374.1 [M+H]<sup>+</sup>; HR-MS calc. [C<sub>24</sub>H<sub>19</sub>ONCl<sup>35</sup>]<sup>+</sup> 372.1150, obs. 372.1154. *One quaternary <sup>13</sup>C signal is not visible in the <sup>13</sup>C NMR.*

Preparative HPLC: Enantiomers were separated on a Phenomenex Cellulose 1 Preparative HPLC column eluting with acetonitrile:water [95:5] at a flow rate of 20 mL/min. The retention times of the enantiomers were 9.8 min and 11.3 min. A total of 220 mg of racemic compound was inject and 55 mg (25%, [ $\alpha$ ]<sub>D</sub><sup>293</sup> -89.3° (c 0.43, CHCl<sub>3</sub>)) of the first eluting enantiomer was isolated. The second eluting enantiomer was not isolated.

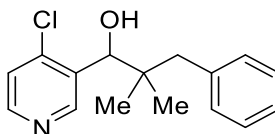
**1-(4-Chloropyridin-3-yl)-3-(p-tolyl)propan-1-ol (60h)**



White solid (192 mg, 20%); Mp: 74-76 °C; <sup>1</sup>H NMR (400 MHz, CDCl<sub>3</sub>) δ 8.69 (s, 1H, Py), 8.21 (d, *J* = 5.3 Hz, 1H, Py), 7.17 (d, *J* = 5.3 Hz, 1H, Py), 7.06 (s, 4H, Ph), 5.07 (dd, *J* = 8.4, 4.0 Hz, 1H, CHOH), 4.62 (s, 1H, OH), 2.87 – 2.75 (m, 1H, CH<sub>2</sub>), 2.76 – 2.64 (m, 1H, CH<sub>2</sub>), 2.29 (s, 3H, CH<sub>3</sub>), 2.15 – 1.91 (m, 2H, CH<sub>2</sub>); <sup>13</sup>C NMR (101 MHz, CDCl<sub>3</sub>) δ 148.9, 148.4, 142.0, 138.7, 138.2, 135.4, 129.1, 128.3, 124.4, 68.5, 39.1, 31.6, 21.1; IR (neat) ν (cm<sup>-1</sup>) 3165 (OH); TOF MS ES+ m/z: 262.2/264.2 [M+H]<sup>+</sup>; HR-MS calc. [C<sub>15</sub>H<sub>17</sub>ONCl<sup>35</sup>]<sup>+</sup> 262.0993, obs. 262.1000.

Preparative HPLC: Enantiomers were separated on a Phenomenex Cellulose 1 Preparative HPLC column eluting with acetonitrile:water [3:2] at a flow rate of 15 mL/min. The retention times of the enantiomers were 37.3 min and 39.2 min. A total of 148 mg of racemic compound was inject and 52 mg (35%) of the first eluting enantiomer was isolated. The second eluting enantiomer was not isolated.

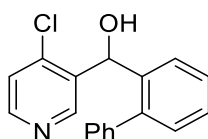
**1-(4-Chloropyridin-3-yl)-2,2-dimethyl-3-phenylpropan-1-ol (82)**



White solid (620 mg, 58%);  $R_f = 0.65$  ( $\text{CH}_2\text{Cl}_2/\text{MeOH} = [9:1]$ ); Mp: 138-140 °C;  $^1\text{H}$  NMR (400 MHz,  $\text{CDCl}_3$ )  $\delta$  8.79 (s, 1H, Py), 8.34 (d,  $J = 5.4$  Hz, 1H, Py), 7.32 – 7.17 (m, 6H, Ph & Py), 5.06 (d,  $J = 3.5$  Hz, 1H,  $\text{CHOH}$ ), 2.84 (d,  $J = 12.8$  Hz, 1H,  $\text{CH}_2$ ), 2.72 (d,  $J = 12.8$  Hz, 1H,  $\text{CH}_2$ ), 2.52 (d,  $J = 3.5$  Hz, 1H, OH), 0.99 (s, 3H,  $\text{CH}_3$ ), 0.80 (s, 3H,  $\text{CH}_3$ );  $^{13}\text{C}$  NMR (101 MHz,  $\text{CDCl}_3$ )  $\delta$  151.5, 148.7, 143.2, 138.2, 135.8, 130.8, 127.9, 126.1, 124.1, 74.1, 44.9, 40.7, 22.8, 21.5; IR (neat)  $\nu$  ( $\text{cm}^{-1}$ ) 3220 (OH); TOF MS ES+  $m/z$ : 276.1/278.1  $[\text{M}+\text{H}]^+$ ; HR-MS calc.  $[\text{C}_{16}\text{H}_{19}\text{ONCl}^{35}]^+$  276.1150, obs. 276.1153.

Preparative HPLC: Enantiomers were separated on a Phenomenex Cellulose 1 Preparative HPLC column eluting with acetonitrile at a flow rate of 10 mL/min. The retention times of the enantiomers were 10.7 min and 13.3 min. A total of 437 mg of racemic compound was injected and 191 mg (44%,  $[\alpha]^{293}_{\text{D}} +28.6^\circ$  (c 0.7,  $\text{CHCl}_3$ )) of the first eluting enantiomer and 163 mg (37%) of the second eluting enantiomer was isolated.

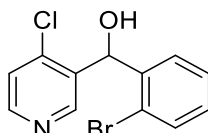
**[1,1'-Biphenyl]-2-yl(4-chloropyridin-3-yl)methanol (87)**



White solid (239 mg, 59%);  $R_f = 0.15$  (hexane/EtOAc = [3:1]); Mp: 149-151 °C;  $^1\text{H}$  NMR (400 MHz,  $\text{CDCl}_3$ )  $\delta$  8.74 (s, 1H, Py), 8.28 (d,  $J = 5.3$  Hz, 1H, Py), 7.43 – 7.24 (m, 9H, Ph), 7.14 (d,  $J = 5.3$  Hz, 1H, Py), 6.12 (s, 1H,  $\text{CHOH}$ ), 3.39 (s, 1H, OH);  $^{13}\text{C}$  NMR (101 MHz,  $\text{CDCl}_3$ )  $\delta$  149.5, 149.1, 142.7, 142.2, 140.6, 138.3, 137.0, 130.4, 129.1, 128.2, 128.1, 127.9, 127.4, 127.2,

124.3, 68.8; IR (neat)  $\nu$  ( $\text{cm}^{-1}$ ) 3077 (OH); TOF MS EI+  $m/z$ : 295.1/297.1  $[\text{M}]^+$ , 277.1/279.1  $[\text{M}-\text{H}_2\text{O}]^+$ ; HR-MS calc.  $[\text{C}_{18}\text{H}_{14}\text{ONCl}^{35}]^+$  295.0758, obs. 295.0767.

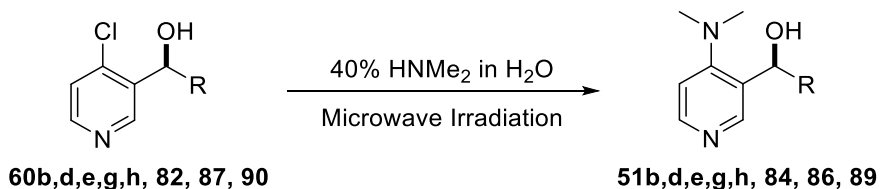
**(2-Bromophenyl)(4-chloropyridin-3-yl)methanol (90)**



Yellow solid (830 mg, 48%);  $R_f$  = 0.44 (EtOAc); Mp: 130-132 °C;  $^1\text{H}$  NMR (400 MHz,  $\text{CDCl}_3$ )  $\delta$  8.51 (s, 1H, Py), 8.40 (d,  $J$  = 5.3 Hz, 1H, Py), 7.57 (dd,  $J$  = 7.9, 1.2 Hz, 1H, Ar), 7.41 (dd,  $J$  = 7.7, 1.9 Hz, 1H, Ar), 7.35 (dd,  $J$  = 7.4, 1.3 Hz, 1H, Ar), 7.32 (d,  $J$  = 5.3 Hz, 1H, Py), 7.20 (ddd,  $J$  = 8.0, 7.3, 1.8 Hz, 1H, Ar), 6.47 (s, 1H,  $\text{CHOH}$ ), 3.51 (s, 1H, OH);  $^{13}\text{C}$  NMR (101 MHz,  $\text{CDCl}_3$ )  $\delta$  149.9, 149.7, 143.6, 140.0, 135.4, 133.1, 129.8, 128.6, 127.8, 124.5, 123.4, 70.7; IR (neat)  $\nu$  ( $\text{cm}^{-1}$ ) 3376 (OH); TOF MS EI+  $m/z$ : 296.9/298.9/300.9  $[\text{M}]^+$ , 218.0/220.0  $[\text{M}-\text{Br}]^+$ ; HR-MS calc.  $[\text{C}_{12}\text{H}_9\text{ONCl}^{35}\text{Br}^{79}]^+$  296.9551, obs. 296.9563.

Preparative HPLC: Enantiomers were separated on a Phenomenex Cellulose 1 Preparative HPLC column eluting with acetonitrile:water [4:1] at a flow rate of 15 mL/min. The retention times of the enantiomers were 6.7 min and 8.1 min. . A total of 468 mg of racemic compound was inject and 162 mg (35%,  $[\alpha]^{293}_{\text{D}} +18.7^\circ$  (c 0.62,  $\text{CHCl}_3$ )) of the first eluting enantiomer was isolated. The second eluting enantiomer was not isolated.

**Synthesis of 51b,d,e,g,h, 84, 86 and 89.**



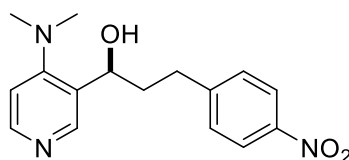
4-Chloropyridine derivative (1.0 equiv.) was added to a stirred solution of  $\text{HNMe}_2$  (40% w/w in  $\text{H}_2\text{O}$ , 2 mL/mmol) in a microwave reaction vessel and heated to the temperature

and time specified (Table 15). The solvent volume was reduced by 75%, basified with saturated aqueous NaHCO<sub>3</sub> (5 mL/mmol) and extracted with CH<sub>2</sub>Cl<sub>2</sub> (3 x 10 mL/mmol). The combined organic extracts were combined, dried over MgSO<sub>4</sub> and evaporated under reduced pressure. The residue was purified by column chromatography (silica, 0-10% MeOH/CH<sub>2</sub>Cl<sub>2</sub>) to give the title compound.

Table 15 - Summary of reagent equivalents and yields for the synthesis of 51b,d,e,g,h, 84, 86 and 89.

Entry	Product	4-Chloropyridine derivative	Scale (mmol)	Temp. (°C)	Time (hrs)	Yield (%)
1	51b	60b	0.06	150	12	≤83
2	51d	60d	0.41	150	12	87
3	51e	60e	0.23	150	8	78
4	51g	60g	0.07	150	12	>99
5	51h	60h	0.21	150	12	90
6	84	82	0.54	150	36	75
7	86	87	0.31	150	12	97
8	89	90	0.40	150	12	70

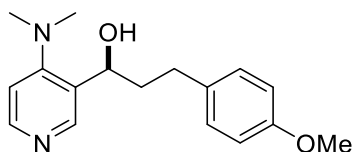
**1-(4-(Dimethylamino)pyridin-3-yl)-3-(4-nitrophenyl)propan-1-ol ((EP)-51b)**



Yellow viscous oil (15 mg, ≤83%<sup>a</sup>); R<sub>f</sub> = 0.61 (CH<sub>2</sub>Cl<sub>2</sub>/MeOH = [9:1]); <sup>1</sup>H NMR (400 MHz, CDCl<sub>3</sub>) δ 8.50 (s, 1H, Py), 8.36 (s, 1H, Py), 8.16 (d, *J* = 8.7 Hz, 2H, Ph), 7.39 (d, *J* = 8.7 Hz, 2H, Ph), 6.92 (d, *J* = 5.5 Hz, 1H, Py), 4.95 (dd, *J* = 9.2, 4.2 Hz, 1H, CHOH), 3.07 – 2.83 (m, 2H, CH<sub>2</sub>), 2.74 (s, 6H, CH<sub>3</sub>), 2.35 – 2.06 (m, 2H, CH<sub>2</sub>); IR (neat) ν (cm<sup>-1</sup>) 3290 (OH); TOF MS ES+ *m/z*: 302.3 [M+H]<sup>+</sup>; HR-MS calc. [C<sub>16</sub>H<sub>20</sub>O<sub>3</sub>N<sub>3</sub>]<sup>+</sup> 302.1499, obs. 302.1513.

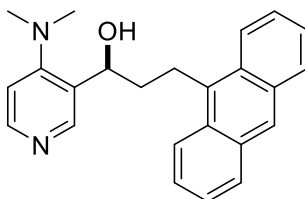
<sup>a</sup> An inseparable decomposition product was observed in the title compound. This was taken through to the next synthetic step. Characterisation is reported omitting this impurity.

**1-(4-(Dimethylamino)pyridin-3-yl)-3-(4-methoxyphenyl)propan-1-ol ((EP)-51d)**



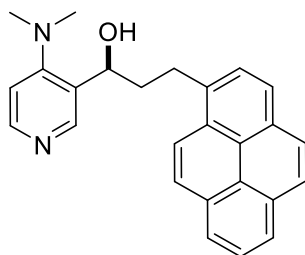
White solid (104 mg, 87%);  $R_f = 0.57$  ( $\text{CH}_2\text{Cl}_2/\text{MeOH} = [4:1]$ ); Mp: 90-93 °C;  $^1\text{H}$  NMR (400 MHz,  $\text{CDCl}_3$ )  $\delta$  8.49 (s, 1H, Py), 8.30 (d,  $J = 5.6$  Hz, 1H, Py), 7.14 (d,  $J = 8.6$  Hz, 2H, Ph), 6.89 – 6.78 (m, 3H, Ph&Py), 4.95 (dd,  $J = 8.9, 4.2$  Hz, 1H,  $\text{CHOH}$ ), 4.33 (s, 1H, OH), 3.79 (s, 3H,  $\text{PhCH}_3$ ), 2.89 – 2.75 (m, 1H,  $\text{CH}_2$ ), 2.72 (s, 6H,  $\text{N}(\text{CH}_3)_2$ ), 2.78 – 2.60 (m, 1H,  $\text{CH}_2$ ), 2.24 – 1.98 (m, 2H,  $\text{CH}_2$ );  $^{13}\text{C}$  NMR (101 MHz,  $\text{CDCl}_3$ )  $\delta$  158.2, 157.8, 149.2, 149.2, 133.7, 132.1, 129.5, 113.8, 113.6, 68.2, 55.3, 44.1, 39.7, 31.5; IR (neat)  $\nu$  ( $\text{cm}^{-1}$ ) 3152 (OH); TOF MS ES+  $m/z$ : 287.2  $[\text{M}+\text{H}]^+$ ; HR-MS calc.  $[\text{C}_{17}\text{H}_{23}\text{O}_2\text{N}_2]^+$  287.1754, obs. 287.1762.

**3-(Anthracen-9-yl)-1-(4-(dimethylamino)pyridin-3-yl)propan-1-ol ((EP)-51e)**



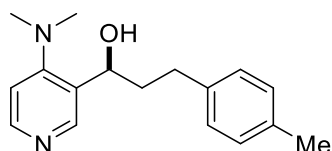
Yellow solid (64 mg, 78%);  $^1\text{H}$  NMR (300 MHz,  $\text{CDCl}_3$ )  $\delta$  8.47 (s, 1H, Py), 8.36 – 8.20 (m, 4H, Ar), 8.03 – 7.87 (m, 2H, Ar), 7.59 – 7.29 (m, 4H, Ar), 6.78 (d,  $J = 5.3$  Hz, 1H, Py), 5.08 (dd,  $J = 8.8, 3.9$  Hz, 1H,  $\text{CHOH}$ ), 3.98 – 3.82 (m, 1H,  $\text{CH}_2$ ), 3.85 – 3.68 (m, 1H,  $\text{CH}_2$ ), 2.58 (s, 6H,  $\text{N}(\text{CH}_3)_2$ ), 2.45 – 2.12 (m, 2H,  $\text{CH}_2$ ).

**1-(4-(Dimethylamino)pyridin-3-yl)-3-(pyren-1-yl)propan-1-ol ((EP)-51g)**



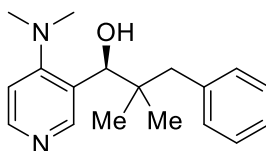
Orange solid (31 mg, 97%);  $R_f = 0.29$  ( $\text{CH}_2\text{Cl}_2/\text{MeOH} = [9:1]$ );  $^1\text{H}$  NMR (300 MHz,  $\text{CDCl}_3$ )  $\delta$  8.54 (s, 1H, Py), 8.32 – 8.21 (m, 2H, Ar), 8.18 – 7.85 (m, 8H, Ar), 6.75 (d,  $J = 5.6$  Hz, 1H, Py), 5.03 (dd,  $J = 8.9, 4.0$  Hz, 1H,  $\text{CHOH}$ ), 3.99 (s, 1H, OH), 3.71 – 3.55 (m, 1H,  $\text{CH}_2$ ), 3.54 – 3.37 (m, 1H,  $\text{CH}_2$ ), 2.55 (s, 6H,  $\text{N}(\text{CH}_3)_2$ ), 2.52 – 2.25 (m, 2H,  $\text{CH}_2$ );  $^{13}\text{C}$  NMR (101 MHz,  $\text{CDCl}_3$ )  $\delta$  162.6, 158.2, 148.9, 148.8, 136.1, 131.9, 131.4, 130.9, 129.9, 128.8, 127.5, 127.3, 126.6, 125.8, 125.1, 125.0, 124.9, 124.8, 124.7, 123.4, 113.4, 68.2, 43.8, 39.6, 30.0; TOF MS ES+  $m/z$ : 381.2  $[\text{M}+\text{H}]^+$ ; HR-MS calc.  $[\text{C}_{26}\text{H}_{25}\text{ON}_2]^+$  381.1961, obs. 381.1968.

**1-(4-(Dimethylamino)pyridin-3-yl)-3-(p-tolyl)propan-1-ol ((EP)-51h)**



White solid (104 mg, 87%);  $R_f = 0.58$  ( $\text{CH}_2\text{Cl}_2/\text{MeOH} = [2:1]$ ); Mp: 117-119 °C;  $^1\text{H}$  NMR (400 MHz,  $\text{CDCl}_3$ )  $\delta$  8.48 (s, 1H, Py), 8.29 (d,  $J = 5.6$  Hz, 1H, Py), 7.15 – 7.05 (m, 4H, Ph), 6.86 (d,  $J = 5.6$  Hz, 1H, Py), 4.96 (dd,  $J = 8.9, 4.3$  Hz, 1H,  $\text{CHOH}$ ), 3.73 (s, 1H, OH), 2.94 – 2.79 (m, 1H,  $\text{CH}_2$ ), 2.72 (s, 6H,  $\text{N}(\text{CH}_3)_2$ ), 2.77 – 2.64 (m, 1H,  $\text{CH}_2$ ), 2.32 (s, 3H,  $\text{PhCH}_3$ ), 2.25 – 2.11 (m, 1H,  $\text{CH}_2$ ), 2.13 – 2.00 (m, 1H,  $\text{CH}_2$ );  $^{13}\text{C}$  NMR (101 MHz,  $\text{CDCl}_3$ )  $\delta$  158.3, 149.2, 149.2, 138.6, 135.3, 132.1, 129.1, 128.4, 113.7, 68.3, 44.1, 39.6, 32.0, 21.0; IR (neat)  $\nu$  ( $\text{cm}^{-1}$ ) 3230 (OH); TOF MS ES+  $m/z$ : 271.3  $[\text{M}+\text{H}]^+$ ; HR-MS calc.  $[\text{C}_{17}\text{H}_{23}\text{ON}_2]^+$  271.1805, obs. 271.1809.

**(S)-1-(4-(Dimethylamino)pyridin-3-yl)-2,2-dimethyl-3-phenylpropan-1-ol ((S)-84)**

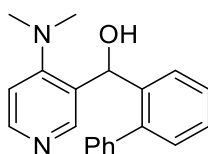


Colourless oil (115 mg, 75%);  $R_f = 0.26$  ( $\text{CH}_2\text{Cl}_2/\text{MeOH} = [9:1]$ );  $^1\text{H}$  NMR (400 MHz,  $\text{CDCl}_3$ )  $\delta$  8.47 (s, 1H, Py), 8.34 (d,  $J = 5.5$  Hz, 1H, Py), 7.33 – 7.16 (m, 5H, Ph), 7.00 (d,  $J = 5.5$  Hz, 1H, Py), 4.85 (s, 1H,  $\text{CHOH}$ ), 2.84 (d,  $J = 12.8$  Hz, 1H,  $\text{CH}_2$ ), 2.65 (s, 6H,  $\text{N}(\text{CH}_3)_2$ ), 2.59 (d,  $J = 12.8$



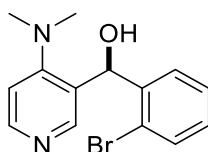
Hz, 1H,  $CH_2$ ), 0.89 (s, 3H,  $CH_3$ ), 0.73 (s, 3H,  $CH_3$ );  $^{13}C$  NMR (101 MHz,  $CDCl_3$ )  $\delta$  160.1, 151.1, 149.1, 138.8, 130.8, 130.5, 127.7, 125.9, 115.3, 75.9, 44.9, 44.8, 40.9, 23.0, 22.0; IR (neat)  $\nu$  ( $cm^{-1}$ ) 3145 (OH); TOF MS ES+  $m/z$ : 285.2  $[M+H]^+$ ; HR-MS calc.  $[C_{18}H_{25}ON_2]^+$  285.1961, obs. 285.1969.

**[1,1'-Biphenyl]-2-yl(4-(dimethylamino)pyridin-3-yl)methanol (86)**



White solid (93 mg, 97%);  $R_f$  = <0.10 (EtOAc); Mp: 223–226 °C;  $^1H$  NMR (400 MHz,  $CDCl_3$ )  $\delta$  8.18 (d,  $J$  = 5.5 Hz, 1H, Py), 7.94 (s, 1H, Py), 7.62 (dd,  $J$  = 7.6, 1.4 Hz, 1H, Ar), 7.36 (td,  $J$  = 7.6, 1.5 Hz, 1H, Ar), 7.29 (td,  $J$  = 7.5, 1.5 Hz, 1H, Ar), 7.24 – 7.12 (m, 4H, Ar), 7.11 – 7.02 (m, 2H, Ar), 6.68 (d,  $J$  = 5.5 Hz, 1H, Py), 6.07 (s, 1H,  $CHOH$ ), 2.54 (s, 6H,  $N(CH_3)_2$ );  $^{13}C$  NMR (101 MHz,  $CDCl_3$ )  $\delta$  157.3, 149.7, 148.4, 140.3, 139.8, 138.6, 130.3, 129.0, 128.0, 126.8, 126.8, 126.5, 126.0, 125.9, 112.2, 67.6, 42.3; IR (neat)  $\nu$  ( $cm^{-1}$ ) 2985 (OH); TOF MS ES+  $m/z$ : 305.2  $[M]^+$ ; HR-MS calc.  $[C_{20}H_{21}ON_2]^+$  305.1648, obs. 305.1657.

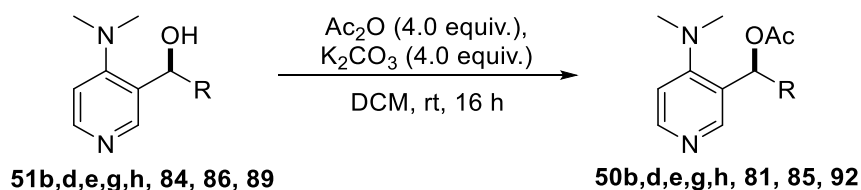
**(2-Bromophenyl)(4-(dimethylamino)pyridin-3-yl)methanol ((EP)-89)**



White solid (86 mg, 70%);  $R_f$  = 0.5 (EtOAc);  $^1H$  NMR (400 MHz,  $CDCl_3$ )  $\delta$  8.36 (d,  $J$  = 5.5 Hz, 1H, Py), 7.92 (s, 1H, Py), 7.65 (dd,  $J$  = 7.7, 1.7 Hz, 1H, Ar), 7.58 (dd,  $J$  = 7.7, 1.3 Hz, 1H, Ar), 7.39 (td,  $J$  = 7.7, 1.3 Hz, 1H, Ar), 7.21 (td,  $J$  = 7.7, 1.7 Hz, 1H, Ar), 6.94 (d,  $J$  = 5.5 Hz, 1H, Py), 6.42 (s, 1H,  $CHOH$ ), 4.62 (s, 1H, OH), 2.91 (s, 6H,  $N(CH_3)_2$ );  $^{13}C$  NMR (101 MHz,  $CDCl_3$ )  $\delta$  158.8, 150.2, 150.0, 140.9, 132.8, 129.5, 129.3, 128.7, 127.8, 123.4, 113.6, 70.9, 43.6; IR

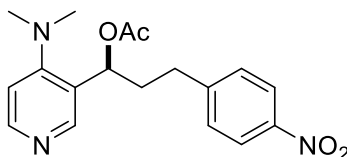
(neat)  $\nu$  ( $\text{cm}^{-1}$ ) 3050 (OH); TOF MS EI+  $m/z$ : 306.0/308.0  $[\text{M}]^+$ , 227.1  $[\text{M}-\text{Br}]^+$ ; HR-MS calc.  $[\text{C}_{14}\text{H}_{15}\text{ON}_2\text{Br}^{79}]^+$  306.0362, obs. 306.0370.

## Synthesis of 50b,d,e,g,h, 81, 85 and 92



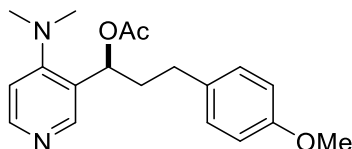
Acetic anhydride (4.0 equiv.) was added to a stirred solution of secondary alcohol (1.0 equiv.) and potassium carbonate (4.0 equiv.) in  $\text{CH}_2\text{Cl}_2$  (0.05 M) at room temperature for 16 hrs. The organic mixture was washed with saturated aqueous  $\text{NaHCO}_3$  (5 mL/mmol), dried over  $\text{MgSO}_4$ , filtered and evaporated to dryness under reduced pressure. The residue was purified by column chromatography (silica, 0-10%  $\text{MeOH}/\text{CH}_2\text{Cl}_2$ ) to give the desired compounds.

### 1-(4-(Dimethylamino)pyridin-3-yl)-3-(4-nitrophenyl)propyl acetate ((+)-50b)



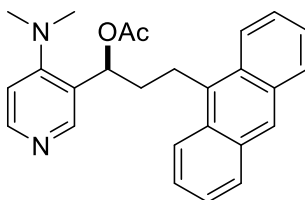
Colourless oil (8 mg, 53%);  $[\alpha]^{293}_{\text{D}} +33.3^\circ$  (c 0.4,  $\text{CHCl}_3$ );  $^1\text{H}$  NMR (400 MHz,  $\text{CDCl}_3$ )  $\delta$  8.49 (s, 1H, Py), 8.35 (d,  $J = 5.5$  Hz, 1H, Py), 8.15 (d,  $J = 8.7$  Hz, 2H, Ar), 7.32 (d,  $J = 8.7$  Hz, 2H, Ar), 6.83 (d,  $J = 5.5$  Hz, 1H, Py), 6.12 (dd,  $J = 8.4, 4.8$  Hz, 1H,  $\text{CHOAc}$ ), 2.88 – 2.76 (m, 1H,  $\text{CH}_2$ ), 2.75 (s, 6H,  $\text{N}(\text{CH}_3)_2$ ), 2.76 – 2.65 (m, 1H,  $\text{CH}_2$ ), 2.35 – 2.21 (m, 1H,  $\text{CH}_2$ ), 2.12 (s, 3H,  $\text{COCH}_3$ ), 2.20 – 2.04 (m, 1H,  $\text{CH}_2$ );  $^{13}\text{C}$  NMR (101 MHz,  $\text{CDCl}_3$ )  $\delta$  170.4, 158.0, 150.0, 148.9, 148.8, 146.5, 143.2, 129.2, 123.7, 113.2, 70.0, 43.7, 36.9, 31.9, 21.2; IR (neat)  $\nu$  ( $\text{cm}^{-1}$ ) 1736 ( $\text{C=O}$ ); TOF MS AP+  $m/z$ : 344.2  $[\text{M}]^+$ ; HR-MS calc.  $[\text{C}_{18}\text{H}_{22}\text{O}_4\text{N}_3]^+$  344.1605, obs. 344.1608.

**1-(4-(Dimethylamino)pyridin-3-yl)-3-(4-methoxyphenyl)propyl acetate ((+)-50d)**



Colourless oil (34 mg, 74%);  $R_f = 0.22$  (EtOAc);  $[\alpha]^{293}_D +21.0^\circ$  (c 1.0,  $\text{CHCl}_3$ );  $^1\text{H}$  NMR (400 MHz,  $\text{CDCl}_3$ )  $\delta$  8.47 (s, 1H, Py), 8.31 (d,  $J = 5.6$  Hz, 1H, Py), 7.07 (d,  $J = 8.6$  Hz, 2H, Ar), 6.82 (d,  $J = 8.6$  Hz, 2H, Ar), 6.78 (d,  $J = 5.6$  Hz, 1H, Py), 6.07 (dd,  $J = 8.9, 4.3$  Hz, 1H,  $\text{CHOAc}$ ), 3.78 (s, 3H,  $\text{OCH}_3$ ), 2.73 (s, 6H,  $\text{N}(\text{CH}_3)_2$ ), 2.76 – 2.63 (m, 1H,  $\text{CH}_2$ ), 2.61 – 2.49 (m, 1H,  $\text{CH}_2$ ), 2.28 – 2.09 (m, 1H,  $\text{CH}_2$ ), 2.10 (s, 3H,  $\text{COCH}_3$ ), 2.09 – 1.95 (m, 1H,  $\text{CH}_2$ );  $^{13}\text{C}$  NMR (101 MHz,  $\text{CDCl}_3$ )  $\delta$  170.5, 157.9, 157.7, 149.6, 148.9, 133.0, 129.3, 128.6, 113.8, 112.8, 70.3, 55.3, 43.5, 37.9, 31.2, 21.2; IR (neat)  $\nu$  ( $\text{cm}^{-1}$ ) 1734 (C=O); TOF MS ES+  $m/z$ : 329.2  $[\text{M}+\text{H}]^+$ ; HR-MS calc.  $[\text{C}_{19}\text{H}_{25}\text{O}_3\text{N}_2]^+$  329.1860, obs. 329.1866.

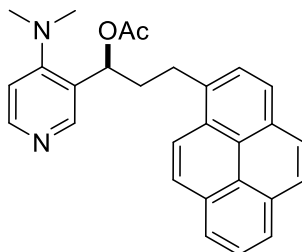
**3-(Anthracen-9-yl)-1-(4-(dimethylamino)pyridin-3-yl)propyl acetate ((+)-50e)**



Orange oil (64 mg, 89%);  $R_f = 0.38$  ( $\text{CH}_2\text{Cl}_2/\text{MeOH}$  [19:1]);  $[\alpha]^{293}_D +45.3^\circ$  (c 0.1,  $\text{CHCl}_3$ );  $^1\text{H}$  NMR (400 MHz,  $\text{CDCl}_3$ )  $\delta$  8.51 (s, 1H, Py), 8.36 – 8.31 (m, 2H, Py & Ar), 8.16 – 8.05 (m, 2H, Ar), 8.03 – 7.93 (m, 2H, Ar), 7.53 – 7.40 (m, 4H, Ar), 6.81 (d,  $J = 5.6$  Hz, 1H, Py), 6.20 (dd,  $J = 8.2, 4.6$  Hz, 1H,  $\text{CHOAc}$ ), 3.76 – 3.54 (m, 2H,  $\text{CH}_2$ ), 2.68 (s, 6H,  $\text{N}(\text{CH}_3)_2$ ), 2.48 – 2.34 (m, 1H,  $\text{CH}_2$ ), 2.34 – 2.16 (m, 1H,  $\text{CH}_2$ ), 2.19 (s, 3H,  $\text{COCH}_3$ );  $^{13}\text{C}$  NMR (101 MHz,  $\text{CDCl}_3$ )  $\delta$  170.5, 157.9, 149.8, 148.6, 133.2, 131.6, 129.5, 129.3, 128.6, 126.0, 125.7, 124.9, 123.9, 113.1,

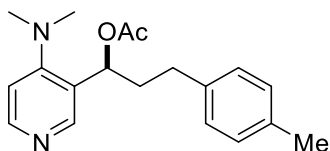
71.3, 43.5, 36.7, 24.0, 21.3; IR (neat)  $\nu$  ( $\text{cm}^{-1}$ ) 1734 (C=O); TOF MS ES+  $m/z$ : 399.2  $[\text{M}+\text{H}]^+$ ; HR-MS calc.  $[\text{C}_{26}\text{H}_{27}\text{O}_2\text{N}_2]^+$  399.2067, obs. 399.2072.

**1-(4-(Dimethylamino)pyridin-3-yl)-3-(pyren-1-yl)propyl acetate ((-)-50g)**



Orange oil (22 mg, 73%);  $R_f$  = 0.49 ( $\text{CH}_2\text{Cl}_2/\text{MeOH}$  [9:1]);  $[\alpha]^{293}_{\text{D}} -50.3^\circ$  (c 0.4,  $\text{CHCl}_3$ );  $^1\text{H}$  NMR (400 MHz,  $\text{CDCl}_3$ )  $\delta$  8.53 (s, 1H, Py), 8.32 (d,  $J$  = 5.6 Hz, 1H, Py), 8.19 – 7.94 (m, 8H, Ar), 7.83 (d,  $J$  = 7.8 Hz, 1H, Ar), 6.75 (d,  $J$  = 5.6 Hz, 1H, Py), 6.18 (dd,  $J$  = 8.6, 4.3 Hz, 1H,  $\text{CHOAc}$ ), 3.56 – 3.44 (m, 1H,  $\text{CH}_2$ ), 3.37 – 3.24 (m, 1H,  $\text{CH}_2$ ), 2.57 (s, 6H,  $\text{N}(\text{CH}_3)_2$ ), 2.60 – 2.40 (m, 1H,  $\text{CH}_2$ ), 2.39 – 2.25 (m, 1H,  $\text{CH}_2$ ), 2.17 (s, 3H,  $\text{COCH}_3$ );  $^{13}\text{C}$  NMR (101 MHz,  $\text{CDCl}_3$ )  $\delta$  170.5, 157.8, 149.7, 148.8, 135.1, 131.4, 130.8, 130.0, 128.6, 128.6, 127.5, 127.4, 127.2, 126.7, 125.9, 125.1, 125.0, 124.9, 124.9, 124.8, 123.0, 113.0, 70.7, 43.4, 37.6, 29.8, 21.3; IR (neat)  $\nu$  ( $\text{cm}^{-1}$ ) 1736 (C=O); TOF MS ES+  $m/z$ : 423.2  $[\text{M}+\text{H}]^+$ ; HR-MS calc.  $[\text{C}_{28}\text{H}_{27}\text{O}_2\text{N}_2]^+$  423.2067, obs. 423.2077.

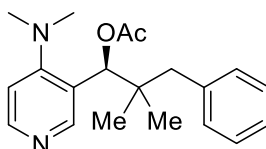
**1-(4-(Dimethylamino)pyridin-3-yl)-3-(p-tolyl)propyl acetate ((+)-50h)**



Colourless oil (26 mg, 75%);  $R_f$  = 0.72 ( $\text{CH}_2\text{Cl}_2/\text{MeOH}$  [4:1]);  $[\alpha]^{293}_{\text{D}} +13.5^\circ$  (c 1.0,  $\text{CHCl}_3$ );  $^1\text{H}$  NMR (400 MHz,  $\text{CDCl}_3$ )  $\delta$  8.47 (s, 1H, Py), 8.31 (d,  $J$  = 5.6 Hz, 1H, Py), 7.06 (d,  $J$  = 9.0 Hz, 4H, Ar), 6.78 (d,  $J$  = 5.6 Hz, 1H, Py), 6.08 (dd,  $J$  = 8.9, 4.3 Hz, 1H,  $\text{CHOAc}$ ), 2.73 (s, 6H,  $\text{N}(\text{CH}_3)_2$ ), 2.77 – 2.65 (m, 1H,  $\text{CH}_2$ ), 2.63 – 2.50 (m, 1H,  $\text{CH}_2$ ), 2.31 (s, 3H,  $\text{PhCH}_3$ ), 2.29 – 2.15 (m, 1H,  $\text{CH}_2$ ), 2.10 (s, 3H,  $\text{COCH}_3$ ), 2.14 – 1.97 (m, 1H,  $\text{CH}_2$ );  $^{13}\text{C}$  NMR (101 MHz,  $\text{CDCl}_3$ )  $\delta$  170.5,

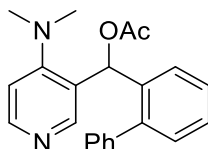
157.7, 149.6, 148.9, 137.8, 135.5, 129.1, 128.6, 128.3, 112.9, 70.4, 43.5, 37.8, 31.7, 21.2, 21.0; IR (neat)  $\nu$  (cm<sup>-1</sup>) 1737 (C=O); TOF MS ES+  $m/z$ : 313.2 [M+H]<sup>+</sup>; HR-MS calc. [C<sub>19</sub>H<sub>25</sub>O<sub>2</sub>N<sub>2</sub>]<sup>+</sup> 313.1911, obs. 313.1917.

**(S)-1-(4-(Dimethylamino)pyridin-3-yl)-2,2-dimethyl-3-phenylpropyl acetate ((S)-81)**



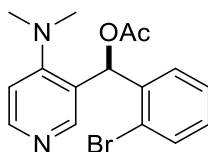
White Solid (123 mg, 99%); Mp: 106-108 °C; [ $\alpha$ ]<sub>D</sub><sup>293</sup> +228.2° (c 0.26, CHCl<sub>3</sub>); <sup>1</sup>H NMR (400 MHz, CDCl<sub>3</sub>)  $\delta$  8.42 (s, 1H, Py), 8.33 (d,  $J$  = 5.6 Hz, 1H, Py), 7.32 – 7.17 (m, 3H, Ph), 7.12 – 7.05 (m, 2H, Ph), 6.85 (d,  $J$  = 5.6 Hz, 1H, Py), 6.03 (s, 1H, CHOAc), 2.76 (s, 6H, N(CH<sub>3</sub>)<sub>2</sub>), 2.64 (s, 2H, CH<sub>2</sub>), 2.17 (s, 3H, COCH<sub>3</sub>), 0.92 (s, 3H, CH<sub>3</sub>), 0.72 (s, 3H, CH<sub>3</sub>); <sup>13</sup>C NMR (101 MHz, CDCl<sub>3</sub>)  $\delta$  170.5, 159.3, 149.4, 149.2, 138.0, 130.8, 127.8, 126.7, 126.1, 113.8, 76.1, 44.8, 43.0, 40.0, 22.3, 22.1, 21.2; IR (neat)  $\nu$  (cm<sup>-1</sup>) 1728 (C=O); TOF MS ES+  $m/z$ : 327.2 [M+H]<sup>+</sup>; HR-MS calc. [C<sub>20</sub>H<sub>27</sub>O<sub>2</sub>N<sub>2</sub>]<sup>+</sup> 327.2067, obs. 327.2074.

**[1,1'-Biphenyl]-2-yl(4-(dimethylamino)pyridin-3-yl)methyl acetate (85)**



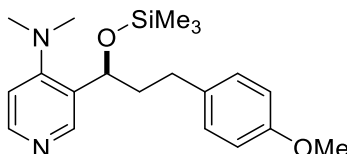
Yellow oil (46 mg, 78%); R<sub>f</sub> = 0.23 (EtOAc); <sup>1</sup>H NMR (400 MHz, CDCl<sub>3</sub>)  $\delta$  8.30 (s, 1H, Py), 8.24 (d,  $J$  = 5.6 Hz, 1H, Py), 7.47 – 7.42 (m, 1H, Ar), 7.39 – 7.29 (m, 5H, Ar), 7.23 – 7.13 (m, 3H, Ar), 6.63 (d,  $J$  = 5.6 Hz, 1H, Py), 6.02 (s, 1H, CHOAc), 2.51 (s, 6H, N(CH<sub>3</sub>)<sub>2</sub>), 2.05 (s, 3H, COCH<sub>3</sub>); <sup>13</sup>C NMR (101 MHz, CDCl<sub>3</sub>)  $\delta$  169.8, 158.3, 151.6, 149.6, 142.0, 140.7, 137.1, 130.4, 128.8, 128.0, 127.9, 127.5, 127.0, 126.5, 126.3, 112.6, 70.2, 43.0, 21.0; IR (neat)  $\nu$  (cm<sup>-1</sup>) 1738 (C=O); TOF MS ES+  $m/z$ : 347.2 [M+H]<sup>+</sup>; HR-MS calc. [C<sub>22</sub>H<sub>23</sub>O<sub>2</sub>N<sub>2</sub>]<sup>+</sup> 347.1754, obs. 347.1757.

**(2-Bromophenyl)(4-(dimethylamino)pyridin-3-yl)methyl acetate ((+)-92)**



Colourless oil (14 mg, 78%);  $[\alpha]^{293}_{\text{D}} +54.7^\circ$  (c 0.4,  $\text{CHCl}_3$ );  $^1\text{H}$  NMR (400 MHz, Tol)  $\delta$  8.71 (s, 1H, Py), 8.38 (s, 1H, Py), 7.60 (s, 1H,  $\text{CHOAc}$ ), 7.24 (dd,  $J = 7.8, 1.2$  Hz, 1H, Ar), 7.17 (dd,  $J = 7.8, 1.6$  Hz, 1H, Ar), 6.79 (td,  $J = 7.8, 1.2$  Hz, 1H, Ar), 6.62 (td,  $J = 7.8, 1.6$  Hz, 1H, Ar), 6.37 (d,  $J = 5.1$  Hz, 1H, Py), 2.39 (s, 6H,  $\text{N}(\text{CH}_3)_2$ ), 1.66 (s, 3H,  $\text{COCH}_3$ );  $^{13}\text{C}$  NMR (101 MHz,  $\text{CDCl}_3$ )  $\delta$  169.7, 158.7, 150.6, 149.4, 138.3, 133.5, 129.9, 128.8, 127.5, 124.4, 114.3, 112.9, 71.8, 43.2, 20.9; IR (neat)  $\nu$  ( $\text{cm}^{-1}$ ) 1742 (C=O); TOF MS AP+  $m/z$ : 349.1/351.1  $[\text{M}]^+$ ; HR-MS calc.  $[\text{C}_{16}\text{H}_{18}\text{O}_2\text{N}_2\text{Br}^{79}]^+$  349.0546, obs. 349.0553.

**3-(3-(4-Methoxyphenyl)-1-((trimethylsilyl)oxy)propyl)-N,N-dimethylpyridin-4-amine ((-)-80)**

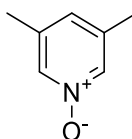


Trimethylsilyl trifluoromethanesulfonate (108  $\mu\text{L}$ , 0.60 mmol, 4.0 equiv.) was added to a solution of **51d** (42 mg, 0.15 mmol, 1.0 equiv.) and triethylamine (84  $\mu\text{L}$ , 0.60 mmol, 4.0 equiv.) in  $\text{CH}_2\text{Cl}_2$  (2 mL) and stirred at room temperature for 16 hours. The reaction mixture was evaporated to dryness under reduced pressure and the residue was purified by column chromatography (silica, 0-10%  $\text{MeOH}/\text{CH}_2\text{Cl}_2$ ) to give the desired compounds as a pale yellow oil (32 mg, 59%);  $[\alpha]^{293}_{\text{D}} -32.4^\circ$  (c 0.3,  $\text{CHCl}_3$ );  $^1\text{H}$  NMR (400 MHz,  $\text{CDCl}_3$ )  $\delta$  8.61 (s, 1H, Py), 8.32 (d,  $J = 5.5$  Hz, 1H, Py), 7.15 (d,  $J = 8.6$  Hz, 2H, Ar), 6.85 (d,  $J = 8.6$  Hz, 2H, Ar), 6.78 (d,  $J = 5.5$  Hz, 1H, Py), 4.96 (dd,  $J = 9.5, 2.8$  Hz, 1H,  $\text{CHOAc}$ ), 3.82 (s, 3H,  $\text{OCH}_3$ ), 2.92 – 2.80 (m, 1H,  $\text{CH}_2$ ), 2.80 – 2.60 (m, 1H,  $\text{CH}_2$ ), 2.67 (s, 6H,  $\text{N}(\text{CH}_3)_2$ ), 2.25 – 2.11 (m, 1H,  $\text{CH}_2$ ), 2.01 – 1.88 (m, 1H,  $\text{CH}_2$ ), 0.00 (s, 9H, TMS);  $^{13}\text{C}$  NMR (101 MHz,  $\text{CDCl}_3$ )  $\delta$  157.7, 156.9,

150.3, 148.9, 133.9, 132.7, 129.5, 113.7, 112.5, 67.6, 55.3, 43.8, 40.5, 31.7, 0.0; IR (neat)  $\nu$  ( $\text{cm}^{-1}$ ) 1592 (C=C); TOF MS ES+  $m/z$ : 359.2  $[\text{M}+\text{H}]^+$ , 287.2  $[\text{M}-\text{TMS}]^+$ ; HR-MS calc.  $[\text{C}_{20}\text{H}_{31}\text{O}_2\text{N}_2\text{Si}]^+$  359.2149, obs. 359.2154.

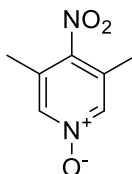
## Synthesis of 3,5-Disubstituted DMAP Derivatives

### 3,5-Dimethylpyridine 1-oxide (**101**)<sup>99</sup>



Peracetic acid (39% w/w in acetic acid, 6 mL, 36 mmol, 1.2 equiv.) was added dropwise at 0 °C to 3,5-lutidine (3.2 g, 30 mmol, 1.2 equiv.) and heated to 85 °C for 2 hrs. The reaction was cooled to 0 °C, neutralised by dropwise addition of aqueous 4M NaOH, extracted with  $\text{CH}_2\text{Cl}_2$  (3 x 100 mL) and the combined organic extracts were dried over  $\text{MgSO}_4$ , filtered and the solvent was removed under reduced pressure to afford a white solid (3.48 g) which was taken forward to the next step without purification.

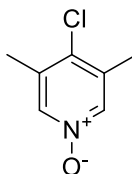
### 3,5-Dimethyl-4-nitropyridine 1-oxide (**102**)<sup>98</sup>



Fuming nitric acid (5.1 mL) was added dropwise to 3,5-dimethylpyridine 1-oxide (**101**, 3.48 g) dissolved in conc. Sulfuric acid (9.6 mL) and heated to 95 °C for 7 hours. The reaction mixture was cooled to room temperature and poured over ice, potassium carbonate was added until pH < 7 and the resulting aqueous mixture was filtered and washed with water. The aqueous filtrate was extracted with  $\text{CH}_2\text{Cl}_2$  (3 x 100 mL) and the combined organic phases were dried over  $\text{MgSO}_4$ , filtered and the solvent was removed under reduced pressure to give a pale yellow solid (3.90 g, 79% over 2 steps); Mp 161-163 °C;  $^1\text{H}$  NMR

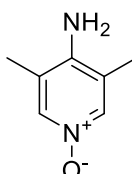
(300 MHz, CDCl<sub>3</sub>)  $\delta$  7.97 (s, 2H, Py), 2.39 (s, 6H, CH<sub>3</sub>); <sup>13</sup>C NMR (101 MHz, CDCl<sub>3</sub>)  $\delta$  139.4, 138.7, 129.4, 15.5; TOF MS EI+ m/z: 168.1 [M]<sup>+</sup>.

#### 4-Chloro-3,5-dimethylpyridine 1-oxide (**103**)<sup>71</sup>



3,5-dimethyl-4-nitropyridine 1-oxide (**102**, 0.5 g, 3.0 mmol, 1.0 equiv.) was dissolved in acetyl chloride (2.5 mL) and heated to 50 °C for 2 hrs. The reaction mixture was poured into aqueous saturated NaHCO<sub>3</sub> (50 mL) and the aqueous mixture was extracted with CH<sub>2</sub>Cl<sub>2</sub> (3 x 50 mL), the organic phases were combined, dried over MgSO<sub>4</sub>, filtered and the solvent was removed under reduced pressure to afford **103** as an off-white solid (223 mg, 48%); Mp 203-204 °C; <sup>1</sup>H NMR (300 MHz, CDCl<sub>3</sub>)  $\delta$  7.98 (s, 2H, Py), 2.32 (s, 6H, CH<sub>3</sub>); <sup>13</sup>C NMR (101 MHz, CDCl<sub>3</sub>)  $\delta$  137.8, 134.6, 133.4, 17.6; TOF MS ES+ m/z: 180.0 [M+Na]<sup>+</sup>.

#### 4-Amino-3,5-dimethylpyridine 1-oxide (**104**)<sup>98</sup>

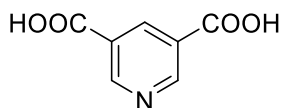


3,5-Dimethyl-4-nitropyridine 1-oxide (**102**, 1.0 g, 6.0 mmol, 1.0 equiv.) was added to a stirred solution of 10% palladium on carbon (0.1g) in ethanol (100 mL) under argon and heated to 90 °C for 1 hour, after which time 55% hydrazine hydrate (3.7 mL, 12.0 mmol, 4.0 equiv.) was added and the reaction was maintained at 90 °C for a further 3 hours. After cooling to room temperature, the reaction mixture was filtered through celite and the filtrate solvent was removed under reduced pressure. The resulting solid was washed with diethyl ether (100 mL) to afford an off-white solid (353 mg, 43%); Mp 230-234 °C; <sup>1</sup>H



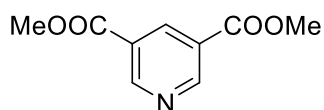
NMR (300 MHz, CDCl<sub>3</sub>)  $\delta$  7.81 (s, 2H, Py), 4.28 (s, 2H, NH<sub>2</sub>), 2.11 (s, 6H, CH<sub>3</sub>); <sup>13</sup>C NMR (101 MHz, CDCl<sub>3</sub>)  $\delta$  143.5, 137.3, 118.5, 14.5; TOF MS ES+ m/z: 161.1 [M+Na]<sup>+</sup>, 139.1 [M+H]<sup>+</sup>.

**Pyridine-3,5-dicarboxylic acid (105)**<sup>100</sup>



3,5-lutidine (8.4 g, 79.0 mmol, 1.0 equiv.) was added to potassium permanganate (26.6 g, 168.0 mmol, 2.1 equiv.) in water (250 mL) at 80 °C and the temperature was raised to 100 °C and maintained for 3 hrs. The reaction temperature was cooled to 80 °C, a further portion of potassium permanganate (26.6 g, 168.0 mmol, 2.1 equiv.) was added and the reaction temperature was raised to 100 °C and maintained for 2 hrs. The reaction mixture was cooled to room temperature, filtered through celite, the filtrate was reduced by 50% and concentrated sulfuric acid was added (95 mL). The resulting precipitate was filtered and washed with diethyl ether (200 mL) to afford a white solid (5.3 g, 44%); Mp >300 °C; <sup>1</sup>H NMR (400 MHz, d<sub>6</sub>-DMSO)  $\delta$  10.37 (s, 2H, OH), 9.26 (d, *J* = 2.1 Hz, 1H, Py), 8.67 (t, *J* = 2.1 Hz, 1H, Py); <sup>13</sup>C NMR (101 MHz, d<sub>6</sub>-DMSO)  $\delta$  165.9, 153.8, 137.9, 127.2; IR (neat)  $\nu$  (cm<sup>-1</sup>) 2870 (OH), 1715 (C=O); TOF MS ES- m/z: 166.2 [M-H]<sup>-</sup>.

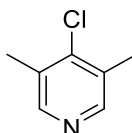
**Dimethyl pyridine-3,5-dicarboxylate (106)**<sup>101</sup>



Dimethylformamide (0.05 mL) was added to pyridine-3,5-dicarboxylic acid (**105**) (1.67 g, 10.0 mmol, 1.0 equiv.) in thionyl chloride (20 mL) and the reaction mixture was heated to reflux for 2 hours, after which time it was cooled to room temperature and the excess reagents were removed under reduced pressure by being azeotroped with toluene. The oily residue was added dropwise to methanol (25 mL) and the reaction mixture was stirred at room temperature for 16 hours. The solvent was removed under reduced pressure, the

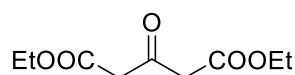
residue was dissolved in CH<sub>2</sub>Cl<sub>2</sub> (100 mL), washed with saturated aqueous NaHCO<sub>3</sub> (2 x 50 mL), dried over MgSO<sub>4</sub>, filtered and the solvent was removed under reduced pressure to give an off-white solid (1.45 g, 74%); Mp 88-90 °C; <sup>1</sup>H NMR (300 MHz, CDCl<sub>3</sub>) δ 9.37 (d, *J* = 2.1 Hz, 2H, Py), 8.87 (t, *J* = 2.1 Hz, 1H, Py), 4.00 (s, 6H, CH<sub>3</sub>); <sup>13</sup>C NMR (101 MHz, CDCl<sub>3</sub>) δ 164.9, 154.2, 138.0, 125.9, 52.7; IR (neat) ν (cm<sup>-1</sup>) 1721 (C=O), 1704 (C=O); TOF MS EI+ *m/z*: 195.1 [M]<sup>+</sup>, 164.1 [M-OMe]<sup>+</sup>.

#### 4-Chloro-3,5-dimethylpyridine (**108**)<sup>102</sup>



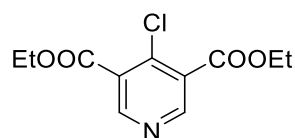
Phosphorous(V) oxychloride (3.7 mL, 40.0 mmol, 4.0 equiv.) was added dropwise to dimethylformamide (55 mL) and stirred at room temperature under argon for 90 mins after which 3-pentanone (**107**, 1.1 mL, 10.0 mmol, 1.0 equiv.) was added dropwise and stirred for 16 hrs. Ammonium acetate (31.0 g, 0.40 mol, 40.0 equiv.) was added, stirred for 90 mins and quenched through the addition of water (200 mL). The reaction mixture was extracted with diethyl ether (3 x 75 mL) and the combined organic extracts were washed with water (2 x 100 mL) followed by brine (2 x 100 mL), dried over MgSO<sub>4</sub>, filtered and the solvent was removed under reduced pressure. The residue was purified by column chromatography (silica, 0-20% EtOAc/Hexane) to afford **108** as a colourless oil (131 mg, 9%); <sup>1</sup>H NMR (300 MHz, CDCl<sub>3</sub>) δ 8.28 (s, 2H, Py), 2.35 (s, 6H, CH<sub>3</sub>); <sup>13</sup>C NMR (101 MHz, CDCl<sub>3</sub>) δ 148.7, 144.2, 131.6, 17.1; TOF MS EI+ *m/z*: 141.0 [M]<sup>+</sup>, 106.1 [M-Cl]<sup>+</sup>; HR-MS calc. [C<sub>7</sub>H<sub>8</sub>NCl<sup>35</sup>]<sup>+</sup> 141.0341, obs. 141.0341.

#### Diethyl 3-oxopentanedioate (**110**)<sup>135</sup>



Citric acid (2.5 g, 13.0 mmol, 1.0 equiv.) was added portionwise to chlorosulfonic acid (3.0 mL, 45.0 mmol, 3.5 equiv.) in CH<sub>2</sub>Cl<sub>2</sub> (3 mL) at 0 °C. The reaction mixture was warmed to room temperature and stirred for 5 hrs, after which it was cooled to 0 °C, ethanol (5 mL) was added dropwise and the reaction mixture was stirred for 2 hours at room temperature. The reaction mixture was quenched through the addition of water (20 mL), extracted with CH<sub>2</sub>Cl<sub>2</sub> (3 x 25 mL) and the combined organic phases were washed with saturated aqueous NaHCO<sub>3</sub> (25 mL), water (25 mL) and brine (25 mL), dried over MgSO<sub>4</sub>, filtered and the solvent was removed under reduced pressure to give **110** as a colourless oil (1.64 g, 63%); <sup>1</sup>H NMR (300 MHz, CDCl<sub>3</sub>) δ 4.21 (q, *J* = 7.2 Hz, 4H, CH<sub>2</sub>CH<sub>3</sub>), 3.61 (s, 4H, CH<sub>2</sub>CO), 1.29 (t, *J* = 7.2 Hz, 6H, CH<sub>3</sub>); <sup>13</sup>C NMR (101 MHz, CDCl<sub>3</sub>) δ 195.5, 166.7, 61.6, 49.0, 14.1; IR (neat) ν (cm<sup>-1</sup>) 1732 (C=O), 1717 (C=O); TOF MS EI+ *m/z*: 202.1 [M]<sup>+</sup>, 157.1 [M-OEt]<sup>+</sup>.

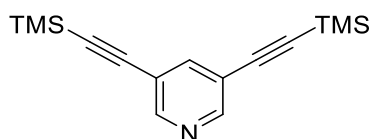
**Diethyl 4-chloropyridine-3,5-dicarboxylate (**111**)**<sup>136</sup>



Phosphorous(V) oxychloride (3.8 mL, 41.0 mmol, 4.1 equiv.) was added dropwise to dimethylformamide (56 mL) and stirred at room temperature under argon for 90 mins, diethyl 3-oxopentanedioate (**110**, 2.0, 9.9 mmol, 1.0 equiv.) was added dropwise and stirred under argon for 16 hrs. Ammonium acetate (31.0 g, 0.4 mol, 40 equiv.) was added, stirred for 90 mins and quenched through the addition of water (200 mL). The reaction mixture was extracted with diethyl ether (3 x 75 mL) and the combined organic extracts were washed with water (2 x 100 mL) followed by brine (2 x 100 mL), dried over MgSO<sub>4</sub>, filtered and the solvent was removed under reduced pressure. The residue was purified by column chromatography (silica, 0-100% EtOAc/Hexane) to afford **111** as an orange oil

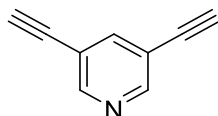
(0.87 g, 32%);  $^1\text{H}$  NMR (300 MHz,  $\text{CDCl}_3$ )  $\delta$  8.60 (s, 2H, Py), 4.43 (q,  $J$  = 7.2 Hz, 4H,  $\text{CH}_2$ ), 1.42 (t,  $J$  = 7.2 Hz, 6H,  $\text{CH}_3$ );  $^{13}\text{C}$  NMR (101 MHz,  $\text{CDCl}_3$ )  $\delta$  163.2, 143.1, 139.2, 116.9, 63.1, 14.1; IR (neat)  $\nu$  ( $\text{cm}^{-1}$ ) 1696 (C=O); TOF MS AP+  $m/z$ : 267.1  $[\text{M}+\text{H}]^+$ ; HR-MS calc.  $[\text{C}_{13}\text{H}_{19}\text{N}_2\text{O}_4]^+$  167.1339, obs. 167.1342.

### 3,5-Bis((trimethylsilyl)ethynyl)pyridine (**113**)<sup>137</sup>



Copper(I) iodide (39 mg, 0.20 mmol, 0.1 equiv.), bis(triphenylphosphine)palladium(II) dichloride (140mg, 0.20 mmol, 0.1 equiv.) and 3,5-dibromopyridine (474 mg, 2.0 mmol, 1.0 equiv.) were dissolved under argon in diisopropylamine (10 mL) and freeze thaw degassed. Trimethylsilylacetylene (1.14 mL, 8.0 mmol, 4.0 equiv.) was added dropwise and the reaction mixture was stirred at 80 °C for 24 hrs. The solvent was removed under reduced pressure and the residue was purified by column chromatography (silica, 0-10% EtOAc/Hexane) to afford **113** as a colourless oil (583 mg, 93%);  $^1\text{H}$  NMR (300 MHz,  $\text{CDCl}_3$ )  $\delta$  8.57 (s, 2H, Py), 7.79 (s, 1H, Py), 0.25 (s, 18H,  $\text{CH}_3$ ); TOF MS EI+  $m/z$ : 271.1  $[\text{M}+\text{H}]^+$ , 256.1  $[\text{M}-\text{Me}]^+$ .

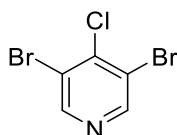
### 3,5-Diethynylpyridine (**114**)<sup>137</sup>



Tetrabutylammonium fluoride in THF (1 M, 8.4 mL, 8.4 mmol, 4.0 equiv.) was added to 3,5-bis((trimethylsilyl)ethynyl)pyridine (**113**, 568 mg, 2.1 mmol, 1.0 equiv.) in THF (10 mL) and stirred at 80 °C for 16 hrs. The reaction mixture was reduced to 1 ml under reduced pressure, diluted with  $\text{CH}_2\text{Cl}_2$  (20 mL), washed with water (20 mL) and brine (20 mL), dried over  $\text{MgSO}_4$ , filtered and the solvent was removed under reduced pressure. The residue

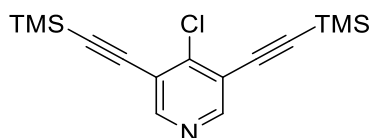
was purified by column chromatography (silica, 0-10% EtOAc/Hexane) to give **114** as a colourless oil (200 mg, 82%);  $^1\text{H}$  NMR (300 MHz,  $\text{CDCl}_3$ )  $\delta$  8.66 (d,  $J$  = 2.0 Hz, 2H, Py), 7.85 (t,  $J$  = 2.0 Hz, 1H, Py), 3.25 (s, 2H, CCH);  $^{13}\text{C}$  NMR (101 MHz,  $\text{CDCl}_3$ )  $\delta$  151.9, 141.9, 119.0, 81.5, 79.4; TOF MS EI+  $m/z$ : 127.1  $[\text{M}]^+$ .

### 3,5-Dibromo-4-chloropyridine (**117**)<sup>37</sup>



Bromine (19 mL, 0.370 mol, 2.0 equiv.) was added dropwise over 30 mins to 4-pyridone (17.5 g, 0.185 mol, 1.0 equiv.) and potassium hydroxide (20.5 g, 0.370 mol, 2.0 equiv.) in water (350 mL) and stirred for 30 mins, the reaction mixture was filtered to give **116** as a pale yellow solid. Phosphorous pentachloride and **116** were heated to 150 °C for 3 hrs, cooled to 0 °C and quenched by the addition of water (100 mL). The resulting mixture was filtered and the solid residue was recrystallised from ethanol to give **117** as a yellow solid (36.6 g, 73%); Mp 100-102 °C;  $^1\text{H}$  NMR (300 MHz,  $\text{CDCl}_3$ )  $\delta$  8.54 (s, 2H, Py);  $^{13}\text{C}$  NMR (101 MHz,  $\text{CDCl}_3$ )  $\delta$  150.9, 144.0, 121.9; TOF MS EI+  $m/z$ : 268.9/270.9/272.9/274.9  $[\text{M}]^+$ .

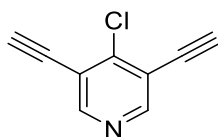
### 4-Chloro-3,5-bis((trimethylsilyl)ethynyl)pyridine (**119**)



Copper(I) iodide (14 mg, 0.07 mmol, 0.1 equiv.), bis(triphenylphosphine)palladium(II) dichloride (52mg, 0.07 mmol, 0.1 equiv.) and **117** (200 mg, 0.74 mmol, 1.0 equiv.) were dissolved under argon in diisopropylamine (10 mL) and freeze thaw degassed. Trimethylsilylacetylene (0.25 mL, 1.76 mmol, 2.4 equiv.) was added dropwise and the reaction mixture was stirred at 80 °C for 72 hrs. The solvent was removed under reduced pressure and the residue was purified by column chromatography (silica, 0-10%

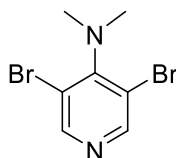
EtOAc/Hexane) to afford **119** as a colourless oil (217 mg, 95%);  $R_f = 0.56$  (Hexane/EtOAc [9:1]);  $^1\text{H}$  NMR (300 MHz,  $\text{CDCl}_3$ )  $\delta$  8.52 (s, 2H, Py), 0.27 (s, 18H,  $\text{CH}_3$ );  $^{13}\text{C}$  NMR (101 MHz,  $\text{CDCl}_3$ )  $\delta$  152.4, 146.9, 120.8, 104.9, 97.9, 0.0; TOF MS EI+  $m/z$ : 305.1/307.1  $[\text{M}]^+$ , 290.1/292.1  $[\text{M-Me}]^+$ .

#### 4-Chloro-3,5-diethynylpyridine (**120**)



Tetrabutylammonium fluoride in THF (1 M, 1.43 mL, 1.43 mmol, 4.0 equiv.) was added to 4-chloro-3,5-bis((trimethylsilyl)ethynyl)pyridine (**119**, 110 mg, 0.36 mmol, 1.0 equiv.) in THF/MeOH (4:2, 6 mL) and stirred at room temperature for 30 mins. The reaction mixture was reduced to 1 ml under reduced pressure, diluted with  $\text{CH}_2\text{Cl}_2$  (20 mL), washed with water (20 mL) and brine (20 mL), dried over  $\text{MgSO}_4$ , filtered and the solvent was removed under reduced pressure. The residue was purified by column chromatography (silica, 0-10% EtOAc/Hexane) to give **120** as a colourless oil (68 mg, >99%);  $R_f = 0.24$  (Hexane/EtOAc [9:1]);  $^1\text{H}$  NMR (300 MHz,  $\text{CDCl}_3$ )  $\delta$  8.62 (s, 2H, Py), 3.54 (s, 2H, CCH);  $^{13}\text{C}$  NMR (101 MHz,  $\text{CDCl}_3$ )  $\delta$  152.9, 147.1, 119.7, 86.1, 76.7; TOF MS EI+  $m/z$ : 161.0/163.0  $[\text{M}]^+$ ; HR-MS calc.  $[\text{C}_9\text{H}_4\text{NCl}^{35}]^+$  161.0027, obs. 161.0027.

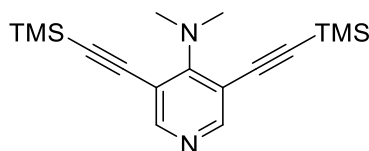
#### 3,5-Dibromo-*N,N*-dimethylpyridin-4-amine (**121**)<sup>138</sup>



3,5-Dibromo-4-chloropyridine (1.5 g, 5.5 mmol, 1.0 equiv.) was added to 40% dimethylamine in water (10 mL) and heated in a microwave reactor for 10 hrs at 140 °C. The solvent was removed under reduced pressure and the solid residue was passed through a  $\text{SiO}_2$  plug (3 cm) with  $\text{CH}_2\text{Cl}_2$  as eluent. The  $\text{CH}_2\text{Cl}_2$  was removed under reduced

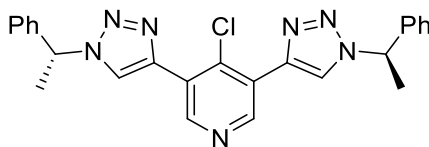
pressure to afford **121** as a white crystalline solid (1.32 g, 85%); Mp 53-55 °C;  $^1\text{H}$  NMR (300 MHz,  $\text{CDCl}_3$ )  $\delta$  8.49 (s, 2H, Py), 3.01 (s, 6H,  $\text{CH}_3$ );  $^{13}\text{C}$  NMR (101 MHz,  $\text{CDCl}_3$ )  $\delta$  155.3, 152.1, 119.7, 42.5; TOF MS ES+  $m/z$ : 277.0/278.9/280.9  $[\text{M}]^+$ .

***N,N*-Dimethyl-3,5-bis((trimethylsilyl)ethynyl)pyridin-4-amine (**122**)**



Copper(I) iodide (19 mg, 0.10 mmol, 0.1 equiv.), bis(triphenylphosphine)palladium(II) dichloride (70 mg, 0.10 mmol, 0.1 equiv.) and **121** (281 mg, 1.00 mmol, 1.0 equiv.) were dissolved under argon in diisopropylamine (5 mL) and freeze thaw degassed. Trimethylsilylacetylene (0.60 mL, 2.40 mmol, 2.4 equiv.) was added dropwise and the reaction mixture was stirred at 80 °C for 16 hrs. The solvent was removed under reduced pressure and the residue was purified by column chromatography (silica, 0-20% EtOAc/Hexane) to afford **122** as a colourless oil (295 mg, 94%);  $^1\text{H}$  NMR (300 MHz,  $\text{CDCl}_3$ )  $\delta$  8.81 (s, 2H, Py), 3.28 (s, 6H,  $\text{N}(\text{CH}_3)_2$ ), 0.24 (s, 18H,  $\text{CH}_3$ );  $^{13}\text{C}$  NMR (101 MHz,  $\text{CDCl}_3$ )  $\delta$  152.4, 146.9, 120.8, 104.9, 97.9, 43.9, -0.1; TOF MS EI+  $m/z$ : 314.2  $[\text{M}]^+$ , 299.2  $[\text{M}-\text{Me}]^+$ , 241.2  $[\text{M}-\text{TMS}]^+$ ; HR-MS calc.  $[\text{C}_{17}\text{H}_{26}\text{N}_2\text{Si}_2]^+$  314.1629, obs. 314.1631.

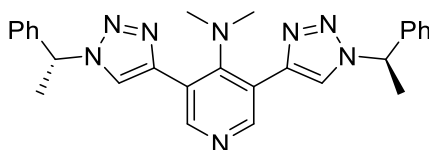
**4-Chloro-3,5-bis(1-((*R*)-1-phenylethyl)-1H-1,2,3-triazol-4-yl)pyridine ((*R,R*)-**124**)**



sodium-L-ascorbate (36 mg, 0.18 mmol, 1.0 equiv.) and  $\text{CuSO}_4 \cdot 5\text{H}_2\text{O}$  (5 mg, 0.018 mmol, 0.1 equiv.) were added to a solution of 4-Chloro-3,5-diethynylpyridine (**120**, 30 mg, 0.18 mmol, 1.0 equiv.) and (*R*)-(1-azidoethyl)benzene (68 mg, 0.46 mmol, 2.5 equiv.) in methanol (5 mL) and stirred for 24 hrs at 50 °C. The reaction mixture was then quenched with the addition of 5% w/v aqueous ammonia solution (10 mL) and extracted with ethyl

acetate (3 x 25 mL). The organic extracts were combined, dried over MgSO<sub>4</sub>, filtered and the solvent was removed under reduced pressure. The residue was purified by column chromatography (silica, 0-100% EtOAc/hexane) to give the desired product as a cream solid (24 mg, 29%); <sup>1</sup>H NMR (400 MHz, CDCl<sub>3</sub>) δ 9.24 (s, 2H, Py), 7.99 (s, 2H, Triazole-*H*), 7.44 – 7.26 (m, 10H, Ph), 5.90 (q, *J* = 7.1 Hz, 2H, CHCH<sub>3</sub>), 2.06 (d, *J* = 7.1 Hz, 6H, CH<sub>3</sub>); <sup>13</sup>C NMR (101 MHz, CDCl<sub>3</sub>) δ 149.7, 141.5, 139.6, 137.6, 129.1, 128.7, 126.5, 126.1, 122.9, 60.6, 21.4; TOF MS ES+ *m/z*: 478.2/480.2 [M+Na]<sup>+</sup>, 456.17 [M+H]<sup>+</sup>; HR-MS calc. [C<sub>25</sub>H<sub>22</sub>N<sub>7</sub>ClNa]<sup>+</sup> 478.1517, obs. 478.1519.

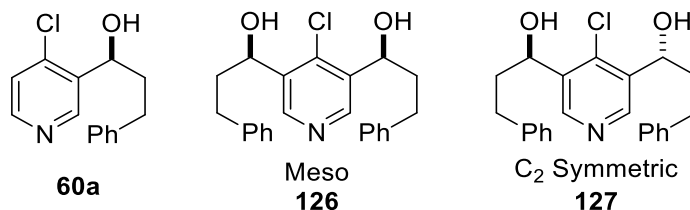
***N,N*-Dimethyl-3,5-bis(1-((*R*)-1-phenylethyl)-1H-1,2,3-triazol-4-yl)pyridin-4-amine ((*R,R*)-125)**



Chloropyridine derivative (***R,R*-124**) (24 mg, 0.052 mmol, 1.0 equiv.) was added to 40% dimethylamine in water (4 mL) and heated in a microwave reactor for 60 hrs at 150 °C. The solvent was removed under reduced pressure and the solid residue was dissolved in CH<sub>2</sub>Cl<sub>2</sub> (10 mL), washed with saturated aqueous NaHCO<sub>3</sub> (2 x 10 mL), dried over MgSO<sub>4</sub>, filtered and the solvent was removed under reduced pressure to afford (***R,R*-125**) as a viscous clear oil (14 mg, 57%); [α]<sub>D</sub><sup>29.3</sup> +29.0° (c 0.4, CHCl<sub>3</sub>); <sup>1</sup>H NMR (400 MHz, CDCl<sub>3</sub>) δ 8.71 (s, 2H, Py), 7.59 (s, 2H, Triazole-*H*), 7.44 – 7.28 (m, 10H, Ph), 5.89 (q, *J* = 7.1 Hz, 2H, CHCH<sub>3</sub>), 2.37 (s, 6H, N(CH<sub>3</sub>)<sub>2</sub>), 2.06 (d, *J* = 7.1 Hz, 6H, CHCH<sub>3</sub>); <sup>13</sup>C NMR (101 MHz, CDCl<sub>3</sub>) δ 154.9, 151.3, 143.8, 139.9, 137.9, 129.1, 128.6, 126.4, 121.4, 60.4, 42.9, 21.4; TOF MS AP+ *m/z*: 465.3 [M+H]<sup>+</sup>; HR-MS calc. [C<sub>27</sub>H<sub>29</sub>N<sub>8</sub>]<sup>+</sup> 465.2514, obs. 465.2510.

**(*Meso*)- 1,1'-(4-chloropyridine-3,5-diyl)bis(3-phenylpropan-1-ol) (126) & (*C*<sub>2</sub>)-1,1'-(4-chloropyridine-3,5-diyl)bis(3-phenylpropan-1-ol) (127)**





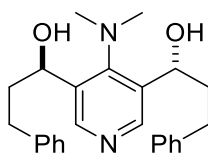
Isopropylmagnesium chloride in THF (1.25M, 4 mL, 5.0 mmol, 1.0 equiv.) was added dropwise to 3,5-dibromo-4-chloropyridine (1.35 g, 5.0 mmol, 1.0 equiv.) in THF (20 mL) at -78 °C under argon and stirred for 2 hrs. Hydrocinnamaldehyde (0.66 mL, 5.0 mmol, 1.0 equiv.) was added and the reaction mixture was warmed to room temperature for 1 hr, then cooled to -78 °C and a second addition of Isopropylmagnesium chloride in THF (1.25M, 6 mL, 7.5 mmol, 1.5 equiv.) was made and stirred for 3 hrs. A second portion of hydrocinnamaldehyde (1.00 mL, 7.5 mmol, 1.0 equiv.) was added and the reaction mixture was warmed to room temperature for 1 hr, quenched through the addition of water (20 mL) and partitioned with CH<sub>2</sub>Cl<sub>2</sub> (50 mL). The phases were separated and the aqueous washed with CH<sub>2</sub>Cl<sub>2</sub> (2 x 20 mL). The combined organic extracts were washed with water (2 x 20 mL) and Brine (2 x 50 mL), dried over MgSO<sub>4</sub>, filtered and the solvent was removed under reduced pressure. The residue was purified by column chromatography (silica, 0-10% MeOH/CH<sub>2</sub>Cl<sub>2</sub>) to give **126** (280 mg, 15%) as a white solid and 900 mg of a mixture of **60a** and **127** as an orange oil. The mixed fractions were purified by column chromatography (silica, 0-5% MeOH/CH<sub>2</sub>Cl<sub>2</sub>) to give **127** (140 mg, 8%) as a white solid and **60a** (400 mg, 32%) as a colourless oil.

**60a**: Colourless oil (400 mg, 32%); <sup>1</sup>H NMR (300 MHz, CDCl<sub>3</sub>) δ 8.70 (s, 1H, Py), 8.25 (d, *J* = 5.3 Hz, 1H, Py), 7.35 – 7.04 (m, 6H, Ph & Py), 5.08 (dd, *J* = 8.2, 4.2 Hz, 1H, CHOH), 4.12 (s, 1H, OH), 2.99 – 2.67 (m, 2H, CH<sub>2</sub>), 2.18 – 1.92 (m, 2H, CH<sub>2</sub>); <sup>13</sup>C NMR (101 MHz, CDCl<sub>3</sub>) δ 148.9, 148.6, 141.9, 141.3, 138.4, 128.5, 128.4, 126.0, 124.4, 68.6, 38.9, 32.0.

**126**: White solid (280 mg, 15%);  $^1\text{H}$  NMR (300 MHz,  $\text{CDCl}_3$ )  $\delta$  7.80 (s, 2H, Py), 7.33 – 6.95 (m, 10H, Ph), 5.75 (s, 2H, OH), 5.09 (t,  $J$  = 6.3 Hz, 2H, CHOH), 2.99 – 2.80 (m, 1H,  $\text{CH}_2$ ), 2.84 – 2.63 (m, 1H,  $\text{CH}_2$ ), 2.10 – 1.94 (m, 2H,  $\text{CH}_2$ ); IR (neat)  $\nu$  ( $\text{cm}^{-1}$ ) 3356 (OH); TOF MS ES+  $m/z$ : 382.2/384.2  $[\text{M}+\text{H}]^+$ ; HR-MS calc.  $[\text{C}_{23}\text{H}_{25}\text{NO}_2\text{Cl}^{35}]^+$  382.1568, obs. 382.1570.

**127**: White solid (140 mg, 8%);  $^1\text{H}$  NMR (300 MHz,  $\text{d}_3\text{-MeOD}$ )  $\delta$  8.63 (s, 2H, Py), 7.31 – 7.11 (m, 10H, Ph), 5.05 (dd,  $J$  = 8.6, 3.7 Hz, 2H, CHOH), 2.90 – 2.69 (m, 4H,  $\text{CH}_2$ ), 2.13 – 1.82 (m, 4H,  $\text{CH}_2$ );  $^{13}\text{C}$  NMR (101 MHz,  $\text{d}_3\text{-MeOD}$ )  $\delta$  146.5, 141.3, 139.5, 138.8, 128.2, 128.0, 125.5, 67.7, 39.1, 31.6; IR (neat)  $\nu$  ( $\text{cm}^{-1}$ ) 3348 (OH); TOF MS ES+  $m/z$ : 382.2/384.2  $[\text{M}+\text{H}]^+$ ; HR-MS calc.  $[\text{C}_{23}\text{H}_{25}\text{NO}_2\text{Cl}^{35}]^+$  382.1568, obs. 382.1571.

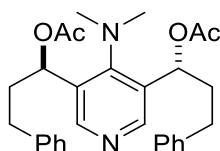
**(C<sub>2</sub>)-1,1'-(4-(Dimethylamino)pyridine-3,5-diyl)bis(3-phenylpropan-1-ol) (128)**



Chloropyridine derivative **127** (40 mg, 0.11 mmol, 1.0 equiv.) was added to 40% dimethylamine in water (3 mL) and heated in a microwave reactor for 40 hrs at 160 °C. The solvent of the resulting reaction mixture was removed under reduced pressure and the oily residue was purified by column chromatography (silica, 0-10% MeOH/ $\text{CH}_2\text{Cl}_2$ ) to afford **128** as a colourless oil (30 mg, 75%);  $R_f$  = 0.17 ( $\text{CH}_2\text{Cl}_2/\text{MeOH}$  [10:1]);  $^1\text{H}$  NMR (400 MHz,  $\text{CDCl}_3$ )  $\delta$  8.42 (s, 2H, Py), 7.33 – 7.24 (m, 4H, Ph), 7.23 – 7.14 (m, 6H, Ph), 4.82 (dd,  $J$  = 9.4, 3.7 Hz, 2H, CHOH), 3.18 (s, 2H, OH), 2.94 – 2.82 (m, 2H,  $\text{CH}_2$ ), 2.80 – 2.67 (m, 2H,  $\text{CH}_2$ ), 2.54 (s, 6H,  $\text{CH}_3$ ), 2.16 – 2.02 (m, 2H,  $\text{CH}_2$ ), 1.97 – 1.83 (m, 2H,  $\text{CH}_2$ );  $^{13}\text{C}$  NMR (101 MHz,  $\text{CDCl}_3$ )  $\delta$  154.6, 149.0, 141.4, 138.5, 128.6, 128.5, 126.0, 68.5, 44.1, 40.7, 32.5; IR (neat)  $\nu$  ( $\text{cm}^{-1}$ ) 3320 (OH); TOF MS ES+  $m/z$ : 391.4  $[\text{M}+\text{H}]^+$ ; HR-MS calc.  $[\text{C}_{25}\text{H}_{31}\text{N}_2\text{O}_2]^+$  391.2380, obs. 391.2387.

Preparative HPLC: Enantiomers were separated on a Phenomenex Cellulose 1 Preparative HPLC column eluting with acetonitrile:water [1:1] at a flow rate of 15 mL/min. The retention times of the enantiomers were 35.0 min and 43.3 min. A total of 30 mg of racemic compound was inject and 10.1 mg (34%) of the first eluting enantiomer was isolated. The second eluting enantiomer was not isolated.

**(C<sub>2</sub>)-(4-(Dimethylamino)pyridine-3,5-diyl)bis(3-phenylpropane-1,1-diyl) diacetate ((+)-**129**)**



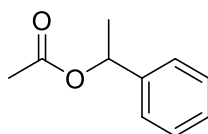
Acetic anhydride (0.1 mL, 1.05 mmol, 40.0 equiv.) was added to a stirred solution of **128** (10.1 mg, 0.026 mmol, 1.0 equiv.) and potassium carbonate (100 mg, 0.724 mmol, 28.0 equiv.) in CH<sub>2</sub>Cl<sub>2</sub> (5 mL) at room temperature for 16 hrs. The reaction mixture was washed with water (10 mL) and saturated aqueous K<sub>2</sub>CO<sub>3</sub> (10 mL), dried over MgSO<sub>4</sub>, filtered and evaporated to dryness under reduced pressure. The residue was purified by column chromatography (silica, 0-10% MeOH/CH<sub>2</sub>Cl<sub>2</sub>) to afford **129** as a colourless oil (5.5 mg, 45% yield); R<sub>f</sub> = 0.55 (CH<sub>2</sub>Cl<sub>2</sub>/MeOH [10:1]); [α]<sup>293</sup><sub>D</sub> +8.5° (c 0.5, CHCl<sub>3</sub>); <sup>1</sup>H NMR (300 MHz, CDCl<sub>3</sub>) δ 8.47 (s, 2H, Py), 7.32 – 7.24 (m, 4H, Ph), 7.24 – 7.11 (m, 6H, Ph), 5.97 (dd, *J* = 9.7, 3.4 Hz, 2H, CHOAc), 2.86 – 2.70 (m, 2H, CH<sub>2</sub>), 2.72 – 2.58 (m, 2H, CH<sub>2</sub>), 2.57 (s, 6H, N(CH<sub>3</sub>)<sub>2</sub>), 2.26 – 2.12 (m, 2H, CH<sub>2</sub>), 2.10 (s, 6H, COCH<sub>3</sub>), 2.00 – 1.84 (m, 2H, CH<sub>2</sub>); <sup>13</sup>C NMR (101 MHz, CDCl<sub>3</sub>) δ 170.4, 154.2, 148.4, 140.8, 135.4, 128.5, 128.5, 126.1, 70.1, 42.9, 38.4, 32.3, 21.1; IR (neat) ν (cm<sup>-1</sup>) 1738 (C=O); TOF MS ES+ *m/z*: 475.3 [M+H]<sup>+</sup>; HR-MS calc. [C<sub>29</sub>H<sub>35</sub>N<sub>2</sub>O<sub>4</sub>]<sup>+</sup> 475.2591, obs. 475.2591.

## Kinetic Resolution of Secondary Alcohols

### *Synthesis of Calibration Standards*

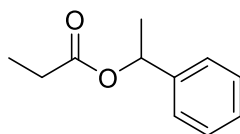
Alcohol (3.3 mmol, 1.0 equiv.) was added to  $\text{NEt}_3$  (7.6 mmol, 0.56 mL, 2.0 equiv.), anhydride (3.9 mmol, 1.2 equiv.) and DMAP (20 mg, 0.16 mmol, 0.05 equiv.) in DCM (5 mL) and stirred for 18 hrs at room temperature. The resulting mixture was washed with 1 M aq. HCl (1 mL), aq. sat.  $\text{NaHCO}_3$  (2 mL) and  $\text{H}_2\text{O}$  (5 mL), dried over  $\text{MgSO}_4$ , filtered through a 1 cm silica plug, washed with ethyl acetate and evaporated under reduced pressure to afford the corresponding esters.

#### **1-Phenylethyl acetate (132)<sup>139</sup>**



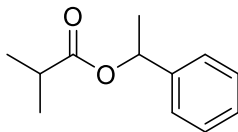
Colourless oil, >99% yield;  $^1\text{H}$  NMR (300 MHz,  $\text{CDCl}_3$ )  $\delta$  7.97 – 7.21 (m, 5H, Ph), 5.88 (q,  $J$  = 6.6 Hz, 1H,  $\text{CHCH}_3$ ), 2.07 (s, 3H,  $\text{COCH}_3$ ), 1.53 (d,  $J$  = 6.6 Hz, 3H,  $\text{CHCH}_3$ );  $^{13}\text{C}$  NMR (101 MHz,  $\text{CDCl}_3$ )  $\delta$  170.3, 141.7, 128.5, 127.9, 126.1, 72.3, 22.2, 21.4; IR (neat)  $\nu$  ( $\text{cm}^{-1}$ ) 1731 ( $\text{C=O}$ ); TOF MS EI+  $m/z$ : 164.2  $[\text{M}]^+$ .

#### **1-Phenylethyl propionate (133)<sup>140</sup>**



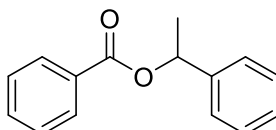
Colourless oil, 91% yield;  $^1\text{H}$  NMR (300 MHz,  $\text{CDCl}_3$ )  $\delta$  7.85 – 6.93 (m, 5H, Ph), 5.81 (q,  $J$  = 6.6 Hz, 1H,  $\text{CHCH}_3$ ), 2.27 (t,  $J$  = 7.6 Hz, 2H,  $\text{CH}_2$ ), 1.45 (d,  $J$  = 6.6 Hz, 3H,  $\text{CHCH}_3$ ), 1.05 (t,  $J$  = 7.6 Hz, 3H,  $\text{CH}_2\text{CH}_3$ );  $^{13}\text{C}$  NMR (101 MHz,  $\text{CDCl}_3$ )  $\delta$  173.7, 141.9, 128.5, 127.8, 126.1, 72.1, 27.9, 22.3, 9.1; IR (neat)  $\nu$  ( $\text{cm}^{-1}$ ) 1734 ( $\text{C=O}$ ); TOF MS EI+  $m/z$ : 178.2  $[\text{M}]^+$ .

**1-Phenylethyl isobutyrate (134)<sup>141</sup>**



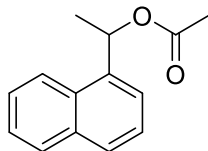
Colourless oil, 90% Yield; <sup>1</sup>H NMR (300 MHz, CDCl<sub>3</sub>) δ 7.59 – 6.83 (m, 5H, Ph), 5.79 (q, *J* = 6.6 Hz, 1H, CHCH<sub>3</sub>), 2.48 (hept, *J* = 7.0 Hz, 1H, CH(CH<sub>3</sub>)<sub>2</sub>), 1.44 (d, *J* = 6.6 Hz, 3H, CHCH<sub>3</sub>), 1.09 (d, *J* = 7.0 Hz, 3H, CH(CH<sub>3</sub>)<sub>2</sub>), 1.07 (d, *J* = 7.0 Hz, 3H, CH(CH<sub>3</sub>)<sub>2</sub>); <sup>13</sup>C NMR (101 MHz, CDCl<sub>3</sub>) δ 176.3, 142.0, 128.5, 127.7, 125.9, 71.9, 34.2, 22.3, 18.9; IR (neat) ν (cm<sup>-1</sup>) 1732 (C=O); TOF MS EI+ *m/z*: 192.3 [M]<sup>+</sup>.

**1-Phenylethyl Benzoate (135)<sup>142</sup>**



Colourless oil, >99% Yield <sup>1</sup>H NMR (300 MHz, CDCl<sub>3</sub>) δ 8.13 – 7.83 (m, 2H, Ph), 7.55 – 6.82 (m, 8H, Ph), 6.01 (q, *J* = 6.6 Hz, 1H, CHCH<sub>3</sub>), 1.53 (d, *J* = 6.6 Hz, 3H, CHCH<sub>3</sub>); <sup>13</sup>C NMR (101 MHz, CDCl<sub>3</sub>) δ 164.7, 140.7, 133.4, 131.8, 128.5, 127.7, 127.2, 126.8, 125.0, 71.8, 21.3; IR (neat) ν (cm<sup>-1</sup>) 1789 (C=C), 1713 (C=O); TOF MS ES+ *m/z*: 249.1 [M+Na]<sup>+</sup>.

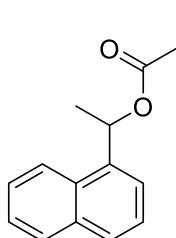
**1-(Naphthalen-1-yl)ethyl acetate (137)<sup>139</sup>**



Colourless oil, 91% Yield; <sup>1</sup>H NMR (300 MHz, CDCl<sub>3</sub>) δ 8.15 (d, *J* = 8.3 Hz, 1H, Ar) 8.0 – 7.77 (m, 2H, Ar), 7.72 – 7.44 (m, 4H, Ar), 6.72 (q, *J* = 6.6 Hz, 1H, CHCH<sub>3</sub>), 2.18 (s, 3H, COCH<sub>3</sub>) 1.77 (d, *J* = 6.6 Hz, 3H, CHCH<sub>3</sub>); <sup>13</sup>C NMR (101 MHz, CDCl<sub>3</sub>) δ 170.4, 137.5, 133.9, 130.3,

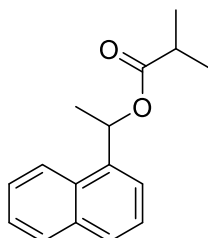
129.0, 128.5, 126.4, 125.7, 125.4, 123.2, 123.2, 69.5, 21.7, 21.4; IR (neat)  $\nu$  ( $\text{cm}^{-1}$ ) 1731 (C=O); TOF MS ES+  $m/z$ : 237.1  $[\text{M}+\text{Na}]^+$ .

**1-(Naphthalen-1-yl)ethyl propionate (138)<sup>16</sup>**



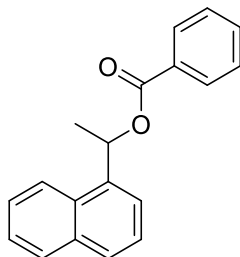
Colourless oil, 79% Yield;  $^1\text{H}$  NMR (300 MHz,  $\text{CDCl}_3$ )  $\delta$  7.97 (d,  $J$  = 8.4 Hz, 1H, Ar) 7.80 – 7.57 (m, 2H, Ar), 7.56 – 7.24 (m, 4H, Ar), 6.55 (q,  $J$  = 6.6 Hz, 1H,  $\text{CHCH}_3$ ), 2.45 – 2.15 (m, 2H,  $\text{CH}_2\text{CH}_3$ ) 1.57 (d,  $J$  = 6.6 Hz, 3H,  $\text{CHCH}_3$ ), 1.03 (t,  $J$  = 7.6 Hz, 3H,  $\text{CH}_2\text{CH}_3$ );  $^{13}\text{C}$  NMR (101 MHz,  $\text{CDCl}_3$ )  $\delta$  173.8, 137.7, 133.9, 130.4, 129.0, 128.5, 126.3, 125.7, 125.4, 123.3, 123.2, 69.3, 28.0, 21.8, 9.2; IR (neat)  $\nu$  ( $\text{cm}^{-1}$ ) 1730 (C=O); TOF MS ES+  $m/z$ : 251.5  $[\text{M}+\text{Na}]^+$ .

**1-(Naphthalen-1-yl)ethyl isobutyrate (139)<sup>143</sup>**



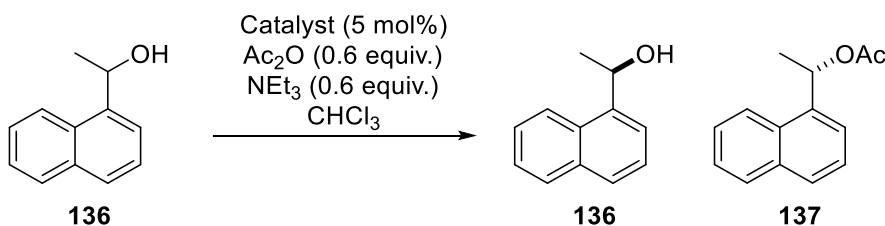
Colourless Oil, 76% Yield;  $^1\text{H}$  NMR (300 MHz,  $\text{CDCl}_3$ )  $\delta$  7.98 (d,  $J$  = 8.2 Hz, 1H, Ar) 7.80 – 7.60 (m, 2H, Ar), 7.57 – 7.15 (m, 4H, Ar), 6.55 (q,  $J$  = 6.6 Hz, 1H,  $\text{CHCH}_3$ ), 2.51 (hept,  $J$  = 7.0 Hz, 1H,  $\text{CH}(\text{CH}_3)_2$ ) 1.59 (d,  $J$  = 6.6 Hz, 3H,  $\text{CHCH}_3$ ), 1.11 (d,  $J$  = 7.0 Hz, 3H,  $\text{CH}(\text{CH}_3)_2$ ), 1.07 (d,  $J$  = 7.0 Hz, 3H,  $\text{CH}(\text{CH}_3)_2$ );  $^{13}\text{C}$  NMR (101 MHz,  $\text{CDCl}_3$ )  $\delta$  176.4, 137.7, 133.9, 130.4, 128.9, 128.4, 126.3, 125.7, 125.4, 123.3, 123.2, 69.2, 34.3, 21.8, 19.0; IR (neat)  $\nu$  ( $\text{cm}^{-1}$ ) 1728 (C=O); TOF MS ES+  $m/z$ : 265.2  $[\text{M}+\text{Na}]^+$ .

### 1-(Naphthalen-1-yl)ethyl benzoate (**140**)<sup>144</sup>



White Solid, 86% Yield; <sup>1</sup>H NMR (300 MHz, CDCl<sub>3</sub>) δ 8.25 - 7.94 (m, 3H, Ar) 7.90 – 7.21 (m, 9H, Ar), 6.81 (q, *J* = 6.6 Hz, 1H, CHCH<sub>3</sub>), 1.76 (d, *J* = 6.6 Hz, 3H, CHCH<sub>3</sub>); <sup>13</sup>C NMR (101 MHz, CDCl<sub>3</sub>) δ 165.9, 137.6, 133.9, 133.0, 130.6, 130.5, 130.3, 129.7, 129.0, 128.5, 128.4, 126.4, 125.7, 125.4, 123.3, 70.3, 22.0; IR (neat) ν (cm<sup>-1</sup>) 1787 (C=C), 1711 (C=O); TOF MS ES+ *m/z*: 299.2 (40) [M+Na]<sup>+</sup>.

### Catalysis Screening Reaction Preparation



Acetic anhydride (5.9 μL, 63 μmol, 0.60 equiv.) was added to a solution of catalyst (5.3 μmol, 0.05 equiv.), triethylamine (8.8 μL, 63 μmol, 0.60 equiv.) and 1-(1-naphthyl)ethanol (18.1 mg, 106 μmol, 1.00 equiv.) in chloroform (1.5 mL) at room temperature and shaken. A 2 μL aliquot was taken every 58 mins and analysed by gas chromatography.

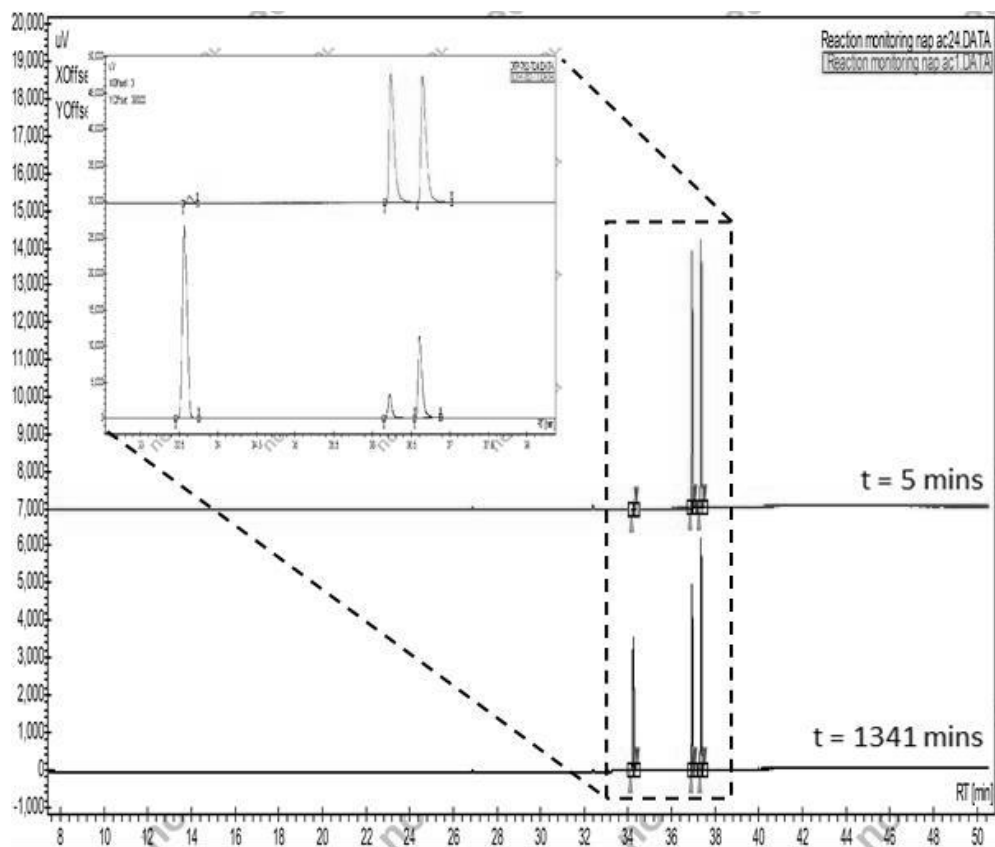


Figure 50 - Representative GC trace for selectivity factor determination for the resolution of 1-(1-naphthyl)ethanol with 50g

## GC Parameters

### Column

Varian WCOT Fused Silica 25M x 0.25 MM Coating CP CHIRASIL-DEX CB DF=0.25

### Injector

Sample penetration depth - 90%

Washes - 9 at 8  $\mu$ L

Draw up speed - 5  $\mu$ L/s

Injector oven temperature - 260  $^{\circ}$ C

Splitter - 500

### Oven

Stabilisation time - 0.5 min

Start temp - 50  $^{\circ}$ C

Ramp rate - 3.7  $^{\circ}$ C/min

Max temp - 200  $^{\circ}$ C

Hold max temp - 10 mins

Run length - 50.54 min

Column flow - 1.0 mL/min

### Detector

Setpoint - 300  $^{\circ}$ C

He flow - 25 mL/min

H2 flow - 30 mL/min



Air flow - 300 mL/min

Acquisition frequency 20.0 Hz

## Gas Chromatography Correction factors and Retention Times

Calibration factors were determined by preparing samples containing known amounts of ester and alcohol. These samples were analysed by chiral GC and their % composition plotted against the observed integration. All best fit lines have  $R^2$  values greater than 0.98.

*Table 16 - GC correction factors and retention times*

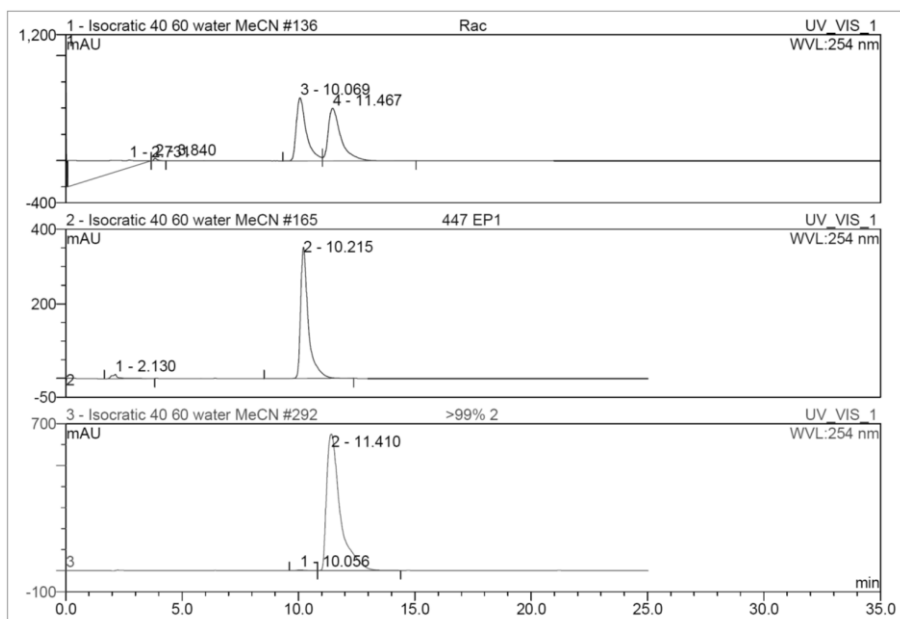
<b>Compound number (OH/Ester)</b>	<b>Alcohol retention time*</b>	<b>Ester retention time*</b>	<b>Alcohol correction factor</b>	<b>Ester correction factor</b>
<b>131/132</b>	$R = 22.4$ min $S = 22.9$ min	$S = 19.3$ min $R = 20.5$ min	$1.0107x+0.222$	$1.0107x-1.2947$
<b>131/133</b>	$R = 22.4$ min $S = 22.9$ min	21.8 min 22.2 min	$1.0073x+3.5874$	$1.0073x-4.3223$
<b>131/134</b>	$R = 22.4$ min $S = 22.9$ min	22.6 min (merged)	$0.9911x+5.8094$	$0.9911x-4.9183$
<b>131/135</b>	$R = 22.4$ min $S = 22.9$ min	36.4 min Merged	$0.9845x+1.4285$	$0.9939x-1.4022$
<b>136/137</b>	36.9 min 37.3 min	34.2 min (merged)	$1.0073x-0.8163$	$1.0073x+0.0865$
<b>136/138</b>	36.9 min 37.3 min	36.4 min (merged) 37.0 min	$1.0152x-1.2022$	$1.0151x-0.3127$
<b>136/139</b>	36.9 min 37.3 min	(merged with alcohol)	n.d.	n.d.
<b>136/140</b>	36.9 min 37.3 min	Not visible	n.d.	n.d.

\*Stereochemistry was determined by synthesis and analysis of commercially available single enantiomer compounds

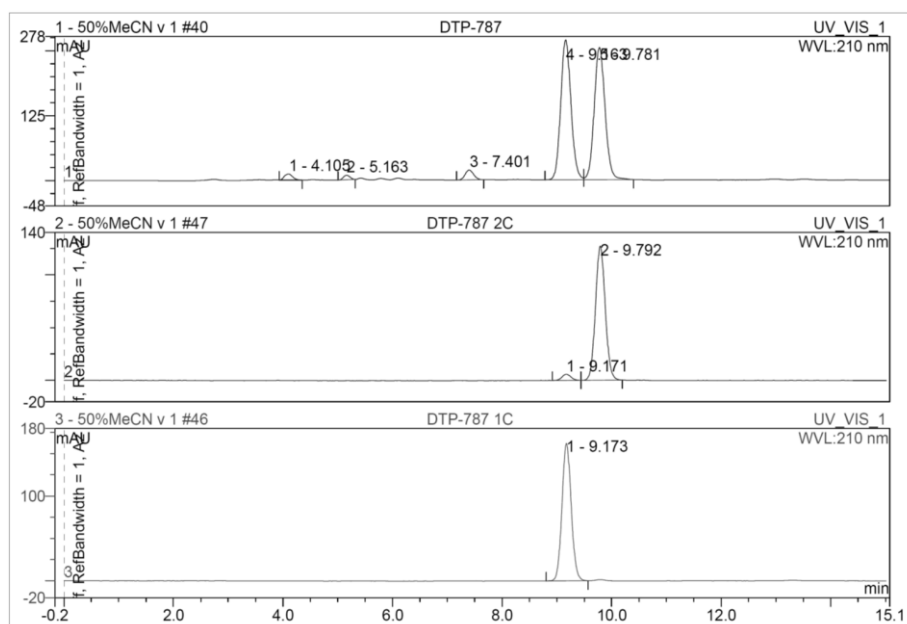
# Appendix

## HPLC Data

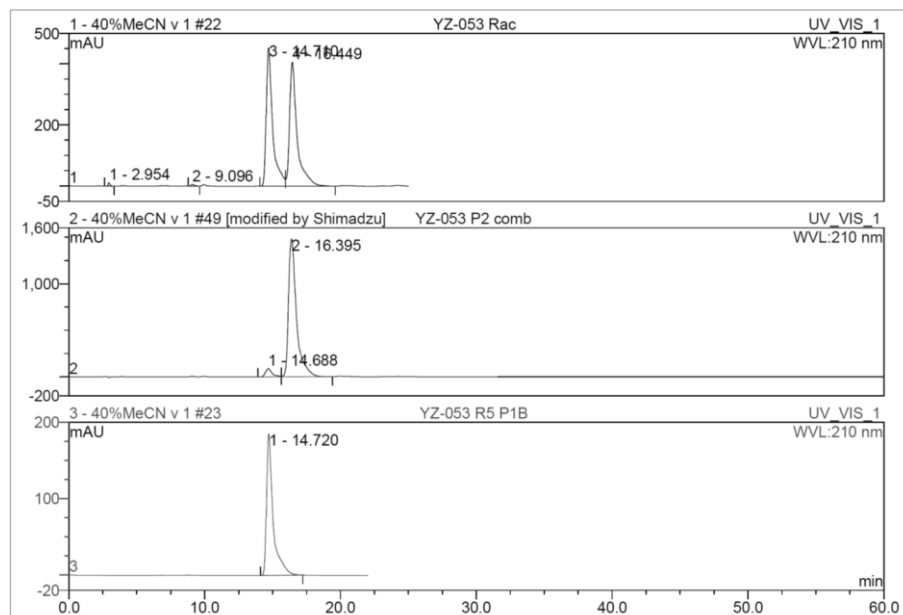
### HPLC separation of *R* and *S* 60a·HCl



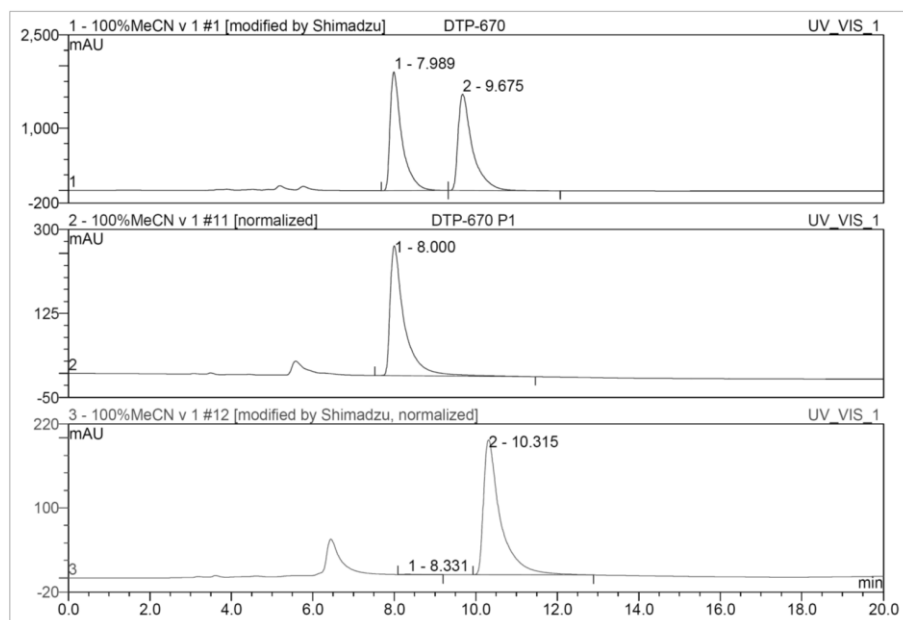
### HPLC separation of *R* and *S* 60b



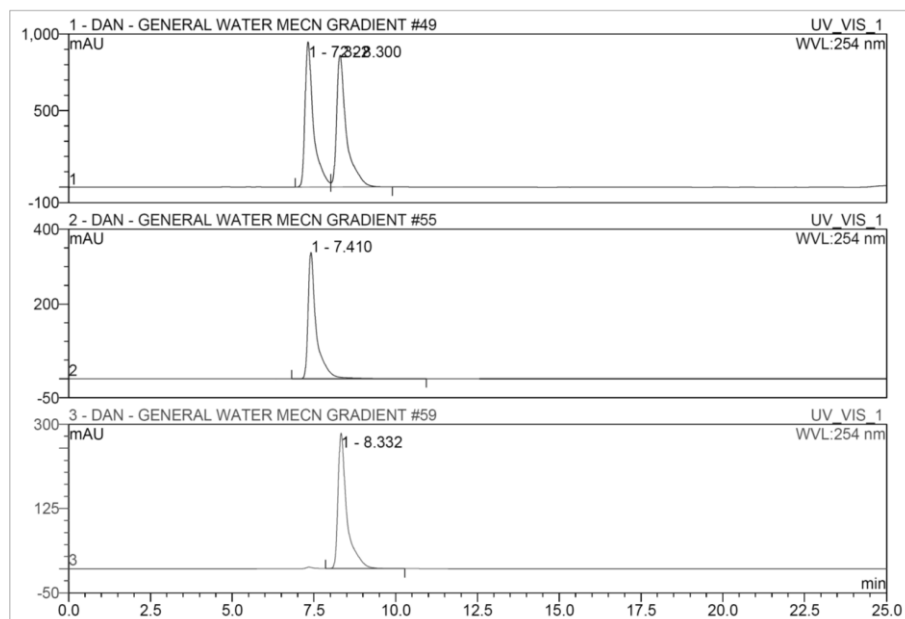
## HPLC separation of *R* and *S* 60d



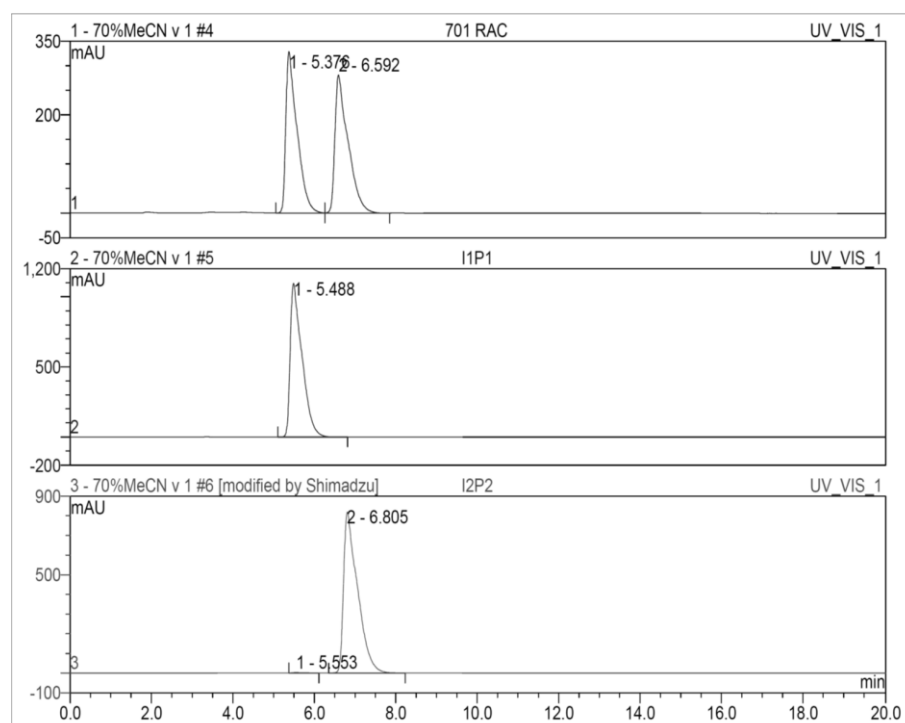
## HPLC separation of *R* and *S* 60e



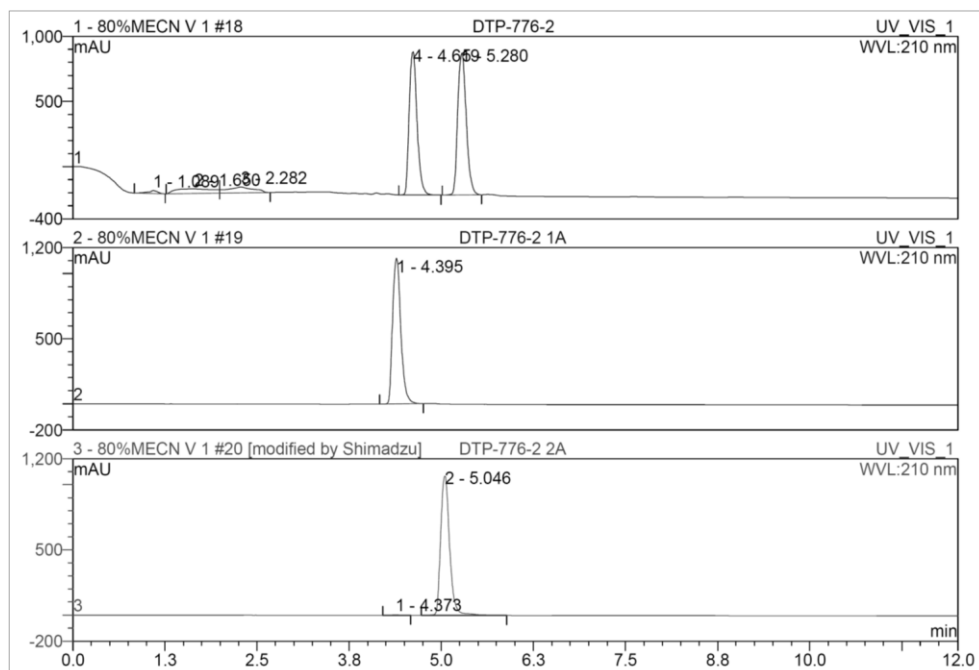
## HPLC separation of *R* and *S* 60g



## HPLC separation of *R* and *S* 82



## HPLC separation of *R* and *S* 90



## X-Ray Structures

### Compound rac-60a

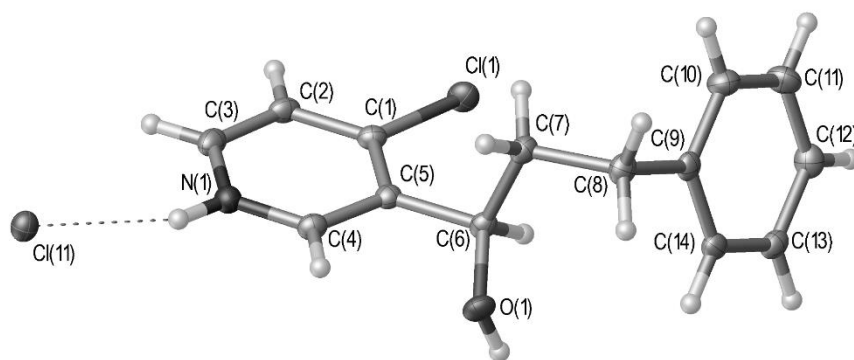


Figure S1 - Crystal structure of rac-60a with ellipsoids drawn at the 50 % probability level.

#### Notes:

The hydrogen atoms bonded to N(1) and O(1) were located in the electron density and the positions and displacement parameters were freely refined. The remaining hydrogen atoms were added at calculated positions and refined by use of a riding model with the isotropic displacement parameters based on the equivalent isotropic displacement parameter (Ueq) of the parent atom. Hydrogen bonding is details in Table 7, Page 8.

**Table 1. Crystal data and structure refinement for rac-60a.**

Identification code DTP-341\_HCl\_Salt

Empirical formula	C <sub>14</sub> H <sub>15</sub> ClNO, Cl
Formula weight	284.17
Temperature	100.00(10) K
Wavelength	1.5418 Å
Crystal system	Orthorhombic
Space group	P bca
Unit cell dimensions	a = 7.66720(10) Å $\alpha$ = 90°. b = 12.7084(3) Å $\beta$ = 90°. c = 28.6450(7) Å $\gamma$ = 90°.
Volume	2791.11(10) Å <sup>3</sup>
Z	8
Density (calculated)	1.353 Mg/m <sup>3</sup>
Absorption coefficient	4.077 mm <sup>-1</sup>
F(000)	1184
Crystal size	0.28 x 0.17 x 0.02 mm <sup>3</sup>
Theta range for data collection	6.55 to 70.07°.
Index ranges	-8 ≤ h ≤ 9, -7 ≤ k ≤ 15, -25 ≤ l ≤ 34
Reflections collected	6629
Independent reflections	2637 [R(int) = 0.0282]
Completeness to theta = 70.07°	99.4 %
Absorption correction	Semi-empirical from equivalents
Max. and min. transmission	1.00000 and 0.78586
Refinement method	Full-matrix least-squares on F <sup>2</sup>
Data / restraints / parameters	2637 / 0 / 171
Goodness-of-fit on F <sup>2</sup>	1.088
Final R indices [I > 2σ(I)]	R1 = 0.0358, wR2 = 0.0916
R indices (all data)	R1 = 0.0414, wR2 = 0.0958
Largest diff. peak and hole	0.331 and -0.303 e.Å <sup>-3</sup>

**Table 2. Atomic coordinates (  $\times 10^4$ ) and equivalent isotropic displacement parameters ( $\text{\AA}^2 \times 10^3$ ) for *rac*-60a U(eq) is defined as one third of the trace of the orthogonalized  $U^{ij}$  tensor.**

	x	y	z	U(eq)
C(1)	1914(3)	8256(2)	822(1)	16(1)
C(2)	719(3)	7605(2)	603(1)	19(1)
C(3)	1317(3)	6722(2)	379(1)	21(1)
C(4)	4213(3)	7137(2)	582(1)	18(1)
C(5)	3697(3)	8036(2)	817(1)	16(1)
C(6)	5050(3)	8700(2)	1069(1)	17(1)
C(7)	5109(3)	8373(2)	1585(1)	19(1)
C(8)	6334(3)	9060(2)	1877(1)	20(1)
C(9)	5713(3)	10182(2)	1920(1)	17(1)
C(10)	4464(3)	10462(2)	2253(1)	24(1)
C(11)	3875(3)	11492(2)	2289(1)	26(1)
C(12)	4525(3)	12259(2)	1991(1)	22(1)
C(13)	5761(3)	11991(2)	1656(1)	20(1)
C(14)	6339(3)	10960(2)	1622(1)	19(1)
N(1)	3036(2)	6516(2)	374(1)	19(1)
O(1)	6728(2)	8541(1)	871(1)	20(1)
Cl(1)	1166(1)	9364(1)	1107(1)	21(1)
Cl(11)	2648(1)	4566(1)	-246(1)	19(1)

**Table 3. Bond lengths [ $\text{\AA}$ ] and angles [ $^\circ$ ] for *rac*-60a..**

C(1)-C(2)	1.385(3)
C(1)-C(5)	1.395(3)
C(1)-Cl(1)	1.727(2)
C(2)-C(3)	1.373(3)

C(2)-H(2)	0.9500
C(3)-N(1)	1.343(3)
C(3)-H(3)	0.9500
C(4)-N(1)	1.339(3)
C(4)-C(5)	1.384(3)
C(4)-H(4)	0.9500
C(5)-C(6)	1.519(3)
C(6)-O(1)	1.422(2)
C(6)-C(7)	1.536(3)
C(6)-H(6)	1.0000
C(7)-C(8)	1.530(3)
C(7)-H(7A)	0.9900
C(7)-H(7B)	0.9900
C(8)-C(9)	1.508(3)
C(8)-H(8A)	0.9900
C(8)-H(8B)	0.9900
C(9)-C(14)	1.391(3)
C(9)-C(10)	1.397(3)
C(10)-C(11)	1.389(3)
C(10)-H(10)	0.9500
C(11)-C(12)	1.388(3)
C(11)-H(11)	0.9500
C(12)-C(13)	1.390(3)
C(12)-H(12)	0.9500
C(13)-C(14)	1.387(3)
C(13)-H(13)	0.9500
C(14)-H(14)	0.9500
N(1)-H(1)	0.91(3)
O(1)-H(1A)	0.86(3)
C(2)-C(1)-C(5)	121.6(2)
C(2)-C(1)-Cl(1)	118.80(16)
C(5)-C(1)-Cl(1)	119.58(16)

C(3)-C(2)-C(1)	118.6(2)
C(3)-C(2)-H(2)	120.7
C(1)-C(2)-H(2)	120.7
N(1)-C(3)-C(2)	119.5(2)
N(1)-C(3)-H(3)	120.3
C(2)-C(3)-H(3)	120.3
N(1)-C(4)-C(5)	120.69(19)
N(1)-C(4)-H(4)	119.7
C(5)-C(4)-H(4)	119.7
C(4)-C(5)-C(1)	116.77(19)
C(4)-C(5)-C(6)	119.61(18)
C(1)-C(5)-C(6)	123.57(19)
O(1)-C(6)-C(5)	110.43(17)
O(1)-C(6)-C(7)	108.63(17)
C(5)-C(6)-C(7)	109.09(17)
O(1)-C(6)-H(6)	109.6
C(5)-C(6)-H(6)	109.6
C(7)-C(6)-H(6)	109.6
C(8)-C(7)-C(6)	112.91(17)
C(8)-C(7)-H(7A)	109.0
C(6)-C(7)-H(7A)	109.0
C(8)-C(7)-H(7B)	109.0
C(6)-C(7)-H(7B)	109.0
H(7A)-C(7)-H(7B)	107.8
C(9)-C(8)-C(7)	112.99(18)
C(9)-C(8)-H(8A)	109.0
C(7)-C(8)-H(8A)	109.0
C(9)-C(8)-H(8B)	109.0
C(7)-C(8)-H(8B)	109.0
H(8A)-C(8)-H(8B)	107.8
C(14)-C(9)-C(10)	118.3(2)
C(14)-C(9)-C(8)	120.86(19)

C(10)-C(9)-C(8)	120.86(19)
C(11)-C(10)-C(9)	120.9(2)
C(11)-C(10)-H(10)	119.5
C(9)-C(10)-H(10)	119.5
C(12)-C(11)-C(10)	120.0(2)
C(12)-C(11)-H(11)	120.0
C(10)-C(11)-H(11)	120.0
C(11)-C(12)-C(13)	119.7(2)
C(11)-C(12)-H(12)	120.1
C(13)-C(12)-H(12)	120.1
C(14)-C(13)-C(12)	119.9(2)
C(14)-C(13)-H(13)	120.1
C(12)-C(13)-H(13)	120.1
C(13)-C(14)-C(9)	121.2(2)
C(13)-C(14)-H(14)	119.4
C(9)-C(14)-H(14)	119.4
C(4)-N(1)-C(3)	122.8(2)
C(4)-N(1)-H(1)	119.7(19)
C(3)-N(1)-H(1)	117.4(19)
C(6)-O(1)-H(1A)	107(2)

---

Symmetry transformations used to generate equivalent atoms:

**Table 4.** Anisotropic displacement parameters ( $\text{\AA}^2 \times 10^3$ ) for *rac*-60a. The anisotropic displacement factor exponent takes the form:  $-2\pi^2 [h^2 a^{*2} U^{11} + \dots + 2 h k a^* b^* U^{12}]$

---

	$U^{11}$	$U^{22}$	$U^{33}$	$U^{23}$	$U^{13}$	$U^{12}$
12						



C(1)	14(1) 1(1)	18(1)	17(1)	3(1)	1(1)
C(2) 2(1)	13(1)	26(1)	18(1)	3(1)	0(1) -
C(3) 6(1)	20(1)	25(1)	17(1)	2(1)	-2(1) -
C(4)	14(1) 1(1)	20(1)	19(1)	2(1)	0(1)
C(5) 1(1)	16(1)	16(1)	15(1)	2(1)	0(1) -
C(6)	12(1) 1(1)	17(1)	22(1)	-1(1)	1(1)
C(7) 2(1)	17(1)	19(1)	21(1)	0(1)	-1(1) -
C(8) 1(1)	16(1)	20(1)	23(1)	-1(1)	-4(1) -
C(9) 2(1)	13(1)	19(1)	19(1)	-3(1)	-4(1) -
C(10) 3(1)	22(1)	25(1)	24(1)	2(1)	5(1) -
C(11)	22(1) 2(1)	31(1)	25(1)	-3(1)	8(1)
C(12)	22(1) 4(1)	20(1)	26(1)	-2(1)	-3(1)
C(13) 5(1)	18(1)	21(1)	20(1)	2(1)	-4(1) -
C(14) 4(1)	14(1)	24(1)	18(1)	-3(1)	-1(1) -
N(1) 1(1)	20(1)	19(1)	19(1)	-1(1)	1(1) -

O(1) 1(1)	13(1)	22(1)	26(1)	2(1)	3(1) -
Cl(1)	16(1) 4(1)	20(1)	27(1)	-1(1)	2(1)
Cl(11)	16(1) 1(1)	18(1)	23(1)	-2(1)	-2(1)

Table 5. Hydrogen coordinates (x 10<sup>4</sup>) and isotropic displacement parameters (Å<sup>2</sup>x 10<sup>3</sup>) for DTP-341\_HCl\_Salt.

	x	y	z	U(eq)
H(2)	-491	7767	608	23
H(3)	523	6259	228	25
H(4)	5415	6958	568	21
H(6)	4726	9460	1045	20
H(7A)	3918	8416	1717	23
H(7B)	5497	7631	1606	23
H(8A)	6442	8752	2193	24
H(8B)	7506	9056	1732	24
H(10)	4012	9940	2457	29
H(11)	3027	11671	2517	31
H(12)	4127	12965	2015	27
H(13)	6210	12513	1451	23
H(14)	7177	10781	1391	22
H(1)	3390(40)	5920(20)	223(11)	41(8)
H(1A)	6970(40)	9090(30)	707(12)	49(10)

Table 6. Torsion angles [°] *rac*-60a.

C(5)-C(1)-C(2)-C(3)	0.3(3)
Cl(1)-C(1)-C(2)-C(3)	-179.63(16)
C(1)-C(2)-C(3)-N(1)	-0.5(3)
N(1)-C(4)-C(5)-C(1)	-0.3(3)
N(1)-C(4)-C(5)-C(6)	177.27(19)
C(2)-C(1)-C(5)-C(4)	0.2(3)
Cl(1)-C(1)-C(5)-C(4)	-179.94(15)
C(2)-C(1)-C(5)-C(6)	-177.33(19)
Cl(1)-C(1)-C(5)-C(6)	2.6(3)
C(4)-C(5)-C(6)-O(1)	24.1(3)
C(1)-C(5)-C(6)-O(1)	-158.46(19)
C(4)-C(5)-C(6)-C(7)	-95.2(2)
C(1)-C(5)-C(6)-C(7)	82.2(2)
O(1)-C(6)-C(7)-C(8)	64.2(2)
C(5)-C(6)-C(7)-C(8)	-175.39(17)
C(6)-C(7)-C(8)-C(9)	66.5(2)
C(7)-C(8)-C(9)-C(14)	-95.9(2)
C(7)-C(8)-C(9)-C(10)	82.5(3)
C(14)-C(9)-C(10)-C(11)	-0.6(3)
C(8)-C(9)-C(10)-C(11)	-179.1(2)
C(9)-C(10)-C(11)-C(12)	0.1(4)
C(10)-C(11)-C(12)-C(13)	0.2(3)
C(11)-C(12)-C(13)-C(14)	-0.1(3)
C(12)-C(13)-C(14)-C(9)	-0.5(3)
C(10)-C(9)-C(14)-C(13)	0.8(3)
C(8)-C(9)-C(14)-C(13)	179.33(19)
C(5)-C(4)-N(1)-C(3)	0.1(3)
C(2)-C(3)-N(1)-C(4)	0.4(3)

Symmetry transformations used to generate equivalent atoms:

**Table 7. Hydrogen bonds for *rac*-60a. [Å and °].**

D-H...A H)	d(D- d(H...A)	d(D...A)	<(DHA)
N(1)- H(1)...Cl(11) 47(3)	0.91(3)	2.26(3)	3.0622(19) 1
O(1)- H(1A)...Cl(11)#1 76(3)	0.86(3)	2.22(3)	3.0805(17) 1

Symmetry transformations used to generate equivalent atoms:  
#1 x+1/2,-y+3/2,-z

## Compound (S)-60a

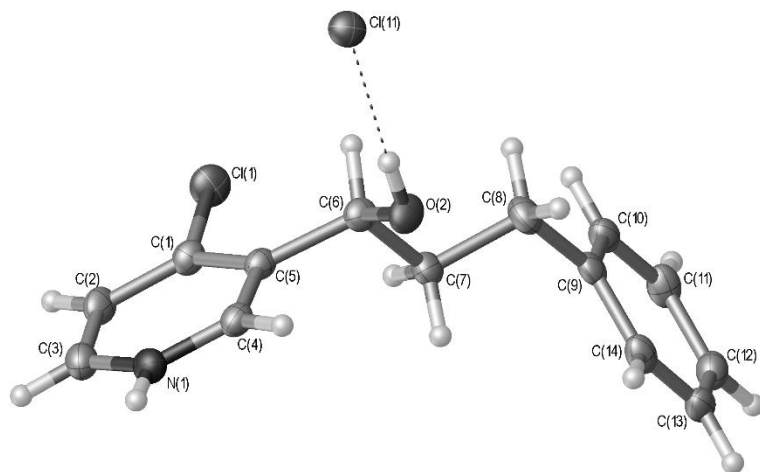


*Figure S2 - X-Ray crystal structure of 60a with ellipsoids drawn at the 50 % probability level. Hydrogen bonding is shown using a dotted line. The absolute structure has been determined, with C(6) being S*

### Notes:

The structure is a polymorph of **rac-60a**, with the same atomic connectivity but different crystal structure. This structure (**(S)-60a**) is chiral. The absolute structure has been determined, with C(6) being S

The hydrogen atoms bonded to O(1) and N(1) were located in the electron density and freely refined while the remaining hydrogen atoms were fixed as riding models.

Hydrogen bonding is detailed in Table 6 below. Other tables in the report give bond lengths, angles and torsion angles with standard deviations given in brackets.

**Table 1 Crystal data and structure refinement for (S)-60a.**

Identification code	DTP-441-SM
Empirical formula	C <sub>14</sub> H <sub>15</sub> NOCl <sub>2</sub>
Formula weight	284.17
Temperature/K	99.9(3)
Crystal system	monoclinic
Space group	P2 <sub>1</sub>
a/Å	5.49156(14)
b/Å	7.73189(16)
c/Å	16.8293(4)
α/°	90
β/°	90.422(3)
γ/°	90
Volume/Å <sup>3</sup>	714.56(3)
Z	2
ρ <sub>calc</sub> /mg/mm <sup>3</sup>	1.321
m/mm <sup>-1</sup>	3.982
F(000)	296.0
Crystal size/mm <sup>3</sup>	0.2204 × 0.1355 × 0.0192
Radiation	CuKα (λ = 1.54184)
2θ range for data collection	10.514 to 151.182°
Index ranges	-6 ≤ h ≤ 5, -9 ≤ k ≤ 9, -21 ≤ l ≤ 21
Reflections collected	13455
Independent reflections	2894 [R <sub>int</sub> = 0.0463, R <sub>sigma</sub> = 0.0311]
Data/restraints/parameters	2894/1/171

Goodness-of-fit on  $F^2$  1.048  
 Final R indexes [ $I \geq 2\sigma(I)$ ]  $R_1 = 0.0321$ ,  $wR_2 = 0.0802$   
 Final R indexes [all data]  $R_1 = 0.0339$ ,  $wR_2 = 0.0815$   
 Largest diff. peak/hole /  $e \text{ \AA}^{-3}$  0.51/-0.26  
 Flack parameter -0.006(9)

**Table 2 Fractional Atomic Coordinates ( $\times 10^4$ ) and Equivalent Isotropic Displacement Parameters ( $\text{\AA}^2 \times 10^3$ ) for (S)-60a.  $U_{eq}$  is defined as 1/3 of the trace of the orthogonalised  $U_{ij}$  tensor.**

Atom	x	y	z	$U_{eq}$
C1	1986(6)	3686(4)	1725.3(17)	22.4(6)
C2	598(7)	2430(4)	1356(2)	26.8(7)
C3	-1285(6)	2957(5)	863.1(19)	28.9(7)
C4	-363(6)	5881(4)	1114.9(19)	23.7(6)
C5	1528(6)	5456(4)	1620.3(18)	20.8(6)
C6	2962(6)	6878(4)	2035.7(18)	22.6(6)
C7	2263(6)	7010(4)	2908.3(19)	24.0(6)
C8	3850(6)	8315(4)	3360.6(19)	29.3(7)
C9	3164(6)	8451(4)	4223.9(19)	22.8(6)
C10	4589(6)	7677(4)	4814(2)	26.2(7)
C11	3926(6)	7770(4)	5605(2)	29.0(7)
C12	1831(7)	8632(4)	5826(2)	29.1(7)
C13	389(6)	9406(4)	5243(2)	28.2(7)
C14	1062(6)	9312(4)	4456.2(19)	26.5(6)
Cl1	4391.7(15)	3033.6(9)	2319.6(5)	30.7(2)
N1	-1692(6)	4647(4)	757.8(17)	25.2(6)
O2	2501(5)	8496(3)	1675.4(14)	26.8(5)
Cl11	6079.0(14)	9078.4(9)	330.7(4)	25.83(18)

**Table 3 Anisotropic Displacement Parameters ( $\text{\AA}^2 \times 10^3$ ) for (S)-60a. The Anisotropic displacement factor exponent takes the form: -  $2\pi^2[h^2a^{*2}U_{11}+2hka^*b^*U_{12}+\dots]$ .**

Atom	$U_{11}$	$U_{22}$	$U_{33}$	$U_{23}$	$U_{13}$	$U_{12}$
C1	25.8(15)	19.5(14)	21.9(13)	1.6(11)	0.9(12)	3.5(12)
C2	32.6(19)	15.2(13)	32.6(17)	0.3(12)	6.4(14)	-0.8(13)
C3	30.6(17)	24.8(15)	31.2(16)	-5.5(14)	4.4(13)	-3.4(15)
C4	26.1(17)	20.1(14)	24.8(15)	-0.9(11)	5.1(12)	1.7(12)
C5	21.7(15)	17.4(14)	23.3(14)	0.8(11)	3.1(12)	1.7(12)
C6	24.3(16)	17.6(13)	26.0(15)	1.8(11)	1.9(12)	0.7(12)
C7	24.5(16)	19.4(14)	28.0(15)	-1.5(12)	1.3(12)	-3.3(12)
C8	30.7(18)	26.0(16)	31.2(16)	-2.1(13)	0.6(13)	-9.4(14)
C9	22.5(16)	15.3(13)	30.7(15)	-1.9(11)	-1.9(12)	-5.2(11)
C10	21.0(15)	20.8(15)	36.7(17)	-6.1(12)	-3.8(12)	1.4(12)
C11	32.7(17)	21.2(15)	33.0(16)	-0.3(12)	-9.9(13)	3.3(14)
C12	33.0(18)	24.8(15)	29.4(15)	-5.4(12)	3.2(14)	-3.8(13)
C13	22.0(16)	21.7(16)	40.9(17)	-10.2(13)	-0.5(13)	2.3(12)
C14	26.6(16)	18.1(14)	34.8(16)	-2.2(12)	-8.0(13)	1.2(13)
Cl1	33.8(4)	23.5(4)	34.8(4)	6.1(3)	-3.4(3)	6.5(3)
N1	24.6(15)	27.9(14)	23.1(13)	-2.9(11)	-1.2(11)	-0.1(12)
O2	35.5(14)	15.7(10)	29.2(11)	3.6(8)	5.6(10)	1.8(9)
Cl11	26.3(4)	22.6(3)	28.6(4)	4.3(3)	0.1(3)	0.7(3)

**Table 4 Bond Lengths for (S)-60a.**

Atom	Atom	Length/ $\text{\AA}$	Atom	Atom	Length/ $\text{\AA}$
------	------	----------------------	------	------	----------------------

C1	C2	1.379(5)	C6	O2	1.412(4)
C1	C5	1.402(4)	C7	C8	1.532(4)
C1	Cl1	1.727(3)	C8	C9	1.507(4)
C2	C3	1.383(5)	C9	C10	1.394(5)
C3	N1	1.337(5)	C9	C14	1.391(5)
C4	C5	1.377(5)	C10	C11	1.385(5)
C4	N1	1.341(5)	C11	C12	1.383(5)
C5	C6	1.519(4)	C12	C13	1.391(5)
C6	C7	1.524(4)	C13	C14	1.378(5)

**Table 5 Bond Angles for (S)-60a.**

Atom	Atom	Atom	Angle/°	Atom	Atom	Atom	Angle/°
C2	C1	C5	122.2(3)	C6	C7	C8	112.1(3)
C2	C1	Cl1	118.2(2)	C9	C8	C7	112.3(3)
C5	C1	Cl1	119.6(3)	C10	C9	C8	120.9(3)
C1	C2	C3	118.1(3)	C14	C9	C8	121.2(3)
N1	C3	C2	119.4(3)	C14	C9	C10	117.9(3)
N1	C4	C5	120.8(3)	C11	C10	C9	120.8(3)
C1	C5	C6	123.8(3)	C12	C11	C10	120.6(3)
C4	C5	C1	116.4(3)	C11	C12	C13	119.2(3)
C4	C5	C6	119.8(3)	C14	C13	C12	120.0(3)
C5	C6	C7	111.0(2)	C13	C14	C9	121.6(3)
O2	C6	C5	110.6(3)	C3	N1	C4	123.1(3)
O2	C6	C7	108.0(3)				

**Table 6 Hydrogen Bonds for (S)-60a.**

D	H	A	d(D-H)/Å	d(H-A)/Å	d(D-A)/Å	D-H-A/°
N1	H1	Cl11 <sup>1</sup>	0.81(5)	2.32(5)	3.047(3)	151(5)
O2	H2A	Cl11	0.84(6)	2.20(6)	3.041(3)	178(6)

<sup>1</sup>-X, -1/2+Y, -Z

**Table 7 Torsion Angles for (S)-60a.**

A	B	C	D	Angle/°	A	B	C	D	Angle/°
C1	C2	C3	N1	0.3(5)	C8	C9	C10	C11	-178.5(3)
C1	C5	C6	C7	-74.4(4)	C8	C9	C14	C13	178.3(3)
C1	C5	C6	O2	165.8(3)	C9	C10	C11	C12	0.0(5)
C2	C1	C5	C4	-1.2(5)	C10	C9	C14	C13	0.0(5)
C2	C1	C5	C6	178.0(3)	C10	C11	C12	C13	0.1(5)
C2	C3	N1	C4	-0.5(5)	C11	C12	C13	C14	-0.3(5)
C4	C5	C6	C7	104.8(3)	C12	C13	C14	C9	0.2(5)
C4	C5	C6	O2	-15.1(4)	C14	C9	C10	C11	-0.1(5)
C5	C1	C2	C3	0.6(5)	Cl1	C1	C2	C3	-178.2(2)
C5	C4	N1	C3	-0.1(5)	Cl1	C1	C5	C4	177.6(2)
C5	C6	C7	C8	174.6(3)	Cl1	C1	C5	C6	-3.2(4)
C6	C7	C8	C9	180.0(3)	N1	C4	C5	C1	0.9(5)
C7	C8	C9	C10	103.9(4)	N1	C4	C5	C6	-178.3(3)
C7	C8	C9	C14	-74.5(4)	O2	C6	C7	C8	-64.0(3)

**Table 8 Hydrogen Atom Coordinates ( $\text{\AA} \times 10^4$ ) and Isotropic Displacement Parameters ( $\text{\AA}^2 \times 10^3$ ) for (S)-60a.**

Atom	x	y	z	U(eq)
H2	927	1237	1439	32
H3	-2281	2126	601	35
H4	-730	7063	1018	28
H6	4740	6613	1999	27
H7A	2432	5858	3160	29
H7B	535	7363	2946	29
H8A	5577	7961	3323	35
H8B	3682	9465	3108	35
H10	6033	7080	4671	31
H11	4918	7236	5999	35
H12	1381	8696	6369	35
H13	-1058	9998	5386	34
H14	67	9848	4063	32
H1	-2830(90)	4890(70)	470(30)	40(13)
H2A	3500(110)	8630(80)	1300(30)	68(18)

### Experimental

Single crystals of  $\text{C}_{14}\text{H}_{15}\text{NOCl}_2$  (**(S)-60a**) were crystallised from acetonitrile.

A suitable crystal was selected on a **SuperNova, Dual, Cu at zero, Atlas** diffractometer. The crystal was kept at 99.9(3) K during data collection. Using Olex2 [1], the structure was solved with the ShelXS [2] structure solution program using Direct Methods and refined with the ShelXL [3] refinement package using Least Squares minimisation.

1. Dolomanov, O.V., Bourhis, L.J., Gildea, R.J., Howard, J.A.K. & Puschmann, H. (2009), J. Appl. Cryst. 42, 339-341.
2. Sheldrick, G.M. (2008). Acta Cryst. A64, 112-122.

3. Sheldrick, G.M. (2008). Acta Cryst. A64, 112-122.

### Crystal structure determination of (S)-60a

**Crystal Data** for  $\text{C}_{14}\text{H}_{15}\text{NOCl}_2$  ( $M = 284.17$ ): monoclinic, space group  $P2_1$  (no. 4),  $a = 5.49156(14) \text{ \AA}$ ,  $b = 7.73189(16) \text{ \AA}$ ,  $c = 16.8293(4) \text{ \AA}$ ,  $\beta = 90.422(3)^\circ$ ,  $V = 714.56(3) \text{ \AA}^3$ ,  $Z = 2$ ,  $T = 99.9(3) \text{ K}$ ,  $\mu(\text{CuK}\alpha) = 3.982 \text{ mm}^{-1}$ ,  $D_{\text{calc}} = 1.321 \text{ g/mm}^3$ , 13455 reflections measured ( $10.514 \leq 2\theta \leq 151.182$ ), 2894 unique ( $R_{\text{int}} = 0.0463$ ,  $R_{\text{sigma}} = 0.0311$ ) which were used in all calculations. The final  $R_1$  was 0.0321 ( $I > 2\sigma(I)$ ) and  $wR_2$  was 0.0815 (all data).

### Refinement model description

Number of restraints - 1, number of constraints - unknown.

Details:

1. Fixed Uiso

At 1.2 times of:

All C(H) groups, All C(H,H) groups

2.a Ternary CH refined with riding coordinates:

C6(H6)

2.b Secondary CH2 refined with riding coordinates:

C7(H7A,H7B), C8(H8A,H8B)

2.c Aromatic/amide H refined with riding coordinates:

C2(H2), C3(H3), C4(H4), C10(H10), C11(H11), C12(H12), C13(H13), C14(H14)

## Compound (S)-51a

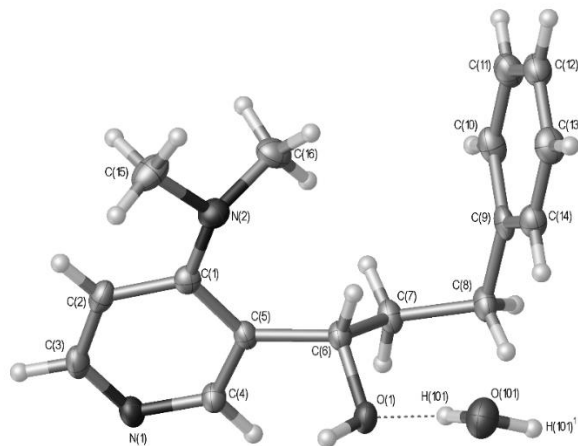


*Figure S3 - Crystal structure of (S)-51a with ellipsoids drawn at the 50 % probability level. Hydrogen bonding is shown using a dotted line. The water molecule lies on a 2-fold rotation axis. Symmetry codes used generate equivalent atoms: \$1: 1-x, y, 1-z.*

### Notes:

The structure contains half a molecule of water per molecule, with the water molecule, H(101)-O(101)-H(101) lying on a 2-fold rotation axis such that only one of the hydrogen atoms is crystallographically unique.

The Flack parameter is -0.02 (11). The standard deviation on this value is too large for the absolute structure to have been determined from the diffraction data (no heavy atoms present). However, in reference to DTP-441-SM it can be stated that C(6) in DTP-441 is S.

The hydrogen atoms bonded to O(1) and O(101) were located in the electron density while the remaining hydrogen atoms were fixed as riding models.

Hydrogen bonding is detailed in Table 6 of the DTP-441\_Tables.html report. Other tables in the report give bond lengths, angles and torsion angles with standard deviations given in brackets.

**Table 1 Crystal data and structure refinement for (S)-51a.**

Identification code	DTP-441
Empirical formula	C <sub>16</sub> H <sub>21</sub> N <sub>2</sub> O <sub>1.5</sub>
Formula weight	265.35
Temperature/K	99.98(11)
Crystal system	monoclinic
Space group	I2
a/Å	18.9063(4)
b/Å	5.67337(14)
c/Å	14.0166(3)
α/°	90
β/°	107.626(2)
γ/°	90
Volume/Å <sup>3</sup>	1432.87(5)
Z	4
ρ <sub>calc</sub> /mg/mm <sup>3</sup>	1.230
m/mm <sup>-1</sup>	0.629
F(000)	572.0
Crystal size/mm <sup>3</sup>	0.2663 × 0.1329 × 0.0982
Radiation	CuKα (λ = 1.54184)
2θ range for data collection	6.942 to 148.6°
Index ranges	-23 ≤ h ≤ 23, -7 ≤ k ≤ 6, -17 ≤ l ≤ 17
Reflections collected	13290
Independent reflections	2781 [R <sub>int</sub> = 0.0281, R <sub>sigma</sub> = 0.0205]
Data/restraints/parameters	2781/2/186

Goodness-of-fit on  $F^2$  1.059  
 Final R indexes [ $I \geq 2\sigma(I)$ ]  $R_1 = 0.0348$ ,  $wR_2 = 0.0879$   
 Final R indexes [all data]  $R_1 = 0.0364$ ,  $wR_2 = 0.0893$   
 Largest diff. peak/hole /  $e \text{ \AA}^{-3}$  0.13/-0.28  
 Flack parameter -0.02(11)

**Table 2 Fractional Atomic Coordinates ( $\times 10^4$ ) and Equivalent Isotropic Displacement Parameters ( $\text{\AA}^2 \times 10^3$ ) for (S)-51a.  $U_{eq}$  is defined as 1/3 of the trace of the orthogonalised  $U_{ij}$  tensor.**

Atom	x	y	z	$U_{eq}$
C1	3169.1(11)	3867(4)	1038.9(14)	20.7(4)
C2	2424.5(12)	3984(4)	431.6(15)	25.4(5)
C3	1901.7(11)	2490(5)	608.8(15)	25.4(5)
C4	2761.5(11)	838(4)	1943.1(15)	22.0(4)
C5	3332.2(10)	2276(4)	1849.9(14)	20.0(4)
C6	4071.3(10)	2145(4)	2683.2(14)	20.9(4)
C7	4444.9(11)	-254(4)	2706.4(16)	23.9(5)
C8	5239.9(11)	-376(4)	3430.0(16)	26.0(5)
C9	5788.1(10)	1017(4)	3065.1(15)	23.3(5)
C10	5977.9(11)	265(4)	2220.9(17)	28.0(5)
C11	6470.7(12)	1533(5)	1865.6(17)	30.0(5)
C12	6789.9(12)	3585(5)	2346.2(17)	29.1(5)
C13	6611.1(12)	4347(4)	3182.8(17)	28.9(5)
C14	6112.0(11)	3073(4)	3536.0(16)	26.0(5)
C15	3462.5(14)	7291(5)	174.8(16)	34.0(5)
C16	4389.0(12)	4253(5)	775.4(17)	30.7(5)
N1	2057.1(9)	873(4)	1335.4(12)	24.3(4)
N2	3712.6(10)	5343(3)	872.1(13)	25.5(4)

O1	3950.1(8)	2422(3)	3637.7(10)	24.6(3)
O101	5000	5275(5)	5000	38.4(6)

**Table 3 Anisotropic Displacement Parameters ( $\text{\AA}^2 \times 10^3$ ) for (S)-51a. The Anisotropic displacement factor exponent takes the form:  $-2\pi^2[h^2a^{*2}U_{11}+2hka^*b^*U_{12}+\dots]$ .**

Atom	$U_{11}$	$U_{22}$	$U_{33}$	$U_{23}$	$U_{13}$	$U_{12}$
C1	21.2(9)	19.8(11)	20.0(9)	-3.0(8)	4.7(7)	-0.1(8)
C2	27.3(10)	26.9(13)	18.3(9)	1.1(8)	1.4(8)	5.0(9)
C3	18.3(9)	32.3(13)	21.5(9)	-5.1(9)	-0.1(7)	2.6(9)
C4	18.2(9)	22.9(12)	22.2(9)	0.9(9)	2.3(7)	-0.5(8)
C5	15.4(8)	21.9(12)	21.3(9)	-1.7(9)	3.5(7)	1.2(8)
C6	16.4(9)	21.9(11)	21.9(9)	1.0(8)	2.2(7)	0.2(8)
C7	17.3(9)	21.4(12)	29.5(10)	-0.5(9)	1.7(8)	0.5(8)
C8	18.3(9)	24.8(13)	30.6(10)	4.6(9)	0.8(8)	3.4(8)
C9	13.8(8)	22.5(12)	28.7(10)	1.4(9)	-0.9(8)	5.1(8)
C10	20.7(9)	25.8(13)	33.5(11)	-7.7(10)	2.3(8)	1.6(9)
C11	22.8(10)	35.6(15)	30.3(11)	-4.4(10)	6.2(9)	3.9(9)
C12	22.4(9)	32.1(14)	30.6(11)	2.6(10)	4.9(8)	0.4(10)
C13	26.1(10)	24.1(14)	32.8(11)	-4.3(10)	3.4(9)	-2.6(9)
C14	22.5(9)	27.0(13)	26.3(10)	-2.7(9)	4.1(8)	3.3(9)
C15	48.3(14)	25.8(13)	24.9(10)	2.6(10)	6.6(9)	-7.5(11)
C16	26.6(10)	35.3(15)	32.4(11)	-3.8(10)	12.4(9)	-6.9(10)
N1	17.1(8)	30.5(11)	22.9(8)	-2.7(8)	2.3(6)	-1.5(7)
N2	28.6(9)	23.5(11)	24.5(8)	1.0(7)	8.0(7)	-2.6(8)
O1	20.0(6)	29.8(9)	20.5(6)	1.0(6)	0.9(5)	4.8(6)
O101	35.8(13)	39.5(17)	34.5(12)	0	2.3(10)	0



**Table 4 Bond Lengths for (S)-51a.**

Atom	Atom	Length/Å	Atom	Atom	Length/Å
C1	C2	1.409(3)	C7	C8	1.539(3)
C1	C5	1.411(3)	C8	C9	1.510(3)
C1	N2	1.399(3)	C9	C10	1.403(3)
C2	C3	1.381(3)	C9	C14	1.388(3)
C3	N1	1.335(3)	C10	C11	1.384(3)
C4	C5	1.390(3)	C11	C12	1.388(3)
C4	N1	1.346(2)	C12	C13	1.384(3)
C5	C6	1.528(2)	C13	C14	1.393(3)
C6	C7	1.529(3)	C15	N2	1.456(3)
C6	O1	1.433(2)	C16	N2	1.463(3)

**Table 5 Bond Angles for (S)-51a.**

Atom	Atom	Atom	Angle/°	Atom	Atom	Atom	Angle/°
C2	C1	C5	116.86(18)	C9	C8	C7	112.74(17)
N2	C1	C2	121.38(19)	C10	C9	C8	120.2(2)
N2	C1	C5	121.70(17)	C14	C9	C8	121.9(2)
C3	C2	C1	120.1(2)	C14	C9	C10	117.9(2)
N1	C3	C2	123.69(18)	C11	C10	C9	121.2(2)
N1	C4	C5	125.4(2)	C10	C11	C12	120.2(2)
C1	C5	C6	124.99(18)	C13	C12	C11	119.4(2)
C4	C5	C1	117.71(17)	C12	C13	C14	120.3(2)
C4	C5	C6	117.12(18)	C9	C14	C13	121.0(2)
C5	C6	C7	111.68(17)	C3	N1	C4	116.10(19)

O1	C6	C5	109.91(14)	C1	N2	C15	117.44(18)
O1	C6	C7	106.34(17)	C1	N2	C16	117.97(18)
C6	C7	C8	114.01(17)	C15	N2	C16	111.95(18)

**Table 6 Hydrogen Bonds for (S)-51a.**

D	H	A	d(D-H)/Å	d(H-A)/Å	d(D-A)/Å	D-H-A/°
O1	H1	N1 <sup>1</sup>	0.95(4)	1.79(4)	2.740(2)	173(3)
O101	H101	O1	0.870(13)	1.944(13)	2.813(2)	177(3)

<sup>1</sup>1/2-X,1/2+Y,1/2-Z

**Table 7 Torsion Angles for (S)-51a.**

A	B	C	D	Angle/°	A	B	C	D	Angle/°
C1	C2	C3	N1	-0.5(3)	C7	C8	C9	C10	-68.8(3)
C1	C5	C6	C7	-118.4(2)	C7	C8	C9	C14	110.4(2)
C1	C5	C6	O1	123.9(2)	C8	C9	C10	C11	179.06(19)
C2	C1	C5	C4	4.5(3)	C8	C9	C14	C13	-179.39(19)
C2	C1	C5	C6	-170.29(19)	C9	C10	C11	C12	0.2(3)
C2	C1	N2	C15	11.1(3)	C10	C9	C14	C13	-0.2(3)
C2	C1	N2	C16	-127.7(2)	C10	C11	C12	C13	0.0(3)
C2	C3	N1	C4	3.4(3)	C11	C12	C13	C14	-0.4(3)
C4	C5	C6	C7	66.8(2)	C12	C13	C14	C9	0.4(3)
C4	C5	C6	O1	-51.0(3)	C14	C9	C10	C11	-0.2(3)
C5	C1	C2	C3	-3.6(3)	N1	C4	C5	C1	-1.7(3)
C5	C1	N2	C15	-165.72(19)	N1	C4	C5	C6	173.5(2)

C5 C1 N2 C16	55.5(3)	N2 C1 C2 C3	179.4(2)
C5 C4 N1 C3	-2.3(3)	N2 C1 C5 C4	-178.48(19)
C5 C6 C7 C8	171.82(17)	N2 C1 C5 C6	6.7(3)
C6 C7 C8 C9	-71.3(2)	O1 C6 C7 C8	-68.3(2)

**Table 8 Hydrogen Atom Coordinates ( $\text{\AA} \times 10^4$ ) and Isotropic Displacement Parameters ( $\text{\AA}^2 \times 10^3$ ) for (S)-51a.**

Atom	x	y	z	U(eq)
H2	2282	5093	-100	30
H3	1403	2619	190	30
H4	2878	-261	2480	26
H6	4409	3418	2587	25
H7A	4458	-636	2023	29
H7B	4139	-1470	2902	29
H8A	5241	236	4092	31
H8B	5400	-2044	3518	31
H10	5764	-1140	1887	34
H11	6591	998	1291	36
H12	7128	4459	2103	35
H13	6830	5744	3518	35
H14	5991	3621	4108	31
H15A	3292	6679	-511	51
H15B	3874	8391	240	51
H15C	3053	8113	326	51
H16A	4479	2759	1144	46
H16B	4811	5314	1050	46
H16C	4331	3955	67	46

H1	3616(17)	3690(70)	3610(20)	49(9)
H101	4683(15)	4410(60)	4560(20)	58

### Experimental

Single crystals of  $\text{C}_{16}\text{H}_{21}\text{N}_2\text{O}_{1.5}$  (**(S)-51a**) were obtained from slow evaporation from *d*-chloroform. A suitable crystal was selected on a **SuperNova, Dual, Cu at zero, Atlas** diffractometer. The crystal was kept at 99.98(11) K during data collection. Using Olex2 [1], the structure was solved with the ShelXS [2] structure solution program using Direct Methods and refined with the ShelXL [3] refinement package using Least Squares minimisation.

1. Dolomanov, O.V., Bourhis, L.J., Gildea, R.J., Howard, J.A.K. & Puschmann, H. (2009), *J. Appl. Cryst.* 42, 339-341.
2. Sheldrick, G.M. (2008). *Acta Cryst.* A64, 112-122.
3. Sheldrick, G.M. (2008). *Acta Cryst.* A64, 112-122.

### Crystal structure determination of (S)-51a

**Crystal Data** for  $\text{C}_{16}\text{H}_{21}\text{N}_2\text{O}_{1.5}$  ( $M = 265.35$ ): monoclinic, space group I2 (no. 5),  $a = 18.9063(4) \text{ \AA}$ ,  $b = 5.67337(14) \text{ \AA}$ ,  $c = 14.0166(3) \text{ \AA}$ ,  $\beta = 107.626(2)^\circ$ ,  $V = 1432.87(5) \text{ \AA}^3$ ,  $Z = 4$ ,  $T = 99.98(11) \text{ K}$ ,  $\mu(\text{CuK}\alpha) = 0.629 \text{ mm}^{-1}$ ,  $D_{\text{calc}} = 1.230 \text{ g/mm}^3$ , 13290 reflections measured ( $6.942 \leq 2\theta \leq 148.6$ ), 2781 unique ( $R_{\text{int}} = 0.0281$ ,  $R_{\text{sigma}} = 0.0205$ ) which were used in all calculations. The final  $R_1$  was 0.0348 ( $I > 2\sigma(I)$ ) and  $wR_2$  was 0.0893 (all data).

### Refinement model description

Number of restraints - 2, number of constraints - unknown.

Details:

1. Fixed Uiso  
At 1.2 times of:  
All C(H) groups, All C(H,H) groups  
At 1.5 times of:

All C(H,H,H) groups, All O(H) groups  
 2. Restrained distances  
 O101-H101  
 0.82 with sigma of 0.01  
 3.a Ternary CH refined with riding coordinates:  
 C6(H6)  
 3.b Secondary CH2 refined with riding coordinates:  
 C7(H7A,H7B), C8(H8A,H8B)  
 3.c Aromatic/amide H refined with riding coordinates:  
 C2(H2), C3(H3), C4(H4), C10(H10), C11(H11), C12(H12), C13(H13),  
 C14(H14)  
 3.d Idealised Me refined as rotating group:  
 C15(H15A,H15B,H15C), C16(H16A,H16B,H16C)

## Compound 67

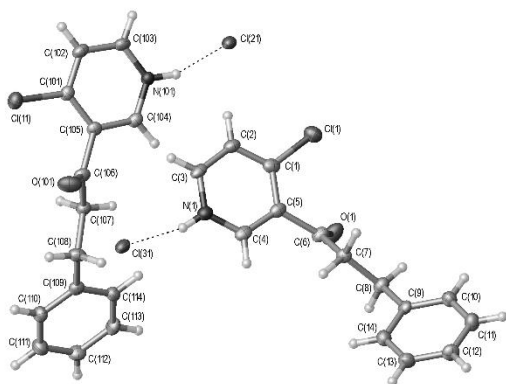


Figure 54 - Crystal structure of 67 with ellipsoids drawn at the 50 % probability level.  
 Hydrogen bonding is shown using dashed lines.

## Notes:

The structure contains two crystallographically-independent molecules, along with two anions.

The hydrogen atoms bonded to N(1) and N(101) were located in the electron density and the positions and displacement parameters were freely refined. The remaining hydrogen atoms were added at calculated positions and refined by use of a riding model with the isotropic displacement parameters based on the equivalent isotropic displacement parameter (Ueq) of the parent atom. Hydrogen bonding is details in Table 7, Page 11.

**Table 1. Crystal data and structure refinement for 67.**

Identification code	DTP-342_HCl_Salt
Empirical formula	C <sub>14</sub> H <sub>13</sub> ClNO, Cl
Formula weight	282.15
Temperature	100.00(10) K
Wavelength	1.5418 Å
Crystal system	Monoclinic
Space group	P 2 <sub>1</sub> /c
Unit cell dimensions	a = 28.5185(11) Å $\beta$ = 90°. b = 5.4659(3) Å $\gamma$ = 107.906(5)°. c = 18.1830(8) Å $\gamma$ = 90°.
Volume	2697.1(2) Å <sup>3</sup>
Z	8
Density (calculated)	1.390 Mg/m <sup>3</sup>
Absorption coefficient	4.219 mm <sup>-1</sup>
F(000)	1168
Crystal size	0.363 x 0.067 x 0.043 mm <sup>3</sup>
Theta range for data collection	6.525 to 66.599°.
Index ranges	-26<=h<=33, -4<=k<=5, -21<=l<=15

Reflections collected	6313
Independent reflections	4316 [R(int) = 0.0146]
Completeness to theta = 67.684°	88.2 %
Absorption correction	Gaussian
Max. and min. transmission	0.748 and 0.301
Refinement method	Full-matrix least-squares on F <sup>2</sup>
Data / restraints / parameters	4316 / 0 / 333
Goodness-of-fit on F <sup>2</sup>	1.213
Final R indices [I>2sigma(I)]	R1 = 0.0785, wR2 = 0.1987
R indices (all data)	R1 = 0.0799, wR2 = 0.1994
Extinction coefficient	n/a
Largest diff. peak and hole	1.606 and -0.432 e.Å <sup>-3</sup>

**Table 2. Atomic coordinates ( x 10<sup>4</sup>) and equivalent isotropic displacement parameters (Å<sup>2</sup> x 10<sup>3</sup>) for 67. U(eq) is defined as one third of the trace of the orthogonalized U<sup>ij</sup> tensor.**

	x	y	z	U(eq)
C(1)	1593(2)	5979(12)	5846(3)	25(1)
C(2)	1834(2)	4769(12)	5403(3)	25(1)
C(3)	2135(2)	2832(12)	5728(3)	25(1)
C(4)	1959(2)	3295(11)	6893(3)	24(1)
C(5)	1652(2)	5255(11)	6606(3)	23(1)
C(6)	1419(2)	6604(11)	7137(3)	21(1)
C(7)	1082(2)	5203(10)	7466(3)	20(1)
C(8)	941(2)	6645(11)	8090(3)	24(1)
C(9)	608(2)	5226(11)	8433(3)	20(1)
C(10)	133(2)	6075(12)	8360(3)	26(1)

C(11)	-165(2)	4835(12)	8720(3)	30(1)
C(12)	3(2)	2729(12)	9141(3)	27(1)
C(13)	470(2)	1880(12)	9208(3)	30(1)
C(14)	772(2)	3101(11)	8855(3)	26(1)
N(1)	2190(2)	2163(10)	6451(3)	22(1)
O(1)	1504(2)	8761(9)	7244(3)	39(1)
Cl(1)	1215(1)	8398(3)	5435(1)	30(1)
C(101)	3426(2)	3749(10)	4288(3)	20(1)
C(102)	3190(2)	4906(12)	3604(3)	25(1)
C(103)	2877(2)	6834(12)	3614(3)	24(1)
C(104)	3051(2)	6488(10)	4954(3)	20(1)
C(105)	3362(2)	4513(10)	4983(3)	19(1)
C(106)	3594(2)	3230(11)	5740(3)	22(1)
C(107)	3904(2)	4736(11)	6404(3)	21(1)
C(108)	4055(2)	3361(12)	7164(3)	27(1)
C(109)	4387(2)	4829(11)	7827(3)	23(1)
C(110)	4855(2)	3990(12)	8226(3)	27(1)
C(111)	5150(2)	5211(12)	8872(3)	31(1)
C(112)	4981(2)	7372(12)	9114(3)	28(1)
C(113)	4518(2)	8231(11)	8710(3)	26(1)
C(114)	4222(2)	7006(11)	8069(3)	25(1)
N(101)	2817(2)	7526(9)	4278(2)	20(1)
O(101)	3544(2)	1068(8)	5779(2)	34(1)
Cl(11)	3814(1)	1345(3)	4261(1)	28(1)
Cl(21)	2152(1)	11861(3)	3916(1)	24(1)
Cl(31)	2843(1)	-2260(3)	6758(1)	26(1)

**Table 3. Bond lengths [Å] and angles [°] for 67**

C(1)-C(2)	1.377(8)
-----------	----------

C(1)-C(5)	1.398(8)
C(1)-Cl(1)	1.725(6)
C(2)-C(3)	1.377(9)
C(2)-H(2)	0.9500
C(3)-N(1)	1.326(7)
C(3)-H(3)	0.9500
C(4)-N(1)	1.337(7)
C(4)-C(5)	1.381(8)
C(4)-H(4)	0.9500
C(5)-C(6)	1.519(8)
C(6)-O(1)	1.208(7)
C(6)-C(7)	1.492(7)
C(7)-C(8)	1.533(8)
C(7)-H(7A)	0.9900
C(7)-H(7B)	0.9900
C(8)-C(9)	1.501(8)
C(8)-H(8A)	0.9900
C(8)-H(8B)	0.9900
C(9)-C(14)	1.391(8)
C(9)-C(10)	1.400(8)
C(10)-C(11)	1.398(8)
C(10)-H(10)	0.9500
C(11)-C(12)	1.384(9)
C(11)-H(11)	0.9500
C(12)-C(13)	1.381(8)
C(12)-H(12)	0.9500
C(13)-C(14)	1.393(8)
C(13)-H(13)	0.9500
C(14)-H(14)	0.9500
N(1)-H(1)	0.85(8)
C(101)-C(102)	1.373(8)
C(101)-C(105)	1.395(7)

C(101)-Cl(11)	1.729(6)
C(102)-C(103)	1.384(8)
C(102)-H(102)	0.9500
C(103)-N(101)	1.326(7)
C(103)-H(103)	0.9500
C(104)-N(101)	1.333(7)
C(104)-C(105)	1.388(8)
C(104)-H(104)	0.9500
C(105)-C(106)	1.506(7)
C(106)-O(101)	1.195(7)
C(106)-C(107)	1.503(7)
C(107)-C(108)	1.516(8)
C(107)-H(17A)	0.9900
C(107)-H(17B)	0.9900
C(108)-C(109)	1.514(8)
C(108)-H(18A)	0.9900
C(108)-H(18B)	0.9900
C(109)-C(110)	1.388(8)
C(109)-C(114)	1.399(9)
C(110)-C(111)	1.386(8)
C(110)-H(110)	0.9500
C(111)-C(112)	1.398(9)
C(111)-H(111)	0.9500
C(112)-C(113)	1.381(8)
C(112)-H(112)	0.9500
C(113)-C(114)	1.383(8)
C(113)-H(113)	0.9500
C(114)-H(114)	0.9500
N(101)-H(101)	0.91(6)
C(2)-C(1)-C(5)	120.9(6)
C(2)-C(1)-Cl(1)	118.2(4)
C(5)-C(1)-Cl(1)	120.9(5)

C(3)-C(2)-C(1)	118.4(5)
C(3)-C(2)-H(2)	120.8
C(1)-C(2)-H(2)	120.8
N(1)-C(3)-C(2)	120.4(5)
N(1)-C(3)-H(3)	119.8
C(2)-C(3)-H(3)	119.8
N(1)-C(4)-C(5)	120.3(5)
N(1)-C(4)-H(4)	119.8
C(5)-C(4)-H(4)	119.8
C(4)-C(5)-C(1)	117.5(5)
C(4)-C(5)-C(6)	119.2(5)
C(1)-C(5)-C(6)	123.2(5)
O(1)-C(6)-C(7)	123.9(5)
O(1)-C(6)-C(5)	118.1(5)
C(7)-C(6)-C(5)	117.9(5)
C(6)-C(7)-C(8)	112.5(5)
C(6)-C(7)-H(7A)	109.1
C(8)-C(7)-H(7A)	109.1
C(6)-C(7)-H(7B)	109.1
C(8)-C(7)-H(7B)	109.1
H(7A)-C(7)-H(7B)	107.8
C(9)-C(8)-C(7)	112.6(5)
C(9)-C(8)-H(8A)	109.1
C(7)-C(8)-H(8A)	109.1
C(9)-C(8)-H(8B)	109.1
C(7)-C(8)-H(8B)	109.1
H(8A)-C(8)-H(8B)	107.8
C(14)-C(9)-C(10)	118.7(5)
C(14)-C(9)-C(8)	120.8(5)
C(10)-C(9)-C(8)	120.5(5)
C(11)-C(10)-C(9)	120.4(6)
C(11)-C(10)-H(10)	119.8

C(9)-C(10)-H(10)	119.8
C(12)-C(11)-C(10)	120.3(5)
C(12)-C(11)-H(11)	119.9
C(10)-C(11)-H(11)	119.9
C(13)-C(12)-C(11)	119.4(5)
C(13)-C(12)-H(12)	120.3
C(11)-C(12)-H(12)	120.3
C(12)-C(13)-C(14)	121.0(6)
C(12)-C(13)-H(13)	119.5
C(14)-C(13)-H(13)	119.5
C(9)-C(14)-C(13)	120.3(5)
C(9)-C(14)-H(14)	119.8
C(13)-C(14)-H(14)	119.8
C(3)-N(1)-C(4)	122.5(6)
C(3)-N(1)-H(1)	116(5)
C(4)-N(1)-H(1)	121(5)
C(102)-C(101)-C(105)	121.3(5)
C(102)-C(101)-Cl(11)	117.7(4)
C(105)-C(101)-Cl(11)	121.1(4)
C(101)-C(102)-C(103)	118.5(5)
C(101)-C(102)-H(102)	120.8
C(103)-C(102)-H(102)	120.8
N(101)-C(103)-C(102)	119.6(5)
N(101)-C(103)-H(103)	120.2
C(102)-C(103)-H(103)	120.2
N(101)-C(104)-C(105)	119.9(5)
N(101)-C(104)-H(104)	120.1
C(105)-C(104)-H(104)	120.1
C(104)-C(105)-C(101)	117.3(5)
C(104)-C(105)-C(106)	119.5(5)
C(101)-C(105)-C(106)	123.1(5)
O(101)-C(106)-C(107)	123.1(5)

O(101)-C(106)-C(105)	119.2(5)
C(107)-C(106)-C(105)	117.6(5)
C(106)-C(107)-C(108)	113.1(5)
C(106)-C(107)-H(17A)	109.0
C(108)-C(107)-H(17A)	109.0
C(106)-C(107)-H(17B)	109.0
C(108)-C(107)-H(17B)	109.0
H(17A)-C(107)-H(17B)	107.8
C(109)-C(108)-C(107)	113.3(5)
C(109)-C(108)-H(18A)	108.9
C(107)-C(108)-H(18A)	108.9
C(109)-C(108)-H(18B)	108.9
C(107)-C(108)-H(18B)	108.9
H(18A)-C(108)-H(18B)	107.7
C(110)-C(109)-C(114)	118.6(5)
C(110)-C(109)-C(108)	120.5(6)
C(114)-C(109)-C(108)	120.9(5)
C(111)-C(110)-C(109)	121.3(6)
C(111)-C(110)-H(110)	119.4
C(109)-C(110)-H(110)	119.4
C(110)-C(111)-C(112)	119.7(5)
C(110)-C(111)-H(111)	120.1
C(112)-C(111)-H(111)	120.1
C(113)-C(112)-C(111)	119.1(5)
C(113)-C(112)-H(112)	120.5
C(111)-C(112)-H(112)	120.5
C(112)-C(113)-C(114)	121.3(6)
C(112)-C(113)-H(113)	119.3
C(114)-C(113)-H(113)	119.3
C(113)-C(114)-C(109)	120.0(5)
C(113)-C(114)-H(114)	120.0
C(109)-C(114)-H(114)	120.0

C(103)-N(101)-C(104)	123.4(5)
C(103)-N(101)-H(101)	120(4)
C(104)-N(101)-H(101)	117(4)

Symmetry transformations used to generate equivalent atoms:

**Table 4.** Anisotropic displacement parameters ( $\text{\AA}^2 \times 10^3$ ) for 67. The anisotropic displacement factor exponent takes the form:  $-2\pi^2 [h^2 a^{*2} U^{11} + \dots + 2 h k a^* b^* U^{12}]$

	U <sup>11</sup>	U <sup>22</sup>	U <sup>33</sup>	U <sup>23</sup>	U <sup>13</sup>	U <sup>12</sup>
C(1)	22(3)	29(4)	22(3)	1(3)	4(2)	-7(2)
C(2)	27(3)	29(4)	18(3)	-2(2)	8(2)	-5(2)
C(3)	25(3)	32(4)	19(3)	-10(3)	9(2)	-9(2)
C(4)	25(3)	25(3)	21(3)	-7(2)	7(2)	-10(2)
C(5)	24(3)	25(3)	21(3)	-4(2)	9(2)	-9(2)
C(6)	28(3)	16(3)	22(3)	-6(2)	10(2)	-7(2)
C(7)	25(3)	14(3)	21(3)	1(2)	7(2)	-3(2)
C(8)	29(3)	22(3)	25(3)	-3(2)	12(2)	-3(2)
C(9)	26(3)	17(3)	19(2)	-4(2)	9(2)	0(2)
C(10)	26(3)	26(3)	26(3)	4(3)	8(2)	4(2)
C(11)	26(3)	31(4)	36(3)	2(3)	13(2)	3(3)
C(12)	29(3)	25(4)	29(3)	4(3)	12(2)	-5(2)
C(13)	31(3)	33(4)	25(3)	7(3)	8(2)	2(3)
C(14)	23(3)	28(4)	26(3)	-1(3)	6(2)	2(2)
N(1)	23(2)	24(3)	20(2)	-2(2)	6(2)	-3(2)
O(1)	57(3)	26(3)	45(3)	-7(2)	32(2)	-13(2)
Cl(1)	31(1)	28(1)	29(1)	3(1)	5(1)	-2(1)

C(101)	22(2)	16(3)	23(3)	-2(2)	9(2)	-4(2)
C(102)	27(3)	31(4)	19(3)	-3(2)	10(2)	-5(2)
C(103)	26(3)	31(4)	17(3)	3(2)	8(2)	-2(2)
C(104)	24(3)	17(3)	21(3)	-3(2)	9(2)	-5(2)
C(105)	22(2)	16(3)	21(3)	1(2)	8(2)	-5(2)
C(106)	26(3)	21(4)	21(3)	2(2)	10(2)	-6(2)
C(107)	23(3)	21(3)	20(3)	-1(2)	7(2)	-2(2)
C(108)	28(3)	30(4)	20(3)	3(3)	4(2)	-3(2)
C(109)	25(3)	23(3)	21(3)	2(2)	9(2)	-3(2)
C(110)	29(3)	23(3)	27(3)	1(3)	9(2)	5(2)
C(111)	26(3)	33(4)	29(3)	0(3)	3(2)	3(3)
C(112)	28(3)	28(4)	24(3)	-5(3)	4(2)	-6(2)
C(113)	33(3)	20(3)	30(3)	-4(3)	14(2)	2(2)
C(114)	22(3)	31(4)	22(3)	2(3)	6(2)	4(2)
N(101)	20(2)	19(3)	20(2)	1(2)	8(2)	1(2)
O(101)	48(3)	23(3)	27(2)	3(2)	5(2)	-14(2)
Cl(11)	29(1)	25(1)	31(1)	-1(1)	13(1)	2(1)
Cl(21)	23(1)	33(1)	17(1)	-1(1)	6(1)	3(1)
Cl(31)	23(1)	36(1)	18(1)	-4(1)	7(1)	-1(1)

**Table 5. Hydrogen coordinates (  $\times 10^4$ ) and isotropic displacement parameters ( $\text{\AA}^2 \times 10^3$ ) for 67.**

	x	y	z	U(eq)
H(2)	1793	5260	4886	30
H(3)	2304	1970	5433	30
H(4)	2007	2750	7407	28

H(7A)	1245	3658	7692	24
H(7B)	779	4778	7046	24
H(8A)	1245	7094	8507	29
H(8B)	774	8178	7862	29
H(10)	12	7502	8065	31
H(11)	-485	5441	8676	37
H(12)	-201	1876	9381	32
H(13)	588	442	9500	36
H(14)	1091	2480	8901	31
H(1)	2410(30)	1100(140)	6640(40)	40(20)
H(102)	3240	4395	3134	30
H(103)	2707	7657	3148	29
H(104)	3004	7098	5416	24
H(17A)	3718	6217	6457	25
H(17B)	4205	5276	6286	25
H(18A)	3754	2889	7294	32
H(18B)	4227	1840	7103	32
H(110)	4976	2551	8054	32
H(111)	5466	4582	9148	37
H(112)	5181	8237	9551	33
H(113)	4400	9692	8875	32
H(114)	3907	7643	7794	30
H(101)	2590(20)	8700(110)	4280(30)	15(14)

**Table 6. Torsion angles [ $^\circ$ ] for 67.**

C(5)-C(1)-C(2)-C(3)	-0.2(8)
Cl(1)-C(1)-C(2)-C(3)	-179.8(4)
C(1)-C(2)-C(3)-N(1)	-0.1(8)
N(1)-C(4)-C(5)-C(1)	0.2(8)



N(1)-C(4)-C(5)-C(6)	-176.3(5)
C(2)-C(1)-C(5)-C(4)	0.1(8)
Cl(1)-C(1)-C(5)-C(4)	179.7(4)
C(2)-C(1)-C(5)-C(6)	176.4(5)
Cl(1)-C(1)-C(5)-C(6)	-4.0(7)
C(4)-C(5)-C(6)-O(1)	120.7(6)
C(1)-C(5)-C(6)-O(1)	-55.5(8)
C(4)-C(5)-C(6)-C(7)	-61.8(7)
C(1)-C(5)-C(6)-C(7)	122.0(6)
O(1)-C(6)-C(7)-C(8)	-12.1(8)
C(5)-C(6)-C(7)-C(8)	170.6(5)
C(6)-C(7)-C(8)-C(9)	-179.1(5)
C(7)-C(8)-C(9)-C(14)	64.7(7)
C(7)-C(8)-C(9)-C(10)	-117.9(6)
C(14)-C(9)-C(10)-C(11)	1.4(9)
C(8)-C(9)-C(10)-C(11)	-176.0(5)
C(9)-C(10)-C(11)-C(12)	-1.2(9)
C(10)-C(11)-C(12)-C(13)	0.7(9)
C(11)-C(12)-C(13)-C(14)	-0.5(9)
C(10)-C(9)-C(14)-C(13)	-1.3(8)
C(8)-C(9)-C(14)-C(13)	176.2(5)
C(12)-C(13)-C(14)-C(9)	0.8(9)
C(2)-C(3)-N(1)-C(4)	0.4(8)
C(5)-C(4)-N(1)-C(3)	-0.5(8)
C(105)-C(101)-C(102)-C(103)	-1.2(8)
Cl(11)-C(101)-C(102)-C(103)	179.9(4)
C(101)-C(102)-C(103)-N(101)	0.6(8)
N(101)-C(104)-C(105)-C(101)	1.9(7)
N(101)-C(104)-C(105)-C(106)	-175.4(5)
C(102)-C(101)-C(105)-C(104)	0.0(8)
Cl(11)-C(101)-C(105)-C(104)	178.8(4)
C(102)-C(101)-C(105)-C(106)	177.1(5)

Cl(11)-C(101)-C(105)-C(106)	-4.1(7)
C(104)-C(105)-C(106)-O(101)	125.7(6)
C(101)-C(105)-C(106)-O(101)	-51.4(8)
C(104)-C(105)-C(106)-C(107)	-57.7(7)
C(101)-C(105)-C(106)-C(107)	125.3(6)
O(101)-C(106)-C(107)-C(108)	-12.3(8)
C(105)-C(106)-C(107)-C(108)	171.2(5)
C(106)-C(107)-C(108)-C(109)	177.3(5)
C(107)-C(108)-C(109)-C(110)	-120.1(6)
C(107)-C(108)-C(109)-C(114)	62.4(7)
C(114)-C(109)-C(110)-C(111)	2.6(9)
C(108)-C(109)-C(110)-C(111)	-175.0(5)
C(109)-C(110)-C(111)-C(112)	-2.0(9)
C(110)-C(111)-C(112)-C(113)	0.9(9)
C(111)-C(112)-C(113)-C(114)	-0.5(9)
C(112)-C(113)-C(114)-C(109)	1.1(9)
C(110)-C(109)-C(114)-C(113)	-2.1(8)
C(108)-C(109)-C(114)-C(113)	175.4(5)
C(102)-C(103)-N(101)-C(104)	1.4(8)
C(105)-C(104)-N(101)-C(103)	-2.6(8)

—  
Symmetry transformations used to generate equivalent atoms:

**Table 7. Hydrogen bonds for 67 [Å and °].**

D-H...A	d(D-H)	d(H...A)	d(D...A)	<(DHA)
N(1)-H(1)...Cl(31)	0.85(8)	2.19(8)	2.997(6)	160(7)
N(101)-H(101)...Cl(21)	0.91(6)	2.12(6)	2.978(5)	158(5)

Symmetry transformations used to generate equivalent atoms:

## Compound 82

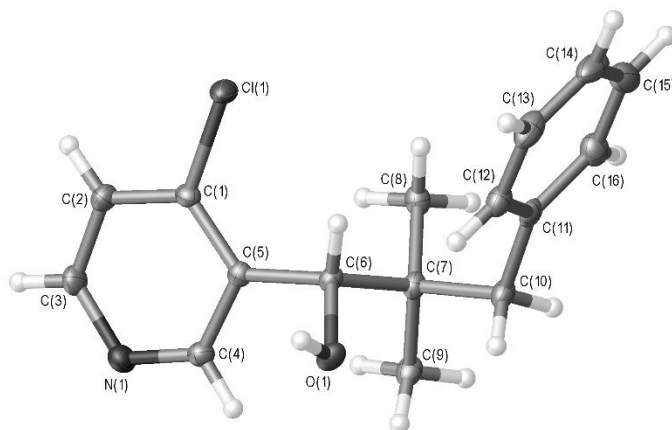


*Figure S5 - Crystal structure of 82 with ellipsoids drawn at the 50 % probability level.  
The absolute structure has been determined from the diffraction data, with the  
stereocentre being S*

### Notes:

This structure is chiral. The absolute structure has been determined from the diffraction data, with C(6) being S

The hydrogen atom bonded to O(1) was located in the electron density and freely refined while the remaining hydrogen atoms were fixed as riding models. Hydrogen bonding is detailed in Table 6 of the DTP-701-EP1\_Tables.html report. Other tables in the report give bond lengths, angles and torsion angles with standard deviations given in brackets.

**Table 1 Crystal data and structure refinement for 82.**

Identification code	DTP-701-EP1
Empirical formula	C <sub>16</sub> H <sub>18</sub> ClNO
Formula weight	275.76
Temperature/K	100.1(9)
Crystal system	monoclinic
Space group	P2 <sub>1</sub>
a/Å	10.07501(9)
b/Å	7.27003(7)
c/Å	10.52824(9)
α/°	90
β/°	111.3486(10)
γ/°	90
Volume/Å <sup>3</sup>	718.234(12)
Z	2
ρ <sub>calc</sub> /cm <sup>3</sup>	1.275
μ/mm <sup>-1</sup>	2.274
F(000)	292.0
Crystal size/mm <sup>3</sup>	0.2628 × 0.1597 × 0.0957
Radiation	CuKα (λ = 1.54184)
2θ range for data collection/°	9.018 to 149.032
Index ranges	-12 ≤ h ≤ 12, -9 ≤ k ≤ 8, -13 ≤ l ≤ 13
Reflections collected	25684
Independent reflections	2841 [R <sub>int</sub> = 0.0205, R <sub>sigma</sub> = 0.0094]
Data/restraints/parameters	2841/1/178
Goodness-of-fit on F <sup>2</sup>	1.078
Final R indexes [I ≥ 2σ (I)]	R <sub>1</sub> = 0.0205, wR <sub>2</sub> = 0.0539
Final R indexes [all data]	R <sub>1</sub> = 0.0207, wR <sub>2</sub> = 0.0540

Largest diff. peak/hole / e Å<sup>-3</sup> 0.17/-0.18  
 Flack parameter -0.003(3)

**Table 2 Fractional Atomic Coordinates (×10<sup>4</sup>) and Equivalent Isotropic Displacement Parameters (Å<sup>2</sup>×10<sup>3</sup>) for 82. U<sub>eq</sub> is defined as 1/3 of the trace of the orthogonalised U<sub>ij</sub> tensor.**

Atom	x	y	z	U(eq)
C1	-1472.9(16)	4160(2)	7927.3(15)	15.5(3)
C2	-2807.6(17)	3842(2)	7994.2(17)	19.5(3)
C3	-3029.3(17)	2191(3)	8521.8(17)	20.8(3)
C4	-742.5(15)	1262(3)	8944.7(14)	17.0(3)
C5	-391.5(15)	2865(2)	8398.5(15)	14.4(3)
C6	1116.1(15)	3108(2)	8405.0(15)	14.3(3)
C7	1391.2(16)	2018(2)	7258.0(15)	15.6(3)
C8	376.7(16)	2705(2)	5874.0(15)	18.4(3)
C9	1185.2(18)	-54(2)	7386.4(18)	19.5(3)
C10	2964.6(16)	2298(2)	7388.9(17)	18.5(3)
C11	3412.8(16)	4198(2)	7131.4(17)	17.8(3)
C12	3899.0(17)	5512(3)	8167.3(18)	21.0(3)
C13	4389.9(18)	7210(3)	7940(2)	27.7(4)
C14	4404.9(19)	7647(3)	6665(2)	30.3(4)
C15	3911.1(17)	6378(3)	5614.3(19)	29.9(4)
C16	3424.2(17)	4668(3)	5845.3(17)	23.6(4)
Cl1	-1194.0(4)	6259.5(5)	7281.4(4)	22.09(1)
N1	-2021.1(15)	892(2)	8996.9(14)	20.3(3)
O1	2117.8(11)	2526.9(17)	9692.2(11)	18.1(3)

**Table 3 Anisotropic Displacement Parameters (Å<sup>2</sup>×10<sup>3</sup>) for 82. The Anisotropic displacement factor exponent takes the form: -2π<sup>2</sup>[h<sup>2</sup>a<sup>2</sup>U<sub>11</sub>+2hka\*b\*U<sub>12</sub>+...].**

Atom	U <sub>11</sub>	U <sub>22</sub>	U <sub>33</sub>	U <sub>23</sub>	U <sub>13</sub>	U <sub>12</sub>
C1	18.3(7)	12.9(8)	16.3(7)	1.2(6)	7.6(6)	0.0(6)
C2	15.2(7)	21.4(9)	22.3(8)	3.3(6)	7.2(6)	4.0(6)
C3	14.9(7)	24.9(9)	24.6(8)	2.7(7)	9.8(6)	-0.6(7)
C4	16.5(6)	16.7(7)	17.6(6)	2.1(7)	5.9(5)	1.1(7)
C5	14.0(7)	15.5(8)	13.4(6)	-0.9(6)	4.6(5)	0.3(6)
C6	12.0(7)	13.9(8)	16.4(7)	-0.7(6)	4.4(5)	0.7(6)
C7	13.5(7)	16.7(8)	17.8(7)	-2.0(6)	7.1(6)	-0.1(6)
C8	17.0(7)	21.2(9)	17.8(7)	-1.7(6)	7.4(6)	-1.8(6)
C9	18.6(7)	15.9(9)	25.8(8)	-3.6(7)	10.2(6)	-0.8(6)
C10	15.4(7)	17.0(9)	25.1(8)	-1.8(7)	9.8(6)	1.1(6)
C11	10.1(6)	19.1(9)	25.2(8)	0.4(7)	7.5(6)	2.6(6)
C12	15.9(7)	21.8(9)	26.4(8)	-2.3(7)	9.0(6)	1.6(6)
C13	20.1(8)	20.1(10)	44.6(10)	-7.5(8)	13.7(7)	-1.3(7)
C14	22.2(9)	17.3(10)	56.0(12)	9.2(8)	19.9(8)	3.6(7)
C15	22.3(8)	34.8(11)	35.6(9)	14.1(9)	13.9(7)	5.3(9)
C16	18.6(8)	28.5(10)	24.2(8)	0.8(7)	8.4(6)	-0.1(7)
Cl1	22.72(18)	15.56(19)	32.1(2)	8.00(16)	14.93(14)	4.46(16)
N1	19.9(6)	20.6(9)	22.0(6)	3.5(5)	9.7(5)	-0.9(6)
O1	15.2(5)	19.8(7)	16.3(5)	-2.2(5)	2.0(4)	2.9(4)

**Table 4 Bond Lengths for 82.**

Atom	Atom	Length/Å	Atom	Atom	Length/Å
C1	C2	1.391(2)	C7	C8	1.527(2)
C1	C5	1.388(2)	C7	C9	1.533(2)
C1	Cl1	1.7352(17)	C7	C10	1.554(2)

C2	C3	1.375(3)
C3	N1	1.343(2)
C4	C5	1.401(2)
C4	N1	1.336(2)
C5	C6	1.527(2)
C6	C7	1.551(2)
C6	O1	1.4274(17)

C10	C11	1.508(2)
C11	C12	1.397(2)
C11	C16	1.400(2)
C12	C13	1.383(3)
C13	C14	1.385(3)
C14	C15	1.386(3)
C15	C16	1.391(3)

**Table 5 Bond Angles for 82.**

Atom	Atom	Atom	Angle/°
C2	C1	Cl1	117.59(13)
C5	C1	C2	121.13(15)
C5	C1	Cl1	121.25(12)
C3	C2	C1	117.88(15)
N1	C3	C2	123.52(14)
N1	C4	C5	125.13(16)
C1	C5	C4	115.36(14)
C1	C5	C6	125.01(14)
C4	C5	C6	119.59(13)
C5	C6	C7	113.39(13)
O1	C6	C5	109.18(12)
O1	C6	C7	108.85(12)
C6	C7	C10	109.25(13)
C8	C7	C6	109.19(13)

Atom	Atom	Atom	Angle/°
C8	C7	C9	109.89(14)
C8	C7	C10	110.40(13)
C9	C7	C6	111.39(14)
C9	C7	C10	106.70(13)
C11	C10	C7	117.82(14)
C12	C11	C10	121.90(15)
C12	C11	C16	117.65(16)
C16	C11	C10	120.37(16)
C13	C12	C11	121.39(17)
C12	C13	C14	120.23(18)
C13	C14	C15	119.55(18)
C14	C15	C16	120.19(17)
C15	C16	C11	120.98(17)
C4	N1	C3	116.93(15)

**Table 6 Hydrogen Bonds for 82.**

D	H	A	d(D-H)/Å	d(H-A)/Å	d(D-A)/Å	D-H-A/°
O1	H1	N1 <sup>1</sup>	0.82(3)	2.03(3)	2.8281(18)	165(2)

<sup>1</sup>-X, 1/2+Y, 2-Z

**Table 7 Torsion Angles for 82.**

A	B	C	D	Angle/°
C1	C2	C3	N1	1.3(3)
C1	C5	C6	C7	-103.84(18)
C1	C5	C6	O1	134.62(15)
C2	C1	C5	C4	-0.6(2)
C2	C1	C5	C6	-178.23(14)
C2	C3	N1	C4	0.2(2)
C4	C5	C6	C7	78.59(17)
C4	C5	C6	O1	-42.94(19)
C5	C1	C2	C3	-1.0(2)
C5	C4	N1	C3	-2.0(2)
C5	C6	C7	C8	61.31(17)
C5	C6	C7	C9	-60.24(18)
C5	C6	C7	C10	-177.86(13)
C6	C7	C10	C11	-66.61(18)
C7	C10	C11	C12	87.60(19)
C7	C10	C11	C16	-95.82(18)
C8	C7	C10	C11	53.48(19)

A	B	C	D	Angle/°
C9	C7	C10	C11	172.85(14)
C10	C11	C12	C13	175.97(14)
C10	C11	C16	C15	-176.34(15)
C11	C12	C13	C14	0.2(2)
C12	C11	C16	C15	0.4(2)
C12	C13	C14	C15	0.6(2)
C13	C14	C15	C16	-1.0(3)
C14	C15	C16	C11	0.4(3)
C16	C11	C12	C13	-0.7(2)
Cl1	C1	C2	C3	-179.15(13)
Cl1	C1	C5	C4	177.46(11)
Cl1	C1	C5	C6	-0.2(2)
N1	C4	C5	C1	2.2(2)
N1	C4	C5	C6	-179.98(14)
O1	C6	C7	C8	-176.97(13)
O1	C6	C7	C9	61.49(17)
O1	C6	C7	C10	-56.14(17)

**Table 8 Hydrogen Atom Coordinates (Å×10<sup>4</sup>) and Isotropic Displacement Parameters (Å<sup>2</sup>×10<sup>3</sup>) for 82.**

Atom	x	y	z	U(eq)
H2	-3527	4719	7692	23
H3	-3926	1961	8551	25
H4	-30	386	9299	20
H6	1272	4418	8288	17
H8A	506	4004	5803	28

H8B	-589	2465	5789	28
H8C	575	2078	5161	28
H9A	196	-307	7192	29
H9B	1736	-447	8297	29
H9C	1495	-704	6750	29
H10A	3571	1934	8302	22
H10B	3155	1459	6760	22
H12	3892	5238	9028	25
H13	4711	8061	8646	33
H14	4744	8785	6514	36
H15	3905	6672	4753	36
H16	3101	3823	5135	28
H1	2160(20)	3390(40)	10210(20)	33(6)

A suitable crystal was selected on a **SuperNova, Dual, Cu at zero, Atlas** diffractometer. The crystal was kept at 100.1(9) K during data collection. Using Olex2 [1], the structure was solved with the ShelXS [2] structure solution program using Direct Methods and refined with the ShelXL [3] refinement package using Least Squares minimisation.

Dolomanov, O.V., Bourhis, L.J., Gildea, R.J., Howard, J.A.K. & Puschmann, H. (2009), J. Appl. Cryst. 42, 339-341.

Sheldrick, G.M. (2008). Acta Cryst. A64, 112-122.

Sheldrick, G.M. (2015). Acta Cryst. C71, 3-8.

Crystal structure determination of **82**

**Crystal Data** for C<sub>16</sub>H<sub>18</sub>ClNO (*M* = 275.76 g/mol): monoclinic, space group P2<sub>1</sub> (no. 4), *a* = 10.07501(9) Å, *b* = 7.27003(7) Å, *c* = 10.52824(9) Å, *β* = 111.3486(10)°, *V* = 718.234(12) Å<sup>3</sup>, *Z* = 2, *T* = 100.1(9) K, *μ*(CuKα) = 2.274 mm<sup>-1</sup>, *D*<sub>calc</sub> = 1.275 g/cm<sup>3</sup>, 25684 reflections measured (9.018° ≤ 2θ ≤ 149.032°), 2841 unique (*R*<sub>int</sub> = 0.0205, *R*<sub>sigma</sub> = 0.0094) which were used in all calculations. The final *R*<sub>1</sub> was 0.0205 (*I* > 2σ(*I*)) and *wR*<sub>2</sub> was 0.0540 (all data).

Refinement model description

Number of restraints - 1, number of constraints - unknown.

Details:

1.Fixed Uiso

At 1.2 times of:

All C(H) groups, All C(H,H) groups

At 1.5 times of:

All C(H,H,H) groups

2.a Ternary CH refined with riding coordinates:

C6(H6)

2.b Secondary CH2 refined with riding coordinates:

C10(H10A,H10B)

2.c Aromatic/amide H refined with riding coordinates:

C2(H2), C3(H3), C4(H4), C12(H12), C13(H13), C14(H14), C15(H15), C16(H16)

2.d Idealised Me refined as rotating group:

C8(H8A,H8B,H8C), C9(H9A,H9B,H9C)

## Compound 87

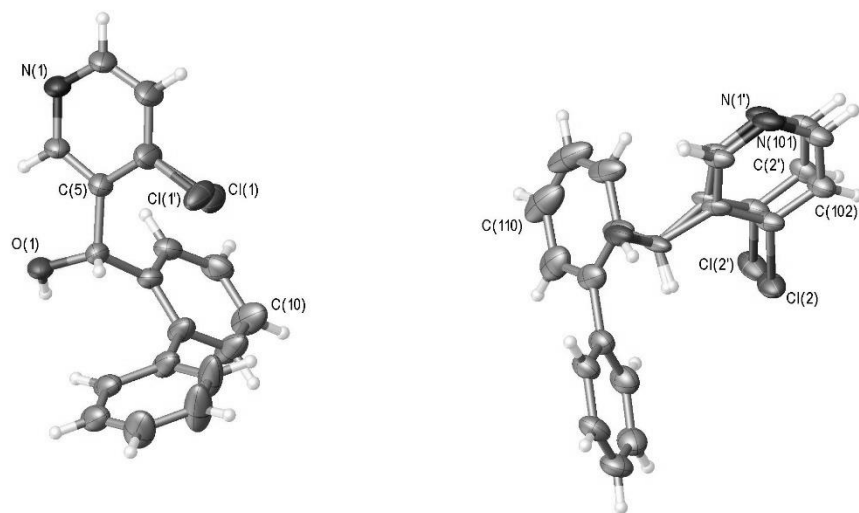


*Figure 56 - Crystal structure of 87 with ellipsoids drawn at the 50 % probability level. The structure contains two crystallographically-independent molecules. In molecule 1 the chlorine atom Cl(1)/Cl(1') is disordered over two positions at a refined percentage occupancy ratio of 58 (4):42 (4). In molecule 2 the group C(101)-C(105), N(101), Cl(2)/C(1')-C(5'), N(1'), Cl(2') is disordered over two positions at a refined percentage occupancy ratio of 52 (7):48 (7).*

### Notes:

The data used in this refinement have been treated with the SQUEEZE algorithm in PLATON due to the presence in the structure of a significant amount of highly disordered solvent (probably mostly chloroform) which it was not possible to refine successfully

The structure contains two crystallographically-independent molecules. In molecule 1 the chlorine atom Cl(1)/Cl(1') is disordered over two positions at a refined percentage occupancy ratio of 58 (4):42 (4). In molecule 2 the group C(101)-C(105), N(101), Cl(2)/C(1')-C(5'), N(1'), Cl(2') is disordered over two positions at a refined percentage occupancy ratio of 52 (7):48 (7).

The structure is in a centrosymmetric space group such that in half the molecules in the unit cell C(6) and C(106) are *S* and in the other half they are *R*. All hydrogen atoms were fixed as riding models.

Hydrogen bonding is detailed in Table 6 of the DTP-713-F4\_sq\_Tables.html report and details of the results from the application of the SQUEEZE algorithm are given in Table 10. Other tables in the report give bond lengths, angles and torsion angles with standard deviations given in brackets.

**Table 1 Crystal data and structure refinement for 87.**

Identification code	DTP-713-F4_sq
Empirical formula	C <sub>18</sub> H <sub>14</sub> ClNO
Formula weight	295.75
Temperature/K	99.96(14)
Crystal system	triclinic
Space group	P-1
a/Å	10.6546(7)
b/Å	12.1477(9)
c/Å	15.0701(11)
α/°	100.532(6)
β/°	97.717(6)
γ/°	93.494(6)
Volume/Å <sup>3</sup>	1892.9(2)
Z	4

$\rho_{\text{calc}}/\text{cm}^3$	1.038
$\mu/\text{mm}^{-1}$	1.763
F(000)	616.0
Crystal size/ $\text{mm}^3$	$0.2482 \times 0.1226 \times 0.0532$
Radiation	$\text{CuK}\alpha$ ( $\lambda = 1.54184$ )
2 $\theta$ range for data collection/ $^\circ$	6.032 to 140.112
Index ranges	$-11 \leq h \leq 12, -13 \leq k \leq 14, -18 \leq l \leq 16$
Reflections collected	11024
Independent reflections	7011 [ $R_{\text{int}} = 0.0448, R_{\text{sigma}} = 0.0553$ ]
Data/restraints/parameters	7011/208/455
Goodness-of-fit on $F^2$	1.039
Final R indexes [ $ I  \geq 2\sigma(I)$ ]	$R_1 = 0.0902, wR_2 = 0.2499$
Final R indexes [all data]	$R_1 = 0.1080, wR_2 = 0.2693$
Largest diff. peak/hole / $\text{e } \text{\AA}^{-3}$	0.59/-0.56

**Table 2 Fractional Atomic Coordinates ( $\times 10^4$ ) and Equivalent Isotropic Displacement Parameters ( $\text{\AA}^2 \times 10^3$ ) for 87.  $U_{\text{eq}}$  is defined as 1/3 of the trace of the orthogonalised  $U_{ij}$  tensor.**

Atom	x	y	z	$U(\text{eq})$
C1	7395(5)	10338(6)	2656(3)	59.7(14)
C2	8661(5)	10497(6)	2541(4)	65.8(16)
C3	8941(4)	10256(5)	1673(3)	55.0(13)
C4	6840(4)	9743(4)	1070(3)	39.5(9)
C5	6443(4)	9966(4)	1911(3)	40.5(9)
C6	5040(4)	9825(4)	2017(3)	37.5(9)
C7	4791(4)	8923(4)	2564(3)	38.9(9)
C8	4001(5)	9082(5)	3244(3)	52.2(12)
C9	3863(6)	8244(6)	3750(5)	73.4(19)

C10	4441(6)	7258(5)	3589(5)	71.8(18)
C11	5206(4)	7100(4)	2905(4)	50.2(11)
C12	5354(4)	7918(4)	2396(3)	41.5(9)
C13	3372(5)	10130(5)	3478(4)	54.1(13)
C14	3531(7)	10714(7)	4380(4)	86(2)
C15	2950(9)	11696(8)	4632(4)	102(3)
C16	2175(7)	12098(6)	3960(4)	76.1(19)
C17	2012(5)	11554(5)	3080(4)	53.5(12)
C18	2600(4)	10575(4)	2827(3)	46.1(10)
Cl1	7007(5)	10385(15)	3763(2)	53(2)
Cl1'	7051(6)	10910(20)	3739(4)	59(3)
N1	8074(3)	9859(4)	934(3)	46.4(9)
O1	4322(3)	9588(3)	1129.9(19)	40.4(7)
C101	9910(8)	6799(8)	10914(7)	35.8(16)
C102	10957(8)	6685(8)	11535(8)	41.8(16)
C103	12025(10)	7410(9)	11592(8)	41.1(18)
C104	11014(19)	8317(12)	10495(12)	35(2)
C105	9932(10)	7617(9)	10361(7)	32.7(18)
C1'	10004(8)	6419(8)	10510(8)	34.5(16)
C2'	11079(8)	6284(8)	11099(8)	37.9(17)
C3'	12098(10)	7083(9)	11249(9)	39.0(19)
C4'	11080(20)	8082(14)	10333(13)	34(2)
C5'	9977(11)	7320(10)	10100(9)	34(2)
C106	8804(3)	7640(4)	9580(4)	46.0(11)
C107	8689(4)	6803(4)	8683(4)	50.1(12)
C108	7503(4)	6275(4)	8239(4)	47.8(11)
C109	7426(6)	5549(5)	7401(4)	62.4(14)
C110	8510(8)	5347(6)	6990(5)	85(2)

C111	9667(8)	5871(6)	7419(6)	88(3)	C10	77(4)	68(4)	98(5)	53(3)	45(3)	38(3)
C112	9755(5)	6574(5)	8254(5)	68.0(18)	C11	38(2)	49(3)	70(3)	20(2)	11(2)	16.6(19)
C113	6306(4)	6436(4)	8637(3)	43.5(10)	C12	27.0(18)	53(2)	46(2)	11.2(19)	8.3(16)	5.4(17)
C114	5583(4)	5482(4)	8762(3)	48.7(11)	C13	52(3)	70(3)	61(3)	42(3)	30(2)	32(2)
C115	4438(4)	5599(4)	9096(4)	52.3(11)	C14	111(5)	121(6)	57(3)	52(4)	37(3)	87(5)
C116	4002(4)	6649(5)	9300(4)	53.2(12)	C15	140(7)	141(7)	53(3)	39(4)	38(4)	110(6)
C117	4710(4)	7591(4)	9189(3)	48.2(11)	C16	90(4)	86(4)	73(4)	38(3)	34(3)	64(4)
C118	5857(4)	7492(4)	8846(3)	40.9(9)	C17	45(2)	65(3)	67(3)	38(3)	22(2)	21(2)
Cl2	8536(2)	5897(3)	10814(3)	47.2(10)	C18	36(2)	57(3)	59(3)	34(2)	20.7(19)	14.1(19)
N101	12079(15)	8234(10)	11091(10)	38(2)	Cl1	43.5(14)	79(5)	34.5(11)	15.0(14)	1.3(8)	-15.0(18)
Cl2'	8719(2)	5420(3)	10316(4)	49.0(12)	Cl1'	51.0(18)	84(8)	35.5(16)	7(2)	8.0(12)	-30(3)
N1'	12118(17)	7971(12)	10886(11)	37(2)	N1	25.6(16)	72(3)	48(2)	26.5(18)	8.9(14)	-1.4(16)
O101	8864(3)	8739(3)	9374(2)	44.8(7)	O1	25.2(13)	55.7(18)	42.5(16)	17.9(13)	5.0(11)	-5.1(12)

**Table 3 Anisotropic Displacement Parameters ( $\text{\AA}^2 \times 10^3$ ) for 87. The Anisotropic displacement factor exponent takes the form: -  $2\pi^2[h^2a^{*2}U_{11}+2hka^*b^*U_{12}+...]$ .**

Atom	U <sub>11</sub>	U <sub>22</sub>	U <sub>33</sub>	U <sub>23</sub>	U <sub>13</sub>	U <sub>12</sub>
C1	35(2)	105(4)	37(2)	13(2)	0.8(18)	-6(2)
C2	30(2)	118(5)	48(3)	25(3)	-2.6(19)	-10(3)
C3	24(2)	93(4)	51(3)	27(3)	1.5(18)	-8(2)
C4	22.8(18)	56(3)	43(2)	19.5(18)	3.8(15)	-2.3(16)
C5	27.6(19)	58(3)	37(2)	15.2(18)	3.1(15)	-0.5(17)
C6	28.6(19)	55(2)	31.8(19)	14.1(17)	7.2(15)	4.7(17)
C7	25.3(18)	56(3)	40(2)	15.8(18)	9.6(15)	7.0(17)
C8	48(3)	71(3)	57(3)	36(2)	30(2)	33(2)
C9	76(4)	88(4)	91(4)	62(4)	56(3)	54(3)



C111	93(5)	74(4)	140(7)	71(5)	84(5)	51(4)
C112	46(3)	71(4)	116(5)	66(4)	41(3)	30(3)
C113	33(2)	52(2)	53(3)	27(2)	6.8(17)	10.0(17)
C114	41(2)	47(2)	62(3)	24(2)	3(2)	6.6(19)
C115	39(2)	59(3)	61(3)	24(2)	2(2)	-6(2)
C116	27(2)	67(3)	67(3)	19(2)	4.7(19)	1(2)
C117	29(2)	56(3)	60(3)	12(2)	1.3(18)	11.6(18)
C118	29.3(19)	43(2)	53(2)	17.0(18)	1.4(17)	6.4(16)
Cl2	30.3(10)	52.2(18)	63(2)	31.5(16)	-0.4(10)	-11.6(10)
N101	20(3)	34(5)	66(5)	17(4)	13(3)	4(3)
Cl2'	33.0(12)	37.7(15)	76(3)	29.0(17)	-9.9(13)	-12.8(10)
N1'	20(3)	33(5)	61(5)	9(4)	12(3)	4(3)
O101	26.4(13)	50.1(17)	71(2)	36.7(16)	16.0(13)	12.6(12)

**Table 4 Bond Lengths for 87.**

Atom	Atom	Length/Å	Atom	Atom	Length/Å
C1	C2	1.390(7)	C103	N101	1.362(16)
C1	C5	1.394(6)	C104	C105	1.360(18)
C1	Cl1	1.765(6)	C104	N101	1.37(2)
C1	Cl1'	1.749(8)	C105	C106	1.571(11)
C2	C3	1.365(7)	C1'	C2'	1.390(12)
C3	N1	1.341(6)	C1'	C5'	1.351(15)
C4	C5	1.376(6)	C1'	Cl2'	1.730(9)
C4	N1	1.360(5)	C2'	C3'	1.377(14)
C5	C6	1.527(5)	C3'	N1'	1.295(18)
C6	C7	1.517(6)	C4'	C5'	1.41(2)
C6	O1	1.419(5)	C4'	N1'	1.32(2)

C7	C8	1.405(6)	C5'	C106	1.495(11)
C7	C12	1.390(6)	C106	C107	1.520(8)
C8	C9	1.391(7)	C106	O101	1.425(5)
C8	C13	1.483(7)	C107	C108	1.405(7)
C9	C10	1.378(8)	C107	C112	1.399(7)
C10	C11	1.391(7)	C108	C109	1.392(8)
C11	C12	1.375(7)	C108	C113	1.488(6)
C13	C14	1.396(9)	C109	C110	1.396(8)
C13	C18	1.401(6)	C110	C111	1.372(13)
C14	C15	1.392(8)	C111	C112	1.375(11)
C15	C16	1.398(8)	C113	C114	1.408(6)
C16	C17	1.352(9)	C113	C118	1.394(6)
C17	C18	1.393(7)	C114	C115	1.386(7)
C101	C102	1.387(12)	C115	C116	1.380(8)
C101	C105	1.409(13)	C116	C117	1.380(7)
C101	Cl2	1.746(8)	C117	C118	1.392(6)
C102	C103	1.378(13)			

**Table 5 Bond Angles for 87.**

Atom	Atom	Atom	Angle/°	Atom	Atom	Atom	Angle/°
C2	C1	C5	121.3(4)	C105	C104	N101	124.2(12)
C2	C1	Cl1	119.4(4)	C101	C105	C106	121.0(8)
C2	C1	Cl1'	115.2(4)	C104	C105	C101	116.5(10)
C5	C1	Cl1	118.5(4)	C104	C105	C106	122.3(10)
C5	C1	Cl1'	122.1(4)	C2'	C1'	Cl2'	118.9(7)
C3	C2	C1	117.4(4)	C5'	C1'	C2'	119.9(8)
N1	C3	C2	123.9(4)	C5'	C1'	Cl2'	121.2(7)

N1	C4	C5	124.2(4)	C3'	C2'	C1'	118.5(9)
C1	C5	C6	122.3(4)	N1'	C3'	C2'	124.4(11)
C4	C5	C1	116.0(4)	N1'	C4'	C5'	126.0(14)
C4	C5	C6	121.7(4)	C1'	C5'	C4'	115.4(11)
C7	C6	C5	111.3(3)	C1'	C5'	C106	123.8(10)
O1	C6	C5	107.7(3)	C4'	C5'	C106	119.8(11)
O1	C6	C7	112.6(3)	C5'	C106	C107	101.5(6)
C8	C7	C6	121.3(4)	C107	C106	C105	119.8(5)
C12	C7	C6	119.8(4)	O101	C106	C105	107.5(5)
C12	C7	C8	118.9(4)	O101	C106	C5'	116.5(6)
C7	C8	C13	122.7(4)	O101	C106	C107	107.6(4)
C9	C8	C7	118.4(4)	C108	C107	C106	121.2(4)
C9	C8	C13	118.8(4)	C112	C107	C106	120.9(5)
C10	C9	C8	122.3(5)	C112	C107	C108	117.9(6)
C9	C10	C11	118.9(5)	C107	C108	C113	122.7(5)
C12	C11	C10	119.7(4)	C109	C108	C107	119.6(5)
C11	C12	C7	121.8(4)	C109	C108	C113	117.6(5)
C14	C13	C8	120.1(4)	C108	C109	C110	120.9(7)
C14	C13	C18	117.2(5)	C111	C110	C109	119.6(7)
C18	C13	C8	122.7(5)	C110	C111	C112	119.9(5)
C15	C14	C13	122.0(5)	C111	C112	C107	122.1(6)
C14	C15	C16	118.6(6)	C114	C113	C108	118.6(4)
C17	C16	C15	120.6(5)	C118	C113	C108	121.9(4)
C16	C17	C18	120.8(5)	C118	C113	C114	119.4(4)
C17	C18	C13	120.8(5)	C115	C114	C113	120.0(5)
C3	N1	C4	117.0(4)	C116	C115	C114	120.1(4)
C102	C101	C105	121.7(8)	C115	C116	C117	120.4(4)
C102	C101	Cl2	118.9(6)	C116	C117	C118	120.5(5)

C105	C101	Cl2	119.4(7)	C117	C118	C113	119.6(4)
C103	C102	C101	117.2(8)	C103	N101	C104	117.2(11)
N101	C103	C102	123.2(10)	C3'	N1'	C4'	115.9(12)

**Table 6 Hydrogen Bonds for 87.**

D	H	A	d(D-H)/Å	d(H-A)/Å	d(D-A)/Å	D-H-A/°
O1	H1	N101 <sup>1</sup>	0.84	2.01	2.805(15)	157.0
O1	H1	N1' <sup>1</sup>	0.84	2.09	2.907(17)	164.7
O101	H101	N1' <sup>2</sup>	0.84	1.94	2.755(5)	163.2

<sup>1</sup>-1+X,+Y,-1+Z; <sup>2</sup>+X,+Y,1+Z

**Table 7 Torsion Angles for 87.**

A	B	C	D	Angle/°	A	B	C	D	Angle/°
C1	C2	C3	N1	-1.3(10)	C104	C105	C106	O101	-25.8(11)
C1	C5	C6	C7	-64.1(6)	C105	C101	C102	C103	0.2(16)
C1	C5	C6	O1	172.1(5)	C105	C104	N101	C103	-1.6(17)
C2	C1	C5	C4	1.5(9)	C105	C106	C107	C108	138.8(6)
C2	C1	C5	C6	-177.8(5)	C105	C106	C107	C112	-44.1(7)
C2	C3	N1	C4	3.0(8)	C1'	C2'	C3'	N1'	1.0(18)
C4	C5	C6	C7	116.7(5)	C1'	C5'	C106	C107	-77.7(11)
C4	C5	C6	O1	-7.2(6)	C1'	C5'	C106	O101	165.8(9)
C5	C1	C2	C3	-1.1(10)	C2'	C1'	C5'	C4'	-1.3(16)
C5	C4	N1	C3	-2.6(7)	C2'	C1'	C5'	C106	-169.7(10)
C5	C6	C7	C8	136.6(5)	C2'	C3'	N1'	C4'	-0.6(18)

C5	C6	C7	C12	-43.1(5)	C4'	C5'	C106	C107	114.4(10)	Cl1'	C1	C5	C4	167.5(11)	C118	C113	C114	C115	-0.4(7)
C6	C7	C8	C9	-176.8(5)	C4'	C5'	C106	O101	-2.1(13)	Cl1'	C1	C5	C6	-11.7(13)	Cl2	C101	C102	C103	179.8(8)
C6	C7	C8	C13	-0.5(8)	C5'	C1'	C2'	C3'	0.0(16)	N1	C4	C5	C1	0.4(7)	Cl2	C101	C105	C104	177.8(8)
C6	C7	C12	C11	176.7(4)	C5'	C4'	N1'	C3'	-0.9(19)	N1	C4	C5	C6	179.7(4)	Cl2	C101	C105	C106	-7.3(13)
C7	C8	C9	C10	-2.0(11)	C5'	C106	C107	C108	139.0(7)	O1	C6	C7	C8	-102.3(5)	N101	C104	C105	C101	3.3(16)
C7	C8	C13	C14	-126.0(6)	C5'	C106	C107	C112	-43.9(7)	O1	C6	C7	C12	78.0(5)	N101	C104	C105	C106	-171.6(10)
C7	C8	C13	C18	54.4(8)	C106	C107	C108	C109	177.4(4)	C101	C102	C103	N101	1.7(17)	Cl2'	C1'	C2'	C3'	180.0(8)
C8	C7	C12	C11	-3.0(7)	C106	C107	C108	C113	-4.1(6)	C101	C105	C106	C107	-77.4(10)	Cl2'	C1'	C5'	C4'	178.7(9)
C8	C9	C10	C11	1.0(12)	C106	C107	C112	C111	-176.2(4)	C101	C105	C106	O101	159.5(8)	Cl2'	C1'	C5'	C106	10.4(16)
C8	C13	C14	C15	-179.4(7)	C107	C108	C109	C110	-0.7(7)	C102	C101	C105	C104	-2.5(15)	N1'	C4'	C5'	C1'	1.9(19)
C8	C13	C18	C17	179.0(4)	C107	C108	C113	C114	-123.4(5)	C102	C101	C105	C106	172.4(9)	N1'	C4'	C5'	C106	170.8(12)
C9	C8	C13	C14	50.4(9)	C107	C108	C113	C118	59.8(6)	C102	C103	N101	C104	-1.1(16)	O101	C106	C107	C108	-98.1(4)
C9	C8	C13	C18	-129.3(6)	C108	C107	C112	C111	0.9(7)	C104	C105	C106	C107	97.2(10)	O101	C106	C107	C112	78.9(4)
C9	C10	C11	C12	-1.0(10)	C108	C109	C110	C111	0.1(8)										
C10	C11	C12	C7	2.1(8)	C108	C113	C114	C115	-177.4(4)										
C12	C7	C8	C9	2.9(8)	C108	C113	C118	C117	177.9(4)										
C12	C7	C8	C13	179.2(5)	C109	C108	C113	C114	55.2(6)										
C13	C8	C9	C10	-178.5(7)	C109	C108	C113	C118	-121.7(5)										
C13	C14	C15	C16	0.6(14)	C109	C110	C111	C112	1.1(8)										
C14	C13	C18	C17	-0.6(8)	C110	C111	C112	C107	-1.6(8)										
C14	C15	C16	C17	-1.1(13)	C112	C107	C108	C109	0.3(6)										
C15	C16	C17	C18	0.8(10)	C112	C107	C108	C113	178.8(4)										
C16	C17	C18	C13	0.1(8)	C113	C108	C109	C110	-179.3(4)										
C18	C13	C14	C15	0.2(11)	C113	C114	C115	C116	0.5(8)										
Cl1	C1	C2	C3	168.5(8)	C114	C113	C118	C117	1.0(7)										
Cl1	C1	C5	C4	-168.2(7)	C114	C115	C116	C117	-1.2(8)										
Cl1	C1	C5	C6	12.5(9)	C115	C116	C117	C118	1.8(8)										
Cl1'	C1	C2	C3	-168.1(11)	C116	C117	C118	C113	-1.7(7)										

Table 8 Hydrogen Atom Coordinates ( $\text{\AA} \times 10^4$ ) and Isotropic Displacement Parameters ( $\text{\AA}^2 \times 10^3$ ) for 87.					
Atom	x	y	z	U(eq)	
H2	9308	10762	3048	79	
H3	9802	10376	1586	66	
H4	6212	9493	550	47	
H6	4803	10554	2351	45	
H9	3352	8357	4224	88	
H10	4319	6695	3939	86	
H11	5623	6431	2790	60	
H12	5856	7792	1917	50	
H14	4053	10433	4835	104	
H15	3077	12085	5249	123	

H16	1759	12759	4122	91
H17	1491	11843	2629	64
H18	2476	10205	2205	55
H1	3787	9037	1087	61
H102	10939	6131	11904	50
H103	12759	7331	12002	49
H104	11033	8900	10153	42
H2'	11111	5655	11392	45
H3'	12833	6977	11645	47
H4'	11072	8734	10068	41
H106	7997	7532	9836	55
H10A	8054	7516	9894	55
H109	6625	5185	7105	75
H110	8447	4850	6418	102
H111	10406	5747	7138	105
H112	10566	6916	8549	82
H114	5879	4759	8617	58
H115	3954	4956	9184	63
H116	3209	6724	9517	64
H117	4413	8312	9348	58
H118	6330	8141	8756	49
H101	8611	9189	9792	67

**Table 9 Atomic Occupancy for 87.**

Atom	Occupancy	Atom	Occupancy	Atom	Occupancy
Cl1	0.58(4)	Cl1'	0.42(4)	C101	0.520(7)
C102	0.520(7)	H102	0.520(7)	C103	0.520(7)

H103	0.520(7)	C104	0.520(7)	H104	0.520(7)
C105	0.520(7)	C1'	0.480(7)	C2'	0.480(7)
H2'	0.480(7)	C3'	0.480(7)	H3'	0.480(7)
C4'	0.480(7)	H4'	0.480(7)	C5'	0.480(7)
H106	0.520(7)	H10A	0.480(7)	Cl2	0.520(7)
N101	0.520(7)	Cl2'	0.480(7)	N1'	0.480(7)

**Table 10 Solvent masks information for 87.**

Number	X	Y	Z	Volume	Electron count	Content
1	-0.005	-0.022	0.500	549	236	

#### Experimental

Single crystals of C<sub>18</sub>H<sub>14</sub>ClNO **87** were obtained by slow evaporation from chloroform-*d*. A suitable crystal was selected on a **SuperNova, Dual, Cu at zero, Atlas** diffractometer. The crystal was kept at 99.96(14) K during data collection. Using Olex2 [1], the structure was solved with the ShelXS [2] structure solution program using Direct Methods and refined with the ShelXL [3] refinement package using Least Squares minimisation.

1. Dolomanov, O.V., Bourhis, L.J., Gildea, R.J., Howard, J.A.K. & Puschmann, H. (2009), *J. Appl. Cryst.* 42, 339-341.
2. Sheldrick, G.M. (2008). *Acta Cryst.* A64, 112-122.
3. Sheldrick, G.M. (2015). *Acta Cryst.* C71, 3-8.

#### Crystal structure determination of 87

**Crystal Data** for C<sub>18</sub>H<sub>14</sub>ClNO (*M* = 295.75 g/mol): triclinic, space group P-1 (no. 2), *a* = 10.6546(7) Å, *b* = 12.1477(9) Å, *c* = 15.0701(11) Å,  $\alpha$  = 100.532(6)°,

$\theta = 97.717(6)^\circ$ ,  $\gamma = 93.494(6)^\circ$ ,  $V = 1892.9(2) \text{ \AA}^3$ ,  $Z = 4$ ,  $T = 99.96(14) \text{ K}$ ,  $\mu(\text{CuK}\alpha) = 1.763 \text{ mm}^{-1}$ ,  $D_{\text{calc}} = 1.038 \text{ g/cm}^3$ , 11024 reflections measured ( $6.032^\circ \leq 2\theta \leq 140.112^\circ$ ), 7011 unique ( $R_{\text{int}} = 0.0448$ ,  $R_{\text{sigma}} = 0.0553$ ) which were used in all calculations. The final  $R_1$  was 0.0902 ( $I > 2\sigma(I)$ ) and  $wR_2$  was 0.2693 (all data).

### Refinement model description

Number of restraints - 208, number of constraints - unknown.

Details:

1. Fixed Uiso

At 1.2 times of:

All C(H) groups, All C(H,H) groups

At 1.5 times of:

All O(H) groups

2. Restrained distances

$\text{Cl1-C1} = \text{Cl1'-C1}$

1.73 with sigma of 0.02

$\text{C105-C106} = \text{C5'-C106}$

1.52 with sigma of 0.02

3. Rigid bond restraints

$\text{C101, C102, C103, C104, C105, C1', C2', C3', C4', C5', N1', N101}$

with sigma for 1-2 distances of 0.005 and sigma for 1-3 distances of 0.005

4. Uiso/Uaniso restraints and constraints

$\text{C101} \approx \text{C102} \approx \text{C103} \approx \text{C104} \approx \text{C105} \approx \text{C1'} \approx \text{C2'} \approx \text{C3'}$

$\approx \text{C4'} \approx \text{C5'} \approx \text{N1'} \approx \text{N101}$ : within 2A with sigma of 0.01 and sigma for terminal atoms of 0.02

5. Others

$\text{Sof}(\text{C1'}) = \text{Sof}(\text{C2'}) = \text{Sof}(\text{H2'}) = \text{Sof}(\text{C3'}) = \text{Sof}(\text{H3'}) = \text{Sof}(\text{C4'}) = \text{Sof}(\text{H4'}) = \text{Sof}(\text{C5'}) =$

$\text{Sof}(\text{H10A}) = \text{Sof}(\text{Cl2'}) = \text{Sof}(\text{N1'}) = 1\text{-FVAR}(1)$

$\text{Sof}(\text{C101}) = \text{Sof}(\text{C102}) = \text{Sof}(\text{H102}) = \text{Sof}(\text{C103}) = \text{Sof}(\text{H103}) = \text{Sof}(\text{C104}) = \text{Sof}(\text{H104}) =$

$\text{Sof}(\text{C105}) = \text{Sof}(\text{H106}) = \text{Sof}(\text{Cl2}) = \text{Sof}(\text{N101}) = \text{FVAR}(1)$

$\text{Sof}(\text{Cl1'}) = 1\text{-FVAR}(2)$

$\text{Sof}(\text{Cl1}) = \text{FVAR}(2)$

6.a Ternary CH refined with riding coordinates:

$\text{C6(H6), C106(H106), C106(H10A)}$

6.b Aromatic/amide H refined with riding coordinates:

$\text{C2(H2), C3(H3), C4(H4), C9(H9), C10(H10), C11(H11), C12(H12), C14(H14), C15(H15), C16(H16), C17(H17), C18(H18), C102(H102), C103(H103), C104(H104),}$

$\text{C2'(H2'), C3'(H3'), C4'(H4'), C109(H109), C110(H110), C111(H111), C112(H112),}$

$\text{C114(H114), C115(H115), C116(H116), C117(H117), C118(H118)}$

6.c Idealised tetrahedral OH refined as rotating group:

$\text{O1(H1), O101(H101)}$

### Compound 126

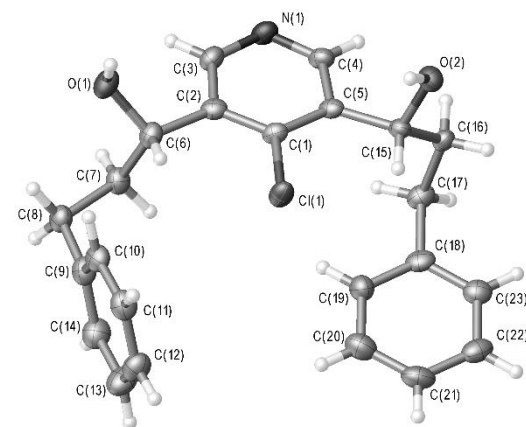


Figure S7 - Crystal structure of 126 with ellipsoids drawn at the 50 % probability level.

Notes:

Despite best efforts in crystal growth and data collection the diffraction was weak, especially at higher diffraction angles due to the small dimensions of the crystal. This has resulted in low Friedel pair coverage and some other quality issues with the

refinement, including somewhat high residual electron density. For this reason, even though the Flack parameter is close to zero with a small standard deviation, we have not claimed that the absolute structure has been determined from the diffraction data.

However, the absolute structure as reported, with the Flack parameter (low Friedel pair coverage) being -0.03 (3), gives C(6) as *S* and C(15) as *R*.

The hydrogen atoms belonging to the hydroxyl group O(1) and O(2) were located in the electron density and their positions refined (subject to bond length restraint for O(1)-H(1)). The remaining hydrogen atoms were fixed as riding models. The U(iso) values for all hydrogen atoms were based on the U(eq) of the parent.

Tables in the report DTP-660-F4\_Tables.html give bond lengths, angles and torsion angles with standard deviations given in brackets.

**Table 1 Crystal data and structure refinement for 126.**

Identification code	DTP-660-F4
Empirical formula	C <sub>23</sub> H <sub>24</sub> ClNO <sub>2</sub>
Formula weight	381.88
Temperature/K	99.97(10)
Crystal system	monoclinic
Space group	P2 <sub>1</sub>
a/Å	9.0658(8)
b/Å	7.3204(5)
c/Å	15.6038(9)
α/°	90
β/°	102.886(7)

γ/°	90
Volume/Å <sup>3</sup>	1009.47(12)
Z	2
ρ <sub>calc</sub> /g/cm <sup>3</sup>	1.256
μ/mm <sup>-1</sup>	1.804
F(000)	404.0
Crystal size/mm <sup>3</sup>	0.5683 × 0.0467 × 0.0426
Radiation	CuKα (λ = 1.54184)
2θ range for data collection/°	5.81 to 136.452
Index ranges	-10 ≤ h ≤ 10, -8 ≤ k ≤ 5, -17 ≤ l ≤ 18
Reflections collected	3690
Independent reflections	2636 [R <sub>int</sub> = 0.0510, R <sub>sigma</sub> = 0.0610]
Data/restraints/parameters	2636/2/250
Goodness-of-fit on F <sup>2</sup>	1.025
Final R indexes [I ≥ 2σ (I)]	R <sub>1</sub> = 0.0598, wR <sub>2</sub> = 0.1561
Final R indexes [all data]	R <sub>1</sub> = 0.0646, wR <sub>2</sub> = 0.1614
Largest diff. peak/hole / e Å <sup>-3</sup>	0.94/-0.43
Flack parameter	-0.03(3)

**Table 2 Fractional Atomic Coordinates (×10<sup>4</sup>) and Equivalent Isotropic Displacement Parameters (Å<sup>2</sup>×10<sup>3</sup>) for 126. U<sub>eq</sub> is defined as 1/3 of of the trace of the orthogonalised U<sub>ij</sub> tensor.**

Atom	x	y	z	U(eq)
C1	6346(6)	5636(7)	1277(3)	22.7(9)
C2	7683(6)	5688(7)	987(3)	24.9(10)
C3	7920(6)	7209(7)	503(3)	26.5(10)
C4	5699(6)	8525(8)	623(3)	26.8(10)
C5	5295(6)	7070(7)	1103(3)	23.2(9)

C6	8890(6)	4212(7)	1179(3)	26.1(10)
C7	10180(6)	4779(7)	1939(3)	28.9(11)
C8	11289(6)	3199(7)	2279(3)	30.5(11)
C9	10602(6)	1826(7)	2792(3)	30.3(11)
C10	9704(6)	374(7)	2379(3)	29.2(11)
C11	8984(6)	-796(7)	2848(3)	32.4(12)
C12	9152(7)	-574(8)	3753(4)	37.2(12)
C13	10070(7)	836(10)	4173(3)	41.2(14)
C14	10778(7)	2015(9)	3700(4)	37.5(12)
C15	3763(5)	7071(7)	1337(3)	23.1(10)
C16	3372(5)	8840(7)	1742(3)	24.4(9)
C17	4448(6)	9300(7)	2629(3)	29.2(11)
C18	4398(6)	7851(7)	3321(3)	28.9(11)
C19	5583(6)	6611(8)	3562(3)	32.4(11)
C20	5527(7)	5245(9)	4184(3)	40.3(13)
C21	4303(7)	5148(9)	4563(3)	38.4(13)
C22	3113(7)	6383(9)	4328(3)	36.2(13)
C23	3172(6)	7723(8)	3701(3)	31.5(11)
Cl1	5937.4(13)	3702.8(15)	1842.5(7)	30.0(3)
N1	6942(5)	8617(7)	317(2)	27.6(8)
O1	9536(4)	3902(6)	436(2)	33.0(8)
O2	2591(4)	6772(5)	561(2)	27.1(7)

C1	33(2)	14(2)	22.0(17)	-1.7(16)	8.3(16)	-2.2(18)
C2	34(3)	21(2)	19.2(17)	-3.9(18)	4.3(16)	-2(2)
C3	31(2)	25(3)	27(2)	-3(2)	11.9(17)	-2(2)
C4	36(2)	22(2)	22.7(17)	3(2)	7.7(16)	4(2)
C5	34(2)	19(2)	17.4(17)	-2.3(16)	5.9(15)	2.7(19)
C6	29(2)	20(2)	31(2)	-5.0(18)	10.1(18)	-0.1(19)
C7	28(3)	24(3)	35(2)	-2(2)	7.2(18)	0(2)
C8	31(3)	26(3)	36(2)	0(2)	11.9(19)	5(2)
C9	30(2)	24(3)	38(2)	-5(2)	7.7(18)	1(2)
C10	34(3)	22(3)	32(2)	-6(2)	8.9(19)	5(2)
C11	33(3)	22(3)	42(3)	-5(2)	6(2)	-2(2)
C12	42(3)	30(3)	43(3)	2(2)	18(2)	-2(2)
C13	45(3)	45(4)	35(2)	-11(3)	13(2)	-6(3)
C14	38(3)	33(3)	41(3)	-8(2)	9(2)	-3(3)
C15	27(2)	23(2)	19.1(17)	2.3(17)	4.8(15)	3.6(19)
C16	28(2)	23(2)	23.9(18)	2.2(19)	11.0(15)	3(2)
C17	38(3)	24(2)	28(2)	-3.5(19)	11.0(19)	-4(2)
C18	43(3)	25(2)	19.2(18)	-5.6(18)	7.5(17)	-3(2)
C19	33(3)	32(3)	32(2)	1(2)	8.2(19)	6(2)
C20	46(3)	36(3)	36(2)	5(2)	2(2)	3(3)
C21	50(3)	35(3)	27(2)	7(2)	2(2)	-3(3)
C22	43(3)	41(3)	25(2)	-3(2)	10(2)	-9(3)
C23	38(3)	28(3)	27(2)	-3(2)	4.4(18)	-3(2)
Cl1	37.2(6)	19.6(6)	37.7(5)	7.7(5)	18.2(4)	4.1(5)
N1	37(2)	20.6(19)	27.5(16)	0.2(19)	12.6(15)	-2(2)
O1	34.0(18)	32(2)	36.5(16)	-9.3(16)	15.4(13)	-3.3(17)
O2	30.4(18)	20.7(18)	28.9(16)	-4.8(13)	3.7(12)	1.9(14)

**Table 3 Anisotropic Displacement Parameters ( $\text{\AA}^2 \times 10^3$ ) for 126. The Anisotropic displacement factor exponent takes the form: -  $2\pi^2[\text{h}^2\text{a}^{*2}\text{U}_{11}+2\text{hka}^*\text{b}^*\text{U}_{12}+\dots]$ .**

Atom	$\text{U}_{11}$	$\text{U}_{22}$	$\text{U}_{33}$	$\text{U}_{23}$	$\text{U}_{13}$	$\text{U}_{12}$
------	-----------------	-----------------	-----------------	-----------------	-----------------	-----------------

**Table 4 Bond Lengths for 126.**

Atom	Atom	Length/Å	Atom	Atom	Length/Å
C1	C2	1.387(7)	C10	C11	1.382(8)
C1	C5	1.403(7)	C11	C12	1.395(8)
C1	Cl1	1.750(5)	C12	C13	1.394(9)
C2	C3	1.389(7)	C13	C14	1.383(9)
C2	C6	1.519(7)	C15	C16	1.517(7)
C3	N1	1.348(7)	C15	O2	1.439(5)
C4	C5	1.397(7)	C16	C17	1.542(6)
C4	N1	1.320(6)	C17	C18	1.522(7)
C5	C15	1.513(7)	C18	C19	1.392(8)
C6	C7	1.525(6)	C18	C23	1.375(8)
C6	O1	1.429(6)	C19	C20	1.402(8)
C7	C8	1.547(7)	C20	C21	1.371(9)
C8	C9	1.503(8)	C21	C22	1.393(9)
C9	C10	1.405(7)	C22	C23	1.395(8)
C9	C14	1.398(7)			

**Table 5 Bond Angles for 126.**

Atom	Atom	Atom	Angle/°	Atom	Atom	Atom	Angle/°
C2	C1	C5	121.4(4)	C11	C10	C9	121.4(4)
C2	C1	Cl1	119.1(4)	C10	C11	C12	120.4(5)
C5	C1	Cl1	119.5(4)	C13	C12	C11	118.8(5)
C1	C2	C3	116.9(5)	C14	C13	C12	120.7(5)
C1	C2	C6	124.0(4)	C13	C14	C9	121.2(5)
C3	C2	C6	119.0(5)	C5	C15	C16	114.4(4)
N1	C3	C2	123.7(5)	O2	C15	C5	110.0(3)

N1	C4	C5	125.4(5)	O2	C15	C16	106.4(4)
C1	C5	C15	125.0(4)	C15	C16	C17	113.6(4)
C4	C5	C1	115.3(4)	C18	C17	C16	111.8(4)
C4	C5	C15	119.6(4)	C19	C18	C17	120.2(5)
C2	C6	C7	110.7(4)	C23	C18	C17	120.5(5)
O1	C6	C2	111.1(4)	C23	C18	C19	119.2(5)
O1	C6	C7	107.0(4)	C18	C19	C20	120.5(5)
C6	C7	C8	113.0(4)	C21	C20	C19	119.5(6)
C9	C8	C7	111.6(4)	C20	C21	C22	120.5(5)
C10	C9	C8	121.9(4)	C21	C22	C23	119.5(5)
C14	C9	C8	120.4(5)	C18	C23	C22	120.8(5)
C14	C9	C10	117.6(5)	C4	N1	C3	117.2(5)

**Table 6 Torsion Angles for 126.**

A	B	C	D	Angle/°	A	B	C	D	Angle/°
C1	C2	C3	N1	1.0(7)	C10	C9	C14	C13	-1.2(8)
C1	C2	C6	C7	-99.7(5)	C10	C11	C12	C13	-0.6(9)
C1	C2	C6	O1	141.6(4)	C11	C12	C13	C14	1.2(9)
C1	C5	C15	C16	135.5(4)	C12	C13	C14	C9	-0.3(10)
C1	C5	C15	O2	-104.8(5)	C14	C9	C10	C11	1.8(8)
C2	C1	C5	C4	-0.1(6)	C15	C16	C17	C18	-61.8(6)
C2	C1	C5	C15	175.5(4)	C16	C17	C18	C19	105.1(6)
C2	C3	N1	C4	0.3(7)	C16	C17	C18	C23	-73.5(6)
C2	C6	C7	C8	169.2(4)	C17	C18	C19	C20	-178.5(5)
C3	C2	C6	C7	79.4(5)	C17	C18	C23	C22	179.2(4)
C3	C2	C6	O1	-39.4(6)	C18	C19	C20	C21	-0.7(8)
C4	C5	C15	C16	-49.1(5)	C19	C18	C23	C22	0.6(7)



C4 C5 C15 O2	70.6(5)	C19 C20 C21 C22	0.6(8)	H14	11382	2951	3992	45
C5 C1 C2 C3	-1.1(6)	C20 C21 C22 C23	0.2(8)	H15	3736	6072	1752	28
C5 C1 C2 C6	177.9(4)	C21 C22 C23 C18	-0.8(8)	H16A	2348	8755	1828	29
C5 C4 N1 C3	-1.8(7)	C23 C18 C19 C20	0.1(8)	H16B	3398	9832	1333	29
C5 C15 C16 C17	-63.0(5)	Cl1 C1 C2 C3	176.7(3)	H17A	5474	9402	2545	35
C6 C2 C3 N1	-178.1(4)	Cl1 C1 C2 C6	-4.2(6)	H17B	4166	10472	2835	35
C6 C7 C8 C9	-73.1(5)	Cl1 C1 C5 C4	-177.9(3)	H19	6417	6690	3309	39
C7 C8 C9 C10	86.2(6)	Cl1 C1 C5 C15	-2.4(6)	H20	6316	4411	4339	48
C7 C8 C9 C14	-90.4(6)	N1 C4 C5 C1	1.6(7)	H21	4266	4250	4979	46
C8 C9 C10 C11	-174.9(5)	N1 C4 C5 C15	-174.2(4)	H22	2285	6315	4587	43
C8 C9 C14 C13	175.6(6)	O1 C6 C7 C8	-69.6(5)	H23	2373	8540	3538	38
C9 C10 C11 C12	-0.9(8)	O2 C15 C16 C17	175.4(4)	H1	9080(80)	3220(90)	60(40)	49
				H2	2730(80)	5720(120)	410(50)	41

**Table 7 Hydrogen Atom Coordinates ( $\text{\AA} \times 10^4$ ) and Isotropic Displacement Parameters ( $\text{\AA}^2 \times 10^3$ ) for 126.**

Atom	x	y	z	U(eq)
H3	8804	7259	294	32
H4	5037	9511	510	32
H6	8440	3075	1332	31
H7A	9758	5226	2418	35
H7B	10735	5775	1747	35
H8A	11565	2596	1784	37
H8B	12204	3693	2651	37
H10	9592	197	1778	35
H11	8383	-1738	2559	39
H12	8661	-1351	4069	45
H13	10207	985	4778	49

## Experimental

A suitable crystal was selected on a **SuperNova, Dual, Cu at zero, Atlas** diffractometer. The crystal was kept at 99.97(10) K during data collection. Using Olex2 [1], the structure was solved with the ShelXS [2] structure solution program using Direct Methods and refined with the ShelXL [3] refinement package using Least Squares minimisation.

1. Dolomanov, O.V., Bourhis, L.J., Gildea, R.J., Howard, J.A.K. & Puschmann, H. (2009), *J. Appl. Cryst.* 42, 339-341.

## Crystal structure determination of 126

**Crystal Data** for  $\text{C}_{23}\text{H}_{24}\text{ClNO}_2$  ( $M = 381.88$  g/mol): monoclinic, space group  $P2_1$  (no. 4),  $a = 9.0658(8)$  Å,  $b = 7.3204(5)$  Å,  $c = 15.6038(9)$  Å,  $\beta = 102.886(7)^\circ$ ,  $V = 1009.47(12)$  Å<sup>3</sup>,  $Z = 2$ ,  $T = 99.97(10)$  K,  $\mu(\text{CuK}\alpha) = 1.804$  mm<sup>-1</sup>,  $D_{\text{calc}} = 1.256$  g/cm<sup>3</sup>, 3690 reflections measured ( $5.81^\circ \leq 2\theta \leq 136.452^\circ$ ), 2636

unique ( $R_{\text{int}} = 0.0510$ ,  $R_{\text{sigma}} = 0.0610$ ) which were used in all calculations. The final  $R_1$  was 0.0598 ( $I > 2\sigma(I)$ ) and  $wR_2$  was 0.1614 (all data).

### Refinement model description

Number of restraints - 2, number of constraints - unknown.

Details:

1. Fixed Uiso

At 1.2 times of:

All C(H) groups, All C(H,H) groups

At 1.5 times of:

All O(H) groups

2. Restrained distances

O1-H1

0.82 with sigma of 0.02

3.a Ternary CH refined with riding coordinates:

C6(H6), C15(H15)

3.b Secondary CH2 refined with riding coordinates:

C7(H7A,H7B), C8(H8A,H8B), C16(H16A,H16B), C17(H17A,H17B)

3.c Aromatic/amide H refined with riding coordinates:

C3(H3), C4(H4), C10(H10), C11(H11), C12(H12), C13(H13), C14(H14),  
C19(H19),

C20(H20), C21(H21), C22(H22), C23(H23)

## References

1. De Rycke, N.; Couty, F.; David, O. R. P., Increasing the Reactivity of Nitrogen Catalysts. *Chem. Eur. J.* **2011**, *17* (46), 12852-12871.
2. Denmark, S. E.; Beutner, G. L., Lewis Base Catalysis in Organic Synthesis. *Angew. Chem. Int. Ed.* **2008**, *47* (9), 1560-1638.
3. Muller, P., Glossary of terms used in physical organic chemistry. *Pure Appl. Chem.* **1994**, *66* (5), 1077-1184.
4. Einhorn, A.; Hollandt, F.; Von Alfred Einhorn, M., Ueber die Acylierung der Alkohole und Phenole in Pyridinlösung. *Liebigs Ann. Chem.* **1898**, *301* (1), 95-115.
5. Litvinen, Lm; Kirichen, Ai, Basicity and stereospecificity in nucleophile catalysis by tertiary amines. *Dokl. Akad. Nauk SSSR* **1967**, *176* (1), 97-&.
6. Shimizu, S.; Watanabe, N.; Kataoka, T.; Shoji, T.; Abe, N.; Morishita, S.; Ichimura, H., Pyridine and Pyridine Derivatives. In *Ullmann's Encyclopedia of Industrial Chemistry*, Wiley-VCH Verlag GmbH & Co. KGaA: 2000.
7. Steglich, W.; Höfle, G., N,N-Dimethyl-4-pyridinamine, a Very Effective Acylation Catalyst. *Angew. Chem. Int. Ed.* **1969**, *8* (12), 981-981.
8. Shaw, S. A.; Aleman, P.; Christy, J.; Kampf, J. W.; Va, P.; Vedejs, E., Enantioselective TADMAP-Catalyzed Carboxyl Migration Reactions for the Synthesis of Stereogenic Quaternary Carbon. *J. Am. Chem. Soc.* **2005**, *128* (3), 925-934.
9. Steglich, W.; Höfle, G., Über eine einfache darstellung von acyl-oxazolinonen-(5) aus 5-acyloxy-oxazolen II. Mitteilung über hypernucleophile acylierungskatalysatoren. *Tetrahedron Lett.* **1970**, *11* (54), 4727-4730.
10. Höfle, G.; Steglich, W.; Vorbrüggen, H., 4-Dialkylaminopyridines as Highly Active Acylation Catalysts. [New synthetic method (25)]. *Angew. Chem. Int. Ed.* **1978**, *17* (8), 569-583.
11. Heinrich, M. R.; Klisa, H. S.; Mayr, H.; Steglich, W.; Zipse, H., Enhancing the Catalytic Activity of 4-(Dialkylamino)pyridines by Conformational Fixation. *Angew. Chem. Int. Ed.* **2003**, *42* (39), 4826-4828.
12. Singh, S.; Das, G.; Singh, O. V.; Han, H., Conformationally restricted 4-dimethylaminopyridine (DMAP) analogs: synthesis and evaluation of catalytic effectiveness. *Tetrahedron Lett.* **2007**, *48* (11), 1983-1986.
13. Hwang, C. K.; Li, W. S.; Nicolaou, K. C., Reactions of hydroxyl groups with tosylchloride-dimethylaminopyridine system. Direct synthesis of chlorides from hydroxycompounds. *Tetrahedron Lett.* **1984**, *25* (22), 2295-2296.
14. Bugarin, A.; Connell, B. T., Acceleration of the Morita–Baylis–Hillman Reaction by a Simple Mixed Catalyst System. *J. Org. Chem.* **2009**, *74* (12), 4638-4641.
15. Hernandez, O.; Chaudhary, S. K.; Cox, R. H.; Porter, J., Synthesis and characterization of 4-dimethylamino-N-triphenylmethylpyridinium chloride, a postulated intermediate in the tritylation of alcohols. *Tetrahedron Lett.* **1981**, *22* (16), 1491-1494.
16. Belmessieri, D.; Joannesse, C.; Woods, P. A.; MacGregor, C.; Jones, C.; Campbell, C. D.; Johnston, C. P.; Duguet, N.; Concellon, C.; Bragg, R. A.; Smith, A. D., Structure-enantioselectivity effects in 3,4-dihydropyrimido[2,1-b]benzothiazole-based isothioureas as enantioselective acylation catalysts. *Org. Biomol. Chem.* **2011**, *9* (2), 559-570.
17. Berlin, J. M.; Fu, G. C., Enantioselective Nucleophilic Catalysis: The Synthesis of Aza- $\beta$ -Lactams through [2+2] Cycloadditions of Ketenes with Azo Compounds. *Angew. Chem. Int. Ed.* **2008**, *47* (37), 7048-7050.
18. Fu, G. C., Asymmetric Catalysis with “Planar-Chiral” Derivatives of 4-(Dimethylamino)pyridine. *Acc. Chem. Res.* **2004**, *37* (8), 542-547.

19. Aitken, A.; Kilenyi, S. N., *Asymmetric Synthesis*. Taylor & Francis: 1992.
20. Kagan, H.; Fiaud, J., Kinetic resolution. *Top. Stereochem* **1988**, *18* (249330), 21.
21. Goodman, J. M.; Köhler, A.-K.; Alderton, S. C. M., Interactive analysis of selectivity in kinetic resolutions. *Tetrahedron Lett.* **1999**, *40* (49), 8715-8718.
22. Goodman, J. M. <http://www-jmg.ch.cam.ac.uk/tools/magnus/KinRes.html> (accessed 20 June 2015).
23. Lee, D.; Choi, Y. K.; Kim, M.-J., Enhancing the Enantioselectivity of Lipase in Transesterification by Substrate Matching: An Enzyme Memory Based Approach. *Org. Lett.* **2000**, *2* (16), 2553-2555.
24. Hu, B.; Meng, M.; Wang, Z.; Du, W.; Fossey, J. S.; Hu, X.; Deng, W.-P., A Highly Selective Ferrocene-Based Planar Chiral PIP (Fc-PIP) Acyl Transfer Catalyst for the Kinetic Resolution of Alcohols. *J. Am. Chem. Soc.* **2010**, *132* (47), 17041-17044.
25. Hu, B.; Meng, M.; Fossey, J. S.; Mo, W.; Hu, X.; Deng, W.-P., Optically pure bulky (hetero)arylalkyl carbinols via kinetic resolution. *Chem. Comm.* **2011**, *47* (38), 10632-10634.
26. Wang, Z.; Ye, J.; Wu, R.; Liu, Y.-Z.; Fossey, J. S.; Cheng, J.; Deng, W.-P., Bi-aryl rotation in phenyl-dihydroimidazoquinoline catalysts for kinetic resolution of arylalkyl carbinols. *Catal. Sci. Tech.* **2014**, *4* (7), 1909-1913.
27. Crittall, M. R.; Fairhurst, N. W. G.; Carbery, D. R., Point-to-helical chirality transfer for a scalable and resolution-free synthesis of a helicoidal DMAP organocatalyst. *Chem. Comm.* **2012**, *48* (91), 11181-11183.
28. Kawabata, T.; Muramatsu, W.; Nishio, T.; Shibata, T.; Schedel, H., A Catalytic One-Step Process for the Chemo- and Regioselective Acylation of Monosaccharides. *J. Am. Chem. Soc.* **2007**, *129* (42), 12890-12895.
29. Spivey, A. C.; Fekner, T.; Adams, H., Synthesis of atropisomeric analogues of DMAP. *Tetrahedron Lett.* **1998**, *39* (48), 8919-8922.
30. Vedejs, E.; Chen, X., Kinetic Resolution of Secondary Alcohols. Enantioselective Acylation Mediated by a Chiral (Dimethylamino)pyridine Derivative. *J. Am. Chem. Soc.* **1996**, *118* (7), 1809-1810.
31. Shaw, S. A.; Aleman, P.; Vedejs, E., Development of Chiral Nucleophilic Pyridine Catalysts: Applications in Asymmetric Quaternary Carbon Synthesis. *J. Am. Chem. Soc.* **2003**, *125* (44), 13368-13369.
32. Ma, G.; Deng, J.; Sibi, M. P., Fluxionally Chiral DMAP Catalysts: Kinetic Resolution of Axially Chiral Biaryl Compounds. *Angew. Chem.* **2014**, *126* (44), 12012-12015.
33. Duffey, T. A.; Shaw, S. A.; Vedejs, E., AcOLeDMAP and BnOLeDMAP: Conformationally Restricted Nucleophilic Catalysts for Enantioselective Rearrangement of Indolyl Acetates and Carbonates. *J. Am. Chem. Soc.* **2009**, *131* (1), 14-+.
34. Mandai, H.; Fujiwara, T.; Noda, K.; Fujii, K.; Mitsudo, K.; Korenaga, T.; Suga, S., Enantioselective Steglich Rearrangement of Oxindole Derivatives by Easily Accessible Chiral N,N-4-(Dimethylamino)pyridine Derivatives. *Org. Lett.* **2015**, *17* (18), 4436-4439.
35. Kawabata, T.; Nagato, M.; Takasu, K.; Fuji, K., Nonenzymatic Kinetic Resolution of Racemic Alcohols through an "Induced Fit" Process. *J. Am. Chem. Soc.* **1997**, *119* (13), 3169-3170.
36. Spivey, A. C.; Fekner, T.; Spey, S. E.; Adams, H., Configurationally stable biaryl analogues of 4-(dimethylamino)pyridine: A novel class of chiral nucleophilic catalysts. *J. Org. Chem.* **1999**, *64* (26), 9430-9443.
37. Spivey, A. C.; Fekner, T.; Spey, S. E., Axially chiral analogues of 4-(dimethylamino)pyridine: Novel catalysts for nonenzymatic enantioselective acylations. *J. Org. Chem.* **2000**, *65* (10), 3154-3159.

38. Ruble, J. C.; Fu, G. C., Chiral  $\pi$ -Complexes of Heterocycles with Transition Metals: A Versatile New Family of Nucleophilic Catalysts. *J. Org. Chem.* **1996**, *61* (21), 7230-7231.
39. Tao, B. T.; Ruble, J. C.; Hoic, D. A.; Fu, G. C., Nonenzymatic kinetic resolution of propargylic alcohols by a planar-chiral DMAP derivative: Crystallographic characterization of the acylated catalyst. *J. Am. Chem. Soc.* **1999**, *121* (21), 5091-5092.
40. Robison, M. M., The Preparation of 1,5-Pyridine. *J. Am. Chem. Soc.* **1958**, *80* (23), 6254-6257.
41. Fu, G. C., Asymmetric catalysis with "planar-chiral" heterocycles. *Pure Appl. Chem.* **2001**, *73* (2), 347-349.
42. Le, Y.; Fu, G. C., A new benchmark for the non-enzymatic enantioselective acylation of amines: use of a planar-chiral derivative of 4-pyrrolidinopyridine as the acylating agent. *Chem. Comm.* **2000**, (2), 119-120.
43. Ruble, J. C.; Latham, H. A.; Fu, G. C., Effective Kinetic Resolution of Secondary Alcohols with a Planar-Chiral Analogue of 4-(Dimethylamino)pyridine. Use of the Fe(C5Ph5) Group in Asymmetric Catalysis. *J. Am. Chem. Soc.* **1997**, *119* (6), 1492-1493.
44. Nguyen, H. V.; Motevalli, M.; Richards, C. J., A C2-Symmetric Metallocene-Pyrrolidinopyridine Nucleophilic Catalyst for Asymmetric Synthesis. *Synlett* **2007**, 2007 (05), 0725-0728.
45. Nguyen, H. V.; Butler, D. C. D.; Richards, C. J., A Metallocene-Pyrrolidinopyridine Nucleophilic Catalyst for Asymmetric Synthesis. *Org. Lett.* **2006**, *8* (4), 769-772.
46. Crittall, M. R.; Rzepa, H. S.; Carbery, D. R., Design, Synthesis, and Evaluation of a Helicenoidal DMAP Lewis Base Catalyst. *Org. Lett.* **2011**, *13* (5), 1250-1253.
47. Dougherty, D. A., The Cation- $\pi$  Interaction. *Acc. Chem. Res.* **2012**, *46* (4), 885-893.
48. Stauffer, D. A.; Barrans, R. E.; Dougherty, D. A., Biomimetic Catalysis of an SN2 Reaction Resulting from a Novel Form of Transition-State Stabilization. *Angew. Chem. Int. Ed.* **1990**, *29* (8), 915-918.
49. Shepodd, T. J.; Petti, M. A.; Dougherty, D. A., Molecular recognition in aqueous media: donor-acceptor and ion-dipole interactions produce tight binding for highly soluble guests. *J. Am. Chem. Soc.* **1988**, *110* (6), 1983-1985.
50. Sunner, J.; Nishizawa, K.; Kebarle, P., Ion-solvent molecule interactions in the gas phase. The potassium ion and benzene. *J. Phys. Chem.* **1981**, *85* (13), 1814-1820.
51. Kim, D.; Hu, S.; Tarakeswar, P.; Kim, K. S.; Lisy, J. M., Cation- $\pi$  Interactions: A Theoretical Investigation of the Interaction of Metallic and Organic Cations with Alkenes, Arenes, and Heteroarenes. *J. Phys. Chem. A* **2003**, *107* (8), 1228-1238.
52. Cabarcos, O. M.; Weinheimer, C. J.; Lisy, J. M., Size selectivity by cation- $\pi$  interactions: Solvation of K<sup>+</sup> and Na<sup>+</sup> by benzene and water. *J. Chem. Phys.* **1999**, *110* (17), 8429-8435.
53. Meot-Ner, M.; Deakyne, C. A., Unconventional ionic hydrogen bonds. 2. NH<sup>+</sup>... $\pi$ . Complexes of onium ions with olefins and benzene derivatives. *J. Am. Chem. Soc.* **1985**, *107* (2), 474-479.
54. Yamada, S.; Fossey, J. S., Nitrogen cation- $\pi$  interactions in asymmetric organocatalytic synthesis. *Org. Biomol. Chem.* **2011**, *9* (21), 7275-7281.
55. Yamada, S., Intramolecular cation- $\pi$  interaction in organic synthesis. *Org. Biomol. Chem.* **2007**, *5* (18), 2903-2912.
56. Chen, W.; Elfeky, S. A.; Nonne, Y.; Male, L.; Ahmed, K.; Amiable, C.; Axe, P.; Yamada, S.; James, T. D.; Bull, S. D.; Fossey, J. S., A pyridinium cation- $\pi$  interaction sensor for the fluorescent detection of alkyl halides. *Chem. Comm.* **2011**, 47 (1), 253-255.
57. Yamada, S.; Yamashita, K., Dynamic kinetic resolution of hemiaminals using a novel DMAP catalyst. *Tetrahedron Lett.* **2008**, *49* (1), 32-35.

58. Yamada, S.; Misono, T.; Iwai, Y.; Masumizu, A.; Akiyama, Y., New Class of Pyridine Catalyst Having a Conformation Switch System: Asymmetric Acylation of Various sec-Alcohols. *J. Org. Chem.* **2006**, *71* (18), 6872-6880.
59. Yamada, S.; Misono, T.; Iwai, Y., Kinetic resolution of sec-alcohols by a new class of pyridine catalysts having a conformation switch system. *Tetrahedron Lett.* **2005**, *46* (13), 2239-2242.
60. Yamada, S., Conformation-control and stereoselective reactions using cation- $\pi$  interactions. *J. Synth. Org. Chem. Jpn.* **2005**, *63* (4), 339-350.
61. Yamada, S.; Morita, C., Face-Selective Addition to a Cation- $\pi$  Complex of a Pyridinium Salt: Synthesis of Chiral 1,4-Dihydropyridines. *J. Am. Chem. Soc.* **2002**, *124* (28), 8184-8185.
62. Yamada, S.; Noguchi, E., Dynamic kinetic resolution of hemiaminals with axially chiral twisted amides. *Tetrahedron Lett.* **2001**, *42* (21), 3621-3624.
63. Huang, Y.-J.; Jiang, Y.-B.; Bull, S. D.; Fossey, J. S.; James, T. D., Diols and anions can control the formation of an exciplex between a pyridinium boronic acid with an aryl group connected via a propylene linker. *Chem. Comm.* **2010**, *46* (43), 8180-8182.
64. Richter, I.; Minari, J.; Axe, P.; Lowe, J. P.; James, T. D.; Sakurai, K.; Bull, S. D.; Fossey, J. S., Intramolecular cation-[small  $\pi$ ] interactions control the conformation of nonrestricted (phenylalkyl)pyridines. *Chem. Comm.* **2008**, *0* (9), 1082-1084.
65. Kawabata, T.; Stragies, R.; Fukaya, T.; Nagaoka, Y.; Schedel, H.; Fuji, K., Preparation and properties of chiral 4-pyrrolidinopyridine (PPY) analogues with dual functional side chains. *Tetrahedron Lett.* **2003**, *44* (8), 1545-1548.
66. Kawabata, T.; Yamamoto, K.; Momose, Y.; Yoshida, H.; Nagaoka, Y.; Fuji, K., Kinetic resolution of amino alcohol derivatives with a chiral nucleophilic catalyst: access to enantiopure cyclic cis-amino alcohols. *Chem. Comm.* **2001**, *0* (24), 2700-2701.
67. Deeming, A., New C-3 derivatised Chiral DMAP Nucleophilic Catalyst for Kinetic Resolution of Secondary Alcohols. *MSci Thesis* **2011**.
68. Groziak, M. P.; Melcher, L. M., The Regioselectivity of Amination of Certain 4-Dimethylaminopyridines. *Heterocycles* **1987**, *26* (11), 2905-2910.
69. Chhattise, P. K.; Ramaswamy, A. V.; Waghmode, S. B., Regioselective, photochemical bromination of aromatic compounds using N-bromosuccinimide. *Tetrahedron Lett.* **2008**, *49* (1), 189-194.
70. Paudler, W. W.; Jovanovic, M. V., Bromination of some pyridine and diazine N-oxides. *J. Org. Chem.* **1983**, *48* (7), 1064-1069.
71. Essery, J. M.; Schofield, K., 961. Some derivatives of 4-amino- and 4-nitro-pyridine. *Journal of the Chemical Society (Resumed)* **1960**, (0), 4953-4959.
72. Poisson, T.; Oudeyer, S.; Levacher, V., Efficient C-3 functionalization of 4-dimethylaminopyridine (DMAP). A straightforward access to new chiral nucleophilic catalysts. *Tetrahedron Lett.* **2012**, *53* (26), 3284-3287.
73. Cailly, T.; Fabis, F.; Lemaître, S.; Bouillon, A.; Rault, S., Synthesis of ortho-substituted cyanopyridines through lithio intermediate trapping. *Tetrahedron Lett.* **2005**, *46* (1), 135-137.
74. Busto, E.; Gotor-Fernández, V.; Gotor, V., Enantioselective Synthesis of 4-(Dimethylamino)pyridines through a Chemical Oxidation-Enzymatic Reduction Sequence. Application in Asymmetric Catalysis. *Adv. Synth. Catal.* **2006**, *348* (18), 2626-2632.
75. Fuglseth, E.; Sundby, E.; Bruheim, P.; Hoff, B. H., Asymmetric reduction using (R)-MeCBS and determination of absolute configuration of para-substituted 2-fluoroarylethanol. *Tetrahedron: Asymmetry* **2008**, *19* (16), 1941-1946.

76. Corey, E. J.; Suggs, J. W., Pyridinium chlorochromate. An efficient reagent for oxidation of primary and secondary alcohols to carbonyl compounds. *Tetrahedron Lett.* **1975**, *16* (31), 2647-2650.
77. Cui J. J., D. J. G., Gu D., Guo C., Johnson M. C., Kania R. S., Kephart S. E., Linton M. A., McAlpine I. J., Pairish M. A., Palmer C. L. WO2009/16460 A2, 2009.
78. Woods, K. W. L., Qun; Sham, Hing L. Farnesyltransferase inhibitors US2003/199542 A1, 2003.
79. Menger, F. M.; Lee, C., Oxidations with solid potassium permanganate. *J. Org. Chem.* **1979**, *44* (19), 3446-3448.
80. Park, C.-M.; Sun, C.; Olejniczak, E. T.; Wilson, A. E.; Meadows, R. P.; Betz, S. F.; Elmore, S. W.; Fesik, S. W., Non-peptidic small molecule inhibitors of XIAP. *Bioorg. Med. Chem. Lett.* **2005**, *15* (3), 771-775.
81. Corey, E. J.; Helal, C. J., Reduction of Carbonyl Compounds with Chiral Oxazaborolidine Catalysts: A New Paradigm for Enantioselective Catalysis and a Powerful New Synthetic Method. *Angew. Chem. Int. Ed.* **1998**, *37* (15), 1986-2012.
82. Zhao, Y. Synthesis of chiral DMAP derivatives. The University of Birmingham, 2015.
83. Hashizume, H.; Ito, H.; Yamada, K.; Nagashima, H.; Kanao, M.; Tomoda, H.; Sunazuka, T.; Kumagai, H.; Omura, S., Synthesis and Biological Activity of New 3-Hydroxy-3-methylglutaryl Coenzyme A (HMG-CoA) Synthase Inhibitors : 2-Oxetanones with a Side Chain Mimicking the Folded Structure of 1233A. *CHEMICAL & PHARMACEUTICAL BULLETIN* **1994**, *42* (3), 512-520.
84. Schwarzer, D.; Kutne, P.; Schröder, C.; Troe, J., Intramolecular vibrational energy redistribution in bridged azulene-anthracene compounds: Ballistic energy transport through molecular chains. *J. Chem. Phys.* **2004**, *121* (4), 1754-1764.
85. Battistuzzi, G.; Cacchi, S.; Fabrizi, G., An Efficient Palladium-Catalyzed Synthesis of Cinnamaldehydes from Acrolein Diethyl Acetal and Aryl Iodides and Bromides. *Org. Lett.* **2003**, *5* (5), 777-780.
86. Noël, S.; Djakovitch, L.; Pinel, C., Influence of the catalytic conditions on the selectivity of the Pd-catalyzed Heck arylation of acrolein derivatives. *Tetrahedron Lett.* **2006**, *47* (23), 3839-3842.
87. Noël, S.; Luo, C.; Pinel, C.; Djakovitch, L., Efficient Heterogeneously Palladium-Catalysed Heck Arylation of Acrolein Diethyl Acetal. Selective Synthesis of Cinnamaldehydes or 3-Arylpropionic Esters. *Adv. Synth. Catal.* **2007**, *349* (7), 1128-1140.
88. Alacid, E.; Nájera, C., Acrolein Diethyl Acetal: A Three-Carbon Homologating Reagent for the Synthesis of  $\beta$ -Arylpropanoates and Cinnamaldehydes by Heck Reaction Catalyzed by a Kaiser Oxime Resin Derived Palladacycle. *Eur. J. Org. Chem.* **2008**, *2008* (18), 3102-3106.
89. Pan, K.; Noël, S.; Pinel, C.; Djakovitch, L., Heck arylation of acrolein acetals using the 9-bromoanthracene: A case of study. *J. Organomet. Chem.* **2008**, *693* (17), 2863-2868.
90. Yang, J. W.; Hechavarria Fonseca, M. T.; List, B., A Metal-Free Transfer Hydrogenation: Organocatalytic Conjugate Reduction of  $\alpha,\beta$ -Unsaturated Aldehydes. *Angew. Chem. Int. Ed.* **2004**, *43* (48), 6660-6662.
91. Frost, C. G.; Hartley, B. C., Tandem Molybdenum Catalyzed Hydrosilylations: An Expedient Synthesis of  $\beta$ -Aryl Aldehydes. *Org. Lett.* **2007**, *9* (21), 4259-4261.
92. Frost, C. G.; Hartley, B. C., Lewis Base-Promoted Hydrosilylation of Cyclic Malonates: Synthesis of  $\beta$ -Substituted Aldehydes and  $\gamma$ -Substituted Amines. *J. Org. Chem.* **2009**, *74* (9), 3599-3602.

93. Andrews, S. P.; Ladlow, M., Convenient Preparation and Use of a New Analytical Construct for the Analysis and Development of Solid-Phase Chemistries. *J. Org. Chem.* **2003**, *68* (14), 5525-5533.
94. Payne, D. T.; Zhao, Y.; Fossey, J. S., Ethylenation of aldehydes to 3-propanal, propanol and propanoic acid derivatives. *Sci. Rep.* **2017**, *7* (1), 1720.
95. Zhang, D.; Chen, Z.; Cai, H.; Zou, X., A new synthetic route to polyfluorobenzyl alcohol. *J. Fluor. Chem.* **2009**, *130* (10), 938-941.
96. Fuchibe, K.; Ohshima, Y.; Mitomi, K.; Akiyama, T., Low-Valent Niobium-Catalyzed Reduction of  $\alpha,\alpha,\alpha$ -Trifluorotoluenes. *Org. Lett.* **2007**, *9* (8), 1497-1499.
97. Faull, A. W.; Brewster, A. G.; Brown, G. R.; Smithers, M. J.; Jackson, R., Dual-Acting Thromboxane Receptor Antagonist/Synthase Inhibitors: Synthesis and Biological Properties of [2-Substituted-4-(3-pyridyl)-1,3-dioxan-5-yl]alkenoic Acids. *J. Med. Chem.* **1995**, *38* (4), 686-694.
98. Fortage, J.; Peltier, C.; Perruchot, C.; Takemoto, Y.; Teki, Y.; Bedioui, F.; Marvaud, V.; Dupeyre, G.; Pospíšil, L.; Adamo, C.; Hromadová, M.; Ciofini, I.; Lainé, P. P., Single-Step versus Stepwise Two-Electron Reduction of Polyarylpyridiniums: Insights from the Steric Switching of Redox Potential Compression. *J. Am. Chem. Soc.* **2012**, *134* (5), 2691-2705.
99. Klán, P., Effect of metal ions on the bromination of 3,5-dimethylpyridine-N-oxide in acetic acid. *Monatshefte für Chemie / Chemical Monthly* **1993**, *124* (3), 327-330.
100. Shi, Q.; Zhang, S.; Wang, Q.; Ma, H.; Yang, G.; Sun, W.-H., Synthesis and crystal structure of metal-organic frameworks  $[\text{Ln}2(\text{pydc}-3,5)3(\text{H}_2\text{O})9]\text{n}3\text{nH}_2\text{O}$  (Ln = Sm, Eu, Gd, Dy; pydc-3,5 = pyridine-3,5-dicarboxylate) along with the photoluminescent property of its europium one. *J. Mol. Struct.* **2007**, *837* (1–3), 185-189.
101. Ehara, T.; Irie, O.; Kosaka, T.; Kanazawa, T.; Breitenstein, W.; Grosche, P.; Ostermann, N.; Suzuki, M.; Kawakami, S.; Konishi, K.; Hitomi, Y.; Toyao, A.; Gunji, H.; Cumin, F.; Schiering, N.; Wagner, T.; Rigel, D. F.; Webb, R. L.; Maibaum, J.; Yokokawa, F., Structure-Based Design of Substituted Piperidines as a New Class of Highly Efficacious Oral Direct Renin Inhibitors. *ACS Med. Chem. Lett.* **2014**, *5* (7), 787-792.
102. Thomas, A. D.; Josemin; Asokan, C. V., Vilsmeier–Haack reactions of carbonyl compounds: synthesis of substituted pyrones and pyridines. *Tetrahedron* **2004**, *60* (23), 5069-5076.
103. Chinchilla, R.; Najera, C., Recent advances in Sonogashira reactions. *Chem. Soc. Rev.* **2011**, *40* (10), 5084-5121.
104. Zeidan, T. A.; Kovalenko, S. V.; Manoharan, M.; Clark, R. J.; Ghiviriga, I.; Alabugin, I. V., Triplet Acetylenes as Synthetic Equivalents of 1,2-Bicarbenes: Phantom  $n,\pi^*$  State Controls Reactivity in Triplet Photocycloaddition. *J. Am. Chem. Soc.* **2005**, *127* (12), 4270-4285.
105. Spivey, A. C.; Fekner, T.; Spey, S. E., Axially Chiral Analogues of 4-(Dimethylamino)pyridine: Novel Catalysts for Nonenzymatic Enantioselective Acylations. *J. Org. Chem.* **2000**, *65* (10), 3154-3159.
106. Liang, L.; Astruc, D., The copper(I)-catalyzed alkyne-azide cycloaddition (CuAAC) “click” reaction and its applications. An overview. *Coordination Chemistry Reviews* **2011**, *255* (23–24), 2933-2945.
107. Brittain, W. D. G.; Buckley, B. R.; Fossey, J. S., Asymmetric Copper-Catalyzed Azide–Alkyne Cycloadditions. *ACS Catalysis* **2016**, *6* (6), 3629-3636.
108. Thompson, A. S.; Humphrey, G. R.; DeMarco, A. M.; Mathre, D. J.; Grabowski, E. J. J., Direct conversion of activated alcohols to azides using diphenyl phosphorazidate. A practical alternative to Mitsunobu conditions. *J. Org. Chem.* **1993**, *58* (22), 5886-5888.



109. Rogers, H. R.; Hill, C. L.; Fujiwara, Y.; Rogers, R. J.; Mitchell, H. L.; Whitesides, G. M., Mechanism of formation of Grignard reagents. Kinetics of reaction of alkyl halides in diethyl ether with magnesium. *J. Am. Chem. Soc.* **1980**, *102* (1), 217-226.
110. Peters, M.; Trobe, M.; Breinbauer, R., A Modular Synthesis of Teraryl-Based  $\alpha$ -Helix Mimetics, Part 2: Synthesis of 5-Pyridine Boronic Acid Pinacol Ester Building Blocks with Amino Acid Side Chains in 3-Position. *Chem. Eur. J.* **2013**, *19* (7), 2450-2456.
111. Narayan, S.; Seelhammer, T.; Gawley, R. E., Microwave assisted solvent free amination of halo-(pyridine or pyrimidine) without transition metal catalyst. *Tetrahedron Lett.* **2004**, *45* (4), 757-759.
112. Tichotová, L.; Matoušová, E.; Špulák, M.; Kuneš, J.; Votruba, I.; Buchta, V.; Pour, M., Synthesis and biological activity of desmethoxy analogues of coruscanone A. *Bioorg. Med. Chem. Lett.* **2011**, *21* (20), 6062-6066.
113. Bigi, F.; Carloni, S.; Ferrari, L.; Maggi, R.; Mazzacani, A.; Sartori, G., Clean synthesis in water. Part 2: Uncatalysed condensation reaction of Meldrum's acid and aldehydes. *Tetrahedron Lett.* **2001**, *42* (31), 5203-5205.
114. Dumas, A. M.; Seed, A.; Zorzitto, A. K.; Fillion, E., A general and practical preparation of alkylidene Meldrum's acids. *Tetrahedron Lett.* **2007**, *48* (40), 7072-7074.
115. Sandhu, H. S.; Sapra, S.; Gupta, M.; Nepali, K.; Gautam, R.; Yadav, S.; Kumar, R.; Jachak, S. M.; Chugh, M.; Gupta, M. K.; Suri, O. P.; Dhar, K. L., Synthesis and biological evaluation of arylidene analogues of Meldrum's acid as a new class of antimalarial and antioxidant agents. *Bioorg. Med. Chem.* **2010**, *18* (15), 5626-5633.
116. Ramachary, D. B.; Kishor, M.; Ramakumar, K., A novel and green protocol for two-carbon homologation: a direct amino acid/K<sub>2</sub>CO<sub>3</sub>-catalyzed four-component reaction of aldehydes, active methylenes, Hantzsch esters and alkyl halides. *Tetrahedron Lett.* **2006**, *47* (5), 651-656.
117. Ramachary, D. B.; Mondal, R.; Venkaiah, C., Rapid two-step synthesis of drug-like polycyclic substances by sequential multi-catalysis cascade reactions. *Org. Biomol. Chem.* **2010**, *8* (2), 321-325.
118. Ramachary, D. B.; Venkaiah, C.; Reddy, Y. V.; Kishor, M., Multi-catalysis cascade reactions based on the methoxycarbonylketene platform: diversity-oriented synthesis of functionalized non-symmetrical malonates for agrochemicals and pharmaceuticals. *Org. Biomol. Chem.* **2009**, *7* (10), 2053-2062.
119. Wright, A. D.; Haslego, M. L.; Smith, F. X., Borohydride reduction of substituted isopropylidene methylenemalonates. *Tetrahedron Lett.* **1979**, *20* (25), 2325-2326.
120. Sharma, A. K.; Subramani, A. V.; Gorman, C. B., Efficient synthesis of halo indanones via chlorosulfonic acid mediated Friedel-Crafts cyclization of aryl propionic acids and their use in alkylation reactions. *Tetrahedron* **2007**, *63* (2), 389-395.
121. Tóth, G.; Kövér, K. E., Simple, Safe, Large Scale Synthesis of 5-Arylmethyl-2,2-dimethyl-1,3-dioxane-4,6-diones and 3-Arylpropanoic Acids. *Synth. Commun.* **1995**, *25* (19), 3067-3074.
122. Lemhadri, M.; Doucet, H.; Santelli, M., Direct synthesis of 3-arylpropionic acids by tetraphosphine/palladium catalysed Heck reactions of aryl halides with acrolein ethylene acetal. *Tetrahedron* **2004**, *60* (50), 11533-11540.
123. Schelkun, R. M.; Yuen, P.-w.; Wustrow, D. J.; Kinsora, J.; Su, T.-Z.; Vartanian, M. G., Heteroaromatic side-chain analogs of pregabalin. *Bioorg. Med. Chem. Lett.* **2006**, *16* (9), 2329-2332.
124. Mizushima, T.; Yoshida, A.; Harada, A.; Yoneda, Y.; Minatani, T.; Murata, S., Pyrene-sensitized electron transport across vesicle bilayers: dependence of transport efficiency on pyrene substituents. *Org. Biomol. Chem.* **2006**, *4* (23), 4336-4344.

125. Cooper, L. C.; Chicchi, G. G.; Dinnell, K.; Elliott, J. M.; Hollingworth, G. J.; Kurtz, M. M.; Locker, K. L.; Morrison, D.; Shaw, D. E.; Tsao, K.-L.; Watt, A. P.; Williams, A. R.; Swain, C. J., 2-Aryl Indole NK1 receptor antagonists: optimisation of indole substitution. *Bioorg. Med. Chem. Lett.* **2001**, *11* (9), 1233-1236.
126. Chitneni, S. K.; Reitman, Z. J.; Gooden, D. M.; Yan, H.; Zalutsky, M. R., Radiolabeled inhibitors as probes for imaging mutant IDH1 expression in gliomas: Synthesis and preliminary evaluation of labeled butyl-phenyl sulfonamide analogs. *Eur. J. Med. Chem.* **2016**, *119*, 218-230.
127. Selvam, P.; Sonavane, S. U.; Mohapatra, S. K.; Jayaram, R. V., Selective reduction of alkenes,  $\alpha,\beta$ -unsaturated carbonyl compounds, nitroarenes, nitroso compounds, N,N-hydrogenolysis of azo and hydrazo functions as well as simultaneous hydrodehalogenation and reduction of substituted aryl halides over PdMCM-41 catalyst under transfer hydrogen conditions. *Tetrahedron Lett.* **2004**, *45* (15), 3071-3075.
128. Gibson, S. E.; Hales, N. J.; Peplow, M. A., Chromium carbonyl complexes as novel traceless linkers. *Tetrahedron Lett.* **1999**, *40* (7), 1417-1418.
129. C. Yang, N.-c.; Minsek, D. W.; Johnson, D. G.; Larson, J. R.; Petrich, J. W.; Gerald, R.; Wasielewski, M. R., Photochemistry of polychromophoric arylamines. *Tetrahedron* **1989**, *45* (15), 4669-4681.
130. Cheung, F. K.; Lin, C.; Minissi, F.; Crivillé, A. L.; Graham, M. A.; Fox, D. J.; Wills, M., An Investigation into the Tether Length and Substitution Pattern of Arene-Substituted Complexes for Asymmetric Transfer Hydrogenation of Ketones. *Org. Lett.* **2007**, *9* (22), 4659-4662.
131. Bucher, J.; Wurm, T.; Nalivela, K. S.; Rudolph, M.; Rominger, F.; Hashmi, A. S. K., Cyclization of Gold Acetylides: Synthesis of Vinyl Sulfonates via Gold Vinylidene Complexes. *Angew. Chem. Int. Ed.* **2014**, *53* (15), 3854-3858.
132. Mamolo, M. G.; Zampieri, D.; Zanette, C.; Florio, C.; Collina, S.; Urbano, M.; Azzolina, O.; Vio, L., Substituted benzylaminoalkylindoles with preference for the  $\sigma^2$  binding site. *Eur. J. Med. Chem.* **2008**, *43* (10), 2073-2081.
133. Bair, K. W.; Tuttle, R. L.; Knick, V. C.; Cory, M.; McKee, D. D., [(1-Pyrenylmethyl)amino] alcohols, a new class of antitumor DNA intercalators. Discovery and initial amine side chain structure-activity studies. *J. Med. Chem.* **1990**, *33* (9), 2385-2393.
134. Xu, G.; Yang, X.; Jiang, B.; Lei, P.; Liu, X.; Wang, Q.; Zhang, X.; Ling, Y., Synthesis and bioactivities of novel piperazine-containing 1,5-Diphenyl-2-penten-1-one analogues from natural product lead. *Bioorg. Med. Chem. Lett.* **2016**, *26* (7), 1849-1853.
135. Poldy, J.; Peakall, R.; Barrow, R. A., Identification of the First Alkenyl Chiloglottone Congener. *Eur. J. Org. Chem.* **2012**, *2012* (29), 5818-5827.
136. Zheng, S.; Thompson, J. D.; Tontcheva, A.; Khan, S. I.; Rubin, Y., Perchloro-2,5,8-triazaphenalenyl Radical. *Org. Lett.* **2005**, *7* (9), 1861-1863.
137. Goto, H.; Heemstra, J. M.; Hill, D. J.; Moore, J. S., Single-Site Modifications and Their Effect on the Folding Stability of m-Phenylene Ethynylene Oligomers. *Org. Lett.* **2004**, *6* (6), 889-892.
138. Spivey, A. C.; Leese, D. P.; Zhu, F.; Davey, S. G.; Jarvest, R. L., New atropisomeric biaryl derivatives of 4-aminopyridine—identification of an improved nucleophilic catalyst for asymmetric acylation of sec-alcohols. *Tetrahedron* **2004**, *60* (20), 4513-4525.
139. Ruble, J. C.; Tweddell, J.; Fu, G. C., Kinetic Resolution of Arylalkylcarbinols Catalyzed by a Planar-Chiral Derivative of DMAP: A New Benchmark for Nonenzymatic Acylation. *J. Org. Chem.* **1998**, *63* (9), 2794-2795.

140. Xia, B.; Cheng, G.; Lin, X.; Wu, Q., Dynamic Double Kinetic Resolution of Amines and Alcohols under the Cocatalysis of Raney Nickel/Candida antarctica Lipase B: From Concept to Application. *Eur. J. Org. Chem.* **2014**, 2014 (14), 2917-2923.
141. Klomp, D.; Djanashvili, K.; Svennum, N. C.; Chantapariyavat, N.; Wong, C.-S.; Vilela, F.; Maschmeyer, T.; Peters, J. A.; Hanefeld, U., Combined epimerisation and acylation: Meerwein-Ponndorf-Verley-Oppenauer catalysts in action. *Org. Biomol. Chem.* **2005**, 3 (3), 483-489.
142. Weng, S.-S.; Ke, C.-S.; Chen, F.-K.; Lyu, Y.-F.; Lin, G.-Y., Transesterification catalyzed by iron(III)  $\beta$ -diketonate species. *Tetrahedron* **2011**, 67 (9), 1640-1648.
143. Larionov, E.; Mahesh, M.; Spivey, A. C.; Wei, Y.; Zipse, H., Theoretical Prediction of Selectivity in Kinetic Resolution of Secondary Alcohols Catalyzed by Chiral DMAP Derivatives. *J. Am. Chem. Soc.* **2012**, 134 (22), 9390-9399.
144. Slungård, S. V.; Krakeli, T.-A.; Thvedt, T. H. K.; Fuglseth, E.; Sundby, E.; Hoff, B. H., Investigation into the enantioselection mechanism of ruthenium–arene–diamine transfer hydrogenation catalysts using fluorinated substrates. *Tetrahedron* **2011**, 67 (31), 5642-5650.